ISSN 1881-7815 Online ISSN 1881-7823

BST BioScience Trends

Volume 20, Number 4
August 2026

IRCA BSSA

IACMHR

www.biosciencetrends.com

BST
BioScience Trends

ISSN: 1881-7815
Online ISSN: 1881-7823
CODEN: BTIRCZ
Issues/Year: 6
Language: English
Publisher: IACMHR Co., Ltd.

BioScience Trends is one of a series of peer-reviewed journals of the International Research and Cooperation Association for Bio & Socio-Sciences Advancement (IRCA-BSSA) Group. It is published bimonthly by the International Advancement Center for Medicine & Health Research Co., Ltd. (IACMHR Co., Ltd.) and supported by the IRCA-BSSA.

BioScience Trends devotes to publishing the latest and most exciting advances in scientific research. Articles cover fields of life science such as biochemistry, molecular biology, clinical research, public health, medical care system, and social science in order to encourage cooperation and exchange among scientists and clinical researchers.

BioScience Trends publishes Original Articles, Brief Reports, Reviews, Policy Forum articles, Communications, Editorials, News, and Letters on all aspects of the field of life science. All contributions should seek to promote international collaboration.

Editorial Board

Editor-in-Chief:

Norihiro KOKUDO
Japan Institute for Health Security, Tokyo, Japan

Co-Editors-in-Chief:

Xishan HAO
Tianjin Medical University, Tianjin, China
Takashi KARAKO
Japan Institute for Health Security, Tokyo, Japan
John J. ROSSI
Beckman Research Institute of City of Hope, Duarte, CA, USA

Senior Editors:

Tetsuya ASAKAWA
The Third People's Hospital of Shenzhen, Shenzhen, China
Yu CHEN
The University of Tokyo, Tokyo, Japan
Xunjia CHENG
Fudan University, Shanghai, China
Yoko FUJITA-YAMAGUCHI
Beckman Research Institute of the City of Hope, Duarte, CA, USA
Jianjun GAO
Qingdao University, Qingdao, China
Michael O. GLOCKER
University of Rostock, Rostock, Germany
Na HE
Fudan University, Shanghai, China
Hongen LIAO
Tsinghua University, Beijing, China
Misao MATSUSHITA
Tokai University, Hiratsuka, Japan
Fanghua QI
Shandong Provincial Hospital, Ji'nan, China
Yasuhiko SUGAWARA
Kumamoto University, Kumamoto, Japan
Timothy Walter SYNOLD
Beckman Research Institute of the City of Hope, Duarte, CA, USA
Ling WANG
Guizhou University of Traditional Chinese Medicine, Guiyang, China

Proofreaders:

Curtis BENTLEY
Roswell, GA, USA
Thomas R. LEBON
Los Angeles, CA, USA

Editorial and Head Office

Pearl City Koishikawa 603,
2-4-5 Kasuga, Bunkyo-ku, Tokyo 112-0003, Japan
E-mail: office@biosciencetrends.com

BioScience Trends

Editorial and Head Office

Pearl City Koishikawa 603, 2-4-5 Kasuga, Bunkyo-ku,
Tokyo 112-0003, Japan

E-mail: office@biosciencetrends.com
URL: www.biosciencetrends.com

Editorial Board Members

Girdhar G. AGARWAL
(Lucknow, India)
Hirotsugu AIGA
(Geneva, Switzerland)
Hidechika AKASHI
(Tokyo, Japan)
Moazzam ALI
(Geneva, Switzerland)
Ping AO
(Shanghai, China)
Hisao ASAMURA
(Tokyo, Japan)
Michael E. BARISH
(Duarte, CA, USA)
Boon-Huat BAY
(Singapore, Singapore)
Yasumasa BESSHO
(Nara, Japan)
Generoso BEVILACQUA
(Pisa, Italy)
Shiuan CHEN
(Duarte, CA, USA)
Yi-Li CHEN
(Yiwu, China)
Yue CHEN
(Ottawa, Ontario, Canada)
Naoshi DOHMAE
(Wako, Japan)
Zhen FAN
(Houston, TX, USA)
Ding-Zhi FANG
(Chengdu, China)
Xiao-Bin FENG
(Beijing, China)
Yoshiharu FUKUDA
(Ube, Japan)
Rajiv GARG
(Lucknow, India)
Ravindra K. GARG
(Lucknow, India)
Makoto GOTO
(Tokyo, Japan)
Demin HAN
(Beijing, China)
David M. HELFMAN
(Daejeon, Korea)
Takahiro HIGASHI
(Tokyo, Japan)
De-Fei HONG
(Hangzhou, China)
De-Xing HOU
(Kagoshima, Japan)
Sheng-Tao HOU
(Guanzhou, China)
Xiaoyang HU
(Southampton, UK)
Yong HUANG
(Ji'ning, China)
Hirofumi INAGAKI
(Tokyo, Japan)
Masamine JIMBA
(Tokyo, Japan)
Chun-Lin JIN
(Shanghai, China)
Kimitaka KAGA
(Tokyo, Japan)
Michael Kahn
(Duarte, CA, USA)
Kazuhiro KAKIMOTO
(Osaka, Japan)
Kiyoko KAMIBEPPU
(Tokyo, Japan)
Haidong KAN
(Shanghai, China)
Kenji KARAKO
(Tokyo, Japan)
Bok-Luel LEE
(Busan, Korea)
Chuan LI
(Chengdu, China)
Mingjie LI
(St. Louis, MO, USA)
Shixue LI
(Ji'nan, China)
Ren-Jang LIN
(Duarte, CA, USA)
Chuan-Ju LIU
(New York, NY, USA)
Lianxin LIU
(Hefei, China)
Xinqi LIU
(Tianjin, China)
Daru LU
(Shanghai, China)
Hongzhou LU
(Guanzhou, China)
Duan MA
(Shanghai, China)
Masatoshi MAKUUCHI
(Tokyo, Japan)
Francesco MAROTTA
(Milano, Italy)
Yutaka MATSUYAMA
(Tokyo, Japan)
Qingyue MENG
(Beijing, China)
Mark MEUTH
(Sheffield, UK)
Michihiro Nakamura
(Yamaguchi, Japan)
Munehiro NAKATA
(Hiratsuka, Japan)
Satoko NAGATA
(Tokyo, Japan)
Miho OBA
(Odawara, Japan)
Xianjun QU
(Beijing, China)
Jean-Pierre Routy
(Montréal, Canada)
Carlos SAINZ-FERNANDEZ
(Santander, Spain)
Yoshihiro SAKAMOTO
(Tokyo, Japan)
Erin SATO
(Shizuoka, Japan)
Takehito SATO
(Isehara, Japan)
Akihito SHIMAZU
(Tokyo, Japan)
Zhifeng SHAO
(Shanghai, China)
Xiao-Ou SHU
(Nashville, TN, USA)
Sarah Shuck
(Duarte, CA, USA)
Judith SINGER-SAM
(Duarte, CA, USA)
Raj K. SINGH
(Dehradun, India)
Peipei SONG
(Tokyo, Japan)
Junko SUGAMA
(Kanazawa, Japan)
Zhipeng SUN
(Beijing, China)
Hiroshi TACHIBANA
(Isehara, Japan)
Tomoko TAKAMURA
(Tokyo, Japan)
Tadatoshi TAKAYAMA
(Tokyo, Japan)
Shin'ichi TAKEDA
(Tokyo, Japan)
Sumihito TAMURA
(Tokyo, Japan)
Puay Hoon TAN
(Singapore, Singapore)
Koji TANAKA
(Tsu, Japan)
John TERMINI
(Duarte, CA, USA)
Usa C. THISYAKORN
(Bangkok, Thailand)
Toshifumi TSUKAHARA
(Nomi, Japan)
Mudit Tyagi
(Philadelphia, PA, USA)
Kohjiro UEKI
(Tokyo, Japan)
Masahiro UMEZAKI
(Tokyo, Japan)
Junming WANG
(Jackson, MS, USA)
Qing Kenneth WANG
(Wuhan, China)
Xiang-Dong WANG
(Boston, MA, USA)
Hisashi WATANABE
(Tokyo, Japan)
Jufeng XIA
(Tokyo, Japan)
Feng XIE
(Hamilton, Ontario, Canada)
Jinfu XU
(Shanghai, China)
Lingzhong XU
(Ji'nan, China)
Masatake YAMAUCHI
(Chiba, Japan)
Aitian YIN
(Ji'nan, China)
George W-C. YIP
(Singapore, Singapore)
Xue-Jie YU
(Galveston, TX, USA)
Rongfa YUAN
(Nanchang, China)
Benny C-Y ZEE
(Hong Kong, China)
Yong ZENG
(Chengdu, China)
Wei ZHANG
(Shanghai, China)
Wei ZHANG
(Tianjin, China)
Chengchao ZHOU
(Ji'nan, China)
Xiaomei ZHU
(Seattle, WA, USA)

(*as of August 2026*)

CONTENTS

Volume 20, Number 4, 2026

Editorial

345-347 **Revisiting long-standing biological questions through evolving technologies**
John J. Rossi

Review

348-360 **Comparison of current global guidelines and consensus on the management of patients with cholangiocarcinoma: A 2026 update**
Enyang He, Yulong Cai, Xianze Xiong, Rongxing Zhou, Fuyu Li, Nansheng Cheng

361-372 **Management of dynamic therapeutic opportunity in hepatocellular carcinoma: Preserving liver function and enabling treatment transitions**
Jiwei Huang, Mingheng Liao, Wei Tang

373-384 **Hepatic arterial infusion chemotherapy–based triplet conversion therapy for hepatocellular carcinoma with portal vein tumor thrombus: Evidence, patient selection, and surgical endpoints**
Chaosheng Xia, Yutao He, Rongfu Hong, Wenda Wang, Hangyu Li, Lin Wang, Zhitian Shi

385-397 **Stem cell-derived extracellular vesicles for rare diseases: A clinical -bottleneck-to-mechanism framework for translation**
Yue Han, Nuo Chen, Peipei Song, Yanling Chen, Wei Tang

398-411 **Immunometabolic reprogramming via GLP-1 receptor agonists in people with HIV: A multidimensional systemic framework**
Liqin Sun, Stephane Isnard, Haipeng Zhu, Jingyi Chen, Yun He, Hongzhou Lu, Jean-Pierre Routy

Original Article

412-424 **PRXL2B facilitates the progression of hepatocellular carcinoma and the therapeutic efficacy of oncolytic adenovirus H101 through the PI3K/AKT/PD-L1 axis**
Ziqi Zhang, Hongli Chen, Yangming Liu, Hao Wang, You Yan, Yanxi Yu, Zuotian Huang, Yanyao Liu, Wei Li, Zhongjun Wu, Meiqing Kang, Xiaoyong Luo, Ping Che, Rui Liao

425-437 **ATP6L impairs vascular stability in colorectal cancer via PDGFB/PDGFRβ signaling**
Xiangdong Tian, Dandan Chen, Jiaqi Duo, Shi Zhang, Lisha Qi

438-449 **Underrecognized cardiovascular complications after hepatectomy: population-level mortality burden from a multicentre populationattributable fraction (PAF) analysis**
Junlong Dai, Zhancheng Qiu, Jimmy Che-To Lai, Yu Zhang, Fei Xie, Yu Yu, Kangyi Jiang, Tinghao Chen, Vincent Wai-Sun Wong, Tianfu Wen, Chuan Li

Brief Report

450-460 **Gene expression profiling of the L4-stage nematode Caenorhabditis elegans following ethanol exposure**
Masaki Miyazawa, Ching Ouyang, Mariko Sezaki, Kayo Yasuda, Naoaki Ishii, Yoko Fujita-Yamaguchi

Editorial

DOI: 10.5582/bst.2026.01089

Revisiting long-standing biological questions through evolving technologies

John J. Rossi*

Center for RNA Biology & Therapeutics, Beckman Research Institute of City of Hope, Duarte, CA, USA.

SUMMARY: Advances in biological sciences and technology have continuously reshaped the questions that researchers are able to address. Over the past several decades, developments in DNA sequencing, mass spectrometry, genome analysis, and omics technologies have transformed not only biomedical research itself, but also the interpretation of observations that previously remained unresolved because of technical limitations. This Editorial reflects on how evolving technologies allow long-standing scientific questions to be revisited across generations of research. Two examples illustrate this process. One concerns the structural re-analysis of a *Streptomyces* lectin first studied in the 1970s, whose molecular features could only later be clarified through advances in mass spectrometry and expanding genetic databases. The second involves a recent transcriptomic re-examination of ethanol-associated lifespan responses in *Caenorhabditis elegans*, where modern RNA-seq approaches provided pathway-level insights that were not technically accessible in earlier studies. Together, these examples highlight that scientific progress often emerges not only from asking new questions, but also from revisiting unresolved observations using new technologies and perspectives.

Keywords: transcriptomics, omics technologies, scientific continuity, biological discovery, RNA sequencing

Recent advances in biological sciences and technology have profoundly influenced biomedical research and the way scientific questions are approached. During the 1970s, when many current senior investigators began their scientific training, technologies in protein chemistry and molecular biology were undergoing rapid development. These methodological advances fundamentally changed what could be experimentally examined and interpreted.

Among the most influential developments was the establishment of amino acid and DNA sequencing technologies. Frederick Sanger first determined the amino acid sequence of insulin, representing a landmark achievement in protein chemistry (*1,2*). Sanger and his colleagues introduced the "dideoxy" chain-termination method for sequencing DNA molecules in 1977, also known as "Sanger Sequencing" (*3*). Though the first DNA sequencing method was introduced by Maxam and Gilbert, which was quickly followed by the more facile Sanger method. This Sanger sequencing was the most widely used form of sequencing for over 40 years, a technology that became the foundation of molecular biology for several decades. These advances enabled increasingly detailed analyses of genomes, gene expression, and cellular regulation, ultimately leading to contemporary genomics and transcriptomics.

The continuing expansion of genetic databases, combined with improvements in sequencing platforms, mass spectrometry, and computational biology, has accelerated biological research since the early 2000s. Modern omics technologies now allow comprehensive analyses of molecular networks, signaling pathways, and dynamic cellular responses at levels that were previously impossible to achieve. As a result, observations that once remained descriptive or mechanistically unresolved can now be revisited using broader and more integrated analytical approaches. Developments of major concepts and technologies in biology are summarized in Table 1.

One example of this process involves earlier work by Dr. Fujita-Yamaguchi on a lectin isolated from *Streptomyces* (*4*). During her doctoral studies in the 1970s at the University of Tokyo, she attempted to determine the primary structure of this lectin protein; however, the available technologies at the time were insufficient to resolve highly similar repetitive domains within the molecule (*5*). After achieving her most important early work of purifying the human insulin receptor (*6*) and conducting research in the insulin and IGF-I signaling field as a PI at Beckman Research Institute of City of Hope (COH) and Tokai University,

Table 1. Developments of concepts & technologies in respective fields of biology

	19th century	Early 20th century	1950's	1960's	1970's	1980's	1990's	2000-
Classical genetics Biochemistry	Mendel, Darwin	Metabolic pathways Enzymes	DNA as genetic material					
Modern genetics		Phage, virus, Drosophila as models	'53: Double-helix model for DNA '57:Central dogma of biology	Discovery of codons & roles of RNAs	DNA sequencing methods	Genome analysis	Genetic databases expansion	**Omics technologies:** Genomics: Transcriptomics: Proteomics: Metabolomics
Protein structure/ function		Isolation of abundant proteins by chromatography X-ray crystal structures of proteins, and other biological molecules	'53: Primary structure of insulin NMR	Affinity chromatography Purification of low expression proteins	Protein data bank expansion	Mass spectrometry Signaling pathway analyses Immunoblots Fluorescent probes Confocal microscopy	LC-MS/MS for protein sequencing	Epigenomics: Spatial Omics: Single-cell Analysis Full genome sequences of organisms CRISPR/Cas9 technology
Genetic engineering Gene manipulation				Restriction enzymes Plasmids	Genetic engineering **'78:Humulin*,** the first biosynthetic human insulin product	Genetic testing for SNPs by PCR **Humanized antibodies**** Antibody therapeutics	Production of a variety of biomedicines	

***In 1978,** scientists at City of Hope and Genentech developed a method for producing biosynthetic human insulin (BHI) using recombinant DNA technology (*10*). Eli Lilly & Co. signed an agreement with Genentech to use the rDNA method to make human insulin commercially available. ****In 1984,** Riggs and Cabilly at City of Hope and Herbert Heyneker and his group at Genentech were able to describe and patent the method for making humanized monoclonal antibodies starting from mouse monoclonal antibodies (*11*).

she returned to COH in 2014 and collaborated with Dr. Markus Kalkum to restart her graduate work, which was never completed. After advances in mass spectrometry and expansion of genetic databases, the lectin structure could finally be clarified through collaborative work at City of Hope (*5,7,8*). These later studies demonstrated how technological progress enabled re-analysis of a biological problem that had remained unresolved for many years.

A similar perspective can be applied to another study presented in this issue of *BioScience Trends* (*9*): "Gene expression profiling of the L4-stage nematode *Caenorhabditis elegans* following ethanol exposure" by Miyazawa *et al*. This research originated from earlier investigations initiated more than two decades ago at Tokai University, where the effects of ethanol exposure on *C. elegans* lifespan were examined using conventional experimental approaches. Although lifespan-associated phenotypes were reproducibly observed, mechanistic analyses at that time were necessarily limited to selected candidate pathways and could not comprehensively evaluate global transcriptional responses.

In the present study, the authors revisited this long-standing experimental framework using time-resolved RNA-seq analysis. Rather than establishing definitive causal mechanisms, the study provides transcriptomic and pathway-level perspectives on stress-response programs and longevity-associated pathways potentially linked to ethanol exposure in *C. elegans*. The observed patterns, including changes in detoxification-related pathways and stress-response signaling, illustrate how modern transcriptomic approaches can provide broader biological context for previously observed phenotypes.

Importantly, the value of such studies may extend beyond the specific biological phenomenon itself. They also demonstrate how scientific observations that once exceeded available technical capabilities can acquire new meaning when revisited through evolving methodologies. In many cases, scientific progress arises not only from generating entirely new questions, but also from returning to unresolved observations with new tools, analytical frameworks, and perspectives.

In this sense, technological advancement does not merely accelerate science; it also allows unfinished scientific questions to be revisited across generations of research.

Funding: None.

Conflict of Interest: The author has no conflicts of interest to disclose.

References

1. Sanger F, Tuppy H. The amino-acid sequence in the phenylalanyl chain of insulin. 2. The investigation of peptides from enzymic hydrolysates. Biochem J. 1951; 49:481-490.
2. Sanger F, Thompson EO. The amino-acid sequence in the glycyl chain of insulin. Biochem J. 1952; 52:iii.
3. Sanger F, Nicklen S, Coulson AR. DNA sequencing with chain-terminating inhibitors. Proc Natl Acad Sci U S A. 1977; 74:5463-5467.
4. Fujita Y, Oishi K, Suzuki K, Imahori K. Purification and properties of an anti-B hemagglutinin produced by Streptomyces sp. Biochemistry. 1975; 14:4465-4470.
5. Fujita-Yamaguchi Y, Bagramyan K, Yamaguchi Y, Ikeda A, Dohmae N, Hong TB, Kalkum M. Mass spectrometric revival of an l-rhamnose- and d-galactose-specific lectin from a lost strain of Streptomyces. J Biol Chem. 2018; 293:368-378.
6. Fujita-Yamaguchi Y, Choi S, Sakamoto Y, Itakura K. Purification of insulin receptor with full binding activity. J Biol Chem. 1983; 258:5045-5049.
7. Fujita-Yamaguchi Y, Muramatsu H, Tapia A, Bagramyan K, Desai M, Takehana Y, Igarashi M, Yamaguchi Y, Kalkum M. Proteolytic Processing, Maturation, and Unique Synteny of the Streptomyces Hemagglutinin SHA. Microbiol Spectr. 2021; 9:e0076621.
8. Quijano JC, Natsuyama H, Tapia A, Bagramyan K, Ortiz JA, Mares J, Kalkum M, Fujita-Yamaguchi Y, Ku HT. A lectin produced by a Streptomyces species targets mammalian pancreatic acinar cells in mice and humans. Sci Rep. 2025; 15:2782.
9. Miyazawa M, Ouyang C, Sezaki M, Yasuda K, Ishii N, Fujita-Yamaguchi Y. Gene expression profiling of the L4-stage nematode Caenorhabditis elegans following ethanol exposure. Biosci Trends. 2026; 20:450-460.
10. Goeddel DV, Kleid DG, Bolivar F, Heyneker HL, Yansura DG, Crea R, Hirose T, Kraszewski A, Itakura K, Riggs AD. Expression in Escherichia coli of chemically synthesized genes for human insulin. Proc Natl Acad Sci U S A. 1979; 76:106-110.
11. Cabilly S, Riggs AD, Pande H, Shively JE, Holmes WE, Rey M, Perry LJ, Wetzel R, Heyneker HL. Generation of antibody activity from immunoglobulin polypeptide chains produced in Escherichia coli. Proc Natl Acad Sci U S A. 1984; 81:3273-3277.

Received April 4, 2026; Accepted May 14, 2026.

**Address correspondence to:*
John J. Rossi, Center for RNA Biology & Therapeutics, Beckman Research Institute of City of Hope, Duarte, CA, USA.
E-mail: jrossi@coh.org

Released online in J-STAGE as advance publication June 2, 2026.

Review

DOI: 10.5582/bst.2026.01104

Comparison of current global guidelines and consensus on the management of patients with cholangiocarcinoma: A 2026 update

Enyang He[1,2,§], Yulong Cai[1,§], Xianze Xiong[1], Rongxing Zhou[1], Fuyu Li[1], Nansheng Cheng[1,2,*]

[1] Department of Bile Duct Surgery, West China Hospital, Sichuan University, Chengdu, Sichuan, China;
[2] Research Center for Biliary Diseases, West China Hospital, Sichuan University, Chengdu, Sichuan, China.

SUMMARY: Cholangiocarcinoma (CCA) is a highly aggressive, molecularly heterogeneous biliary tract malignancy and the second most common primary liver cancer, and it has an increasing global incidence and persistently poor prognosis. Recent updates of international guidelines, including those from the NCCN, ESMO, EASL, CSCO, BSG, and Japanese societies, along with rapid advances in precision oncology, have substantially changed the clinical management of CCA. This review systematically compares current global guidelines, highlighting both areas of consensus and regional differences in epidemiology, risk factors, screening strategies, diagnostic approaches, pathological and molecular classification, staging systems, surgical indications, systemic therapy, and multidisciplinary management. This review also summarizes recent advances in molecular diagnostics, including next-generation sequencing, liquid biopsy, circulating tumor DNA, extracellular vesicles, artificial intelligence-assisted imaging, radiomics, and emerging prognostic biomarkers. The evolving roles of immune checkpoint inhibitors, molecularly targeted therapies against FGFR2, IDH1, HER2, BRAF, NTRK, and MSI-H/dMMR, liver transplantation, locoregional treatment, and conversion (translational) therapy are also discussed. Finally, this review addresses current challenges, including drug resistance, limited access to molecular testing, regional disparities in healthcare resources, and the lack of universally accepted screening strategies. By integrating updated guideline recommendations with the latest clinical evidence, this review provides a comprehensive reference for evidence-based clinical decision-making and future translational research in CCA.

Keywords: cholangiocarcinoma, clinical guideline, precision oncology, molecular profiling, immunotherapy, targeted therapy

1. Introduction

Cholangiocarcinoma (CCA) constitutes a highly aggressive, molecularly diverse, and anatomically heterogeneous cluster of biliary tract malignancies originating from the epithelial cells of the biliary tree and is the second most common primary liver cancer after hepatocellular carcinoma (*1,2*). Based on anatomical location, CCA is classified into intrahepatic cholangiocarcinoma (iCCA), perihilar cholangiocarcinoma (pCCA), and distal cholangiocarcinoma (dCCA), with pCCA and dCCA collectively referred to as extrahepatic cholangiocarcinoma (eCCA) (*3,4*). The 2019 WHO classification further recognizes mixed hepatocellular-cholangiocarcinoma (cHCC-CCA) as a distinct subtype (*5*). Due to the lack of specific early symptoms and the heterogeneity of tumor biology, most patients with CCA are diagnosed in an advanced stage, resulting in a median overall survival (OS) of only 24 months after initial diagnosis (*2*).

In recent years, with advances in medical research and mounting clinical evidence, numerous clinical practice guidelines for CCA management have been updated globally, including those from the National Comprehensive Cancer Network (NCCN), the European Association for the Study of the Liver (EASL), the Chinese Society of Clinical Oncology (CSCO), the British Society of Gastroenterology (BSG), the European Society for Medical Oncology (ESMO), and the Japanese Society of Hepato-Biliary-Pancreatic Surgery (JSHBPS) (*6*). These guidelines provide important references for clinical decision-making, but their recommendations differ due to differences in regional medical resources, epidemiological characteristics, and the incorporation of new evidence. The rapid development of targeted therapy and immunotherapy has significantly changed the treatment landscape of advanced CCA, requiring timely

integration into clinical practice guidelines and clinical decision-making (*7,8*).

This review systematically compares the core content of current CCA guidelines, analyzing their similarities and differences in epidemiology, risk factors, screening and diagnosis, staging, and treatment (Table 1). It then cites recent key studies to corroborate the latest progress in targeted therapy, immunotherapy, surgical techniques, and prognostic biomarkers in order to provide a comprehensive and up-to-date reference for the clinical management and scientific research of CCA.

2. Epidemiology and risk factors

2.1. Epidemiology

CCA is universally recognized as a rare malignancy, accounting for less than 1% of all human cancers; however, its incidence and mortality exhibit marked geographical heterogeneity. Its global age-standardized incidence ranges from 0.3 to 3.5 cases per 100,000 population in Europe, the US, and Australasia but is as high as 85 cases per 100,000 in liver fluke–endemic regions such as northeastern Thailand (*8,25*).

Notably, the incidence of iCCA has been rising steadily worldwide, and particularly in Western nations (*26*). From 2000-2019, the incidence of iCCA increased from 0.92 to 1.94 in the US (*27*). This trend is attributed to advances in diagnostic imaging, demographic shifts including migration, and the escalating burden of chronic liver disease (*7*). Conversely, the incidence of eCCA has remained the same or slightly declined in most regions (*28*). GBC, another subtype of biliary tract cancer, exhibits distinct epidemiological patterns: it is declining in most regions worldwide but remains elevated in South Korea and Japan (*10*).

2.2. Risk factors

Global guidelines uniformly identify chronic inflammation of the biliary epithelium as the core common risk factor for CCA, but there are differences in emphasis on subtype-specific risk factors (*25,29*).

The ESMO and EASL-ILCA guidelines list key risk factors for iCCA including cirrhosis, hepatitis B virus, hepatitis C virus, non-alcoholic fatty liver disease, diabetes, obesity, and hormonal contraceptives (*30*). According to the BSG guidelines, alcohol consumption and cigarette smoking are also associated with an increased risk of iCCA (*8,21*).

The main risk factors for pCCA are primary sclerosing cholangitis (PSC) in Western countries and hepatobiliary flukes or hepatolithiasis in Asian countries (*31*). The ESMO guidelines specify that the annual incidence of CCA in PSC patients is 0.6-1.5%, with a lifetime risk of up to 20%. The BSG guidelines add that choledochal cysts and choledocholithiasis are also high-risk factors for pCCA (*8,23*).

Gallstones are the strongest risk factor for GBC, followed by porcelain gallbladder, gallbladder polyps, PSC, chronic Salmonella typhi or Helicobacter bilis infection, congenital biliary tract malformations, and obesity. The ESMO guidelines emphasize that the incidence of GBC increases with age and that GBC is more common in women (*8*).

Notably, the bEASL-ILCA and BSG guidelines both mention that 60-70% of iCCA cases have no identifiable risk factors, highlighting the need for further exploration of unknown etiologies.

2.3. Hereditary cancer syndromes

A rapidly growing consensus across international guidelines in 2026 is the formal recognition of CCA within the expanding spectrum of hereditary cancer syndromes. CCA is part of the spectrum of hereditary cancer syndromes, including hereditary breast-ovarian

Table 1. Overview of recent major clinical practice guidelines and consensus statements on biliary tract cancers

Guidelines	Year	Country/Geographical area	Language	Tumor	*Ref.*
ENS guideline	2026	Europe	English	iCCA, pCCA, dCCA	(*9*)
NCCN guideline	2025	USA	English	iCCA, pCCA, dCCA and GBC	(*10*)
CSCO guideline	2025	China	Chinese	pCCA	(*11*)
Expert consensus	2025	China	English	pCCA	(*12*)
EASL guideline	2025	Europe	English	pCCA, dCCA	(*13*)
ESMO guideline update	2025	Europe	English	iCCA, pCCA, dCCA and GBC	(*14*)
SEOM-GEMCAD-TTD clinical guidelines	2025	Spain	English	iCCA, pCCA, dCCA and GBC	(*15*)
AFEF guideline	2024	French	English	iCCA, pCCA,	(*16*)
ILTS-ILCA guideline	2024	Europe	English	iCCA, HCC	(*17*)
IHPBA-APHPBA guideline	2024	USA	English	GBC	(*18*)
National guidelines	2024	Pakistan	English	hCCA	(*19*)
Canada guideline	2023	Canada	English	iCCA, pCCA, dCCA and GBC	(*20*)
EASL-ILCA	2023	Europe	English	iCCA	(*21*)
Italian guideline	2023	Italy	English	iCCA, pCCA, dCCA	(*22*)
BSG guideline	2023	UK	English	iCCA, pCCA, dCCA	(*23*)
ESMO guideline	2023	Europe	English	iCCA, pCCA, dCCA and GBC	(*8*)
JSHBPS guideline	2019	Japan	English	iCCA, pCCA, dCCA	(*24*)

cancer syndromes associated with BRCA1 and BRCA2 germline mutations, as well as germline mutations in ATM, CHEK2, and PALB2, and Lynch syndrome linked to mismatch repair deficiency (*32*). Studies have identified germline mutations in 2 to 16% of patients with CCA, including variants in APC, ATM, BAP1, BRCA1, BRCA2, FANCA, PALB2, PMS2, MUTYH, RAD51D, MLH1, and MLH2 (*33-35*). In patients with pCCA/dCCA, germline variants including BRCA1, BRCA2, MLH1, MSH6, MUTYH, ATM, CHEK2, FANCA, and APC have been documented (*34-36*). The BSG guidelines strongly advocate for taking a comprehensive family history to exclude familial cancer syndromes, specifically recommending that patients presenting with an unusual familial pattern of cancer or exceptionally early-onset disease be promptly referred to clinical geneticists (*23*).

3. Screening and diagnosis

3.1. Screening strategies

Due to the lack of universal screening standards, guidelines recommend targeted screening for high-risk populations based on regional risk factors. For PSC patients, the ESMO and EASL-ILCA guidelines recommend annual non-invasive imaging surveillance (ultrasound, MRI/MRCP) combined with CA 19-9 detection (*21,37*). The BSG guidelines support this recommendation, noting that PSC-related CCA may be the first manifestation of previously undiagnosed PSC. The EASL-ILCA guidelines strongly recommend abdominal ultrasound surveillance every 6 months for liver fluke-infected populations. Educational campaigns to prevent liver fluke infection are also advocated for as a primary prevention strategy. For patients with choledochal cysts or hepatolithiasis, guidelines suggest individualized surveillance, but specific protocols lack sufficient evidentiary support (*38*).

3.2. Diagnostic methods

3.2.1 Serological diagnosis

All of the guidelines recognize CA 19-9 as the main serum biomarker for CCA diagnosis and prognosis evaluation, but it is non-specific. CEA is an auxiliary marker, and when combined with CA 19-9 it may improve diagnostic accuracy, but none of the guidelines recommend it as a standalone diagnostic tool (*39*).

As technology has advanced, several novel approaches have been developed. Multiple single-center pilot studies have identified miRNAs and circular RNAs in biological fluids (such as serum, plasma, urine, and bile) with diagnostic and/or prognostic potential for CCA (*9,40*). Levels of miR-21 and miR-122 expression in plasma from iCCA patients were significantly higher than those in controls (*41*). Conversely, levels of miRNA-150 expression in patient serum were markedly lower (*42*).

Analysis of mutations in bile cfDNA aids in differentiating benign from malignant biliary strictures when biliary obstruction is suspected (*43*). Moreover, ctDNA plays a crucial role as a prognostic biomarker and monitoring tool for patients with resected eCCA. Patients with persistently negative ctDNA had significantly longer disease-free survival (*44*). Moreover, ctDNA-based genotyping demonstrated acceptable concordance with tissue genomic profiling, establishing liquid biopsy using ctDNA as a valuable adjunct to the genomic analysis of tissue in BTC (*45*).

Emerging translational evidence also strong corroborates the contention that serum extracellular vesicles contain unique protein biomarkers useful for early, sensitive, and specific diagnosis of PSC, CCA, and HCC (*46*). Serum EVs can be used to predict CCA, diagnose it early, and to predict its prognosis. These biomarkers can be detected through whole serum analysis, which is a form of liquid biopsy using tumor cells (*47*).

3.2.2. Diagnostic imaging

All of the guidelines emphasize a multimodal imaging approach for accurate diagnosis and staging. Abdominal ultrasound (US) is the preferred initial imaging method for CCA diagnosis due to its non-invasiveness and accessibility, and it can identify biliary dilatation, intrahepatic masses, and the site of obstruction (*48*). Contrast-enhanced ultrasound (CEUS) can assist in characterizing indeterminate lesions but is not routinely recommended (*49,50*). The ESMO and BSG guidelines recommend contrast-enhanced multiphase CT as an examination for basic staging, evaluating the extent of the primary tumor, determining vascular and lymph node involvement, and identifying metastases. For pCCA and iCCA, MRI/MRCP is preferred to delineate the biliary tree and vascular anatomy. The clinical utility of 18F-fluorodeoxyglucose positron emission tomography (FDG-PET) remains a point of slight but notable international divergence. The BSG and NCCN guidelines strongly recommend PET-CT for the highly sensitive detection of occult regional nodal involvement and distant metastatic disease to aggressively prevent futile staging laparotomies and non-curative resections. Conversely, the ESMO guidelines caution against its routine baseline use for primary diagnosis and local hilar staging due to an unacceptably poor specificity (often identifying false-positive inflammatory nodes stemming from cholangitis or stent placement), reserving it primarily for resolving ambiguous distant metastases or confirming the suspected recurrence of disease. Common examinations and their indications are shown in Table 2.

Images contain vast amounts of data and quantitative

Table 2. Summary of diagnostic imaging modalities in cholangiocarcinoma per major guidelines

Diagnostic modality	Primary clinical indication in CCA guidelines	Guideline consensus
Abdominal ultrasound	Serves as the initial screening and triage modality for patients with jaundice; enables the identification of severe biliary dilatation and macroscopic abdominal masses.	Universally recognized as the first-line triage tool for preliminary CCA evaluation.
Multiphasic CT	Applied for anatomical staging of primary cholangiocarcinoma, assessment of macroscopic vascular invasion, and detection of distant metastatic lesions.	Established as the standard diagnostic care recommended by ESMO, EASL, BSG, and NCCN guidelines.
MRI / MRCP	Provides high-precision delineation of biliary tract anatomical structures; evaluates hilar tumor resectability in pCCA.	Accepted as the gold standard for local tumor staging of CCA (ESMO, EASL).
FDG-PET / CT	Facilitates the detection of occult regional lymph node metastasis and unidentified distant metastases in CCA patients.	Recommended for selective clinical application (BSG, NCCN); not preferred for routine local tumor staging (ESMO).
ERCP / Cholangioscopy	Enables direct visual evaluation of biliary lesions and targeted pathological tissue sampling for pCCA and dCCA.	The preferred invasive modality for pathological tissue acquisition in CCA diagnosis.

features that are imperceptible to the human eye. Radiomics plays a pivotal role in analyzing these features, which provide information on tumor shape, size, volume, and other characteristics (*51*). Novel imaging techniques such as AI-assisted diagnostic imaging and multimodal image fusion demonstrate promising efficacy in lesion diagnosis, achieving an accuracy rate (ACC) of 94.7% for distinguishing benign from malignant tumors (*52*). CNN-based computer vision represents the most promising approach for diagnosing extrahepatic CCA through image recognition (*53*). Integrating models with MRI images enables differentiation between high-risk and low-risk CCA groups and lymph node metastasis (*54*). Notably, data quality, scale, and instability significantly impact model research. Recognition algorithms require extensive datasets for validation, which are often difficult to obtain. Concurrently, addressing overfitting and enhancing model robustness and reproducibility remain critical challenges (*55*).

3.2.3. Histological diagnosis

Pathological confirmation is the gold standard for CCA diagnosis, with guidelines emphasizing the importance of tissue sampling for both diagnosis and molecular profiling (*7*):

Biopsy methods: For resectable tumors, the ESMO and BSG guidelines caution against percutaneous biopsy to avoid tumor seeding, suggesting that pathological confirmation can be achieved with surgical specimens (*8,23*). For unresectable or metastatic disease, EUS-guided fine needle aspiration/biopsy (FNA/FNB) is preferred for p/dCCA and GBC, while US/CT-guided biopsy is suitable for iCCA. ERCP/PTC-guided biopsy or cholangioscopy-directed biopsy can be used for biliary strictures, but sensitivity is limited, and combining multiple sampling methods may improve yield.

The 5th WHO classification of biliary tract tumors distinguishes two distinct subtypes of iCCA: the large duct type and the small duct type. The small duct type harbors IDH1/2 mutations and FGFR2 fusions, which are treatable with targeted therapies, while the large duct type often presents with KRAS and SMAD4 mutations similar to pCCA and dCCA (*56,57*).

Immunohistochemistry (IHC): The EASL-ILCA and BSG guidelines recommend IHC panels to distinguish CCA subtypes and exclude metastases: iCCA is typically CK7(+), CK19(+), CK20(-); colon metastases are CK7(-), CK20(+), CDX2(+); lung metastases are TTF-1(+); and breast metastases are GATA3(+). Moreover, iCCA is histologically stratified into small duct (SD) and large duct (LD) subtypes, which exhibit distinct anatomical distributions, growth patterns, and immunophenotypes.

SD-iCCA typically manifests as a mass-forming tumor in the peripheral liver and CD56 and N-cadherin are positive. while LD-iCCA typically affects the perihilar region or extrahepatic bile duct and expresses S100p and mucicarmine (*21,23,58,59*).

Molecular profiling: The ESMO, Canadian, and BSG guidelines strongly recommend next-generation sequencing (NGS) for advanced CCA patients eligible for systemic therapy (*8,20,23*). The core gene panel includes IDH1, FGFR2, HER2, BRAF, and NTRK, with RNA sequencing preferred for detecting FGFR2 and NTRK fusions. Liquid biopsies (cell-free DNA) can be used when tissue is insufficient.

4. Staging and classification

The American Joint Committee on Cancer (AJCC)/ Union for International Cancer Control (UICC) TNM staging system represents the most widely adopted staging framework for CCA and is recommended by the majority of clinical guidelines (*60*).

For different CCA subtypes, guidelines emphasize subtype-specific staging criteria and clinical assessment considerations. All major guidelines endorse the 8th edition of the UICC TNM staging system, with the following subtype-specific modifications:

For iCCA: Staging is determined by tumor size, multifocality, vascular invasion, lymph node involvement, and distant metastasis. The ESMO and EASL-ILCA guidelines note that the AJCC/UICC system classifies liver metastases without extrahepatic involvement as early-stage disease. However, the European Network for the Study of Cholangiocarcinoma (ENS-CCA) has proposed a new "M1a stage" for multiple liver lesions, as these patients have a poorer prognosis compared to other early-stage patients. Patients with iCCA and liver metastases (approximately 20% of patients) have a significantly worse prognosis than patients with solitary tumors, regardless of lymph node status (*61*).

For pCCA: In addition to TNM staging, the Bismuth-Corlette classification is widely used to characterize the extent of biliary obstruction, which informs surgical planning and biliary drainage strategies.

Type I: Tumor strictly below the primary biliary confluence.

Type II: Tumor involving the primary confluence without extension into secondary ducts.

Type IIIa/IIIb: Tumor extending into the right (IIIa) or left (IIIb) secondary intrahepatic ducts.

Type IV: Bilateral extension into secondary intrahepatic ducts, or multifocal disease precluding standard resection.

All global guidelines stress that the final determination of resectability must not rely on a single clinician's assessment but must be reached through an expert multidisciplinary team (MDT) including hepatobiliary surgeons, medical oncologists, interventional radiologists, endoscopists, and pathologists.

For dCCA: Staging parallels that for pancreatic head carcinoma, with particular emphasis on assessing pancreatic invasion and lymph node metastasis.

In clinical practice, however, staging classifications often diverge from actual patient circumstances, primarily due to inadequate risk stratification. Several alternative staging systems have been proposed to address these limitations. The KKU staging system has been developed specifically for iCCA staging (*62*), and a modified TNM staging system has been used for the long-term OS stratification of iCCA patients (*63*). Additionally, evidence suggests that when tumors directly invade visceral peritoneal surfaces without involving local extrahepatic structures, survival rates do not differ significantly (*64*). Therefore, further refinement of staging systems requires larger-scale, evidence-based validation studies.

5. Treatment

Therapeutic strategies for CCA are categorized into resectable and unresectable cases. The corresponding treatment algorithm is shown in Figure 1. This review focuses on discussing the concept of translational therapy.

5.1. Treatment of resectable CCA

Surgical resection remains the potentially curative treatment modality for CCA, with achieving an R0

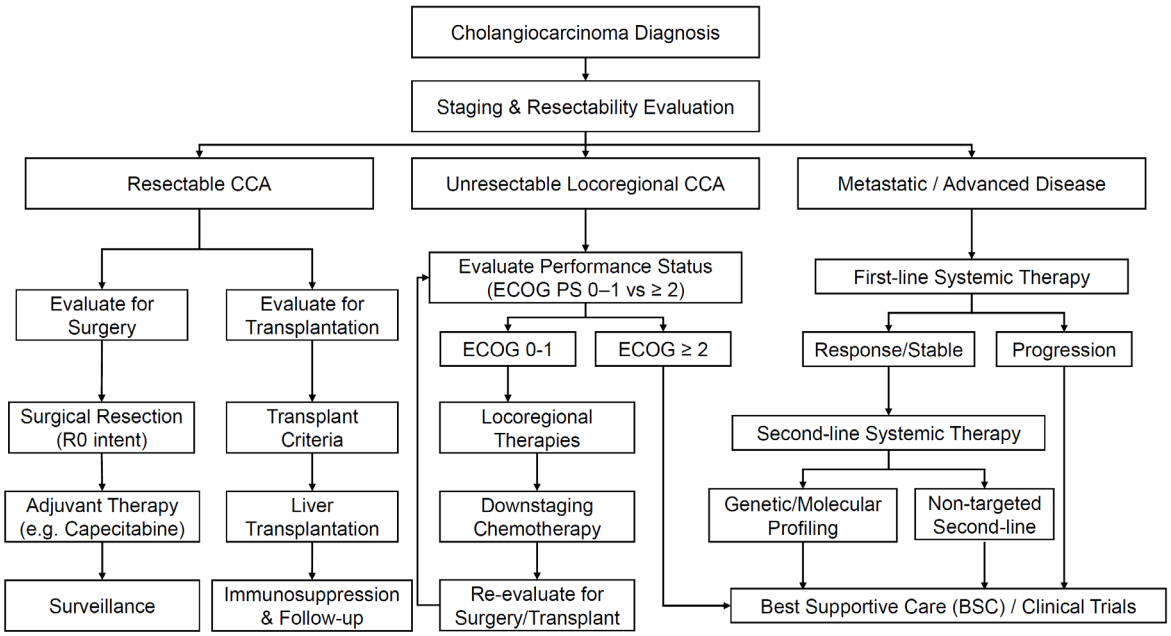


Figure 1. Therapeutic algorithm for cholangiocarcinoma (CCA). This flowchart outlines the corresponding treatment strategies for CCA cases and serves as a visual framework for the subsequent discussion of the concept of therapy in this review.

resection serving as the primary therapeutic objective (*6*). While major clinical guidelines share consistent overarching principles, they differ in certain technical recommendations depending on the CCA subtype.

iCCA: Anatomical hepatectomy—such as hemihepatectomy or segmentectomy—is preferred, accompanied by routine lymphadenectomy with a minimum of six lymph nodes harvested for accurate pathological staging in NCCN. However, large-scale studies at Chinese centers have indicated that while LND is unquestionably critical for accurate N-staging, the procedure itself does not independently improve OS or RFS in patients with clinically node-negative iCCA. Consequently, the primary clinical utility of LND has shifted from a presumed therapeutic clearance to a vital diagnostic tool for risk stratification. The EASL–ILCA guidelines emphasize that anatomical resection is associated with superior survival outcomes compared to non-anatomical resection in patients with stage IB/II iCCA without vascular invasion. Portal vein embolization (PVE) is recommended to augment the future liver remnant (FLR) when the FLR volume is < 25% in patients with normal liver parenchyma or < 40% in those with underlying chronic liver disease (*21*).

For pCCA, extended hepatectomy combined with bile duct resection and caudate lobectomy represents the standard surgical strategy; notably, the BSG guidelines underscore the requirement for preoperative biliary drainage of the FLR, with bilateral drainage indicated in patients presenting with persistent jaundice or cholangitis (*65*). Portal vein or hepatic artery resection and reconstruction may be necessary to achieve R0 margins in advanced Bismuth-Corlette types. In contrast, dCCA is conventionally managed with pancreaticoduodenectomy (Whipple procedure), which routinely includes extended bile duct resection and regional lymphadenectomy.

For GBC, the 2024 IHPBA-APHPBA Delphi Consensus has definitively resolved the long-standing controversy surrounding the surgical management of pT1b GBC, which is defined by tumor invasion of the perimuscular connective tissue without serosal penetration. The optimal extent of hepatic resection for pT1b GBC has frequently been debated in clinical practice. Aggressive surgical strategies have traditionally recommended formal anatomical resection of hepatic segments IVB and V to achieve thorough clearance of deep hepatic parenchymal tissue, whereas alternative approaches have favored a less invasive non-anatomical wedge resection of the gallbladder bed. Notably, the IHPBA-APHPBA Delphi consensus unequivocally recommends margin-negative wedge resection of the gallbladder bed as the sufficient and oncologically radical hepatic procedure for pT1b GBC. In contrast, formal bisegmentectomy of segments IVB/V is strictly reserved for T2 and T3 GBC with confirmed or highly suspected deep hepatic parenchymal invasion (*18*).

Liver transplantation: Liver transplantation is strictly restricted by the ESMO and BSG guidelines to highly selected patients with pCCA arising in the setting of primary sclerosing cholangitis (*8,23*). Eligibility criteria include a tumor size < 3 cm, absence of extrahepatic disease, and completion of neoadjuvant chemoradiotherapy, yielding 5-year survival rates ranging from 55 to 82%. For iCCA, the ILTS-ILCA 2024 and ENS-CCA 2026 guidelines suggest that transplantation be considered only for early-stage tumors (< 3 cm) in patients with underlying cirrhosis (*9,17*). Although current evidence supporting liver transplantation as a therapeutic modality for CCA remains limited by the lack of large-scale, prospective, multicenter studies, it represents an important treatment option for selected patient populations (*66*).

Adjuvant therapy: All of the major clinical guidelines endorse six months of oral capecitabine as standard adjuvant therapy based on the landmark BILCAP trial, which noted a significant OS benefit. The Japanese ASCOT trial further supports the efficacy of S-1 as an alternative adjuvant regimen, particularly in Asian populations. Additionally, the ESMO and BSG guidelines suggest considering adjuvant chemoradiotherapy for R1-resected GBC or p/dCCA, although the supporting evidence remains limited.

Large-scale retrospective evidence further substantiates the role of adjuvant therapy in resectable CCA. In 4,519 patients with CCA who underwent surgical resection, adjuvant therapy was associated with favorable outcomes in low-risk resectable disease, defined as patients with R0 resection margins and negative regional lymph nodes (hazard ratio (HR): 0.86, 95% confidence interval (CI): 0.78–0.95) (*67*). Similarly, for high-risk individuals who underwent surgical resection between 2010 and 2018, the implementation of adjuvant chemotherapy (AC) contributed to improved clinical outcomes (*68*).

5.2. Treatment of unresectable CCA

The stark reality of CCA is that the majority of patients present with locally advanced, unresectable, or metastatic disease. In this setting, management focuses on prolonging survival, maintaining quality of life, and aggressively alleviating symptoms such as biliary obstruction and cancer-related pain.

5.2.1. First-line therapy

As first-line therapy for advanced CCA, gemcitabine plus cisplatin (GemCis) has long been the standard systemic regimen. The phase III TOPAZ-1 trial demonstrated that the addition of durvalumab, a PD-L1 inhibitor, to GemCis significantly improves overall survival, leading the ESMO, Canadian, and BSG guidelines to endorse GemCis combined with durvalumab as the preferred first-line treatment. Similarly, the KEYNOTE-966 trial reported a survival benefit with pembrolizumab plus

GemCis, although this regimen is currently approved only in select regions. In Asian populations, particularly per the CSCO guidelines, the combination of gemcitabine with S-1 is considered non-inferior to GemCis, offering an alternative backbone with a favorable toxicity profile. For patients with a poor performance status (ECOG PS = 2), gemcitabine monotherapy is recommended as a less toxic alternative. In cases of renal impairment, oxaliplatin may be substituted for cisplatin to avoid nephrotoxicity while maintaining therapeutic efficacy (*8,20,23,69*).

5.2.2. Second-line therapy

In the second-line and subsequent treatment of advanced CCA, FOLFOX (5-fluorouracil, leucovorin, and oxaliplatin) is established as the standard regimen based on the ABC-06 trial, which noted that it had a significant overall survival benefit. Liposomal irinotecan combined with 5-FU/leucovorin represents an alternative option, although its efficacy varies between Western and Asian populations (*16*).

For molecularly selected patients, targeted therapies play a critical role: FGFR2 fusions can be treated with FDA- and EMA-approved inhibitors—pemigatinib, infigratinib, and futibatinib—yielding a median PFS of 6.9–9.0 months, and they are recommended by the ESMO and Canadian guidelines after first-line progression (*14*). Ivosidenib, an IDH1 inhibitor, significantly improves PFS in IDH1-mutant BTC and is FDA-approved, though it lacks EMA approval and Canadian reimbursement. For tumors harboring BRAF V600E mutations, combination therapy with dabrafenib and trametinib demonstrates robust activity (objective response rate (ORR): 51%; median OS: 14 months) and is endorsed for eligible patients. NTRK gene fusions, although exceedingly rare (< 0.1% of BTC), are targetable with the tumor-agnostic TRK inhibitors larotrectinib or entrectinib. Similarly, RET inhibitors have also shown efficacy in some patients. In HER2-amplified BTC, dual HER2 blockade with pertuzumab plus trastuzumab or antibody–drug conjugates such as trastuzumab deruxtecan show modest efficacy (ORR: 23–36%) and are generally offered within clinical trials or special access programs. Finally, pembrolizumab is recommended for the subset of patients with high microsatellite instability (MSI-H) or mismatch repair–deficient (dMMR) CCA, based on KEYNOTE-158 data indicating an ORR of 40.9% and a median OS of 24.3 months. (Table 3)

5.2.3. Locoregional therapy

Locoregional treatments (LRT) are critical for palliation, symptom control, and prolonging survival, particularly in liver-predominant unresectable disease or cases presenting with profound obstructive jaundice. Biliary drainage is of the utmost importance so that malignant biliary obstruction is promptly relieved in order to prevent ascending cholangitis, alleviate pruritus, and reverse hyperbilirubinemia, thus enabling the safe administration of systemic chemotherapy. For dCCA, the EASL and BSG guidelines prefer endoscopic biliary drainage (EBD) *via* ERCP over percutaneous transhepatic biliary drainage (PTBD) due to lower risks of hemorrhage and external tube dislocation. Endoscopic drainage is technically arduous in pCCA (Bismuth III/IV). The current EASL and BSG consensus indicates parity between ERCP and PTBD; the choice depends strictly on local MDT expertise and anatomical feasibility.

In addition to biliary drainage, local treatment of the tumor tissue is also imperative. According to the ESMO and EASL–ILCA guidelines, thermal ablation is recommended for patients with unresectable iCCA lesions ≤3 cm, demonstrating a pooled complete ablation rate of 93% and a median OS of 30.2 months. For liver-confined disease, transarterial approaches—including transarterial chemoembolization (TACE), transarterial radioembolization (TARE), and hepatic arterial infusion chemotherapy (HAIC)—represent feasible therapeutic options that may enhance ORRs and facilitate secondary resection, particularly when integrated with systemic therapy. Notably, transarterial therapeutic approaches may demonstrate optimal efficacy in larger lesions (>4 cm) with peripheral enhancement, potentially reflecting increased dependence on arterial blood supply, thereby

Table 3. Actionable molecular targets in cholangiocarcinoma: Prevalence, targeted agents, and corroborating guideline

Molecular target	Prevalence	Targeted agent(s)	Corroborating guideline (NCCN / ESMO)
FGFR2 fusions	10-15% (iCCA)	Pemigatinib, Futibatinib, Erdafitinib	Category 2A / ESCAT I-B
IDH1 mutations	15-20% (iCCA)	Ivosidenib	Category 1 / ESCAT I-A
HER2 amplification	5-15% (GBC, eCCA)	Trastuzumab deruxtecan, Zanidatamab, Trastuzumab + Pertuzumab	Category 2A / ESCAT I-C
BRAF V600E	3-5% (iCCA)	Dabrafenib + Trametinib	Category 2A / ESCAT I-B
MSI-H / dMMR	1-2% (all subtypes)	Pembrolizumab,	Category 2A / ESCAT I-C
		Dostarlimab	Category 2B / ESCAT I-C
NTRK fusions	<1% (all subtypes)	Larotrectinib, Entrectinib, Repotrectinib	Category 2A / ESCAT I-C
RET fusions	<1% (all subtypes)	Pralsetinib	Category 2B / ESCAT I-C
		Selpercatinib	Category 2A / ESCAT I-C
None (wild-type)	~60% (all subtypes)	mFOLFOX or Nal-IRI + 5-FU	Category 1 (FOLFOX)

augmenting treatment effectiveness (*70*).

Stereotactic body radiotherapy (SBRT) provides effective palliative control for locally advanced iCCA, with a reported 1-year local control rate of 83%. However, SBRT is not recommended as a definitive treatment modality outside the context of clinical trials. The optimal management strategy for patients with locally advanced CCA involves a rational combination of multiple locoregional therapeutic approaches, complemented by continually evolving systemic treatment regimens. In the absence of Level 1 evidence to guide clinical decision-making, all patients with CCA should undergo comprehensive evaluation at experienced centers with multidisciplinary expertise (*71*).

5.2.4. Translational therapy

Translational therapy represents a treatment paradigm that integrates systemic and local therapeutic modalities to render initially unresectable advanced carcinoma amenable to curative surgical intervention (*72*). The core mechanism entails combining targeted therapy and immunotherapy with local interventions, including TACE and HAIC. This multimodal approach induces tumor regression, thereby facilitating tumor downstaging.

Multi-agent regimens (*e.g.*, GemCis + immunotherapy) can achieve substantial tumor shrinkage, allowing successful R0 resections in iCCA or pCCA that was previously deemed inoperable. Immunotherapy has emerged as a promising therapeutic strategy across various malignancies in clinical oncology. The fundamental principle of tumor immunotherapy involves modulating the tumor microenvironment (TME) and restoring immune surveillance of tumor cells to achieve antitumor action. Notably, specific patient subpopulations derive substantial benefits from targeted immunotherapeutic interventions, underscoring the increasing importance of precision medicine in identifying eligible candidates for CCA management. Among the classic diagnostic methodologies, including immunohistochemistry (IHC), fluorescence in situ hybridization (FISH), and polymerase chain reaction (PCR)-based assays, the latter demonstrates superior efficiency in detecting single-gene mutations (*73*).

CCA is characterized by a prominent stromal component comprising heterogeneous cell populations, including both innate and adaptive immune cells. Tumor-associated macrophages (TAMs), myeloid-derived suppressor cells (MDSCs), and cancer-associated fibroblasts (CAFs) collectively shape the immune microenvironment of CCA (*74*). Elevated expression of immune checkpoint molecules, including programmed cell death protein 1 (PD-1), its ligand PD-L1, and cytotoxic T-lymphocyte-associated protein 4 (CTLA-4), on tumor-infiltrating immune cells reflects an immunosuppressive milieu (*75*). Consequently, the tumor-infiltrating immune environment (TIME) promotes tumor progression, immune evasion, and chemoresistance, contributing to the limited efficacy of immune checkpoint inhibitor (ICI) therapy observed in clinical trials (*76*).

Current clinical guidelines provide specific recommendations for ICI therapy in CCA. The 2025 NCCN guidelines endorse pembrolizumab, an anti-PD-1 ICI, as monotherapy for unresectable or metastatic CCA exhibiting MSI-H or dMMR. This recommendation is consistent with the 2022 ESMO guidelines for biliary tract cancers (*10,14,77*). Moreover, ESMO recommends NGS for comprehensive molecular profiling in CCA (*78*). Recurrent genomic alterations in advanced CCA include FGFR2 fusions (*79*), ERBB2 (HER2) amplifications (*80*) and mutations (*81*), and BRAF mutations (*82*). Although FGFR inhibitors demonstrate clinical benefit in CCA harboring FGFR2 fusions or rearrangements, therapeutic outcomes remain suboptimal. Their clinical utility is further constrained by dose-dependent toxicities and the inevitable emergence of acquired resistance (*79,83*). Similarly, despite limitations including small cohort sizes and the absence of control groups, mounting evidence suggests that HER2-targeted therapy holds promise for patients with CCA (*84*).

IDH1 mutations represent a rare metabolic enzyme alteration in CCA. While emerging data indicate potential OS benefits, the current understanding of resistance mechanisms remains limited (*85*). Notably, the Japanese guidelines do not currently provide recommendations for patients with genomic alterations in the FGFR or IDH genes (*86*).

In summary, although treatment options beyond standard chemotherapy may be available for patients with CCA, additional prospective data need to be gathered to establish the efficacy of incorporating targeted therapies in various treatment stages or combining them with chemotherapy and other therapeutic modalities (*87*).

6. Discussion

CCA remains a highly aggressive and molecularly heterogeneous malignancy with a persistently poor prognosis. The management of CCA is complex, necessitating a synthesis of the global consensus on stratified care while accounting for significant regional disparities driven by local etiologies and resource availability.

Regional disparities significantly influence the management of CCA, with clinical guidelines tailored to local etiologies and resource availability. In Asia, screening and treatment strategies prioritize liver fluke infection and hepatolithiasis-related CCA, and the oral fluoropyrimidine S-1 is commonly used in both adjuvant and palliative settings. The "Lawa model" program in Thailand, combining anthelmintic treatment, intensive health education, ecosystem monitoring, and community participation, reduced infection rates in cyprinoid fish

(the intermediate host) from 70% to less than 1% (*88,89*). Conversely, Europe and North America focus on PSC-associated CCA, benefiting from broader access to immunotherapies (*e.g.*, durvalumab) and targeted agents such as FGFR inhibitors. In resource-limited regions, cost constraints necessitate reliance on US-based surveillance and gemcitabine-based chemotherapy, while NGS and molecularly targeted therapies remain largely inaccessible. These geographic variations underscore the need for context-specific guideline development and equitable access to advanced therapeutics (*90,91*).

Despite these geographic differences, the core principle of optimizing outcomes relies on stratified management based on resectability status. First, patients with initially resectable CCA undergo upfront curative-intent resection, the only established radical therapy, in 20–30% of newly diagnosed cases. Adjuvant capecitabine for 6 months is universally recommended following R0 resection and is corroborated by evidence from the phase III BILCAP trial (*92*). Second, patients with borderline resectable CCA receive neoadjuvant systemic therapy to facilitate downstaging, followed by resection and adjuvant treatment, in order to improve margin-negative resection rates and reduce recurrence (*9,15*).

Third, patients with initially unresectable CCA responding to treatment receive first-line therapy combining cisplatin, gemcitabine, and anti–PD-1/PD-L1 inhibitors (TOPAZ-1, KEYNOTE-966); eligible patients then undergo salvage resection or liver transplantation, a validated curative approach for selected intrahepatic and perihilar CCA (*93,94*). Fourth, patients with persistently unresectable/metastatic C receive palliative systemic therapy to prolong survival[1]. Second-line FOLFOX is standard for patients without actionable alterations (ABC-06), whereas matched targeted agents are used for IDH1 mutations (ClarIDHy), FGFR2 fusions, BRAF V600E, or HER2 amplification (*95-97*).

Emerging research underscores the importance of molecular subtyping in guiding therapeutic decision-making. According to the EASL-ILCA recommendations, SD-iCCA frequently harbors IDH1/2 mutations and FGFR2 fusions, whereas LD-iCCA and eCCA have abundant KRAS and SMAD4 alterations (*21*). These molecular distinctions may inform subtype-specific treatment strategies and patient stratification. Despite therapeutic advances over the past decade, improvements in survival rates for advanced CCA remain limited. This observation highlights the critical need for identifying specific biomarkers to improve patient prognosis and therapeutic efficacy. Priority must be given to preventive measures, early diagnosis, and the identification of predictive biomarkers to achieve optimal patient stratification (*98,99*).

Drug resistance remains a major challenge in CCA management (*100*). Resistance to FGFR and IDH1 inhibitors arises through secondary gatekeeper mutations or activation of bypass pathways, prompting investigation into irreversible FGFR inhibitors and rational combinations with immunotherapy (*101*). Similarly, the limited efficacy of immune checkpoint inhibitors—attributed to a low tumor mutational burden and an immunosuppressive microenvironment—is being addressed through multimodal approaches, including chemotherapy, anti-VEGF agents, and personalized vaccines. Chemoresistance mechanisms involving DNA repair dysregulation and drug efflux pumps are actively being studied, with PARP inhibitors showing potential in BRCA1/2-mutated subsets. These findings suggest that combination strategies targeting multiple pathways simultaneously may overcome resistance mechanisms more effectively than monotherapy.

For refractory disease, a precision oncology approach is advocated, including repeat molecular profiling *via* tissue re-biopsy or liquid biopsy to uncover acquired actionable alterations (*102,103*), prioritized enrollment in clinical trials evaluating emerging agents (*e.g.*, Claudin 18.2 or MET inhibitors), and integration of locoregional therapies for oligoprogressive disease. Appropriate patient selection, resection with negative surgical margins, and rational administration of systemic chemotherapy remain critical factors for ensuring optimal long-term survival outcomes (*104*).

Critical gaps persist in prevention and early detection (*21*). Prospective data validating the cost-effectiveness of screening high-risk cohorts remain lacking, and novel non-invasive biomarkers, such as circulating tumor DNA and microRNAs, require further validation. Moreover, the long-term impact of public health interventions—particularly educational campaigns in liver fluke-endemic areas—on the incidence of CCA has yet to be quantified. These limitations highlight the need for large-scale, prospective, multicenter studies to establish evidence-based screening protocols.

The integration of spatial transcriptomics with radiomics, encompassing comprehensive analysis of bulk, single-cell, and spatial transcriptomics, holds promise for predicting prognosis and immunotherapeutic benefits, thereby facilitating precision oncology in treatment decision-making for iCCA patients (*105*). This emerging technology may enable more accurate patient stratification and treatment personalization in future clinical practice.

Concurrently, early palliative care involvement is essential to managing complications such as biliary obstruction, pain, and malnutrition, thereby optimizing quality of life, and particularly in patients with a poor performance status for whom best supportive care may be most appropriate. This multidisciplinary approach should be integrated throughout the disease continuum rather than reserved for end-stage disease.

7. Conclusion

Current CCA guidelines share core principles

in epidemiology, diagnosis, and treatment but differ in regional adaptations and resource-based recommendations. The integration of recent key studies has enriched the treatment landscape, with immunotherapy combined with chemotherapy becoming the new first-line standard, and targeted therapies providing personalized options for molecularly defined subgroups. However, several issues remain unaddressed, including drug resistance, lack of universal screening standards, and limited access to advanced therapies in resource-limited regions. Future research should focus on clarifying molecular mechanisms, developing novel biomarkers, optimizing combination therapies, and validating prevention strategies to improve the prognosis for CCA patients.

Acknowledgements

The authors wish to acknowledge the public databases for their contributions to medicine through the vast volumes of data they have shared.

Funding: None.

Conflict of Interest: The authors have no conflicts of interest to disclose.

References

1. Razumilava N, Gores GJ. Cholangiocarcinoma. Lancet. 2014; 383:2168-2179.
2. Cai Y, Cheng N, Ye H, Li F, Song P, Tang W. The current management of cholangiocarcinoma: A comparison of current guidelines. Biosci Trends. 2016; 10:92-102.
3. Cardinale V. Classifications and misclassification in cholangiocarcinoma. Liver Internatl. 2019; 39:260-262.
4. Valle JW, Kelley RK, Nervi B, Oh DY, Zhu AX. Biliary tract cancer. Lancet. 2021; 397:428-444.
5. Nagtegaal ID, Odze RD, Klimstra D, Paradis V, Rugge M, Schirmacher P, Washington KM, Carneiro F, Cree IA. The 2019 WHO classification of tumours of the digestive system. Histopathol. 2020; 76:182-188.
6. Zhang X, Cai Y, Xiong X, Liu A, Zhou R, You Z, Li F, Cheng N. Comparison of current guidelines and consensus on the management of patients with cholangiocarcinoma: 2022 update. Intractable & Rare Diseases Res. 2022; 11:161-172.
7. Colangelo M, Di Martino M, Polidoro MA, Forti L, Tober N, Gennari A, Pagano N, Donadon M. Management of intrahepatic cholangiocarcinoma: A review for clinicians. Gastroenterol Rep (Oxf). 2025; 13:goaf005.
8. Vogel A, Bridgewater J, Edeline J, Kelley RK, Klümpen HJ, Malka D, Primrose JN, Rimassa L, Stenzinger A, Valle JW, Ducreux M. Biliary tract cancer: ESMO Clinical Practice Guideline for diagnosis, treatment and follow-up. Ann Oncol. 2023; 34:127-140.
9. Banales JM, Rodrigues PM, Affò S, *et al*. Cholangiocarcinoma 2026: Status quo, unmet needs and priorities. Nat Rev Gastroenterol Hepatol. 2026; 23:65-96.
10. Benson AB, 3rd, D'Angelica MI, Abrams T, *et al*. Biliary Tract Cancers, Version 2.2025, NCCN Clinical Practice Guidelines In Oncology. J Natl Compr Canc Netw. 2025; 23:403-418.
11. HPBS-CRHA. Guideline for diagnosis and treatment of perihilar cholangiocarcinoma (2025 edition). Chinese J Hepatic Surg (Electronic Ed). 2025; 24:1-20.
12. Liu S, Jiang J, Jian Q, *et al*. Chinese multicenter expert consensus on the diagnosis and treatment of hilar cholangiocarcinoma: 2025 edition. Biosci Trends. 2025; 19:379-403.
13. EASL Clinical Practice Guidelines on the management of extrahepatic cholangiocarcinoma. J Hepatol. 2025; 83:211-238.
14. Vogel A, Ducreux M. ESMO Clinical Practice Guideline interim update on the management of biliary tract cancer. ESMO Open. 2025; 10:104003.
15. Macarulla T, Adeva J, Cano Osuna MT, Ruiz Casado A, Jiménez Gordo AM, Lamarca A, López Muñoz AM, Pazo Cid RA, Saurí T, Gallego Plazas J. SEOM-GEMCAD-TTD clinical guidelines for biliary tract cancer (2025). Clin Transl Oncol. 2025; 27:3293-3306.
16. Neuzillet C, Decraecker M, Larrue H, *et al*. Management of intrahepatic and perihilar cholangiocarcinomas: Guidelines of the French Association for the Study of the Liver (AFEF). Liver Internatl. 2024; 44:2517-2537.
17. Kodali S, Kulik L, D'Allessio A, *et al*. The 2024 ILTS-ILCA consensus recommendations for liver transplantation for HCC and intrahepatic cholangiocarcinoma. Liver Transpl. 2025; 31:815-831.
18. Palepu J, Endo I, Chaudhari VA, *et al*. 'IHPBA-APHPBA clinical practice guidelines': International Delphi consensus recommendations for gallbladder cancer. HPB (Oxford). 2024; 26:1311-1326.
19. Dar FS, Abbas Z, Ahmed I, *et al*. National guidelines for the diagnosis and treatment of hilar cholangiocarcinoma. World J Gastroenterol. 2024; 30:1018-1042.
20. Ramjeesingh R, Chaudhury P, Tam VC, Roberge D, Lim HJ, Knox JJ, Asselah J, Doucette S, Chhiber N, Goodwin R. A practical guide for the systemic treatment of biliary tract cancer in Canada. Curr Oncol. 2023; 30:7132-7150.
21. EASL-ILCA Clinical Practice Guidelines on the management of intrahepatic cholangiocarcinoma. J Hepatol. 2023; 79:181-208.
22. Rimassa L, Brandi G, Niger M, Normanno N, Melisi D. Diagnosis and treatment of cholangiocarcinoma in Italy: A Delphi consensus statement. Crit Rev Oncol Hematol. 2023; 192:104146.
23. Rushbrook SM, Kendall TJ, Zen Y, *et al*. British Society of Gastroenterology guidelines for the diagnosis and management of cholangiocarcinoma. Gut. 2023; 73:16-46.
24. Nagino M, Hirano S, Yoshitomi H, *et al*. Clinical practice guidelines for the management of biliary tract cancers 2019: The 3rd English edition. J Hepatobiliary Pancreat Sci. 2021; 28:26-54.
25. Qurashi M, Vithayathil M, Khan SA. Epidemiology of cholangiocarcinoma. Eur J Surg Oncol. 2025; 51:107064.
26. Florio AA, Ferlay J, Znaor A, Ruggieri D, Alvarez CS, Laversanne M, Bray F, McGlynn KA, Petrick JL. Global trends in intrahepatic and extrahepatic cholangiocarcinoma incidence from 1993 to 2012. Cancer. 2020; 126:2666-2678.
27. Zou Z, Wang X, Huang B, Shi H, Yin K, Fu T, Han Z. Incidence trends and disparities in infection-related malignancies of the liver among US adults, 2000-2019. Gastroenterol Rep (Oxf). 2025; 13:goaf050.
28. Bertuccio P, Malvezzi M, Carioli G, Hashim D,

Boffetta P, El-Serag HB, La Vecchia C, Negri E. Global trends in mortality from intrahepatic and extrahepatic cholangiocarcinoma. J Hepatol. 2019; 71:104-114.
29. Khan SA, Tavolari S, Brandi G. Cholangiocarcinoma: Epidemiology and risk factors. Liver Internatl. 2019; 39 Suppl 1:19-31.
30. Tyson GL, El-Serag HB. Risk factors for cholangiocarcinoma. Hepatol. 2011; 54:173-184.
31. Sripa B, Kaewkes S, Sithithaworn P, Mairiang E, Laha T, Smout M, Pairojkul C, Bhudhisawasdi V, Tesana S, Thinkamrop B, Bethony JM, Loukas A, Brindley PJ. Liver fluke induces cholangiocarcinoma. PLoS Med. 2007; 4:e201.
32. Bonadona V, Bonaïti B, Olschwang S, *et al*. Cancer risks associated with germline mutations in MLH1, MSH2, and MSH6 genes in Lynch syndrome. JAMA. 2011; 305:2304-2310.
33. Okawa Y, Iwasaki Y, Johnson TA, *et al*. Hereditary cancer variants and homologous recombination deficiency in biliary tract cancer. J Hepatol. 2023; 78:333-342.
34. Uson Junior PL, Kunze KL, Golafshar MA, *et al*. Germline cancer susceptibility gene testing in unselected patients with hepatobiliary cancers: A multi-center prospective study. Cancer Prev Res (Phila). 2022; 15:121-128.
35. Yu H, Xu Y, Gao W, Li M, He J, Deng X, Xing W. Comprehensive germline and somatic genomic profiles of Chinese patients with biliary tract cancer. Front Oncol. 2022; 12:930611.
36. Lin J, Shi J, Guo H, *et al*. Alterations in DNA Damage Repair Genes in Primary Liver Cancer. Clin Cancer Res. 2019; 25:4701-4711.
37. Charatcharoenwitthaya P, Enders FB, Halling KC, Lindor KD. Utility of serum tumor markers, imaging, and biliary cytology for detecting cholangiocarcinoma in primary sclerosing cholangitis. Hepatol. 2008; 48:1106-1117.
38. Bergquist A, von Seth E. Epidemiology of cholangiocarcinoma. Best Pract Res Clin Gastroenterol. 2015; 29:221-232.
39. Selvaggi F, Lopetuso LR, Delli Pizzi A, Melchiorre E, Murgiano M, Taraschi AL, Cotellese R, Diana M, Vivarelli M, Mocchegiani F, Catalano T, Aceto GM. Diagnosis of cholangiocarcinoma: The new biological and technological horizons. Diagnostics (Basel, Switzerland). 2025; 15.
40. Han JY, Ahn KS, Kim YH, Kim TS, Baek WK, Suh SI, Kang KJ. Circulating microRNAs as biomarkers in bile-derived exosomes of cholangiocarcinoma. Annals of surgical treatment and research. 2021; 101:140-150.
41. Hu J, Wang YN, Song DJ, Tan JP, Cao Y, Fan J, Wang Z, Zhou J. A high-accuracy model based on plasma miRNAs diagnoses intrahepatic cholangiocarcinoma: A single center with 1001 samples. Diagnostics (Basel, Switzerland). 2021; 11.
42. Salem PES, Ghazala RA, El Gendi AM, Emara DM, Ahmed NM. The association between circulating MicroRNA-150 level and cholangiocarcinoma. J Clin Lab Anal. 2020; 34:e23397.
43. Arechederra M, Rullán M, Amat I, *et al*. Next-generation sequencing of bile cell-free DNA for the early detection of patients with malignant biliary strictures. Gut. 2022; 71:1141-1151.
44. Yoo C, Jeong H, Jeong JH, *et al*. Circulating tumor DNA status and dynamics predict recurrence in patients with resected extrahepatic cholangiocarcinoma. J Hepatol. 2025; 82:861-870.
45. Hwang S, Woo S, Kang B, Kang H, Kim JS, Lee SH, Kwon CI, Kyung DS, Kim HP, Kim G, Kim C, Chon HJ. Concordance of ctDNA and tissue genomic profiling in advanced biliary tract cancer. J Hepatol. 2025; 82:649-657.
46. Arbelaiz A, Azkargorta M, Krawczyk M, *et al*. Serum extracellular vesicles contain protein biomarkers for primary sclerosing cholangitis and cholangiocarcinoma. Hepatology. 2017; 66:1125-1143.
47. Lapitz A, Azkargorta M, Milkiewicz P, *et al*. Liquid biopsy-based protein biomarkers for risk prediction, early diagnosis, and prognostication of cholangiocarcinoma. J Hepatol. 2023; 79:93-108.
48. Cao J, Srinivas-Rao S, Mroueh N, Anand R, Kongboonvijit S, Sertic M, Shenoy-Bhangle AS, Kambadakone A. Cholangiocarcinoma imaging: From diagnosis to response assessment. Abdominal radiology (New York). 2024; 49:1699-1715.
49. Guo HL, Zheng X, Cheng MQ, Zeng D, Huang H, Xie XY, Lu MD, Kuang M, Wang W, Xian MF, Chen LD. Contrast-enhanced ultrasound for differentiation between poorly differentiated hepatocellular carcinoma and intrahepatic cholangiocarcinoma. J Ultrasound Med. 2022; 41:1213-1225.
50. Zhu MR, Zhao CK, Sun YK, Li XL, Yin HH, Lu D, Ye X, Hu XY, Wang X, Xia HS, Han H, Zhou BY, Xu HX, Wang LF. Subtype prediction of intrahepatic cholangiocarcinoma using dynamic contrast-enhanced ultrasound. Insights into imaging. 2024; 15:119.
51. Zerunian M, Polidori T, Palmeri F, Nardacci S, Del Gaudio A, Masci B, Tremamunno G, Polici M, De Santis D, Pucciarelli F, Laghi A, Caruso D. Artificial intelligence and radiomics in cholangiocarcinoma: A comprehensive review. Diagnostics (Basel, Switzerland). 2025; 15.
52. Wei Y, Yang M, Zhang M, *et al*. Focal liver lesion diagnosis with deep learning and multistage CT imaging. Nature communications. 2024; 15:7040.
53. Njei B, Kanmounye US, Seto N, McCarty TR, Mohan BP, Fozo L, Navaneethan U. Artificial intelligence in medical imaging for cholangiocarcinoma diagnosis: A systematic review with scientometric analysis. J Gastroenterol Hepatol. 2023; 38:874-882.
54. Haghbin H, Aziz M. Artificial intelligence and cholangiocarcinoma: Updates and prospects. World J Clin Oncol. 2022; 13:125-134.
55. Granata V, Fusco R, De Muzio F, *et al*. Risk assessment and cholangiocarcinoma: Diagnostic management and artificial intelligence. Biology. 2023; 12.
56. Akita M, Fujikura K, Ajiki T, Fukumoto T, Otani K, Azuma T, Itoh T, Ku Y, Zen Y. Dichotomy in intrahepatic cholangiocarcinomas based on histologic similarities to hilar cholangiocarcinomas. Mod Pathol. 2017; 30:986-997.
57. Hayashi A, Misumi K, Shibahara J, Arita J, Sakamoto Y, Hasegawa K, Kokudo N, Fukayama M. Distinct Clinicopathologic and genetic features of 2 histologic subtypes of intrahepatic cholangiocarcinoma. Am J Surg Pathol. 2016; 40:1021-1030.
58. Beyersdorf J, Zhang ML. Extrahepatic cholangiocarcinoma: Current concepts in histopathology, immunohistochemistry, and molecular diagnostics. Semin Diagn Pathol. 2025; 42:150949.
59. De Santis A, Zhu L, Tao J, Reißfelder C, Schölch S. Molecular subtypes of intrahepatic cholangiocarcinoma.

Trends Mol Med. 2025; 31:755-769.
60. Chun YS, Pawlik TM, Vauthey JN. 8th Edition of the AJCC Cancer Staging Manual: Pancreas and Hepatobiliary Cancers. Ann Surg Oncol. 2018; 25:845-847.
61. Lamarca A, Santos-Laso A, Utpatel K, *et al*. Liver metastases of intrahepatic cholangiocarcinoma: Implications for an updated staging system. Hepatology. 2021; 73:2311-2325.
62. Sa-Ngiamwibool P, Aphivatanasiri C, Sangkhamanon S, *et al*. Modification of the AJCC/UICC 8th edition staging system for intrahepatic cholangiocarcinoma: Proposal for an alternative staging system from cholangiocarcinoma-prevalent Northeast Thailand. HPB (Oxford). 2022; 24:1944-1956.
63. Zhang XF, Xue F, He J, *et al*. Proposed modification of the eighth edition of the AJCC staging system for intrahepatic cholangiocarcinoma. HPB (Oxford). 2021; 23:1456-1466.
64. Wu RY, Yang ZM, Feng J, Zhang L, Zhang G. Evaluation and recommendation of the 8th edition of American Joint Committee on Cancer (AJCC) staging system for intrahepatic cholangiocarcinoma (ICC) in 820 patients from the Surveillance, Epidemiology, and End Results (SEER) database. J Gastrointest Surg. 2021; 25:145-154.
65. Wiggers JK, Groot Koerkamp B, Cieslak KP, Doussot A, van Klaveren D, Allen PJ, Besselink MG, Busch OR, D'Angelica MI, DeMatteo RP, Gouma DJ, Kingham TP, van Gulik TM, Jarnagin WR. Postoperative mortality after liver resection for perihilar cholangiocarcinoma: Development of a risk score and importance of biliary drainage of the future liver remnant. J Am Coll Surg. 2016; 223:321-331.e321.
66. Anteby R, Vierra BM, Shah SA. Liver transplant for intrahepatic cholangiocarcinoma: Current evidence and clinical practice recommendations. J Gastrointest Surg. 2025; 29:102211.
67. Munir MM, Ruff SM, Endo Y, Lima HA, Alaimo L, Moazzam Z, Shaikh C, Pawlik TM. Does adjuvant therapy benefit low-risk resectable cholangiocarcinoma? An evaluation of the NCCN Guidelines. J Gastrointest Surg. 2023; 27:511-520.
68. Rhodin KE, Liu A, Bartholomew A, *et al*. Trends in receipt of adjuvant chemotherapy and its impact on survival in resected biliary tract cancers. Ann Surg Oncol. 2023; 30:4813-4821.
69. Xu R, Zhou J, Yang J, Yu Y, Wang H, Zhang Z, Yang J, Zhang G, Liao R. First-line systemic therapy and sequencing options in advanced biliary tract cancer: A systematic review and network meta-analysis. Biosci Trends. 2025; 18:555-562.
70. Mosconi C, Solaini L, Vara G, Brandi N, Cappelli A, Modestino F, Cucchetti A, Golfieri R. Transarterial chemoembolization and radioembolization for unresectable intrahepatic cholangiocarcinoma-A systemic review and meta-analysis. Cardiovasc Intervent Radiol. 2021; 44:728-738.
71. Blair AB, Alobuia WM, Palta M, Raman SS, Levine MH, Benson AB, 3rd, D'Angelica MI, Cloyd JM. Locoregional treatment options for locally advanced intrahepatic cholangiocarcinoma. J Natl Compr Canc Netw. 2025; 23.
72. Zhang W, Zhou H, Wang Y, Zhang Z, Cao G, Song T, Zhang T, Li Q. Systemic treatment of advanced or recurrent biliary tract cancer. Biosci Trends. 2020; 14:328-341.
73. Zhang D, Dorman K, Westphalen CB, Haas M, Ormanns S, Neumann J, Seidensticker M, Ricke J, De Toni EN, Klauschen F, Algül H, Reisländer T, Boeck S, Heinemann V. Unresectable biliary tract cancer: Current and future systemic therapy. Eur J Cancer. 2024; 203:114046.
74. Ilyas SI, Affo S, Goyal L, Lamarca A, Sapisochin G, Yang JD, Gores GJ. Cholangiocarcinoma - Novel biological insights and therapeutic strategies. Nat Rev Clin Oncol. 2023; 20:470-486.
75. Loeuillard E, Yang J, Buckarma E, Wang J, Liu Y, Conboy C, Pavelko KD, Li Y, O'Brien D, Wang C, Graham RP, Smoot RL, Dong H, Ilyas S. Targeting tumor-associated macrophages and granulocytic myeloid-derived suppressor cells augments PD-1 blockade in cholangiocarcinoma. J Clin Invest. 2020; 130:5380-5396.
76. Fabris L, Sato K, Alpini G, Strazzabosco M. The tumor microenvironment in cholangiocarcinoma progression. Hepatology. 2021; 73 Suppl 1:75-85.
77. Liu J, Shu J. Immunotherapy and targeted therapy for cholangiocarcinoma: Artificial intelligence research in imaging. Crit Rev Oncol Hematol. 2024; 194:104235.
78. Mosele MF, Westphalen CB, Stenzinger A, *et al*. Recommendations for the use of next-generation sequencing (NGS) for patients with advanced cancer in 2024: A report from the ESMO Precision Medicine Working Group. Ann Oncol. 2024; 35:588-606.
79. Goyal L, Meric-Bernstam F, Hollebecque A, *et al*. Futibatinib for FGFR2-rearranged intrahepatic cholangiocarcinoma. N Engl J Med. 2023; 388:228-239.
80. Harding JJ, Fan J, Oh DY, *et al*. Zanidatamab for HER2-amplified, unresectable, locally advanced or metastatic biliary tract cancer (HERIZON-BTC-01): A multicentre, single-arm, phase 2b study. Lancet Oncol. 2023; 24:772-782.
81. Harding JJ, Piha-Paul SA, Shah RH, *et al*. Antitumour activity of neratinib in patients with HER2-mutant advanced biliary tract cancers. Nature Communications. 2023; 14:630.
82. Subbiah V, Kreitman RJ, Wainberg ZA, *et al*. Dabrafenib plus trametinib in BRAFV600E-mutated rare cancers: The phase 2 ROAR trial. Nat Med. 2023; 29:1103-1112.
83. Javle M, Roychowdhury S, Kelley RK, *et al*. Infigratinib (BGJ398) in previously treated patients with advanced or metastatic cholangiocarcinoma with FGFR2 fusions or rearrangements: Mature results from a multicentre, open-label, single-arm, phase 2 study. Lancet Gastroenterol Hepatol. 2021; 6:803-815.
84. Ten Haaft BH, Pedregal M, Prato J, Klümpen HJ, Moreno V, Lamarca A. Revolutionizing anti-HER2 therapies for extrahepatic cholangiocarcinoma and gallbladder cancer: Current advancements and future perspectives. Eur J Cancer. 2024; 199:113564.
85. Ellis H, Braconi C, Valle JW, Bardeesy N. Cholangiocarcinoma targeted therapies: Mechanisms of action and resistance. Am J Pathol. 2025; 195:437-452.
86. Buettner S, Groot Koerkamp B. The Japanese Clinical Practice Guidelines for intrahepatic cholangiocarcinoma: A comparison with Western guidelines. Hepatobiliary surgery and nutrition. 2023; 12:244-247.
87. Wheless M, Agarwal R, Goff L, Lockney N, Padmanabhan C, Heumann T. Current standards, multidisciplinary approaches, and future directions in the management of extrahepatic cholangiocarcinoma. Curr Treat Options Oncol. 2024; 25:127-160.
88. Songserm N, Namwong W, Woradet S, Sripa B, Ali A. Public health interventions for preventing re-infection of

Opisthorchis viverrini: Application of the self-efficacy theory and group process in high-prevalent areas of Thailand. Trop Med Int Health. 2021; 26:962-972.
89. Laithavewat L, Grundy-Warr C, Khuntikeo N, Andrews RH, Petney TN, Yongvanit P, Banchonhattakit P, Sithithaworn P. Analysis of a school-based health education model to prevent opisthorchiasis and cholangiocarcinoma in primary school children in northeast Thailand. Global Health Promotion. 2020; 27:15-23.
90. Ouyang G, Liu Q, Wu Y, Liu Z, Lu W, Li S, Pan G, Chen X. The global, regional, and national burden of gallbladder and biliary tract cancer and its attributable risk factors in 195 countries and territories, 1990 to 2017: A systematic analysis for the Global Burden of Disease Study 2017. Cancer. 2021; 127:2238-2250.
91. Chen S, Han K, Song Y, Liu S, Li X, Wang S, Li H, Li R, Wang J, He Y, Liu M. Current status, trends, and predictions in the burden of gallbladder and biliary tract cancer in China from 1990 to 2019. Chin Med J (Engl). 2022; 135:1697-1706.
92. Bridgewater J, Fletcher P, Palmer DH, *et al*. Long-term outcomes and exploratory analyses of the randomized phase III BILCAP study. J Clin Oncol. 2022; 40:2048-2057.
93. Oh DY, He AR, Bouattour M, *et al*. Durvalumab or placebo plus gemcitabine and cisplatin in participants with advanced biliary tract cancer (TOPAZ-1): Updated overall survival from a randomised phase 3 study. Lancet Gastroenterol Hepatol. 2024; 9:694-704.
94. Kelley RK, Ueno M, Yoo C, *et al*. Pembrolizumab in combination with gemcitabine and cisplatin compared with gemcitabine and cisplatin alone for patients with advanced biliary tract cancer (KEYNOTE-966): A randomised, double-blind, placebo-controlled, phase 3 trial. Lancet. 2023; 401:1853-1865.
95. Lamarca A, Palmer DH, Wasan HS, *et al*. Second-line FOLFOX chemotherapy versus active symptom control for advanced biliary tract cancer (ABC-06): A phase 3, open-label, randomised, controlled trial. Lancet Oncol. 2021; 22:690-701.
96. Zhu AX, Macarulla T, Javle MM, *et al*. Final overall survival efficacy results of ivosidenib for patients with advanced cholangiocarcinoma with IDH1 Mutation: The phase 3 randomized clinical ClarIDHy trial. JAMA oncology. 2021; 7:1669-1677.
97. Subbiah V, Lassen U, Élez E, *et al*. Dabrafenib plus trametinib in patients with BRAF(V600E)-mutated biliary tract cancer (ROAR): A phase 2, open-label, single-arm, multicentre basket trial. Lancet Oncol. 2020; 21:1234-1243.
98. Li Z, Aliseda D, Jones O, Rajendran L, Magyar C, Grant R, O'Kane GM, Saborowski A, Sapisochin G, Vogel A. Recent advances in systemic therapy for advanced biliary tract cancer: A systematic review and meta-analysis using reconstructed RCT survival data. JHEP reports : innovation in hepatology. 2025; 7:101290.
99. Vedeld HM, Grimsrud MM, Andresen K, *et al*. Early and accurate detection of cholangiocarcinoma in patients with primary sclerosing cholangitis by methylation markers in bile. Hepatology. 2022; 75:59-73.
100. Cleary JM, Raghavan S, Wu Q, *et al*. FGFR2 extracellular domain in-frame deletions are therapeutically targetable genomic alterations that function as oncogenic drivers in cholangiocarcinoma. Cancer Discov. 2021; 11:2488-2505.
101. Meric-Bernstam F, Bahleda R, Hierro C, Sanson M, Bridgewater J, Arkenau HT, Tran B, Kelley RK, Park JO, Javle M, He Y, Benhadji KA, Goyal L. Futibatinib, an irreversible FGFR1-4 inhibitor, in patients with advanced solid tumors harboring FGF/FGFR aberrations: A phase I dose-expansion study. Cancer Discov. 2022; 12:402-415.
102. Verdaguer H, Saurí T, Acosta DA, *et al*. ESMO scale for clinical actionability of molecular targets driving targeted treatment in patients with cholangiocarcinoma. Clin Cancer Res. 2022; 28:1662-1671.
103. Bekaii-Saab TS, Bridgewater J, Normanno N. Practical considerations in screening for genetic alterations in cholangiocarcinoma. Ann Oncol. 2021; 32:1111-1126.
104. Ruff SM, Cloyd JM, Pawlik TM. Annals of Surgical Oncology Practice Guidelines Series: Management of primary liver and biliary tract cancers. Ann Surg Oncol. 2023; 30:7935-7949.
105. Ji GW, Xu ZG, Liu SC, Cao SY, Jiao CY, Lu M, Zhang B, Yang Y, Xu Q, Wu XF, Wang K, Xia YX, Li XC, Wang XH. Radiogenomics of intrahepatic cholangiocarcinoma predicts immunochemotherapy response and identifies therapeutic target. Clinical Molec Hepatol. 2025; 31:935-959.

Received April 23, 2026; Revised July 12, 2026; Accepted July 24, 2026.

[§]These authors contributed equally to this work.
**Address correspondence to:*
Nansheng Cheng, Department of Bile Duct Surgery, West China Hospital, Sichuan University, Chengdu 610041, Sichuan, China.
E-mail: nanshengcheng@yeah.net

Released online in J-STAGE as advance publication July 31, 2026.

Review

DOI: 10.5582/bst.2026.01219

Management of dynamic therapeutic opportunity in hepatocellular carcinoma: Preserving liver function and enabling treatment transitions

Jiwei Huang[1,§], Mingheng Liao[1,§], Wei Tang[2,3,*]

[1] Division of Liver Surgery, Department of Surgery and Laboratory of Liver Surgery, West China Hospital, Sichuan University, Chengdu, China;
[2] National Center for Global Health and Medicine, Japan Institute for Health Security, Tokyo, Japan;
[3] Hepato-Biliary-Pancreatic Surgery Division, Department of Surgery, Graduate School of Medicine, University of Tokyo, Tokyo, Japan.

SUMMARY: Hepatocellular carcinoma (HCC) is governed by malignant progression and deterioration of the organ in which the cancer arises. Modern management has therefore outgrown static stage-to-treatment allocation. We define dynamic therapeutic opportunity as the time-varying set of clinically credible treatment options available to an individual patient, determined by hepatic reserve, oncological tractability, physiological reserve, prior therapeutic exposure, patient goals, and real-world deliverability. This framework does not replace validated staging systems or liver-function scores; it asks how each intervention changes the circumstances under which the next decision will be made. Evidence for curative-intent conversion remains dominated by selected cohorts, although the interim results of the randomized TALENTop trial provide the first prospective comparative signal supporting resection in a narrowly defined post-induction population. We review liver-sparing surgery, locoregional-systemic integration, conversion therapy, and modifiers such as frailty and metabolic dysfunction-associated steatotic liver disease. We then propose a trial architecture that complements tumor endpoints with hepatic decompensation, sustained ALBI deterioration, subsequent-treatment access, curative-intent transition, functional independence, and patient-reported outcomes. Modern HCC management should evaluate not only whether an intervention controls the present tumor but also whether it preserves, expands, or eliminates the patient's future set of clinically meaningful treatment options.

Keywords: treatment sequencing, transarterial chemoembolization, conversion therapy, frailty, ALBI grade, clinical trial endpoints

1. Introduction: HCC is not just a cancer

Hepatocellular carcinoma is the predominant form of primary liver cancer and remains a major cause of cancer death worldwide. Its management is unlike that of most solid tumors because prognosis reflects both tumor biology and the trajectory of chronic liver disease. A patient may die from cancer progression, portal-hypertensive complications, hepatic decompensation, treatment-related liver injury, or an interaction among these processes. Contemporary guidelines consequently integrate tumor burden, liver function, performance status, and patient preference rather than relying on anatomical stage alone (*1-4*).

This dual-risk structure creates a paradox. An intervention can suppress tumor growth and extend life, and yet it can also reduce hepatic or physiological reserve enough to make the next effective treatment unsafe. Conversely, a treatment that produces only modest radiological shrinkage may be valuable if it controls disease while preserving the circumstances required for later systemic therapy, ablation, radiotherapy, resection, or transplantation. The clinically relevant unit is therefore not the isolated treatment episode but the evolving treatment pathway.

We use the term "dynamic therapeutic opportunity" to describe the patient's time-varying set of clinically credible systemic, locoregional, and curative-intent options. "Reserve" is retained for internal capacities such as hepatic and physiological reserve; opportunity also depends on prior exposure, access, timing, and preference, and is therefore a state and set of options, not a score.

This Review develops that concept through a structured narrative review. PubMed/MEDLINE and key guideline, trial-registry and society sources were searched for English-language reports published from January 1, 2000 to August 13, 2026, with an emphasis on guidelines, randomized phase 3 trials, prospective

studies, large international cohorts, meta-analyses and concept-defining papers. Historical surgical reports published before 2000 were included when essential. This is not a systematic review and no claim of exhaustive evidence capture is made.

2. The Makuuchi legacy: Balancing curability and hepatic safety

A modern account should not portray historical HCC care as simply tumor-centered. The Makuuchi school established a different question: how much of the liver could safely be removed while retaining the possibility of a cure? Decision algorithms based on ascites, serum bilirubin, and indocyanine green retention at 15 minutes linked the extent of resection to functional reserve rather than tumor anatomy alone (*5,6*). Anatomical resection, portal vein embolization, future-liver-remnant assessment, and meticulous parenchymal preservation operationalized the principle that oncological ambition must be bounded by hepatic safety (*7,8*). A Japanese nationwide analysis of 15,597 resections later found lower operative mortality among patients who met Makuuchi's criteria than among those who exceeded them (*9*).

The framework was primarily optimized around the safety and oncological adequacy of an index intervention, although recurrence surveillance, repeat resection, and local treatment were integral to Japanese practice. What was not yet available was the present diversity of effective systemic and multimodal transitions capable of reopening local or surgical options. The contemporary extension is therefore not from episodic to longitudinal care, but from an established longitudinal surgical tradition to a much larger and more frequently changing treatment space.

This historical continuity matters. Dynamic opportunity management extends, rather than repudiates, liver-sparing surgery. The same logic that once constrained the volume of resection now needs to govern the intensity and repetition of TACE, the timing of systemic therapy, the management of portal hypertension, the prevention of sarcopenia, and the selection of conversion procedures (Figure 1).

3. Why static treatment allocation is no longer sufficient

Staging systems remain indispensable for prognosis, communication, and evidence-based recommendations. The 2026 BCLC update goes beyond stage allocation by formalising multidisciplinary deliberation, patient vulnerability, biological, psychosocial and contextual factors, and the CUSE framework for complexity, uncertainty, subjectivity, and emotion (*10*). EASL 2025, ESMO 2025, AASLD, the Japanese Society of Hepatology 2025, and the Chinese 2026 guidelines likewise require integration of tumor burden, liver function, comorbidity, local expertise, and patient context (*1-4,11,12*). Dynamic therapeutic opportunity is complementary rather than competitive: BCLC 2026 structures decisions under complexity, whereas the current framework focuses on the longitudinal state and set of options left by each intervention and on how that state should be measured in trials.

Static allocation is especially fragile in BCLC-B disease. Patients grouped together for having "intermediate stage" disease may have a solitary large tumor, multifocal disease within one vascular territory, diffuse bilobar disease, variable portal hypertension, and very different ALBI grades. The same label can therefore encompass patients suitable for selective embolization, systemic therapy, radiation, resection at expert centers, or a planned combination strategy. A one-time label cannot capture how

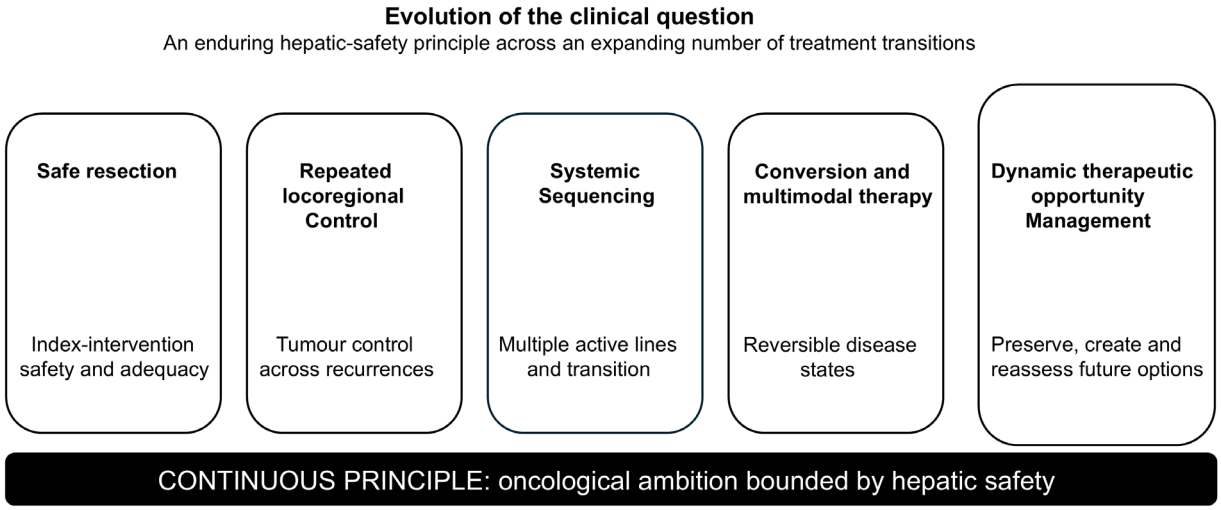


Figure 1. Evolution of the clinical question in HCC management. The Makuuchi-era principle of balancing oncological ambition with hepatic safety is not replaced; it remains a continuous thread as the decision horizon expands and the number of possible treatment transitions grows.

the disease state changes after the first intervention.

Dynamic management requires prospective transition rules. Before treatment begins, the team should specify when reassessment will occur, what constitutes adequate benefit, what degree of deterioration in liver function is unacceptable, when a switch or combination will be considered, and what findings will trigger re-review for curative-intent therapy. Without such rules, repeated treatment can become inertia disguised as continuity.

The practical implication is not continuous restaging for its own sake. Reassessment should be linked to a decision that can still be changed. For systemic treatment, early imaging may identify rapid progression, but biochemical toxicity, portal-hypertensive events, and functional decline may require action before radiological progression. For TACE, the relevant checkpoint may be after the first technically adequate treatment, when residual viable burden and the hepatic functional cost can be assessed together. For a patient approaching a local or surgical window, review may need to occur before maximal radiological response because waiting can consume liver function, allow resistant clones to emerge, or eliminate an operable interval. A dynamic model therefore replaces reactive rescue with planned decision windows.

4. Therapeutic opportunity as a dynamic clinical state

Dynamic therapeutic opportunity is the clinically credible set of options at a particular time. Four domains help identify what currently limits that set; none is sufficient alone.

Hepatic reserve includes synthetic function, portal-hypertensive status, prior decompensation, renal vulnerability, biliary injury, future liver remnant, and the liver's tolerance of embolization, radiation, surgery, and systemic therapy. Child–Pugh class remains clinically familiar but includes subjective components and coarse categories. The ALBI model, derived from albumin and bilirubin, provides an objective continuous measure and distinguishes among prognoses even within Child–Pugh A disease (*13*). Modified ALBI subdivisions improve granularity, but neither ALBI nor Child–Pugh captures portal hypertension, prior decompensation, or procedure-specific functional risk. Dynamic change is generally more informative than a baseline label alone.

Oncological tractability describes whether the cancer remains amenable to meaningful control. It includes burden, distribution, vascular invasion, extrahepatic spread, growth kinetics, AFP or PIVKA-II dynamics, response depth and durability, and the possibility of local clearance. Circulating tumor DNA (ctDNA) kinetics, Wnt/β-catenin activation, tumor mutational burden, microsatellite instability, and features of the immune microenvironment may eventually refine this domain. At present, however, these are investigational in HCC: Wnt/β-catenin-associated immune exclusion is biologically compelling but not uniformly predictive, and neither ctDNA nor molecular profiling should be used as a routine gatekeeper for immunotherapy or conversion outside the context of a validated assay or clinical study (*14-16*). Tractability is not synonymous with radiological response: stable disease with favorable biology may create a local-treatment window, whereas rapid regrowth after an impressive early response may signal limited surgical benefit.

Physiological reserve includes performance status, frailty, muscle quantity and function, nutrition, cognition, cardiopulmonary reserve, renal function, and comorbidity. ECOG performance status is useful but insufficient. Meta-analyses suggest that sarcopenia is common in HCC and is associated with worse survival across surgical, locoregional, and systemic therapies (*17,18*). Age alone should not determine treatment intensity; the relevant issue is resilience and recovery capacity.

Therapeutic optionality is the remaining space for treatment: the availability of active systemic therapy lines, the feasibility of embolization, ablation, or radiation, transplant or resection candidacy, cumulative toxicity, bleeding and vascular risk, organ function, previous drug exposure, and regional access. Patient goals, financial constraints, travel burden, and institutional expertise can narrow this space even when a treatment is technically available.

The framework is deliberately multidirectional. Tumor response can increase opportunity by reducing burden or vascular invasion. The same intervention can eliminate opportunity through decompensation, immune toxicity, vascular complications, or functional decline. Conversely, antiviral treatment, portal-hypertension management, nutrition, and rehabilitation may expand opportunity without directly shrinking the tumor.

Measurement should be parsimonious enough for routine care. At a minimum, each major reassessment should record tumor distribution and response, albumin, bilirubin, platelet count, renal function, portal-hypertensive events, ECOG performance status, weight or muscle trajectory, treatment toxicity, locally available next options, and patient priorities. Baseline values alone are insufficient: a change from ALBI grade 1 to 2a, a new episode of ascites, or a decline in walking capacity can be more decision-relevant than a stable categorical stage. The purpose is not to create a large checklist but to reveal which domain is becoming rate-limiting. Interventions can then be directed toward that domain—for example, selective rather than lobar embolization, treatment of portal hypertension, dose adaptation, prehabilitation, or an early switch to a non-overlapping mechanism (Figure 2 and Table 1).

5. Evidence reshaping treatment boundaries

5.1 Advanced HCC: Multiple effective first-line strategies

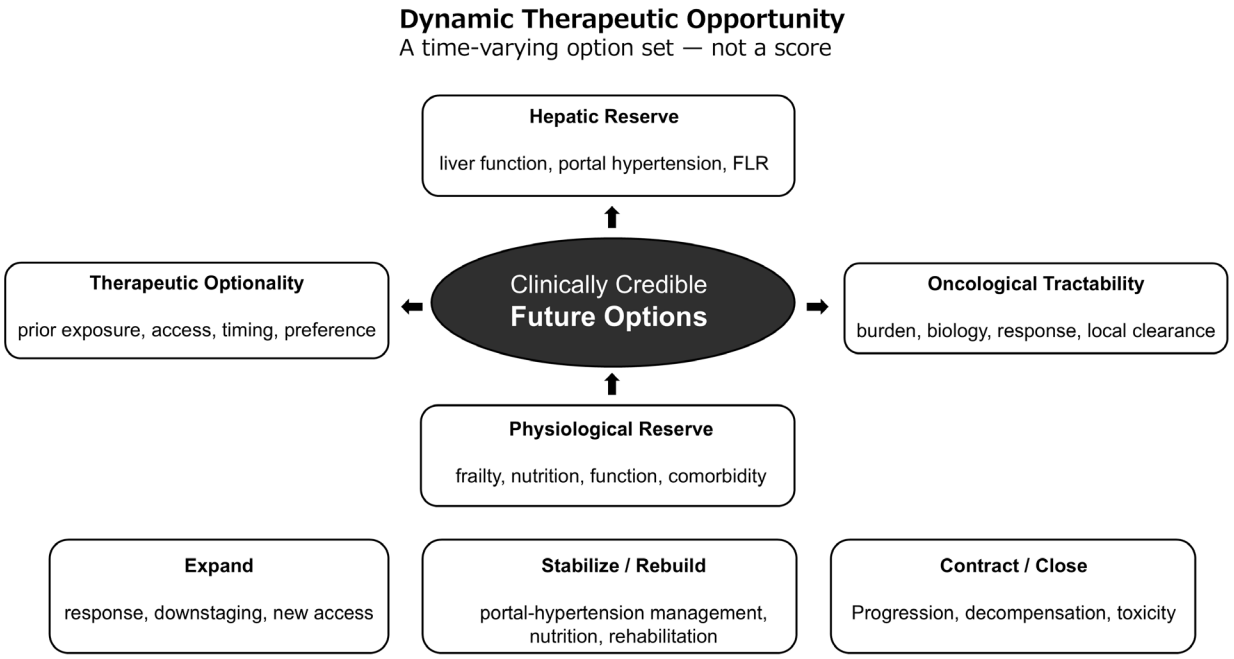


Figure 2. Dynamic therapeutic opportunity as a time-varying set of options. Any domain may become rate-limiting. Tumor response or new access can expand options; progression, decompensation, and toxicity can contract them; supportive care can stabilize or reopen them. The diagram is conceptual and does not imply a numerical score. FLR, future liver remnant.

Table 1. From conventional efficacy endpoints to longitudinal opportunity endpoints

Endpoint	Primary construct	Strength	Limitation for HCC opportunity management	Recommended role
ORR / DoR	Tumor shrinkage / durability	Early antitumor signal; relevant to conversion	Response does not establish resectability, organ preservation or net benefit	Retain; link to predefined MDT reassessment
PFS / RFS	Time to progression or recurrence	Efficient comparison of disease control	Sensitive to assessment rules; may not predict OS or future eligibility	Retain; report with liver and subsequent-treatment data
OS	Time to death	Patient-important and regulatory standard	Affected by competing liver events, cross-over, and later therapy	Primary long-term outcome
ALBI deterioration	Dynamic liver-function change	Objective and repeatable	Does not capture portal hypertension or clinical decompensation alone	Core longitudinal measure with sustained-change definition
Hepatic decompensation	Ascites, bleeding, encephalopathy, jaundice	Directly clinically meaningful	Definitions and competing-risk methods remain inconsistent	Prospectively adjudicated opportunity endpoint
Subsequent-treatment access	Receipt of later systemic/ local therapy	Measures pathway preservation	Confounded by access, preference, and practice variation	Report reasons for receipt and non-receipt
Curative-intent conversion	Transition to resection, ablation or transplant pathway	Captures state change	Selection bias; definitions vary; not synonymous with ORR	Predefine criteria and central MDT review
PROs / functional independence	Patient experience and resilience	Captures benefit beyond imaging	Instrument choice and missing data	Co-primary supportive outcome in longitudinal trials

The first-line systemic landscape has shifted from one dominant multikinase inhibitor to several mechanistically diverse combinations. IMbrave150, HIMALAYA, CARES-310 and CheckMate 9DW each established survival benefit over sorafenib or an investigator-choice TKI in their trial populations (*19-24*). The early crossing of the CheckMate 9DW survival curves may reflect delayed immune benefit together with early progression and treatment-related risk; the relative contribution of these mechanisms cannot be established from the curves alone. This uncertainty makes baseline hepatic and physiological vulnerability clinically relevant before dual-checkpoint blockade.

These trials do not create one universally best regimen. Therapy that includes bevacizumab requires careful assessment and management of bleeding risk and portal hypertension. Dual-checkpoint blockade avoids continuous anti-VEGF exposure but carries a distinct risk of severe immune-mediated toxicity. TKIs remain relevant when immunotherapy is contraindicated, for later-line therapy, or in healthcare systems where access differs. A treatment-opportunity perspective asks not only which regimen maximizes first-line efficacy but also which preserves a credible second-line pathway for the individual patient.

Evidence after modern immunotherapy is far flimsier than first-line evidence. Regorafenib, cabozantinib, and ramucirumab were validated mainly after sorafenib (*25-27*), while nivolumab-based evidence also arose in an earlier sequencing context (*28*). Post-immunotherapy practice therefore relies heavily on cross-trial reasoning and retrospective cohorts; randomized comparisons of complete sequences remain an unmet need. Such studies should document why subsequent treatment was or was not delivered, organ state at the transition, and whether the next therapy addressed resistance, toxicity, or a new curative-intent opportunity.

5.2 Intermediate and locally advanced HCC: From repeated embolization to selectively delivered and systemically integrated locoregional strategies

TACE transformed liver-limited HCC management but benefit depends on selection and technique. Unsuitability should be recognized before treatment or at the first meaningful reassessment when distribution, expected response, or hepatic vulnerability makes an embolization-led strategy unlikely to provide net benefit; refractoriness is declared only after inadequate response despite technically appropriate treatment. Repeated TACE has been associated with persistent ALBI deterioration, and a randomized-cohort secondary analysis documented 3-month ALBI-grade deterioration even after selective procedures (*29-33*). These data support reassessment, not an automatic prohibition: tumor burden, selectivity, recovery within 90 days, and alternatives must be considered together.

Randomized phase 3 trials now define a more complex boundary. EMERALD-1 improved PFS with durvalumab, bevacizumab, and TACE (*34*). LEAP-012 improved PFS, but failed to demonstrate a statistically significant overall survival (OS) benefit; the sponsors subsequently ended the study after a prespecified interim assessment indicated a low probability of meeting the protocol-defined OS threshold (*35,36*). At ASCO 2026, the conference-reported EMERALD-3 trial showed improved PFS with STRIDE plus lenvatinib and TACE *vs.* TACE alone (median 13.0 *vs.* 9.8 months; HR 0.70), with an immature, non-significant OS trend and substantially more grade 3–4 treatment-related adverse events (*37*). Full peer-reviewed reporting of hepatic trajectories, subsequent treatment, and mature OS remains essential. Together, these studies show that longer PFS does not by itself establish preserved survival, liver function, or future treatment access.

Selectively delivered strategies broaden the choice beyond TACE. In FOHAIC-1, modified FOLFOX hepatic arterial infusion chemotherapy (HAIC) improved median OS *vs.* sorafenib in predominantly high-burden, locally advanced HCC and enabled downstaging; another randomized trial in portal-vein invasion favored sorafenib plus FOLFOX-HAIC (*38,39*). These Asia-predominant data require attention to expertise, catheter risk, and external validity but support HAIC as a non-embolizing option when high tumor burden or a portal vein tumor thrombus makes repeated TACE unattractive.

Transarterial radioembolization (TARE) and stereotactic body radiotherapy (SBRT) can similarly concentrate treatment while limiting injury to the uninvolved liver. Randomized phase 2 comparisons reported longer time to progression with yttrium-90 TARE than with conventional or drug-eluting-bead TACE in selected patients (*40,41*). NRG/RTOG 1112 found that SBRT followed by sorafenib improved progression-free survival (PFS) and showed an adjusted OS advantage *vs.* sorafenib alone in locally advanced HCC, although the unadjusted primary comparison narrowly missed its prespecified significance threshold (*42*). These modalities are not intrinsically low-risk to the liver: dosimetry, treated volume, baseline function, and portal hypertension determine risk. Their opportunity value lies in avoiding repeated whole-territory ischemia, treating vascular invasion or focal residual disease, and creating a bridge to resection, ablation, or transplantation at expert centers.

Trials should therefore report selectivity, treated liver volume, procedure number, HAIC catheter complications, TARE dosimetry, SBRT dose-volume constraints, ALBI trajectory, decompensation, and subsequent-treatment eligibility. Technique is part of the causal pathway; none of these modalities is intrinsically organ-sparing.

5.3 Early and potentially resectable HCC: Perioperative uncertainty

Perioperative evidence is no longer uniformly negative. The early recurrence-free-survival advantage of adjuvant atezolizumab plus bevacizumab in IMbrave050 was not sustained with longer follow-up (*43,44*). By contrast, CARES-009, a randomized phase 2/3 trial in resectable HCC at intermediate or high recurrence risk, reported longer event-free survival with perioperative camrelizumab plus rivoceranib than with surgery alone (median 42.1 *vs.* 19.4 months; HR: 0.59), with grade 3 or worse treatment-related adverse events in approximately 38% of the patients (*45*). Generalizability beyond the trial population and mature OS remain unresolved.

The contrast is not a simple negative-versus-positive verdict. IMbrave050 cautions against adopting an advanced-disease regimen for purely postoperative use; CARES-009 suggests that perioperative timing, biological selection, and population may alter the result. Neoadjuvant exposure can test biology but can also delay surgery or cause immune and vascular toxicity. Trials must report the proportion reaching surgery, pathological response, postoperative liver function, recurrence patterns, and OS, and not EFS alone. (Table 2)

6. Conversion as an MDT-governed transition

Conversion is not a drug regimen. It is a transition from a disease state in which curative-intent treatment has an unfavorable or infeasible risk–benefit ratio to one in which such treatment becomes feasible. This definition separates conversion from neoadjuvant therapy, which begins with a planned operation, and from downstaging, which describes a change in measurable disease but does not by itself establish net surgical benefit.

Conversion evidence remains dominated by selected cohorts but is no longer entirely non-randomized. In the interim phase 3 TALENTop analysis, patients with locally advanced HCC, macrovascular invasion, and no extrahepatic spread in whom PR or SD was achieved after atezolizumab plus bevacizumab and who were already judged suitable for R0 resection were randomized to resection followed by therapy or continued systemic treatment. Median time to treatment failure was 20.4 *vs.* 11.8 months (HR 0.60); OS was immature (*46*). This is the first prospective comparative signal for surgery after induction in a narrowly defined population, not evidence that all responding or once-unresectable HCC should be resected. RACB and retrospective cohorts are informative for feasibility and selection but remain vulnerable to guarantee-time bias (*47-49*).

An MDT conversion review should use three safety gates. Biological safety asks whether response is durable rather than transient: sustained AFP or PIVKA-

Table 2. Landmark evidence that changes treatment boundaries—and what it does not yet establish

Clinical problem / study	Primary construct	Liver/opportunity information	Implication for the framework
Advanced first line—IMbrave150	Phase 3; atezolizumab–bevacizumab improved OS and PFS *vs* sorafenib	Selected Child–Pugh A population; later pathways not randomized	Establishes high-efficacy first line, not an optimal sequence
Advanced first line—HIMALAYA	Phase 3; STRIDE improved OS *vs* sorafenib	No continuous anti-VEGF exposure; immune toxicity can alter reserve	Offers a mechanistically distinct option; selection matters
Advanced first line—CheckMate 9DW	Phase 3; nivolumab–ipilimumab improved OS *vs* lenvatinib/sorafenib	Early crossing of curves and immune-related mortality require attention	Median OS alone does not describe early risk or future options
TACE combination—EMERALD-1	Phase 3; durvalumab–bevacizumab–TACE improved PFS	OS and longitudinal hepatic-state data needed	Validates integration; does not yet prove preserved opportunity
TACE combination—LEAP-012	Phase 3; improved PFS but no statistically significant OS benefit; study discontinued for low probability of meeting OS threshold	Liver-function trajectory and subsequent treatment incompletely reported	Demonstrates why PFS cannot stand alone
TACE combination—EMERALD-3	Phase 3 conference abstract; STRIDE–lenvatinib–TACE improved PFS; OS immature	Grade 3–4 toxicity increased; longitudinal hepatic-state data awaited	Promising but requires full peer review and mature OS
Adjuvant—IMbrave050 update	Phase 3; early RFS benefit not sustained; updated HR 0.90	One year of treatment after curative-intent therapy adds exposure and toxicity	Warns against premature extrapolation of intermediate endpoints
Perioperative—CARES-009	Randomized phase 2/3; perioperative camrelizumab–rivoceranib improved EFS vs surgery	More treatment exposure and grade ≥ 3 toxicity; OS immature	Timing and selection may determine perioperative value
Conversion—TALENTop interim	Randomized phase 3; post-induction resection improved TTF *vs*. continued atezolizumab–bevacizumab	Only patients with PR/SD, macrovascular invasion, no extrahepatic spread, and R0-resectability	First comparative signal; not generalizable to all conversion candidates

II decline, control of vascular invasion and extrahepatic disease, and radiological stability for approximately 3–4 months are reasonable expert-practice signals, not validated universal cut-offs. Washout safety addresses wound healing, bleeding, and immune injury. The bevacizumab label requires it to be withheld for at least 28 days before elective surgery; many hepatobiliary teams use approximately 4–6 weeks, but the exact interval should accord with the agent, procedure, toxicity, and institutional protocol (*50*). Active or recent immune-related hepatitis must be resolved and hepatic recovery demonstrated before surgery. Future-liver-remnant safety requires volumetric adequacy plus functional assessment appropriate to the center, such as ICG-R15 or 99mTc-galactosyl human serum albumin scintigraphy, rather than anatomy alone. R0 technical feasibility is therefore necessary but insufficient.

These gates resolve the apparent conflict between oncological tractability and marginal hepatic reserve. When tumor response makes local clearance attractive but reserve is borderline, the default is not maximal treatment intensity. The team should first ask whether the same oncological objective can be achieved with a smaller resection, ablation, SBRT, TARE, or staged strategy; treat portal hypertension and malnutrition; and repeat the functional assessment. If reserve remains the rate-limiting domain, preserving the effective systemic regimen or choosing lower-hepatic-cost consolidation may offer greater net benefit than immediate major hepatectomy.

Liver transplantation creates a distinct downstaging and bridging window because pre-transplant immune activation may persist after tumor control. Small series linked intervals shorter than 3 months between the last immune-checkpoint inhibitor dose and transplantation with severe rejection, and an individual-patient-data meta-analysis of 91 recipients reported rejection in 26.4%; a modeled median washout of 94 days corresponded to a rejection probability of 20% or less (*51,52*). These observational estimates do not establish a universal 90-day rule. Drug type, immune-related adverse events, urgency, donor timing, and immunosuppression protocol all matter, so ICI use for bridging or downstaging should trigger early transplant-center review and a documented, center-specific washout plan.

TALENTop also clarifies endpoint design. Its primary result concerns time to treatment failure, not mature OS, and applies only after induction response and resectability selection. Future studies should predefine the date of conversion eligibility, resectability criteria, central MDT review, competing local options, postoperative liver function, treatment-free survival, recurrence, and patient-reported recovery. Because randomization occurred only after induction response and confirmation of R0 resectability, TALENTop cannot estimate the intention-to-treat effect of an induction-to-conversion strategy in all initially unresectable patients.

The principal analytical challenge is guarantee-time bias: patients must survive, respond, and remain fit long enough to undergo conversion, so direct comparisons to non-converted patients will exaggerate benefit. Landmark analyses, target-trial emulation, and time-dependent exposure models can reduce but not eliminate confounding. Randomization at the moment of resectability may sometimes be feasible—for example, continued systemic therapy *vs.* local consolidation—but patient and clinician preferences will be strong. Even without randomization, prospective registries can improve inference by recording the first date on which conversion was considered, reasons for rejection, central review findings, and outcomes for all eligible patients, not only those who reached the operating room (Figure 3 and Table 3).

7. Aging, frailty, and MASLD are modifiers, not appendices

The HCC population is aging, particularly in countries with successful viral hepatitis control. Chronological age is a poor substitute for physiological reserve. Older adults with preserved function may tolerate intensive therapy, whereas younger patients with decompensated cirrhosis, sarcopenia, or cognitive impairment may have little recovery capacity. Comprehensive geriatric and nutritional assessment can reveal vulnerabilities that ECOG performance status misses.

Sarcopenia is especially relevant because it can be both a baseline risk and a treatment-emergent loss of reserve. A meta-analysis of 42 studies estimated a prevalence of 39% and an adjusted hazard ratio for overall mortality of 1.84 (*17*). Among patients receiving systemic therapy, the pooled prevalence of low skeletal-muscle mass was approximately 43%, with worse OS and PFS (*18*). These associations do not prove that reversing sarcopenia improves survival, but they justify routine screening, resistance exercise, nutritional support, and early rehabilitation as opportunity-preserving interventions.

MASLD changes both surveillance and treatment. HCC can occur without cirrhosis, and yet its absolute incidence in non-cirrhotic MASLD is generally too low for population-wide surveillance. Current guidance prioritizes cirrhosis and recommends stepwise fibrosis assessment: a simple blood-based score such as FIB-4 can identify low-risk patients, while an indeterminate or elevated result should prompt second-line assessment with vibration-controlled transient elastography (VCTE/FibroScan) or an equivalent validated method (*53,54*). These tools stratify fibrosis risk; they do not replace HCC staging or direct tumor treatment. Once HCC develops, cardiovascular, renal, and metabolic comorbidity can influence surgical risk, anti-VEGF eligibility, and recovery. These variables belong inside the core opportunity assessment, not in an etiological footnote.

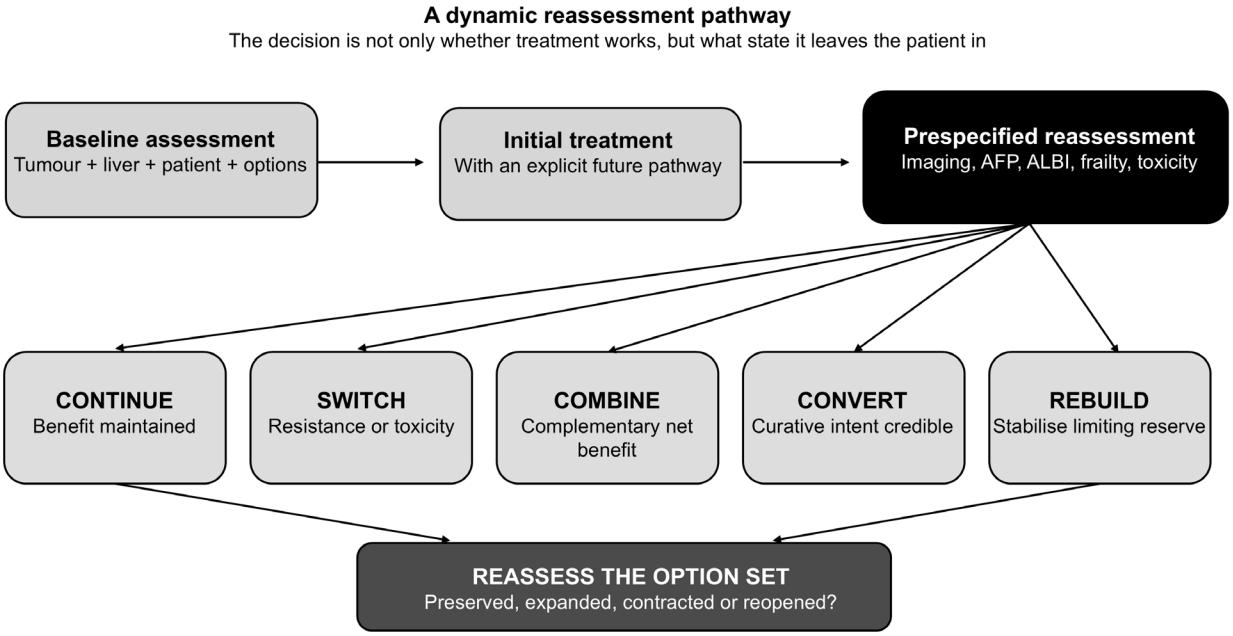


Figure 3. Dynamic reassessment pathway. Prespecified review can lead to continuation, switching, combination, conversion, or stabilization/rebuilding of a rate-limiting reserve. Each transition is followed by reassessment of the clinically credible set of options.

Table 3. Illustrative decision matrix for dynamic therapeutic-opportunity reassessment

Scenario and trigger	Domain signal	Question for the MDT	Possible transition	Required clarification
A. After one round of technically adequate TACE: CR/PR, but ALBI 1 → 2b	Tumor improves; hepatic reserve may be rate-limiting	Is the decline persistent and attributable to TACE, and does expected benefit justify further embolization?	Trigger review of alternatives, including systemic therapy or focal ablation/SBRT; defer repeat TACE while recovery and selectivity are assessed.	ALBI recovery, portal-hypertensive events, treated volume, residual distribution, and available alternatives.
B. IImmune-checkpoint inhibitor + anti-VEGF for 6 months: SD, AFP falls, 20% shrinkage, ALBI 1	Reserve stable; biology favorable; local-clearance potential	Does the distribution now permit a credible curative or consolidative option with acceptable hepatic cost?	Formal review for resection, SBRT, or TARE while comparing therapy to continued systemic control.	Durability, resectability/targetability, anti-VEGF washout. and FLR safety.
C. Third line: slow progression with new mild ascites	Cause and reversibility of hepatic deterioration are uncertain	Is ascites tumor-related, treatment-related or cirrhotic, and what is the immediate oncological risk?	Consider temporary interruption or dose adaptation while investigating and treating reversible causes; escalation may remain appropriate if tumor risk dominates.	Infection, portal-vein thrombosis, renal function, diuretic response, tumor kinetics, and current treatment benefit.
Conflict rule	Oncological tractability favors intensity, but hepatic reserve is marginal	Identify the rate-limiting domain and ask whether the same tumor objective can be achieved at lower hepatic cost.	Prefer smaller resection, ablation, SBRT/TARE, staged therapy or continued effective systemic treatment; defer major intervention if functional safety remains inadequate.	Document the alternative rejected, the locally defined safety threshold, patient preference, and the date for repeat MDT review; no universal numerical threshold has been validated.

8. From an MDT meeting to longitudinal team-based care

Multidisciplinary care is associated with better treatment receipt and survival, although the supporting studies are observational and heterogeneous. A meta-analysis of 12 studies including 15,365 patients found an association between multidisciplinary care and improved OS, but heterogeneity exceeded 90% for several outcomes (*55*). This finding supports team care while cautioning against attributing all benefit to the meeting itself.

Three concepts should be distinguished. An MDT meeting is a time-limited case discussion; multimodality treatment combines interventions; longitudinal team-based care assigns responsibility for reassessment, supportive care, and transitions across the disease course. The last

model is the organizational counterpart to management of dynamic therapeutic opportunity.

Core membership may include hepatology, hepatobiliary surgery, transplant medicine, interventional and diagnostic radiology, radiation oncology, medical oncology, pathology, specialized nursing, nutrition, rehabilitation, geriatrics, and palliative care. Not every discipline must attend every discussion. What matters is a trigger-based process: review at diagnosis, after a prespecified number of treatment cycles or TACE sessions, at meaningful response, at hepatic or functional deterioration, at progression, and whenever curative-intent eligibility might change. The patient and family should be represented in the decision, directly or through structured elicitation of goals.

Implementation requires ownership. One clinician or nurse navigator should maintain the longitudinal problem list, confirm that reassessment occurs on schedule, and record the chosen transition together with the alternatives considered. The MDT output should state not only the recommended treatment but also the contingency plan: what finding would prompt continuation, switch, combination, conversion review, or supportive-care intensification. This reduces the risk that responsibility disappears between specialties. Institutions should audit the time from trigger to review, the proportion of eligible patients receiving the recommended next therapy, unplanned admissions for decompensation, and discordance between patient goals and delivered care. Such measures evaluate the care pathway rather than the frequency of meetings.

9. Redesigning endpoints around clinical-state preservation

OS remains the most consequential endpoint, but it is increasingly affected by long post-progression survival, cross-over, subsequent treatment, and competing liver-related events. ORR and PFS are valuable measures of tumor effect; they cannot by themselves show whether a therapy leaves the patient fit for the next intervention. Both the divergence between early and updated IMbrave050 results and the still-maturing survival data after TACE combinations illustrate the danger of treating an intermediate endpoint as a complete account of clinical value.

Hepatic decompensation should be treated as a major clinical event and not merely an adverse-event category. A 2025 proposal argued for its incorporation as a prognostically relevant intermediate endpoint during systemic therapy (*56*). Standardization is essential: ascites requiring treatment, variceal bleeding, overt encephalopathy, and clinically meaningful jaundice should be defined prospectively, with competing-risk methods that account for tumor progression and death.

We propose a two-layer endpoint architecture. The tumor layer includes ORR, duration of response, PFS, recurrence-free survival, pathological response, and OS. The opportunity layer includes time to first hepatic decompensation, time to sustained ALBI deterioration, maintenance of Child–Pugh A or ALBI grade 1/2a, access to second- and third-line therapy, time to loss of local-treatment eligibility, conversion to curative-intent treatment, treatment-free survival, functional independence, and patient-reported outcomes. A future composite such as "time with an effective treatment option remaining" is conceptually attractive but not ready for regulatory use because option availability varies by geography, expertise, and patient preference. This two-layer architecture operationalizes components of dynamic therapeutic opportunity without collapsing them into a single DTO score; components should be reported separately or combined only through a prespecified hierarchical or multistate analysis.

Endpoint collection should continue after protocol therapy. Without documenting subsequent treatment, local procedures, transplant evaluation, rehabilitation, and reasons for treatment non-receipt, trials cannot determine whether a therapy preserved opportunity or merely postponed radiographic progression.

This approach also changes statistical design. HCC pathways are naturally represented as multistate processes: compensated disease, treatment response, hepatic deterioration, progression, curative-intent transition, recurrence, and death. A conventional Kaplan–Meier curve collapses these clinically distinct transitions into one event time. Multistate models can estimate how an intervention changes the probability of preserving an opportunity-preserved state over time; joint models can relate repeated ALBI or functional measurements to progression and mortality.

A hierarchical composite analyzed with the win ratio could compare patient pairs in an order that reflects clinical priority: death first, then severe hepatic decompensation, then failure to achieve predefined curative-intent conversion, and finally progression (*57*). This prevents an earlier but less important radiological event from outweighing survival or organ failure, although the hierarchy, time windows, and conversion eligibility must be prespecified and sensitivity-tested. When proportional hazards are doubtful—as with early crossing under immunotherapy—restricted mean survival time (RMST) at clinically chosen horizons can express event-free time gained without assuming a constant hazard ratio (*58*). Win-ratio and RMST analyses should be complementary estimands, not post hoc devices used to rescue a negative primary endpoint.

10. A research agenda for dynamic HCC management

The framework is useful only if it generates testable work. Five priorities follow.

(*i*) Define dynamic therapeutic opportunity operationally using repeated, domain-specific variables

rather than an unvalidated summary score.

(*ii*) Standardize sustained ALBI deterioration and clinically adjudicated hepatic decompensation, with competing-risk analyses.

(*iii*) Require prospective trials of systemic therapy to capture subsequent local treatment, transplant assessment, and curative-intent conversion using predefined criteria.

(*iv*) Compare complete treatment strategies in pragmatic trials, including switch timing after TACE and sequencing after immunotherapy.

(*v*) Create a core longitudinal dataset incorporating frailty, sarcopenia, patient-reported outcomes, barriers to access, and reasons that eligible treatment was not delivered.

Methodologically, multistate and joint longitudinal-survival models are likely to be more informative than conventional analyses that treat each line as independent. Clinically, digital monitoring and imaging analytics may assist with repeated assessment, but they should be evaluated against decisions that matter: prevention of decompensation, timely transition, and preservation of curative-intent eligibility. AI and liquid biopsy are tools, not paradigms; their value depends on whether they improve those decisions.

Healthcare economics and equity must be built into this agenda. A sequence that is biologically attractive but unavailable after the first line does not preserve real-world optionality. Trials and registries should therefore report geographic region, insurance or reimbursement constraints, travel burden, referral delay, and access to transplant, radiation and interventional expertise. Cost-effectiveness models should value avoided decompensation, maintained independence, and access to later therapy rather than drug acquisition and progression alone. This is particularly important because the framework could otherwise widen disparities by favoring centers with the most treatment options. A valid opportunity assessment must report biological eligibility and actual deliverability as separate dimensions, identify reasons for the gap, and avoid attributing access-related non-receipt to the biological effect of the initial therapy.

11. Conclusion

The central question in contemporary HCC care is no longer merely which treatment is best for a given stage, but how each intervention changes the patient's future therapeutic possibilities. Preserving liver function is therefore not an ancillary goal and not the whole goal; it is one component of maintaining therapeutic opportunity.

The next paradigm will be defined by the ability to control cancer, prevent hepatic decompensation, preserve physiological resilience, enable treatment transitions, and repeatedly reassess curative-intent options. Static staging and established efficacy endpoints remain necessary, but they should be embedded within longitudinal, multidisciplinary management. The decisive measure of progress will be not only how long a treatment delays tumor growth but also how effectively it keeps meaningful treatment options open.

Funding: This work was supported by the National Key Research and Development Program of China (grant No. 2023YFB3810004; JH).

Conflict of Interest: The authors have no conflicts of interest to disclose.

References

1. European Association for the Study of the Liver. EASL Clinical Practice Guidelines on the management of hepatocellular carcinoma. J Hepatol. 2025; 82:315-374.
2. Singal AG, Llovet JM, Yarchoan M, *et al.* AASLD Practice Guidance on prevention, diagnosis, and treatment of hepatocellular carcinoma. Hepatology. 2023; 78:1922-1965.
3. Vogel A, Martinelli E; ESMO Guidelines Committee. Updated treatment recommendations for hepatocellular carcinoma from the ESMO Clinical Practice Guideline. Ann Oncol. 2021; 32:801-805.
4. Department of Medical Administration, National Health Commission of the People′s Republic of China. Guideline for diagnosis and treatment of primary liver cancer (2026 edition). Chinese Journal of Digestive Surgery, 2026; 25:423-482. (in Chinese)
5. Makuuchi M, Kosuge T, Takayama T, Yamazaki S, Kakazu T, Miyagawa S, Kawasaki S. Surgery for small liver cancers. Semin Surg Oncol. 1993; 9:298-304.
6. Imamura H, Sano K, Sugawara Y, Kokudo N, Makuuchi M. Assessment of hepatic reserve for indication of hepatic resection: Decision tree incorporating indocyanine green test. J Hepatobiliary Pancreat Surg. 2005; 12:16-22.
7. Makuuchi M, Thai BL, Takayasu K, Takayama T, Kosuge T, Gunven P, Yamazaki S, Hasegawa H, Ozaki H. Preoperative portal embolization to increase safety of major hepatectomy for hilar bile duct carcinoma: A preliminary report. Surgery. 1990; 107:521-527.
8. Hasegawa K, Kokudo N, Imamura H, Matsuyama Y, Aoki T, Minagawa M, Sano K, Sugawara Y, Takayama T, Makuuchi M. Prognostic impact of anatomic resection for hepatocellular carcinoma. Ann Surg. 2005; 242:252-259.
9. Aramaki O, Takayama T, Matsuyama Y, *et al.* Reevaluation of Makuuchi's criteria for resecting hepatocellular carcinoma: A Japanese nationwide survey. Hepatol Res. 2023; 53:127-134.
10. Reig M, Sanduzzi-Zamparelli M, Forner A, *et al.* BCLC strategy for prognosis prediction and treatment recommendations: The 2026 update. J Hepatol. 2026; 84:631-654.
11. Vogel A, Chan SL, Dawson LA, Kelley RK, Llovet JM, Meyer T, Ricke J, Rimassa L, Sapisochin G, Vilgrain V, Zucman-Rossi J, Ducreux M. Hepatocellular carcinoma: ESMO Clinical Practice Guideline for diagnosis, treatment and follow-up. Ann Oncol. 2025; 36:491-506.
12. Japan Society of Hepatology. Clinical practice guidelines for hepatocellular carcinoma 2025. Japan Society of Hepatology, Tokyo, Japan, 2025. Japanese.
13. Johnson PJ, Berhane S, Kagebayashi C, *et al.* Assessment of liver function in patients with hepatocellular carcinoma:

A new evidence-based approach—the ALBI grade. J Clin Oncol. 2015; 33:550-558.
14. Ruiz de Galarreta M, Bresnahan E, Molina-Sanchez P, *et al.* β-Catenin activation promotes immune escape and resistance to anti-PD-1 therapy in hepatocellular carcinoma. Cancer Discov. 2019; 9:1124-1141.
15. Harding JJ, Nandakumar S, Armenia J, *et al.* Prospective genotyping of hepatocellular carcinoma: clinical implications of next-generation sequencing for matching patients to targeted and immune therapies. Clin Cancer Res. 2019; 25:2116-2126.
16. Ao H, Xin Z, Jian Z. Liquid biopsy to identify biomarkers for immunotherapy in hepatocellular carcinoma. Biomark Res. 2021; 9:91.
17. Jiang C, Wang Y, Fu W, Zhang G, Feng X, Wang X, Wang F, Zhang L, Deng Y. Association between sarcopenia and prognosis of hepatocellular carcinoma: A systematic review and meta-analysis. Front Nutr. 2022; 9:978110.
18. Kuo MH, Tseng CW, Hsu CS, Chen YC, Kao IT, Wu CY, Shao SC. Prevalence and effect of low skeletal muscle mass among hepatocellular carcinoma patients undergoing systemic therapy: A systematic review and meta-analysis. Cancers (Basel). 2023; 15:2426.
19. Finn RS, Qin S, Ikeda M, *et al.* Atezolizumab plus bevacizumab in unresectable hepatocellular carcinoma. N Engl J Med. 2020; 382:1894-1905.
20. Cheng AL, Qin S, Ikeda M, *et al.* Updated efficacy and safety data from IMbrave150: atezolizumab plus bevacizumab vs sorafenib for unresectable hepatocellular carcinoma. J Hepatol. 2022; 76:862-873.
21. Abou-Alfa GK, Lau G, Kudo M, *et al.* Tremelimumab plus durvalumab in unresectable hepatocellular carcinoma. NEJM Evid. 2022; 1:EVIDoa2100070.
22. Sangro B, Kudo M, Qin S, *et al.* Four-year overall survival update from the phase III HIMALAYA study of tremelimumab plus durvalumab in unresectable hepatocellular carcinoma. Ann Oncol. 2024; 35:448-457.
23. Qin S, Chan SL, Gu S, *et al.* Camrelizumab plus rivoceranib versus sorafenib as first-line therapy for unresectable hepatocellular carcinoma (CARES-310): A randomised, open-label, international phase 3 study. Lancet. 2023; 402:1133-1146.
24. Yau T, Galle PR, Decaens T, *et al.* Nivolumab plus ipilimumab versus lenvatinib or sorafenib as first-line treatment for unresectable hepatocellular carcinoma (CheckMate 9DW). Lancet. 2025; 405:1851-1864.
25. Bruix J, Qin S, Merle P, *et al.* Regorafenib for patients with hepatocellular carcinoma who progressed on sorafenib treatment (RESORCE). Lancet. 2017; 389:56-66.
26. Abou-Alfa GK, Meyer T, Cheng AL, *et al.* Cabozantinib in patients with advanced and progressing hepatocellular carcinoma. N Engl J Med. 2018; 379:54-63.
27. Zhu AX, Kang YK, Yen CJ, *et al.* Ramucirumab after sorafenib in patients with advanced hepatocellular carcinoma and increased alpha-fetoprotein concentrations (REACH-2). Lancet Oncol. 2019; 20:282-296.
28. Melero I, Yau T, Kang YK, *et al.* Nivolumab plus ipilimumab combination therapy in patients with advanced hepatocellular carcinoma previously treated with sorafenib: 5-year results from CheckMate 040. Ann Oncol. 2024; 35:537-548.
29. Kudo M, Han G, Finn RS, *et al.* Brivanib as adjuvant therapy to transarterial chemoembolization in patients with hepatocellular carcinoma: A randomized phase III trial. Hepatology. 2014; 60:1697-1707.
30. Kudo M, Han KH, Ye SL, *et al.* A changing paradigm for the treatment of intermediate-stage hepatocellular carcinoma: Asia-Pacific Primary Liver Cancer Expert consensus statements. Liver Cancer. 2020; 9:245-260.
31. Kudo M, Ueshima K, Chan S, *et al.* Lenvatinib as an initial treatment in patients with intermediate-stage hepatocellular carcinoma beyond up-to-seven criteria and Child-Pugh A liver function: A proof-of-concept study. Cancers (Basel). 2019; 11:1084.
32. Arizumi T, Ueshima K, Chishina H, Kono M, Takita M, Kitai S, Inoue T, Yada N, Hagiwara S, Minami Y, Sakurai T, Nishida N, Kudo M. Validation of the criteria of transcatheter arterial chemoembolization failure or refractoriness in patients with advanced hepatocellular carcinoma proposed by the Liver Cancer Study Group of Japan. Oncology. 2014; 87 Suppl 1:32-36.
33. Kodama Y, Ikeda M, Arai Y, *et al.* Change in liver function after selective transarterial chemoembolization for unresectable hepatocellular carcinoma: JIVROSG-2001 PRESIDENT-ALBI, a secondary analysis of a multicenter randomized controlled trial. Liver Cancer. Published online December 5, 2025.
34. Sangro B, Kudo M, Erinjeri JP, *et al.* Durvalumab with or without bevacizumab with transarterial chemoembolisation in hepatocellular carcinoma (EMERALD-1). Lancet. 2025; 405:216-232.
35. Kudo M, Ren Z, Guo Y, *et al.* Transarterial chemoembolisation combined with lenvatinib plus pembrolizumab versus dual placebo for unresectable, non-metastatic hepatocellular carcinoma (LEAP-012). Lancet. 2025; 405:203-215.
36. Merck & Co., Inc.; Eisai Co., Ltd. Merck and Eisai provide update on phase 3 LEAP-012 trial in unresectable, non-metastatic hepatocellular carcinoma. *https://www.merck.com/news/merck-and-eisai-provide-update-on-phase-3-leap-012-trial-in-unresectable-non-metastatic-hepatocellular-carcinoma/* (accessed August 15, 2026).
37. Abou-Alfa GK, Ren Z, Erinjeri JP, *et al.* Efficacy and safety results from EMERALD-3: tremelimumab plus durvalumab with or without lenvatinib combined with TACE in embolization-eligible HCC. J Clin Oncol. 2026; 44(suppl 17):LBA4000.
38. Lyu N, Wang X, Li JB, Lai JF, Chen QF, Li SL, Deng HJ, He M, Mu LW, Zhao M. Arterial chemotherapy of oxaliplatin plus fluorouracil versus sorafenib in advanced hepatocellular carcinoma: A biomolecular exploratory, randomized, phase III trial (FOHAIC-1). J Clin Oncol. 2022; 40:468-480.
39. He M, Li Q, Zou R, *et al.* Sorafenib plus hepatic arterial infusion of oxaliplatin, fluorouracil, and leucovorin versus sorafenib alone for hepatocellular carcinoma with portal vein invasion: A randomized clinical trial. JAMA Oncol. 2019; 5:953-960.
40. Salem R, Gordon AC, Mouli S, *et al.* Y90 radioembolization significantly prolongs time to progression compared with chemoembolization in patients with hepatocellular carcinoma. Gastroenterology. 2016; 151:1155-1163.e2.
41. Dhondt E, Lambert B, Hermie L, Huyck L, Vanlangenhove P, Geerts A, Verhelst X, Aerts M, Vanlander A, Berrevoet F, Troisi RI, Van Vlierberghe H, Defreyne L. Y-90 radioembolization versus drug-eluting bead chemoembolization for unresectable hepatocellular carcinoma: Results from the TRACE phase II randomized

controlled trial. Radiology. 2022; 303:699-710.
42. Dawson LA, Winter KA, Knox JJ, *et al.* Stereotactic body radiotherapy vs sorafenib alone in hepatocellular carcinoma: The NRG Oncology/RTOG 1112 phase 3 randomized clinical trial. JAMA Oncol. 2025; 11:136-144.
43. Qin S, Chen M, Cheng AL, *et al.* Atezolizumab plus bevacizumab versus active surveillance in patients with resected or ablated high-risk hepatocellular carcinoma (IMbrave050). Lancet. 2023; 402:1835-1847.
44. Yopp A, Chen M, Cheng AL, Kaseb A, Kudo M, Lee HC, Cha E, Hack SP, Lian Q, Spahn J, Wu C, Qin S, Chow PKH. Updated data from IMbrave050: Adjuvant atezolizumab plus bevacizumab for high-risk hepatocellular carcinoma. J Hepatol. 2026; 84:1102-1111.
45. Wang Z, Fan J, Zhou S, *et al.* Perioperative camrelizumab plus rivoceranib versus surgery alone in patients with resectable hepatocellular carcinoma at intermediate or high risk of recurrence (CARES-009): A randomized phase 2/3 trial. Lancet. 2025; 406:2089-2099.
46. Sun HC, Shen F, Liu L, *et al.* Liver resection versus continued atezolizumab plus bevacizumab in locally advanced hepatocellular carcinoma after atezolizumab plus bevacizumab treatment (TALENTop): A multicentre, open-label, randomised phase 3 trial. Ann Oncol. 2025; 36(suppl):abstract 1469MO.
47. Okuno M, Ishii T, Ichida A, Soyama A, Takemura N, Hirono S, Eguchi S, Hasegawa K, Sasaki Y, Uemura K, Kokudo N, Hatano E. Protocol of the RACB study: A multicenter, single-arm, prospective study to evaluate the efficacy of resection of initially unresectable hepatocellular carcinoma with atezolizumab combined with bevacizumab. BMC Cancer. 2023; 23:780.
48. Shimose S, Saeki I, Ito T, *et al.* The benefit of conversion therapy for patients with unresectable hepatocellular carcinoma receiving atezolizumab plus bevacizumab using oncological resectability criteria in Japan. Hepatol Int. 2025; 19:846-855.
49. Takeuchi Y, Sue M, Miyake N, *et al.* Borderline resectable classification identifies candidates for conversion therapy in unresectable hepatocellular carcinoma treated with atezolizumab and bevacizumab. Hepatol Res. 2026; 56:830-839.
50. National Library of Medicine. DailyMed: Avastin (bevacizumab) injection, solution. *https://dailymed.nlm.nih.gov/dailymed/drugInfo.cfm?setid=939b5d1f-9fb2-4499-80ef-0607aa6b114e* (accessed August 15, 2026).
51. Schnickel GT, Fabbri K, Hosseini M, Misel M, Berumen J, Parekh J, Mekeel K, Dehghan Y, Kono Y, Ajmera V. Liver transplantation for hepatocellular carcinoma following checkpoint inhibitor therapy with nivolumab. Am J Transplant. 2022; 22:1699-1704.
52. Rezaee-Zavareh MS, Yeo YH, Wang T, *et al.* Impact of pre-transplant immune checkpoint inhibitor use on post-transplant outcomes in HCC: A systematic review and individual patient data meta-analysis. J Hepatol. 2025; 82:107-119.
53. European Association for the Study of the Liver, European Association for the Study of Diabetes, European Association for the Study of Obesity. EASL-EASD-EASO Clinical Practice Guidelines on the management of metabolic dysfunction-associated steatotic liver disease: executive summary. Diabetologia. 2024; 67:2375-2392.
54. Rinella ME, Neuschwander-Tetri BA, Siddiqui MS, Abdelmalek MF, Caldwell S, Barb D, Kleiner DE, Loomba R. AASLD Practice Guidance on the clinical assessment and management of nonalcoholic fatty liver disease. Hepatology. 2023; 77:1797-1835.
55. El Dahan KS, Reczek A, Daher D, Rich NE, Yang JD, Hsiehchen D, Zhu H, Patel MS, del Pilar Bayona Molano M, Sanford N, Gopal P, Parikh ND, Yopp AC, Singal AG. Multidisciplinary care for patients with HCC: A systematic review and meta-analysis. Hepatol Commun. 2023; 7:e0143.
56. Cabibbo G, Celsa C, Bhoori S, Reiberger T, Pinato DJ, Cammà C. Establishing hepatic decompensation as a meaningful clinical outcome during systemic therapy for hepatocellular carcinoma. J Hepatol. 2025; 83:1443-1451.
57. Pocock SJ, Ariti CA, Collier TJ, Wang D. The win ratio: A new approach to the analysis of composite endpoints in clinical trials based on clinical priorities. Eur Heart J. 2012; 33:176-182.
58. Uno H, Claggett B, Tian L, *et al.* Moving beyond the hazard ratio in quantifying the between-group difference in survival analysis. J Clin Oncol. 2014; 32:2380-2385.

Received July 9, 2026; Revised August 21, 2026; Accepted August 25, 2026.

[§]These authors contributed equally to this work.

**Address correspondence to:*
Wei Tang, National Center for Global Health and Medicine, Japan Institute for Health Security, 1-21-1 Toyama, Shinjuku-ku, Tokyo 162-8655, Japan.
E-mail: politang-tky@umin.ac.jp

Released online in J-STAGE as advance publication August 28, 2026.

Review

DOI: 10.5582/bst.2026.01217

Hepatic arterial infusion chemotherapy–based triplet conversion therapy for hepatocellular carcinoma with portal vein tumor thrombus: Evidence, patient selection, and surgical endpoints

Chaosheng Xia[§], Yutao He[§], Rongfu Hong, Wenda Wang, Hangyu Li, Lin Wang[*], Zhitian Shi[*]

Hepatobiliary and Pancreatic Surgery, The Second Affiliated Hospital of Kunming Medical University, Kunming, China.

SUMMARY: Portal vein tumor thrombus (PVTT) is a biologically aggressive and clinically heterogeneous form of hepatocellular carcinoma (HCC). Global guidelines generally classify macrovascular invasion as advanced disease and prioritize systemic therapy, whereas selected East Asian practice pathways incorporate hepatic arterial infusion chemotherapy (HAIC), radiotherapy, or resection. This review critically evaluates HAIC combined with an antiangiogenic agent and immune checkpoint inhibitor as a conversion strategy for HCC with PVTT. Randomized trials substantiate the efficacy of HAIC-based treatment in contrast to controls from the days of sorafenib but do not establish the incremental benefit of the contemporary triplet. Across prospective single-arm studies, RECIST 1.1 objective response rates ranged from approximately 36 to 77%, with higher estimates in some studies using mRECIST. Retrospective PVTT-focused comparisons also suggest longer progression-free and overall survival than with dual systemic therapy or HAIC alone, but these figures remain vulnerable to confounding by indication, heterogeneous regimens, inconsistent response criteria, and immortal-time bias related to surgery. Conversion should be defined as a prospectively documented transition from unresectable disease to an R0-resectable state with adequate liver reserve, not as radiological response alone. We propose an explicitly unvalidated multidisciplinary framework for candidate selection, reassessment, and perioperative management. Current evidence supports protocol-based use in clinical trials or experienced centers rather than routine global adoption. Randomized PVTT-stratified trials comparing the triplet to contemporary immunotherapy, with intention-to-treat reporting of resection and pathological response, are required.

Keywords: hepatectomy, downstaging, immune checkpoint inhibition, antiangiogenesis, portal hypertension

1. Introduction

Hepatocellular carcinoma (HCC) remains a leading cause of cancer mortality worldwide, and macroscopic portal-vein invasion is one of its most adverse phenotypes (*1,2*). Portal vein tumor thrombus (PVTT) is not merely a staging variable. It accelerates intrahepatic dissemination, reduces portal inflow, worsens portal hypertension, and narrows the therapeutic window by eroding hepatic reserve. The label also encompasses very different anatomical states: a segmental branch thrombus that can be removed with the involved lobe is not clinically equivalent to a tumor extending into the main trunk or contralateral portal vein.

This heterogeneity is explained by a persistent East-West divergence. The BCLC 2026, EASL 2025, AASLD, ESMO, and ASCO frameworks generally place macrovascular invasion on a systemic-therapy pathway (*3-7*). Japanese, Korean, and Chinese guidance accepts broader use of liver-directed therapy, and the 2026 Chinese PVTT guideline explicitly recommends individualized combinations of hepatic arterial infusion chemotherapy (HAIC), transarterial chemoembolization (TACE), radiotherapy, targeted agents, and immunotherapy for unresectable disease (*8-11*). Observational surgical data further suggest that selected patients with limited PVTT may outlive non-surgical comparators, although selection is profound (*12,13*).

The central question is therefore not whether a triplet can shrink tumors. It is whether adding HAIC to a modern systemic doublet creates a reproducible, oncologically meaningful conversion-to-resection opportunity, without consuming liver reserve or delaying effective systemic control. This review is organized around that question.

We performed a targeted narrative review updated through July 29, 2026. MEDLINE/PubMed, Embase, Web of Science, the Cochrane Library, ClinicalTrials.gov, WHO ICTRP-linked records, and Chinese guideline sources were searched using combinations of hepatocellular carcinoma, portal vein tumor thrombus or portal vein invasion, HAIC or hepatic arterial infusion,

FOLFOX, immune checkpoint blockade, antiangiogenic therapy, conversion, downstaging, resection, and pathological response. References listed in key trials and major guidelines were also screened. The review was not protocol-registered and did not use duplicate screening or a PRISMA selection process; it should therefore be interpreted as a critical narrative synthesis rather than an exhaustive systematic review.

We prioritized PVTT-specific randomized or prospective studies, contemporary systemic-therapy trials with macrovascular-invasion data, comparative HAIC-based cohorts, and studies reporting conversion, R0 resection, or pathological response. General unresectable-HCC studies were retained only when they provided information on the HAIC backbone, safety, mechanism, or trial design. RECIST 1.1 and mRECIST outcomes were identified and presented independently. No quantitative meta-analysis was performed because the available studies mixed single-arm and comparative designs, incompatible control regimens, different PVTT strata, and non-equivalent response criteria; a pooled estimate would therefore imply a precision and exchangeability that the evidence does not support.

2. Clinical context and biological rationale

The Japanese Vp classification is anatomically explicit: Vp1 denotes invasion distal to second-order branches, Vp2 invasion of second-order branches, Vp3 invasion of a first-order branch, and Vp4 invasion of the main trunk or a contralateral branch. Cheng type I-IV is commonly used in China and is similar but not directly interchangeable. Reporting both systems, along with the exact vessels involved, is preferable to collapsing disease into "PVTT present" (Table 1).

Resectability must be divided into technical and oncological components. Technical unresectability includes inadequate future liver remnant (FLR), inability to obtain negative margins, prohibitive portal reconstruction, or unacceptable surgical risk. Oncological unresectability includes rapidly progressive extrahepatic disease, diffuse bilobar intrahepatic dissemination, or a tumor biology indicating that major surgery would be unlikely to provide meaningful disease-free survival. Conversion therapy should document which barriers existed at the baseline and which barriers were overcome.

The dominant competing risk is liver failure. Portal occlusion, varices, thrombocytopenia, and a large tumor burden can make apparent antitumor activity clinically irrelevant if treatment worsens hepatic reserve. Child-Pugh class alone is insufficient; the ALBI grade, bilirubin trajectory, platelet count, ascites, variceal risk, portal collaterals, and quantitative FLR should be integrated.

HAIC is not the only liver-directed option for PVTT. External-beam radiotherapy, transarterial chemoembolization, and transarterial radioembolization are used in selected anatomical and regional settings, but their potential utility depends heavily on the extent of PVTT, liver reserve, arterial anatomy, and local expertise (*4,8-11*). This review focuses on HAIC-based triplet therapy and does not claim comparative superiority over these alternatives.

Atezolizumab plus bevacizumab and durvalumab plus tremelimumab are established immunotherapy-based first-line therapies for unresectable HCC, with camrelizumab plus rivoceranib (CARES-310 interim and final analyses; (*17*,*20*)), sintilimab plus a bevacizumab biosimilar, and nivolumab plus ipilimumab further broadening the global treatment landscape (*14-20*). These regimens were not designed as conversion programs and their eligibility criteria generally favored Child-Pugh A and ECOG 0-1 populations. Importantly, drug classes are not interchangeable: LEAP-002 did not meet its prespecified superiority boundaries for pembrolizumab plus lenvatinib *vs.* lenvatinib (*21*). Treating all 'TKI plus PD-1' combinations as a validated class is therefore scientifically unsafe.

Vp4 disease illustrates the unmet need. In the exploratory IMbrave150 analysis, median overall survival was 7.6 months with atezolizumab-bevacizumab and 5.5 months with sorafenib (HR: 0.62, 95% CI: 0.34-1.11) (*15*). This small, underpowered subgroup analysis should

Table 1. PVTT anatomy and implications for conversion planning

Category	Anatomical extent	Usual clinical implication	Conversion question
Vp1 / Cheng I	Distal segmental branches	May be technically resectable with limited hepatectomy in selected patients	Is biology favorable enough for upfront surgery or short neoadjuvant therapy?
Vp2 / Cheng I-II	Second-order portal branches	Resection possible in experienced centers if future liver remnant (FLR) and portal pressure are acceptable	Will induction therapy reduce early systemic and intrahepatic failure?
Vp3 / Cheng II	First-order right or left portal branch	Often technically complex; may require thrombectomy or en-bloc portal resection	Can PVTT regress to permit an oncologically credible R0 surgery?
Vp4 / Cheng III-IV	Main trunk and/or contralateral branch; superior mesenteric vein extension in Cheng IV	Advanced, high-risk disease; portal hypertension and hepatic decompensation are central hazards	Can treatment restore portal flow, maintain FLR, and exclude rapidly progressive systemic biology?

not be used for indirect superiority claims, but it is a clinically relevant benchmark: outcomes in main-trunk or contralateral-branch invasion remain substantially worse than in the trial population overall.

HAIC delivers chemotherapy through the hepatic artery without permanent embolization. In China, FOLFOX-HAIC is common; Japan and Korea have longer experience with cisplatin/5-fluorouracil or related regimens. Avoiding embolization can be attractive when portal inflow is compromised, although catheterization, arterial anatomy, and repeated procedures introduce distinct risks.

Randomized evidence validates the efficacy of HAIC in treating portal vein invasion. In 247 patients, sorafenib plus FOLFOX-HAIC improved median overall survival from 7.13 to 13.37 months (HR 0.35) and objective response from 2.5 to 40.8% *vs.* sorafenib alone (*22*). A randomized phase II trial restricted to Vp3/Vp4 disease reported a median overall survival of 16.3 *vs.* 6.5 months with sorafenib plus 3cir-OFF HAIC *vs.* sorafenib (HR 0.28) (*23*). FOHAIC-1 similarly favored HAIC over sorafenib in a high-risk advanced population, although it was not a PVTT-specific trial (*24*). Conversely, the randomized phase III FOLFOX-HAIC *vs.* TACE study in large HCC excluded major vascular invasion and extrahepatic spread; it provided evidence of local efficacy but cannot be cited as high-level evidence for treating PVTT (*25*).

Oxaliplatin can trigger hallmarks of immunogenic cell death, including calreticulin exposure, ATP release, and HMGB1 release, potentially increasing antigen presentation (*26*). Anti-VEGF/VEGFR treatment may transiently normalize abnormal vasculature and reduce immunosuppressive myeloid signaling, while checkpoint blockade can restore effector T-cell function (*27,28*). These concepts provide a plausible sequence from cytoreduction to immune engagement, but direct evidence from treated patients with PVTT is limited. Dose, drug identity, and timing matter: excessive vessel pruning may aggravate hypoxia or alter HAIC delivery.

PVTT itself may be immunologically distinct. Single-cell profiling has identified enrichment of immunosuppressive C5aR-positive tumor-associated macrophages in venous tumor thrombus, while other transcriptomic work describes immune-desert or immune-excluded features (*29,30*). These data strengthen the rationale for PVTT-specific translational sampling, but they do not prove that adding any particular TKI or antibody to HAIC reverses those states (Figure 1).

3. Clinical evidence for HAIC-based triplet therapy

Prospective single-arm studies have provided evidence of variable but clinically relevant antitumor activity, but they have not quantified the incremental effect of HAIC. Lenvatinib, toripalimab, and FOLFOX-HAIC were reported to result in a RECIST 1.1 ORR of 63.9% and a median PFS of 10.4 months in 36 patients with high-risk advanced HCC (*31*). The TRIPLET phase II study of camrelizumab, apatinib, and FOLFOX-HAIC enrolled 35 BCLC C patients and reported a confirmed

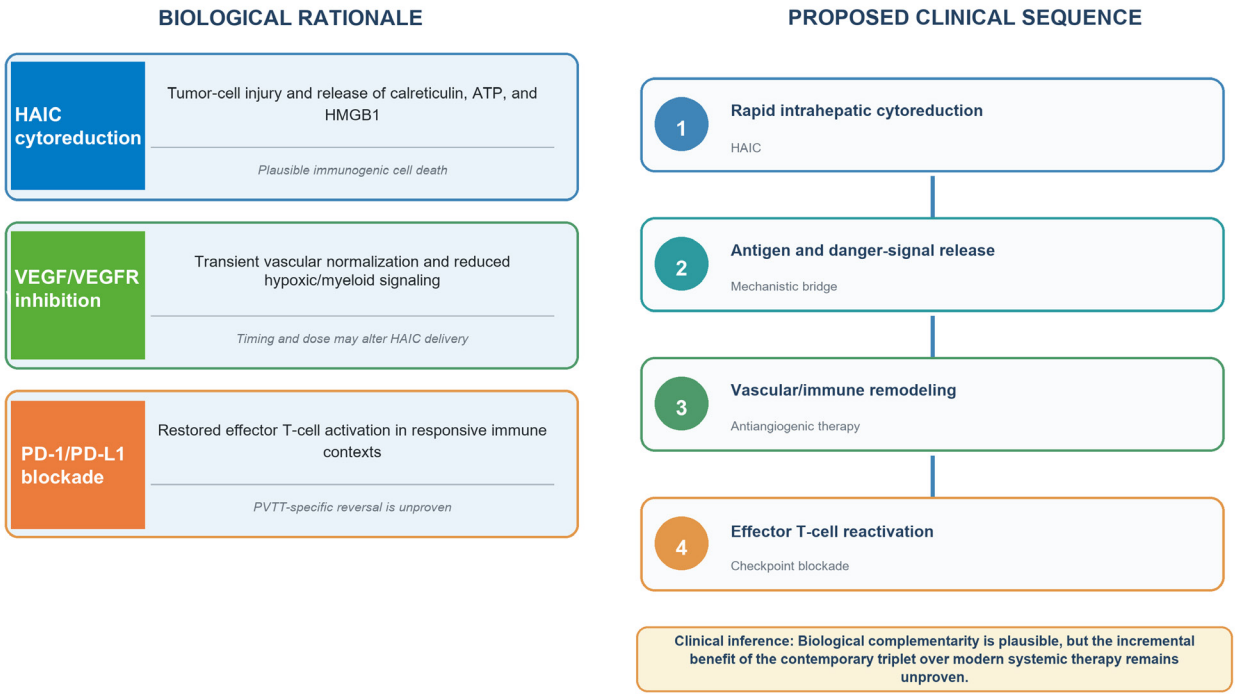


Figure 1. The biological and clinical logic of HAIC-based triplet therapy. This figure separates the mechanistic rationale from clinical inference. HAIC-induced cytoreduction, VEGF/VEGFR inhibition, and checkpoint blockade may be biologically complementary, but the incremental clinical benefit of the contemporary triplet over modern systemic therapy has not been established.

RECIST ORR of 77.1% and a median PFS of 10.38 months (*32*). Cal Era used raltitrexed-oxaliplatin HAIC with camrelizumab-lenvatinib in 39 evaluable patients, resulting in an ORR of 66.7% and a median PFS and OS of 13.8 and 21.2 months, respectively, but grade 3–4 treatment-related events occurred in 79.5% of the patients (*33*).

Not all prospective signals are uniformly strong. Double-IA-001, a small phase II study of FOLFOX-HAIC, camrelizumab, and sorafenib, did not meet its prespecified first-stage activity requirement; the median OS was 8.87 months and grade 3 or higher treatment-related events occurred in 76% of patients (*34*). Negative or modest studies are important because they counter publication-driven assumptions that any triplet is synergistic (Table 2).

PVTT-specific comparative evidence expanded substantially between 2024 and 2026. In a four-center study including 411 patients with PVTT, camrelizumab plus rivoceranib with or without HAIC was compared. After propensity score matching, the triplet regimen achieved significantly longer median OS (18.7 *vs*. 11.0 months) and PFS (10.0 *vs*. 5.6 months); however, the ORR remained identical in both groups (42.2%). These findings suggest that the observed survival advantage was driven primarily by improved disease control and delayed progression rather than greater tumor shrinkage (*35*). This distinction underscores that radiographic response, survival outcomes, and conversion to resectability represent related but non-interchangeable endpoints. Therefore, while the study supports a beneficial effect of HAIC on disease control and time-to-event outcomes, it does not provide evidence that HAIC enhanced conversion eligibility or increased the likelihood of R0 resection through additional cytoreduction.

In a multicenter high-risk cohort defined by Vp4 and/or tumor diameter of at least 10 cm, FOLFOX-HAIC plus heterogeneous TKIs and PD-1 inhibitors was compared to TKI-PD-1 therapy. After matching 194 pairs, median OS was 24.6 *vs.* 11.9 months, PFS was 10.0 *vs.* 7.7 months, and ORR was 57.7% *vs.* 28.9%; grade 3–4 events were also higher (59.2% *vs.* 47.4%) (*36*). Only one-third of the original cohort had Vp4, so the result cannot be assumed to represent all main-trunk PVTT.

More anatomically focused data are informative but remain retrospective. In Vp4 disease, HAIC-lenvatinib-tislelizumab was associated with a median OS of 23.2 *vs.* 6.9 months and a tumor ORR of 77.1% *vs.* 42.9% compared to HAIC alone after matching 35 patients per group (*37*). A 2026 single-arm Vp4 cohort of 35 patients reported an mRECIST ORR of 60%, a median OS of 313 days, and grade 3–4 events in 45.7% (*38*). Another 2026 weighted comparison of 97 Vp4 patients found that adding a PD-1 blockade to HAIC-TKI improved the adjusted median OS from 10.1 to 14.6 months (HR 0.47) and PFS from 5.5 to 7.3 months (HR 0.48) (*39*). These estimates are hypothesis-generating, not practice-defining.

The large TACE-HAIC study by Yuan *et al*. is often cited as triplet evidence, but the intervention combines embolization, infusion chemotherapy, a targeted agent, and immunotherapy; it should not be pooled conceptually with HAIC-only triplets (*40*). Similarly, examination of the extrahepatic-metastasis cohort by Guan *et al*. suggests that intrahepatic control may still matter when distant disease is present, but residual confounding and liver-dominant selection limit causal interpretation (*41*) (Table 2).

By study, ORR, conversion, resection, pathological response, and grade 3–4 toxicity are therefore summarized descriptively in Table 2. The ranges should not be interpreted as pooled effects: patient selection, the extent of PVTT, drug combinations, response criteria, adverse-event attribution, and denominators differ materially across studies.

Conversion endpoints are especially susceptible to inflation. In a study by Luo *et al*., pCR was achieved in 7 of 27 patients who underwent resection (25.9%) but in only 7 of all 145 treated patients (4.8%) (*42*). In a study by Liu *et al*., a radiological complete response, and not a pathological complete response, was achieved in 22.2% (*43*). In a 19-patient prospective conversion study, 14 were considered eligible for resection, nine underwent R0 resection, and pCR was achieved in two: The conversion and R0 resection rates were 73.7% (14/19) and 47.4% (9/19), respectively; pCR was 22.2% (2/9) among resected patients and 10.5% (2/19) in the intention-to-treat population (*44*). High-quality reviews must report all denominators.

Comparing patients who underwent surgery to those who did not is also biased: surgery is only possible after a period of survival and favorable response. Conventional Kaplan-Meier analyses from treatment initiation create guarantee-time bias, also known as immortal time bias. Landmark analysis, time-dependent exposure modeling, or target-trial methods are required. The CHANCE2416 publication is a protocol for a retrospective target-trial emulation and has not reported hypothesized survival figures as results (*45*).

4. Conversion criteria, patient selection, and safety

The optimal candidate is not defined by PVTT alone. As a pragmatic and explicitly unvalidated MDT framework, consideration may be given to patients with an ECOG performance status of 0–1, Child-Pugh A or carefully selected B7 liver function, ALBI grade 1 or favorable grade 2, adequate marrow and renal function, controlled HBV, no uncontrolled ascites or encephalopathy, and manageable portal hypertension. Disease should be liver-dominant and the barrier to R0 resection should be anatomically resolvable. Vp1/Vp2 disease may already be directly resectable in selected patients; Vp3/

Table 2. Evidence from randomized HAIC backbones, prospective triplets, comparative cohorts, and conversion studies. RECIST 1.1 and mRECIST are retained as reported and are not combined; no pooled effect is presented because designs, comparators, populations, and denominators are heterogeneous

Study	Design; Population	Treatment	Key outcomes	Main limitation
He *et al*. (*22*)	randomized, *n* = 247; HCC with portal-vein invasion	Sorafenib + FOLFOX-HAIC *vs.* sorafenib	OS 13.37 *vs.* 7.13 mos; HR 0.35; RECIST ORR 40.8% *vs.* 2.5%	Outdated systemic comparator
Zheng *et al*. (*23*)	randomized phase II, *n* = 64; Vp3/Vp4, treatment-naive	Sorafenib + 3cir-OFF HAIC *vs.* sorafenib	OS 16.3 *vs.* 6.5 mos; HR 0.28; ORR 41% *vs.* 3%	Small study; port-catheter regimen
Lai *et al*. (*31*)	phase II, *n* = 36; High-risk advanced HCC; mixed high-risk criteria	Lenvatinib + toripalimab + FOLFOX-HAIC	RECIST ORR 63.9%; PFS 10.4 mos; extended OS 17.9 mos	Single center; no control
TRIPLET (*32*)	phase II, *n* = 35; BCLC C HCC	Camrelizumab + apatinib + FOLFOX-HAIC	RECIST ORR 77.1%; PFS 10.38 mos	Small, single arm; not PVTT-specific
Cal Era (*33*)	phase II, *n* = 39; BCLC B/C HCC	Camrelizumab + lenvatinib + RALOX-HAIC	ORR 66.7%; PFS 13.8 mos; OS 21.2 mos; grade 3-4 TRAE 79.5%	Non-FOLFOX HAIC; exploratory biomarkers
Double-IA-001 (*34*)	phase II, *n* = 25; BCLC C HCC	Camrelizumab + sorafenib + FOLFOX-HAIC	ORR 44%; PFS 4.87 mos; OS 8.87 mos; primary endpoint not met	Small; modest activity; high toxicity
Luo *et al*. (*42*)	Single-center retrospective, *n* = 145 uHCC	Single-arm HAIC + ICI + TKI	mRECIST ORR 57.2%; PFS 9.7 mos	Resection 27/145 (18.6%); pCR 7/27 (25.9%) among resected, 7/145 (4.8%) ITT
Liu *et al*. (*43*)	Retrospective, *n* = 27; 70.4% PVTT; heavily pretreated	Single-arm HAIC + anti-PD-1 + TKI	ORR 63%; radiological CR 22.2%; PFS 10.6 mos	No pathological proof for the reported CR; grade ≥ 3 AE 55.6%
Li *et al*. (*35*)	Multicenter retrospective PVTT, *n* = 411; PSM 83 pairs	HAIC + camrelizumab + rivoceranib *vs.* systemic doublet	Matched OS 18.7 *vs.* 11.0 mos; PFS 10.0 *vs.* 5.6 mos; ORR 42.2% in both arms	DCR 94.0% *vs.* 78.3%; grade 3–4 TRAE 70.5% *vs.* 62.2%
Zuo *et al*. (*36*)	Multicenter high-risk HCC, *n* = 466; PSM 194 pairs	HAIC + TKI + PD-1 *vs.* TKI + PD-1	Matched OS 24.6 *vs.* 11.9 mos; PFS 10.0 *vs.* 7.7 mos; ORR 57.7% *vs.* 28.9%	Resection/ablation 16.5% *vs.* 9.2%; only 33.3% had Vp4 before matching
Tang *et al*. (*37*)	Multicenter Vp4, *n* = 155; PSM 35 pairs	HAIC + lenvatinib + tislelizumab *vs*. HAIC	OS 23.2 *vs.* 6.9 mos; PFS 6.6 *vs*. 2.4 mos; tumor ORR 77.1% *vs.* 42.9%	Hepatectomy 15.8% *vs.* 0.9%; small matched sample
Wang *et al*. (*38*)	Retrospective Vp4, *n* = 35	Single-arm HAIC + TKI + PD-1	mRECIST ORR 60%; OS 313 days; PFS 204 days	Grade 3-4 AE 45.7%; 97.1% HBV; no control
Liu *et al*. (*39*)	Retrospective Vp4, *n* = 97; sIPTW	HAIC + TKI + PD-1 *vs.* HAIC + TKI	Adjusted OS 14.6 *vs.* 10.1 mos (HR 0.47); PFS 7.3 *vs.* 5.5 mos (HR 0.48)	Single center; potential cohort overlap; RECIST 1.1
Yalikun *et al*. (*44*)	Prospective single arm, *n* = 19 uHCC; no extrahepatic spread	HAIC + camrelizumab + apatinib	RECIST ORR 47.4%; mRECIST ORR 89.5%; survival immature	Resectable 14/19 (73.7%); R0 9/19 (47.4%); pCR 2/9 (22.2%) resected and 2/19 (10.5%) ITT; grade ≥ 3 TRAE 73.7%

Vp4 disease has a greater need for local control but less physiological margin for error. These categories should not be interpreted as a validated selection rule (Table 2).

Extrahepatic disease is not an absolute biological prohibition, but it changes the endpoint. Limited, controllable metastases may permit a consolidated strategy in exceptional cases; widespread or rapidly progressing metastases make major hepatectomy difficult to justify. The benefit reported in an extrahepatic-metastasis cohort should be viewed as evidence that liver control matters, not proof that surgery is curative in disseminated disease (*41*) (Figure 2 and Table 3).

Reassessment after approximately two HAIC cycles, often 6–8 weeks, is a pragmatic practice-based approach rather than a prospectively validated universal interval. RECIST 1.1 and mRECIST should be reported separately because size reduction and loss of arterial enhancement measure different effects. Operability requires more than response: R0 resection must be anatomically feasible; FLR and liver function must be adequate; portal inflow and outflow must be reconstructable; and extrahepatic disease must be absent or controllable. Stability at one reassessment may help exclude rapidly progressive biology, although excessive delay risks cumulative toxicity or regrowth.

Radiological CR is not pathological CR. Residual viable cells may persist in a non-enhancing mass or thrombus, and immune-related patterns can complicate imaging. Observational data and recent meta-analyses have yet to demonstrate that non-surgical observation after complete response is equivalent to resection (*46*). Pathology should report the viable tumor percentage separately for the hepatic lesion and PVTT, margin status, microvascular invasion, nodal disease, and treatment effect.

Triplet therapy combines non-overlapping and overlapping toxicities. FOLFOX-HAIC causes marrow suppression, transaminase elevation, nausea, abdominal pain, and cumulative oxaliplatin neuropathy; catheter complications include dissection, thrombosis, infection, and extrahepatic perfusion. Antiangiogenic agents cause hypertension, proteinuria, bleeding, thrombosis, and impaired wound healing, whereas immune checkpoint inhibitors may cause hepatitis, colitis, pneumonitis, endocrinopathy, myocarditis, or other immune toxicities. Across contemporary studies, grade 3 or higher event rates ranged from approximately 46 to 80%, but the definitions, regimens, populations, and follow-up differed (*33,35,36,38,44*). These rates should therefore be presented by study rather than pooled as a single safety estimate.

Before administering therapy that includes bevacizumab, clinically significant varices and other manifestations of portal hypertension should be assessed and managed according to current portal-hypertension guidance (*47*). Perioperative interruption must be

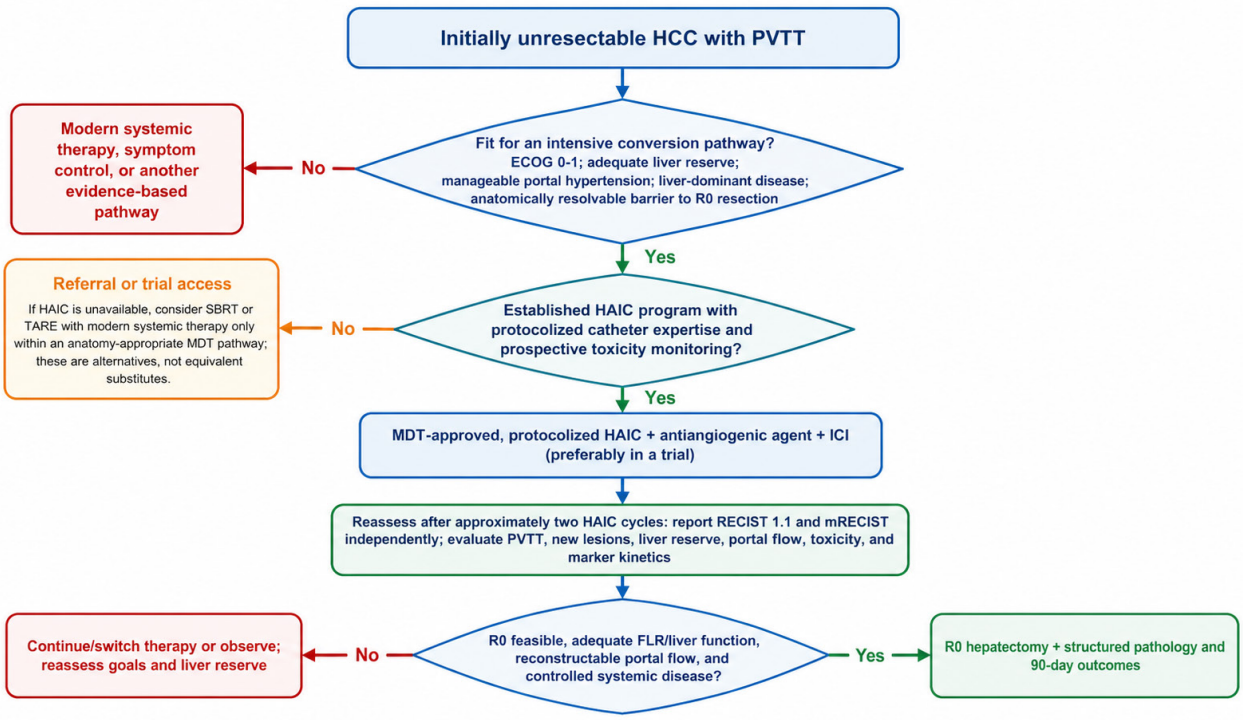


Figure 2. Multidisciplinary selection and reassessment pathway. This unvalidated framework distinguishes centers with an established HAIC program from settings in which referral, structured training, SBRT, or TARE may be considered. Alternative locoregional modalities are not presented as equivalent substitutes for HAIC. RECIST 1.1 and mRECIST should be reported independently. This class-level pathway does not imply interchangeability among HAIC backbones, antiangiogenic agents, or ICIs; any regimen should be protocol-specified and evidence-informed. *Abbreviations*: MDT, multidisciplinary team; FLR, future liver remnant; SBRT, stereotactic body radiotherapy; TARE, transarterial radioembolization.

Table 3. Practical selection, reassessment, and perioperative checklist

Domain	Before treatment	At each reassessment	Before surgery
Tumor anatomy	Triphasic CT or MRI; PVTT extent; arterial anatomy; liver volumetry	RECIST 1.1 and mRECIST separately; PVTT regression; new lesions	R0 plan; portal reconstruction; FLR and inflow/outflow; exclude progression
Liver reserve	Child-Pugh, ALBI, bilirubin, INR, platelets, ascites, ICG where used	Trend rather than a single value; treatment-related injury	No unresolved hepatitis or decompensation; adequate FLR (context-specific)
Portal hypertension	Endoscopy when anti-VEGF therapy is planned; collaterals, spleen, platelets	Bleeding, ascites, portal-flow changes	Variceal control; operative bleeding strategy
Systemic biology	Chest imaging; bone/brain imaging if symptomatic; AFP and DCP	Marker kinetics; extrahepatic response; tempo of disease	No uncontrolled systemic progression
Treatment safety	Neuropathy, marrow, renal function, cardiovascular and immune history	Cumulative oxaliplatin toxicity; hypertension/proteinuria; immune hepatitis; catheter events	Agent-specific washout; normalized coagulation and marrow; steroid plan if prior irAE
Patient-centered factors	Goals, uncertainty, procedure burden, costs and access	Quality of life and preference at each decision point	Informed trade-off between surgery, continued therapy, and observation
Program capability	Trained interventional oncology team; catheter and rescue protocols; MDT review; referral pathway if unavailable	Procedure-level quality assurance; catheter complications; center-level outcome registry	Experienced hepatobiliary surgery, anesthesia, portal reconstruction, pathology, and 90-day outcome capture

individualized to drug half-life, bleeding and wound-healing risks, immune toxicity, and surgical urgency. A longer interval is generally required for bevacizumab than for oral TKIs, but a universal window cannot be inferred from the HAIC-triplet literature; it should be governed by current product information and institutional protocols. Surgery should be deferred after clinically significant immune hepatitis until toxicity has resolved and immunosuppression has been appropriately tapered. In Vp4 disease with complete main-trunk occlusion, uncontrolled or recent variceal bleeding, or worsening liver reserve, antiangiogenic therapy and repeated HAIC catheterization should be deferred or avoided until portal-hypertension risk is stabilized and an MDT judges the residual risk acceptable.

HBV status and HBV DNA should be assessed before treatment, antiviral therapy should be optimized when indicated, and reactivation surveillance should continue during and after anticancer therapy (*49*). Nutritional status, sarcopenia, and patient-reported outcomes also deserve systematic attention because repeated HAIC procedures impose travel, hospitalization, and financial burdens not discernable from conventional adverse-event tables.

5. Evidence gaps and future directions

Most modern HAIC-triplet data originate from HBV-predominant Chinese cohorts treated at high-volume centers. Whether those data can be generalized to HCV, alcohol-, or metabolic-dysfunction-associated HCC is uncertain. Arterial techniques, inpatient infrastructure, drug availability, and surgical thresholds differ between regions. The Japanese and Korean experience also involves regimens that are not identical to Chinese FOLFOX-HAIC (*8-10*).

For centers without an established HAIC program, triplet adoption should not precede a formal implementation pathway: referral or proctorship from a high-volume center, protocol-based catheter training, standardized FOLFOX preparation and dose modification, prospective catheter- and liver-toxicity surveillance, hepatobiliary surgical participation, and independent radiology review. Where that infrastructure is unavailable, anatomy-appropriate stereotactic body radiotherapy (SBRT) or transarterial radioembolization (TARE) may be paired with contemporary systemic therapy as part of an experienced MDT or clinical trial (*4,5,8-11*). These modalities should be viewed as alternative locoregional strategies, not interchangeable substitutes for HAIC, because direct comparative conversion data are lacking. Institutional registries should include all treated patients, including those who deteriorate before the first response scan, to prevent survivorship-biased internal impressions.

No biomarker currently indicates which patients to select for HAIC-based triple therapy. AFP and des-gamma-carboxy prothrombin kinetics are useful adjuncts but cannot replace imaging. Baseline ALBI, the neutrophil-to-lymphocyte ratio, tumor size, and tumor number are repeatedly associated with outcome, and yet they may be prognostic rather than predictive. Small exploratory studies have proposed CCL28/BTC or IL-2/CXCL13/CCL19 signatures (*31,33*); these require assay standardization and validation in treatment-interaction analyses.

The most promising research direction is longitudinal

multi-compartment profiling. Paired primary tumor and PVTT tissue can resolve the myeloid, stromal, and hypoxic programs highlighted by single-cell and spatial studies (*29,30,48*). Serial circulating tumor DNA may help identify molecular residual disease after radiological response or resection, while radiomics and digital pathology may quantify thrombus viability and treatment effect. Models should be established and judged by calibration and clinical utility, not only discrimination.

A decisive trial should enroll cohorts with untreated HCC and prospectively stratified Vp3 and Vp4 disease, Child-Pugh A, and clearly defined B7, and extrahepatic spread should be separately stratified. The control must be a contemporary immunotherapy regimen, not sorafenib. The experimental arm should specify one HAIC regimen, one antiangiogenic agent, one ICI, a catheter technique, dose-modification rules, a response review, and surgical criteria. A registered randomized phase II study, NCT04947826, compares HAIC plus HLX10 and HLX04 to HAIC plus a placebo in major PVTT; its registration is evidence of an appropriate design, not evidence of efficacy (*50*).

Overall survival should remain the primary endpoint, with blinded central review of RECIST 1.1 and mRECIST reported simultaneously but independently; hepatic, PVTT, and extrahepatic responses should also be described separately. Future conversion trials should prespecify the full intention-to-treat population as the mandatory denominator for conversion, R0 resection, major pathological response, and pCR. Surgical-cohort percentages may be reported only as secondary conditional estimates and must never replace intention-to-treat rates. Ninety-day mortality, major morbidity, patient-reported quality of life, time to hepatic decompensation, and grade 3–5 toxicity should be key secondary endpoints. Surgery should be analyzed as a time-dependent exposure with a prespecified landmark sensitivity analysis.

Randomization alone will not solve every question. Embedded translational studies should examine whether HAIC changes antigenicity, T-cell clonality, myeloid states, or ctDNA clearance and whether those changes interact with treatment. Health-economic and implementation analyses are essential because repeated arterial procedures, specialized catheter skills, and costly systemic therapy may worsen inequity in access. Trial reports should include center volume, operator experience, catheter technique, admission burden, and cross-over to SBRT or TARE so that geographic transferability can be judged.

A review-length synthesis should also contrast HAIC with other liver-directed strategies rather than treating HAIC as the sole local platform. In a randomized trial of 90 patients with liver-confined HCC and macroscopic vascular invasion, TACE plus external-beam radiotherapy improved PFS and OS *vs.* sorafenib and enabled curative resection in five patients (*51*). NRG/RTOG 1112 subsequently showed that SBRT followed by sorafenib produced a clinically meaningful, although not statistically significant, improvement in

Table 4. Competing locoregional strategies in HCC with PVTT: evidence signal, selection logic, and limitations

Strategy	Evidence signal	Most plausible selection context	Conversion relevance	Key limitation
HAIC + antiangiogenic agent + ICI	High ORR in small prospective cohorts; favorable retrospective comparisons (*31-39*)	Liver-dominant, high-burden disease; preserved liver reserve; experienced HAIC/MDT program	Potential cytoreduction and PVTT regression; few ITT R0 and pathological endpoints	No randomized comparison to a contemporary ICI regimen
TACE + external-beam RT	Randomized benefit versus sorafenib in liver-confined macroscopic vascular invasion (*51*)	Preserved unilateral portal flow, Child-Pugh A, liver-confined disease	Five of 45 patients underwent curative resection in the randomized trial	Single-center, sorafenib-era comparator; embolic ischemia risk
SBRT + systemic therapy	Phase III RTOG 1112 showed clinically meaningful but non-significant OS improvement (*52*)	Focal or anatomically targetable PVTT; adequate uninvolved liver; radiotherapy expertise	May eliminate vascular invasion and preserve arterial options	Not a PVTT-specific conversion trial; liver-dose constraints
TARE (yttrium-90)	PVTT-focused meta-analysis suggests activity, but SARAH/SIRveNIB did not improve ITT OS (*54-56*)	Liver-dominant disease, favorable shunt/dosimetry, preserved liver reserve, expert center	Potential lobar control without macroembolization	Selection and dosimetry heavily influence outcomes; limited resection data
Selective TACE	Systematic-review signal in selected PVTT populations (*53*)	Peripheral PVTT with preserved portal flow and superselective access	May facilitate local control in combination programs	Main-trunk occlusion and poor reserve increase hepatic failure risk

Note: The table is a clinical-reasoning comparison, not a network-derived treatment ranking. *Abbreviations*: ICI, immune checkpoint inhibitor; ITT, intention-to-treat; MDT, multidisciplinary team; OS, overall survival; RT, radiotherapy; TACE, transarterial chemoembolization; TARE, transarterial radioembolization.

Table 5. Minimum endpoint and denominator framework for PVTT conversion studies

Domain	Required definition	Denominator and time origin	Minimum report
Whole-tumor response	RECIST 1.1, independently reviewed when feasible (*59*)	All treated patients; baseline to prespecified scan times	CR, PR, SD, PD; confirmed/unconfirmed ORR; missing scans counted explicitly
Viable-tumor response	mRECIST reported separately, not merged with RECIST 1.1 (*60*)	All treated patients and response-evaluable subset	Enhancing viable diameter; discordance with RECIST 1.1
PVTT response	Predefined change in Vp/Cheng extent, enhancement, portal flow, and surgical clearance	All patients with baseline PVTT; fixed imaging schedule	PVTT CR/PR definition, recanalization, differentiation from bland thrombus
Conversion eligibility	Prospectively specified technical and oncological resectability at MDT review	All patients starting conversion therapy	Date, reason, and criteria for resectability; reasons for non-conversion
Resection and margin	Surgery attempted, completed hepatectomy, R0/R1/R2, thrombectomy or en-bloc resection	ITT and underwent surgery as denominators, both stated	ITT resection and R0 rates; 90-day morbidity/mortality
Pathological response	Viable tumor percentage in liver lesion and PVTT separately; MPR and pCR thresholds prespecified	ITT and underwent resection as denominators, both stated	pCR/MPR in each denominator; margins, nodes, microvascular invasion
Liver reserve and safety	Child-Pugh components, ALBI, portal-hypertension events, CTCAE grade (*61*)	Baseline and each cycle; safety population defined	Decompensation, bilirubin/albumin trajectory, grade 3–5 events, catheter complications
Survival and surgery effect	OS/PFS from treatment start; surgery as time-dependent exposure or landmark analysis (*62,63*)	All treated patients; time zero aligned with eligibility and assignment	ITT Kaplan-Meier; adjusted time-dependent/landmark estimate; loss to follow-up

Abbreviations: CR, complete response; CTCAE, Common Terminology Criteria for Adverse Events; ITT, intention-to-treat; MDT, multidisciplinary team; MPR, major pathological response; ORR, objective response rate; OS, overall survival; pCR, pathological complete response; PD, progressive disease; PFS, progression-free survival; PR, partial response; SD, stable disease.

OS over sorafenib alone in locally advanced HCC (*52*). Systematic reviews have substantiated the effectiveness of carefully selected TACE and TARE approaches in PVTT (*53,54*), but the negative results of the SARAH and SIRveNIB phase III trials with regard to OS caution against extrapolating a favorable single-center TARE series to unselected advanced HCC (*55,56*). Broader meta-analytic and network comparisons are useful for generating hypotheses but remain limited by era effects, treatment heterogeneity, and indirectness (*57,58*). Table 4 therefore presents selection logic rather than a treatment ranking.

Response and conversion reporting also require a common measurement architecture. RECIST 1.1 should quantify the whole tumor burden, whereas mRECIST should independently quantify enhancing viable HCC; neither framework alone adequately describes PVTT regression, recanalization, or surgical clearance (*59,60*). Baseline and longitudinal liver reserve should be reported with Child-Pugh components and an objective score such as ALBI because radiological response without preserved hepatic function cannot produce a safe conversion (*61*). Table 5 specifies the minimum denominators, time origins, and endpoint definitions needed to compare future studies.

For observational conversion cohorts, eligibility, treatment assignment, the start of follow-up, and surgical status must be aligned. A target-trial protocol should be specified before analysis (*62*), and surgery should be modeled as a time-dependent exposure or evaluated with a prespecified landmark analysis to prevent immortal time bias (*63*). These methods do not remove unmeasured confounding, but they make the causal question and principal assumptions auditable.

6. Conclusion

HAIC-based triple therapy is one of the most active conversion strategies under investigation for HCC with PVTT. The rationale is compelling and early response, survival, and resection signals are clinically meaningful. And yet the evidence has an important asymmetry: randomized trials have established the value of HAIC in contrast to controls from the days of sorafenib, whereas the modern triplet is mainly substantiated by small prospective cohorts and retrospective comparisons in a limited geographic setting. Its superiority to contemporary ICI-based systemic therapy has not been established.

The appropriate current position is neither dismissal nor routine universal adoption. In experienced multidisciplinary centers, carefully selected patients with preserved liver function, liver-dominant high-burden disease, and anatomically actionable PVTT

may reasonably be placed on a protocolized conversion pathway, preferably as part of a trial. Centers that lack HAIC capability should prioritize referral, structured training, or anatomy-appropriate alternative locoregional strategies such as SBRT or TARE rather than informal replication. Every claim of success should preserve the intention-to-treat denominator, report RECIST 1.1 and mRECIST independently, distinguish radiological from pathological response, and demonstrate that technically feasible surgery is also oncologically worthwhile.

Funding: This work was supported by the National Natural Science Foundation of China (82372810); the Key Research and Development Program of Yunnan Province (202403AC100023); Kunming Medical University's Project to Create a First-class Team in the Discipline (2024XKTDYS04); Yunnan Province's Support Program for Personnel to Develop the Province: Special Project for Young Talent (2025 Zhitian Shi); the Yunnan Provincial Health Commission's Medical Personnel Development Program (H-2024056); and the Joint Special Project of the Science and Technology Department of Yunnan Province and Kunming Medical University (202601AY070001-191).

Conflict of Interest: The authors have no conflicts of interest to disclose.

References

1. Bray F, Laversanne M, Sung H, Ferlay J, Siegel RL, Soerjomataram I, Jemal A. Global cancer statistics 2022: GLOBOCAN estimates of incidence and mortality worldwide for 36 cancers in 185 countries. CA Cancer J Clin. 2024; 74:229-263.
2. Llovet JM, Kelley RK, Villanueva A, Singal AG, Pikarsky E, Roayaie S, Lencioni R, Koike K, Zucman-Rossi J, Finn RS. Hepatocellular carcinoma. Nat Rev Dis Primers. 2021; 7:6.
3. Reig M, Sanduzzi-Zamparelli M, Forner A, *et al*. BCLC strategy for prognosis prediction and treatment recommendations: The 2026 update. J Hepatol. 2026; 84:631-654.
4. European Association for the Study of the Liver. EASL clinical practice guidelines on the management of hepatocellular carcinoma. J Hepatol. 2025; 82:315-374.
5. Singal AG, Llovet JM, Yarchoan M, *et al*. AASLD practice guidance on prevention, diagnosis, and treatment of hepatocellular carcinoma. Hepatology. 2023; 78:1922-1965.
6. Vogel A, Chan SL, Dawson LA, Kelley RK, Llovet JM, Meyer T, Ricke J, Rimassa L, Sapisochin G, Vilgrain V, Zucman-Rossi J, Ducreux M, ESMO Guidelines Committee. Hepatocellular carcinoma: ESMO clinical practice guideline for diagnosis, treatment and follow-up. Ann Oncol. 2025; 36:491-506.
7. Gordan JD, Kennedy EB, Abou-Alfa GK, *et al*. Systemic therapy for advanced hepatocellular carcinoma: ASCO guideline update. J Clin Oncol. 2024; 42:1830-1850.
8. Lau G, Obi S, Zhou J, *et al*. APASL clinical practice guidelines on systemic therapy for hepatocellular carcinoma-2024. Hepatol Int. 2024; 18:1661-1683.
9. Korean Liver Cancer Association (KLCA) and National Cancer Center (NCC) Korea. 2022 KLCA-NCC Korea practice guidelines for the management of hepatocellular carcinoma. Clin Mol Hepatol. 2022; 28:583-705.
10. Hasegawa K, Takemura N, Yamashita T, *et al*. Clinical practice guidelines for hepatocellular carcinoma: The Japan Society of Hepatology 2021 version (5th JSH-HCC guidelines). Hepatol Res. 2023; 53:383-390.
11. Chinese Association of Liver Cancer and Chinese Medical Doctor Association. Guidelines for diagnosis and treatment of hepatocellular carcinoma with portal vein tumor thrombus in China (2026 edition) (in Chinese). Zhonghua Yi Xue Za Zhi. 2026; 106:41-55.
12. Kokudo T, Hasegawa K, Matsuyama Y, Takayama T, Izumi N, Kadoya M, Kudo M, Ku Y, Sakamoto M, Nakashima O, Kaneko S, Kokudo N, Liver Cancer Study Group of Japan. Survival benefit of liver resection for hepatocellular carcinoma associated with portal vein invasion. J Hepatol. 2016; 65:938-943.
13. Cheng S, Chen M, Cai J, Sun J, Guo R, Bi X, Lau WY, Wu M. Chinese expert consensus on multidisciplinary diagnosis and treatment of hepatocellular carcinoma with portal vein tumor thrombus (2018 edition). Liver Cancer. 2020; 9:28-40.
14. Finn RS, Qin S, Ikeda M, *et al*. Atezolizumab plus bevacizumab in unresectable hepatocellular carcinoma. N Engl J Med. 2020; 382:1894-1905.
15. Finn RS, Galle PR, Ducreux M, Cheng AL, Reilly N, Nicholas A, Hernandez S, Ma N, Merle P, Salem R, Li D, Breder V. Efficacy and safety of atezolizumab plus bevacizumab versus sorafenib in hepatocellular carcinoma with main trunk and/or contralateral portal vein invasion in IMbrave150. Liver Cancer. 2024; 13:655-668.
16. Abou-Alfa GK, Lau G, Kudo M, *et al*. Tremelimumab plus durvalumab in unresectable hepatocellular carcinoma. NEJM Evid. 2022; 1:EVIDoa2100070.
17. Qin S, Chan SL, Gu S, *et al*. Camrelizumab plus rivoceranib versus sorafenib as first-line therapy for unresectable hepatocellular carcinoma (CARES-310): A randomised, open-label, international phase 3 study. Lancet. 2023; 402:1133-1146.
18. Ren Z, Xu J, Bai Y, *et al*. Sintilimab plus a bevacizumab biosimilar (IBI305) versus sorafenib in unresectable hepatocellular carcinoma (ORIENT-32): A randomised, open-label, phase 2-3 study. Lancet Oncol. 2021; 22:977-990.
19. Yau T, Galle PR, Decaens T, *et al*. Nivolumab plus ipilimumab versus lenvatinib or sorafenib as first-line treatment for unresectable hepatocellular carcinoma (CheckMate 9DW): An open-label, randomised, phase 3 trial. Lancet. 2025; 405:1851-1864.
20. Qin S, Gu S, Chan SL, *et al*. Camrelizumab plus rivoceranib versus sorafenib as first-line therapy for unresectable hepatocellular carcinoma (CARES-310): Final analysis of a randomised, open-label, international, phase 3 study. Lancet Oncol. 2025; 26:1598-1611.
21. Llovet JM, Kudo M, Merle P, *et al*. Lenvatinib plus pembrolizumab versus lenvatinib plus placebo for advanced hepatocellular carcinoma (LEAP-002): A randomised, double-blind, phase 3 trial. Lancet Oncol. 2023; 24:1399-1410.
22. He M, Li Q, Zou R, *et al*. Sorafenib plus hepatic arterial infusion of oxaliplatin, fluorouracil, and leucovorin vs sorafenib alone for hepatocellular carcinoma with portal

vein invasion: A randomized clinical trial. JAMA Oncol. 2019; 5:953-960.
23. Zheng K, Zhu X, Fu S, *et al*. Sorafenib plus hepatic arterial infusion chemotherapy versus sorafenib for hepatocellular carcinoma with major portal vein tumor thrombosis: A randomized trial. Radiology. 2022; 303:455-464.
24. Lyu N, Wang X, Li JB, Lai JF, Chen QF, Li SL, Deng HJ, He M, Mu LW, Zhao M. Arterial chemotherapy of oxaliplatin plus fluorouracil versus sorafenib in advanced hepatocellular carcinoma: A biomolecular exploratory, randomized, phase III trial (FOHAIC-1). J Clin Oncol. 2022; 40:468-480.
25. Li QJ, He MK, Chen HW, Fang WQ, Zhou YM, Xu L, Wei W, Zhang YJ, Guo Y, Guo RP, Chen MS, Shi M. Hepatic arterial infusion of oxaliplatin, fluorouracil, and leucovorin versus transarterial chemoembolization for large hepatocellular carcinoma: A randomized phase III trial. J Clin Oncol. 2022; 40:150-160.
26. Galluzzi L, Vitale I, Warren S, *et al*. Consensus guidelines for the definition, detection and interpretation of immunogenic cell death. J Immunother Cancer. 2020; 8:e000337.
27. Fukumura D, Kloepper J, Amoozgar Z, Duda DG, Jain RK. Enhancing cancer immunotherapy using antiangiogenics: Opportunities and challenges. Nat Rev Clin Oncol. 2018; 15:325-340.
28. Shigeta K, Datta M, Hato T, *et al*. Dual programmed death receptor-1 and vascular endothelial growth factor receptor-2 blockade promotes vascular normalization and enhances antitumor immune responses in hepatocellular carcinoma. Hepatology. 2020; 71:1247-1261.
29. Zhou KQ, Zhong YC, Song MF, Sun YF, Zhu W, Cheng JW, Xu Y, Zhang ZF, Wang PX, Tang Z, Zhou J, Zhang LY, Fan J, Yang XR. Distinct immune microenvironment of venous tumor thrombus in hepatocellular carcinoma at single-cell resolution. Hepatology. 2025; 82:566-581.
30. Tong W, Zhong J, Yang Q, Lin H, Chen B, Lu T, Chen J, Luo N. Single-cell and bulk transcriptomic datasets enable the development of prognostic models based on dynamic changes in the tumor immune microenvironment in patients with hepatocellular carcinoma and portal vein tumor thrombus. Front Immunol. 2024; 15:1414121.
31. Lai Z, He M, Bu X, Xu Y, Huang Y, Wen D, Li Q, Xu L, Zhang Y, Wei W, Chen M, Kan A, Shi M. Lenvatinib, toripalimab plus hepatic arterial infusion chemotherapy in patients with high-risk advanced hepatocellular carcinoma: A biomolecular exploratory, phase II trial. Eur J Cancer. 2022; 174:68-77.
32. Zhang TQ, Geng ZJ, Zuo MX, Li JB, Huang JH, Huang ZL, Wu PH, Gu YK. Camrelizumab (a PD-1 inhibitor) plus apatinib (an VEGFR-2 inhibitor) and hepatic artery infusion chemotherapy for hepatocellular carcinoma in Barcelona Clinic Liver Cancer stage C (TRIPLET): A phase II study. Signal Transduct Target Ther. 2023; 8:413.
33. Zang M, Li Q, Hu X, Pang H, Li R, Li W, Chen Y, Zhu P, Su K, Yuan G, Li Y, Li Y, Chen J. Camrelizumab combined with lenvatinib and RALOX-hepatic arterial infusion chemotherapy for unresectable hepatocellular carcinoma (Cal Era): A prospective, single-arm, phase II trial. Liver Cancer. 2025; 14:731-742.
34. Shen L, Cao F, Liu Y, Nuerhashi G, Lin L, Tan H, Wen C, Wang Y, Chen S, Zou H, Xie L, Fan W. Hepatic artery infusion of FOLFOX chemotherapy plus camrelizumab combined with sorafenib for advanced hepatocellular carcinoma in Barcelona Clinic Liver Cancer stage C (Double-IA-001): A phase II trial. BMC Med. 2025; 23:275.
35. Li Y, Guo J, Liu W, Pang H, Song Y, Wu S, Zhang F, Yan D, Chen J, An C, Li C. Hepatic artery infusion chemotherapy combined with camrelizumab plus rivoceranib for hepatocellular carcinoma with portal vein tumor thrombosis: A multicenter propensity score-matching analysis. Hepatol Int. 2024; 18:1286-1298.
36. Zuo M, Zheng G, Cao Y, Lu H, Li D, An C, Fan W. Hepatic arterial chemotherapy infusion combined with tyrosine kinase inhibitors and PD-1 inhibitors for advanced hepatocellular carcinoma with high risk: A propensity score matching study. Int J Surg. 2025; 111:104-112.
37. Tang S, Shi F, Xiao Y, Cai H, Ma P, Zhou Y, Wu Z, Chen S, Guo W. HAIC plus lenvatinib and tislelizumab for advanced hepatocellular carcinoma with Vp4 portal vein invasion. Hepatol Int. 2025; 19:106-117.
38. Wang X, Chen S, Yu W, Liu W, Fang Z. A retrospective study of hepatic arterial infusion chemotherapy combined with tyrosine kinase inhibitors and PD-1 inhibitors in hepatocellular carcinoma patients with main portal vein tumor thrombus (Vp4). J Hepatocell Carcinoma. 2026; 13:562766.
39. Liu W, Zhang K, Chen S, Wang X, Yu W. Hepatic arterial infusion chemotherapy plus tyrosine kinase inhibitors with or without PD-1 inhibitors for advanced hepatocellular carcinoma with Vp4 portal vein tumor thrombosis: A retrospective cohort study. Front Immunol. 2026; 17:1832313.
40. Yuan Y, He W, Yang Z, Qiu J, Huang Z, Shi Y, Lin Z, Zheng Y, Chen M, Lau WY, Li B, Yuan Y. TACE-HAIC combined with targeted therapy and immunotherapy versus TACE alone for hepatocellular carcinoma with portal vein tumour thrombus: A propensity score matching study. Int J Surg. 2023; 109:1222-1230.
41. Guan R, Zhang N, Deng M, Lin Y, Huang G, Fu Y, Zheng Z, Wei W, Zhong C, Zhao H, Mei J, Guo R. Patients with hepatocellular carcinoma extrahepatic metastases can benefit from hepatic arterial infusion chemotherapy combined with lenvatinib plus programmed death-1 inhibitors. Int J Surg. 2024; 110:4062-4073.
42. Luo L, Xiao Y, Zhu G, Huang A, Song S, Wang T, Ge X, Xie J, Deng W, Hu Z, Wen W, Mei H, Wan R, Shan R. Hepatic arterial infusion chemotherapy combined with PD-1 inhibitors and tyrosine kinase inhibitors for unresectable hepatocellular carcinoma: A tertiary medical center experience. Front Oncol. 2022; 12:1004652.
43. Liu BJ, Gao S, Zhu X, Guo JH, Kou FX, Liu SX, Zhang X, Wang XD, Cao G, Chen H, Liu P, Xu HF, Gao QZ, Yang RJ. Real-world study of hepatic artery infusion chemotherapy combined with anti-PD-1 immunotherapy and tyrosine kinase inhibitors for advanced hepatocellular carcinoma. Immunotherapy. 2021; 13:1395-1405.
44. Yalikun K, Li Z, Zhang J, *et al*. Hepatic artery infusion chemotherapy combined with camrelizumab and apatinib as conversion therapy for patients with unresectable hepatocellular carcinoma: A single-arm exploratory trial. BMC Cancer. 2025; 25:838.
45. Liu J, Zhang S, Shao H. Hepatic arterial infusion chemotherapy plus lenvatinib and PD-1 inhibitors versus lenvatinib plus PD-1 inhibitors as first-line treatment for hepatocellular carcinoma with high tumour burden and portal vein tumour thrombus (CHANCE 2416): Study protocol of a multicentre, retrospective, target trial

emulation design. BMJ Open. 2025; 15:e099510.
46. Wang J, Hu Y, Zhou L, Yang Y, Chen J, Chen H, Wang H. Non-surgery strategy versus hepatectomy in hepatocellular carcinoma patients with complete response after conversion therapy: A meta-analysis. World J Surg Oncol. 2024; 22:349.
47. de Franchis R, Bosch J, Garcia-Tsao G, Reiberger T, Ripoll C, Baveno VII Faculty. Baveno VII - Renewing consensus in portal hypertension. J Hepatol. 2022; 76:959-974.
48. Han T, Chen L, Liu N, *et al*. Repurposed acarbose targets nidogen-1 to remodel the tumor stroma and suppress portal vein tumor thrombus in hepatocellular carcinoma. Research (Wash D C). 2026; 9:1161.
49. Hwang JP, Feld JJ, Hammond SP, Wang SH, Alston-Johnson DE, Cryer DR, Hershman DL, Loehrer AP, Sabichi AL, Symington BE, Terrault N, Wong ML, Somerfield MR, Artz AS. Hepatitis B virus screening and management for patients with cancer prior to therapy: ASCO provisional clinical opinion update. J Clin Oncol. 2020; 38:3698-3715.
50. ClinicalTrials.gov. Combination therapy of HAIC and HLX10 and HLX04 in HCC with major portal vein tumor thrombosis (NCT04947826). *https://clinicaltrials.gov/study/NCT04947826* (accessed August 13, 2026).
51. Yoon SM, Ryoo BY, Lee SJ, Kim JH, Shin JH, An JH, Lee HC, Lim YS. Efficacy and safety of transarterial chemoembolization plus external beam radiotherapy vs sorafenib in hepatocellular carcinoma with macroscopic vascular invasion: A randomized clinical trial. JAMA Oncol. 2018; 4:661-669.
52. Dawson LA, Winter KA, Knox JJ, *et al*. Stereotactic body radiotherapy vs sorafenib alone in hepatocellular carcinoma: The NRG Oncology/RTOG 1112 phase 3 randomized clinical trial. JAMA Oncol. 2025; 11:136-144.
53. Silva JP, Berger NG, Tsai S, Christians KK, Clarke CN, Mogal H, White S, Rilling W, Gamblin TC. Transarterial chemoembolization in hepatocellular carcinoma with portal vein tumor thrombosis: A systematic review and meta-analysis. HPB (Oxford). 2017; 19:659-666.
54. Kim PH, Choi SH, Kim JH, Park SH. Comparison of radioembolization and sorafenib for the treatment of hepatocellular carcinoma with portal vein tumor thrombosis: A systematic review and meta-analysis of safety and efficacy. Korean J Radiol. 2019; 20:385-398.
55. Vilgrain V, Pereira H, Assenat E, *et al*. Efficacy and safety of selective internal radiotherapy with yttrium-90 resin microspheres compared with sorafenib in locally advanced and inoperable hepatocellular carcinoma (SARAH): An open-label randomised controlled phase 3 trial. Lancet Oncol. 2017; 18:1624-1636.
56. Chow PKH, Gandhi M, Tan SB, *et al*. SIRveNIB: Selective internal radiation therapy versus sorafenib in Asia-Pacific patients with hepatocellular carcinoma. J Clin Oncol. 2018; 36:1913-1921.
57. Liu B, Grindrod N, Meyers BM, Freiburger S, Boldt G, Malik A, Jairam MP, Brahmania M, Cardarelli Leite L, Simone CB 2nd, Chow R, Lock M. Treatment modalities to manage hepatocellular carcinoma patients with portal vein thrombosis: A systematic review and meta-analysis. Ann Palliat Med. 2023; 12:1165-1174.
58. Leung JH, Wang SY, Leung HWC, Chan ALF. Comparative efficacy and safety of multimodality treatment for advanced hepatocellular carcinoma with portal vein tumor thrombus: Patient-level network meta-analysis. Front Oncol. 2024; 14:1344798.
59. Eisenhauer EA, Therasse P, Bogaerts J, *et al*. New response evaluation criteria in solid tumours: Revised RECIST guideline (version 1.1). Eur J Cancer. 2009; 45:228-247.
60. Lencioni R, Llovet JM. Modified RECIST (mRECIST) assessment for hepatocellular carcinoma. Semin Liver Dis. 2010; 30:52-60.
61. Johnson PJ, Berhane S, Kagebayashi C, *et al*. Assessment of liver function in patients with hepatocellular carcinoma: A new evidence-based approach-the ALBI grade. J Clin Oncol. 2015; 33:550-558.
62. Hernan MA, Robins JM. Using big data to emulate a target trial when a randomized trial is not available. Am J Epidemiol. 2016; 183:758-764.
63. Hernan MA, Sauer BC, Hernandez-Diaz S, Platt R, Shrier I. Specifying a target trial prevents immortal time bias and other self-inflicted injuries in observational analyses. J Clin Epidemiol. 2016; 79:70-75.

Received July 12, 2026; Revised August 22, 2026; Accepted August 25, 2026.

[§]These authors contributed equally to this work.
**Address correspondence to:*
Lin Wang and Zhitian Shi, Second Department of Hepatobiliary and Pancreatic Surgery, The Second Affiliated Hospital of Kunming Medical University, Kunming 650101, China.
E-mail: wlgcpkmu@163.com (LW); sztkmmu@163.com (ZS)

Released online in J-STAGE as advance publication August 28, 2026.

Review

DOI: 10.5582/bst.2026.01150

Stem cell-derived extracellular vesicles for rare diseases: A clinical -bottleneck-to-mechanism framework for translation

Yue Han[1], Nuo Chen[1], Peipei Song[2], Yanling Chen[3,4,*], Wei Tang[2,3,5,*]

[1] Department of Dermatology, The Union Hospital, Fujian Medical University, Fuzhou, Fujian, China;
[2] Japan Institute for Health Security, Tokyo, Japan;
[3] Department of Hepatobiliary Surgery, Fujian Institute of Hepatobiliary Surgery, Fujian Medical University Union Hospital, Fuzhou, Fujian, China;
[4] Fujian Key Laboratory of Tumor Microbiology, Department of Medical Microbiology, Fujian Medical University, Fuzhou, Fujian, China;
[5] Hepato-Biliary-Pancreatic Surgery Division, Department of Surgery, Graduate School of Medicine, The University of Tokyo, Tokyo, Japan.

SUMMARY: Rare diseases impose a disproportionate clinical burden, and yet therapeutic progress is hindered by small cohorts, biological heterogeneity, and limited disease-specific options. Stem cell-derived extracellular vesicles (EVs), and especially exosome-enriched products, are emerging as adaptable cell-free therapeutics that preserve key paracrine activities of parent cells while offering improved controllability, engineering flexibility, and potentially lower acute immunogenicity than living-cell products. This review proposes a clinically driven bottleneck-to-mechanism framework for rare-disease translation, matching each disease class to its dominant pathological barrier, mechanism-relevant EV function, route-aware delivery strategy, and measurable potency endpoint. Using this framework, EVs may enable immune circuit rewiring in autoimmune disorders, neuroprotection and toxic-protein clearance in neurodegeneration, osteogenic and matrix-supportive repair in skeletal/connective tissue diseases, and metabolic rescue in lysosomal or mitochondrial disorders. We further highlight a key conceptual distinction between EVs as active biologics and EVs as engineered delivery vehicles. Successful translation will depend on integrating cargo design, surface targeting, biodistribution-aware administration, scalable manufacturing, and quality-by-design control, while anticipating repeat-dose pharmacokinetics/pharmacodynamics (PK/PD), immunogenicity, complement activation, procoagulant risk, impurity control, and off-target organ-accumulation challenges. Multi-omics and artificial intelligence may further refine target selection and precision engineering. Overall, stem cell-derived EVs constitute a versatile platform for treating rare diseases, but clinical success requires closer alignment among mechanism, disease specificity, product definition, and translational endpoints.

Keywords: extracellular vesicles, exosomes, rare diseases, mesenchymal stem cells, cargo engineering, surface targeting, artificial intelligence

1. Introduction

Rare diseases, despite their low individual prevalence, collectively impose a major medical and societal burden. Their marked genetic heterogeneity, limited number of patients, and often severe phenotypes complicate mechanistic studies, biomarker discovery, and therapeutic development (*1-3*). Conventional drug-development pipelines are particularly strained in this setting because small trial populations restrict statistical power, lengthen recruitment, and lessen commercial incentives. As a result, many rare disorders still lack disease-modifying therapies, highlighting the need for therapeutic platforms that can be adapted across mechanistically distinct indications (*4,5*).

Stem cell-based interventions have emerged as one such platform, with mesenchymal stem cells (MSCs) receiving particular attention because of their immunomodulatory activity, trophic secretome, and relative ease of procurement from bone marrow, adipose tissue, the umbilical cord, or related sources (*6-8*). However, direct cell transplantation faces persistent barriers, including variable engraftment, potential immunogenicity, theoretical tumorigenicity, ethical and manufacturing concerns, and inconsistent *in vivo* behavior across donors and culture conditions (*9,10*). These limitations have motivated interest in cell-free strategies that retain biological activity while improving safety, controllability, and scalability.

Among these strategies, stem cell-derived extracellular vesicles (EVs), and particularly exosome-enriched EV preparations, have become especially

attractive. EVs are lipid bilayer membrane-delimited particles released by cells; exosomes refer to an endosome-derived subtype, but most studies cannot prove biogenesis and should therefore report EV subtypes operationally and transparently. This terminology and reporting rigor are codified in minimal information for studies of extracellular vesicles (MISEV) guidelines, most recently updated as MISEV2023 (*11*). Importantly, EVs can recapitulate many beneficial paracrine effects of their parent cells while reducing risks associated with living-cell administration, such as ectopic engraftment or uncontrolled proliferation (*12,13*). Their relative stability in biological fluids, low immunogenicity, and ability to traverse selected biological barriers further enhance their appeal as rare–disease therapeutics (*14,15*).

The therapeutic logic of mesenchymal stem cell-derived EVs (MSC-EVs) is increasingly being defined at the level of mechanism rather than broad claims of regeneration. Here, regeneration is treated as a phenotypic outcome category; our emphasis is on mechanism-linked, testable endpoints that can serve as potency readouts and guide translation under small-cohort constraints. Their cargo can reshape inflammatory signaling, attenuate apoptosis, promote angiogenesis and tissue repair, and support metabolic homeostasis in recipient cells (*16-19*). In immune-mediated settings, MSC-EVs can reprogram macrophages, T-cell subsets, and cytokine networks; in neurological disease, they can provide trophic support and modulate neuroinflammation; and in tissue-fragility or metabolic disorders, they can be engineered to enhance pathway-specific correction (*20-23*).

Nonetheless, clinical translation remains constrained by unresolved issues in product definition, large-scale manufacturing, biodistribution, route selection, and potency testing. EV composition varies with cell source, donor state, priming conditions, and purification workflow, making batch comparability a central challenge rather than a secondary technical detail (*24-27*). Accordingly, progress in treating rare diseases will depend on integrating mechanistic precision, rare-disease clinical bottlenecks, engineering design, and regulatory–grade manufacturing into a single development framework.

At the same time, the pathways discussed in EV studies are not inherently novel therapeutic targets. Cytokine networks, AKT/ERK-linked survival signaling, Wnt-associated repair programs, and phagocyte responses are already addressed to varying degrees by existing biologics or small molecules. The justification for developing EV therapeutics is therefore not simply that they can affect these pathways but that they may combine multi-cargo biologic signaling, intracellular or nucleic-acid delivery, and route- or barrier-aware tissue access within a single platform, which may be especially relevant when rare-disease pathology involves several coupled bottlenecks that are not easily addressed by a single conventional agent. Conversely, when an approved drug already provides robust pathway control with acceptable safety, EV development should be justified by a clear added value such as improved tissue access, lower systemic exposure, combination-cargo capability, or the ability to support mutation-directed delivery rather than pathway modulation alone.

Compared to enzyme replacement therapy (ERT), antisense oligonucleotides (ASOs), AAV gene therapy, small-molecule chaperones, and immune biologics, EVs should not be considered to be intrinsically superior in treating every rare disease. Their realistic value is context-dependent: multi-cargo delivery when inflammatory, metabolic, and repair pathways must be modulated together; route-aware tissue access through local, intranasal, or matrix-retained delivery; lower systemic exposure when pathology is regional; surface/cargo engineering that combines targeting ligands with RNA, protein, enzyme, or small-molecule payloads; and adjunctive use with ERT, ASO, AAV, or biologics to improve tissue residence, reduce local inflammation, or broaden pathway coverage. Thus, EV development should be justified indication by indication by a measurable added value over available modalities.

As shown in Figure 1, the development pathway of stem cell-derived exosome therapy for rare diseases extends from fundamental exosome features and core therapeutic mechanisms to disease-specific preclinical advances in genetic metabolic, neurodegenerative, and skeletal or connective-tissue rare disorders, and then onward to clinical translation. In this review, we intentionally adopt a clinical-bottleneck-to-mechanism framework and focus on representative rare-disease classes where *i*) a dominant bottleneck can be identified, *ii*) EV mechanisms can be linked to measurable endpoints, and *iii*) translational constraints can be discussed in specific terms. We do not aim for exhaustive coverage of all rare diseases; instead, we emphasize design logic that can be re-used across indications. We emphasize four themes that are especially important for rare-disease translation: disease-matched mechanism selection, engineering logic for cargo and surface modification, clinically relevant delivery-route design, and manufacturing/regulatory strategies that can facilitate scalable and reproducible products (*28,29*).

2. Biological characteristics of stem cell-derived exosomes and their potential mechanisms in the treatment of rare diseases

2.1. Biogenesis, composition, and functions of exosomes

Exosomes are small EVs generated through the endosomal pathway, in which inward budding of endosomal membranes forms multivesicular bodies that subsequently fuse with the plasma membrane to release vesicles into the extracellular space. This biogenesis route shapes both membrane composition and cargo architecture, yielding vesicles enriched in canonical

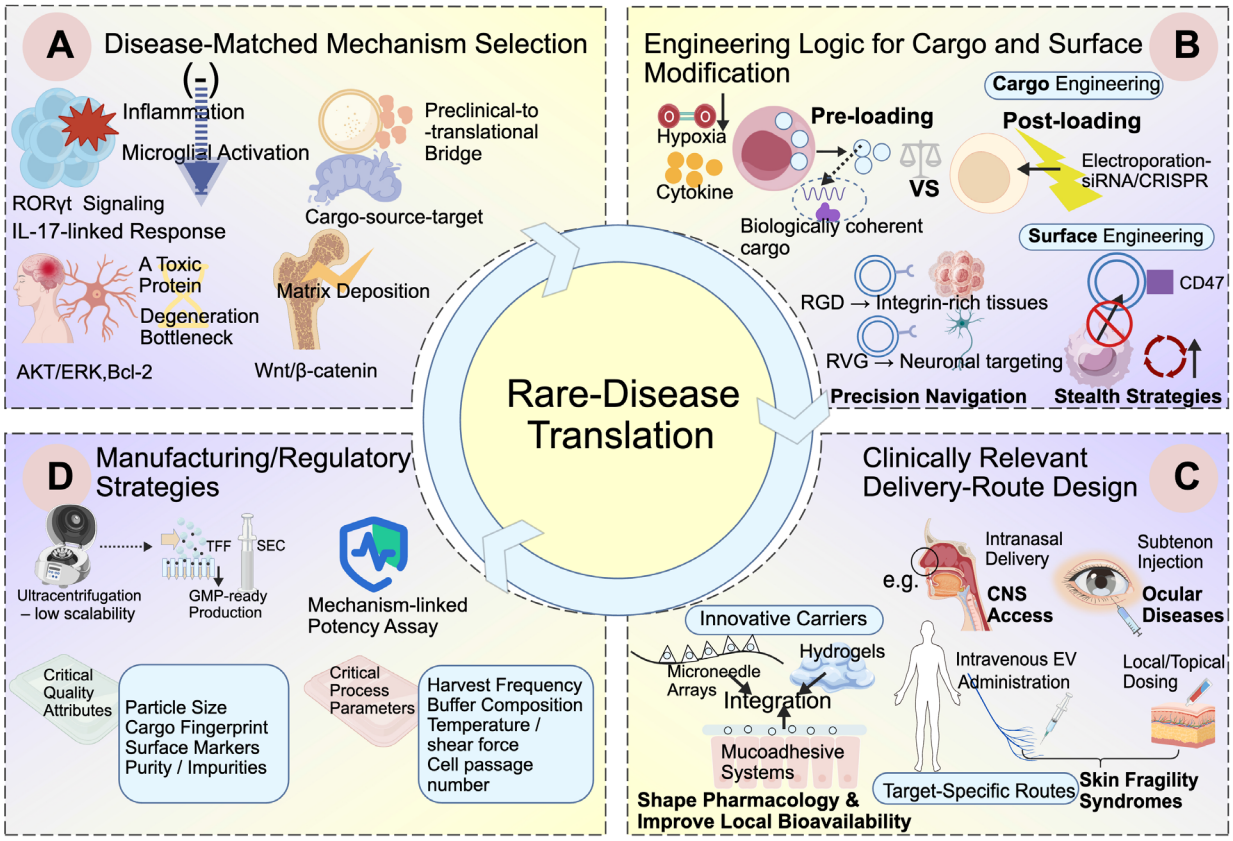


Figure 1. Clinically aligned translational workflow for stem cell-derived EV therapy in rare diseases. (A) Disease-matched mechanism selection: dominant disease bottlenecks are first defined and paired with EV functions, including suppression of inflammation and microglial activation, inhibition of RORγt/IL-17-linked immune responses, AKT/ERK–Bcl-2-associated neuroprotection, and Wnt/β-catenin-mediated matrix or bone repair. **(B)** Cargo and surface engineering: EVs may be modified through pre-loading strategies such as hypoxia or cytokine priming to enrich biologically coherent cargo or through post-loading methods such as electroporation to deliver siRNA, CRISPR-related components, or other defined payloads. Surface ligands, including RGD- or RVG-like motifs and CD47-based stealth modules, can improve tissue navigation and reduce phagocytic clearance. **(C)** Delivery-route design: intranasal, subtenon, intravenous, local, or topical administration is selected according to target tissue, while hydrogels, microneedle arrays, and mucoadhesive systems improve retention and local bioavailability. **(D)** Manufacturing and regulatory strategies: scalable purification, GMP-compatible production, critical quality attributes, critical process parameters, and mechanism-linked potency assays support reproducibility. **(E)** Integrated rare-disease translation: mechanism, engineering, route, manufacturing, and clinical endpoints are iteratively aligned.

markers such as CD9, CD63, and CD81, together with lipids, miRNAs, mRNAs, circular RNAs, enzymes, cytokines, and growth-related proteins (*30,31*). Because definitive assignment to "exosomes" requires evidence of biogenesis, we refer to "EVs" or "exosome-enriched EVs" when appropriate, and emphasize transparent reporting consistent with MISEV guidelines.

From a translational perspective, EV product information can be organized into three interacting layers (Figure 2): a payload layer consisting of miRNA, mRNA, proteins, lipids, enzymes, and any engineered therapeutic cargo; a navigation layer consisting of integrins, tetraspanins, adhesion molecules, targeting ligands, and anti-phagocytic or stealth modules that influence tissue tropism and uptake; and a manufacturing layer consisting of the source cell type, donor variability, passage number, culture and priming conditions, the method of purification, storage, and release testing. This layered framework explains why two products labeled simply as MSC-exosome may display markedly different *in vivo* behavior even when their operational identity-marker profiles appear similar.

MSC-EVs are particularly relevant to rare diseases because they often carry pro-repair and immunoregulatory cargo, including miR-21, miR-146a, members of the let-7 family, HGF, and VEGF, while also retaining membrane features that can influence uptake in target tissues (*17,31,32*). Together, these properties position EVs as natural nanocarriers that couple biological signaling with delivery potential. For rare-disease applications, however, descriptive marker panels are insufficient; functional interpretation must be linked to the disease bottleneck the vesicles are intended to overcome.

2.2. Core mechanisms underlying the therapeutic effects of EVs on rare diseases

A more clinically useful framework is to map a dominant EV mechanism to a dominant disease bottleneck (Figure 3). Importantly, rare-disease relevance is established by

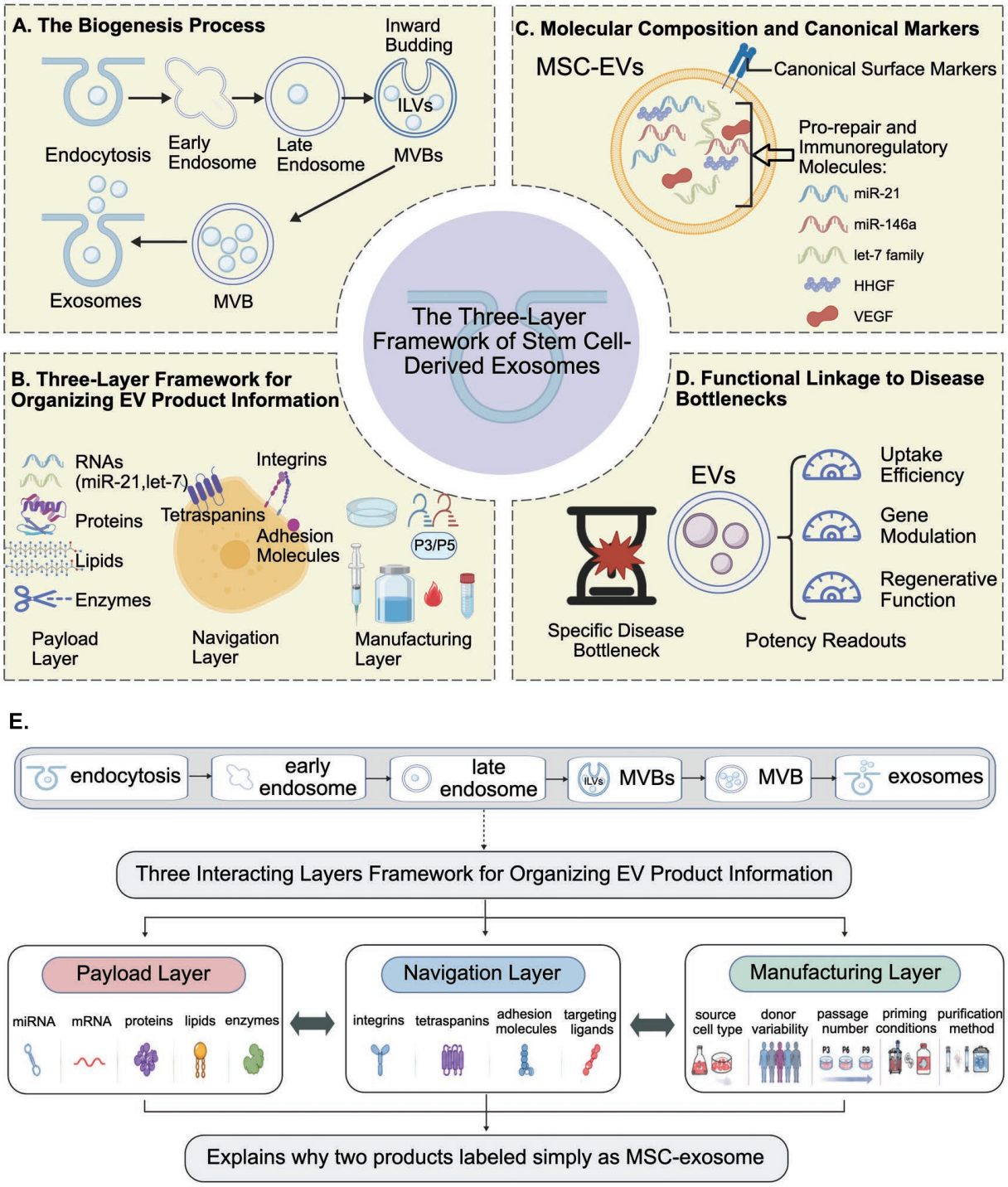


Figure 2. Biological characteristics of stem cell-derived exosomes. (A) Biogenesis process: exosomes arise from the endosomal pathway, in which endocytosis forms early endosomes, late endosomes, and multivesicular bodies; fusion of multivesicular bodies with the plasma membrane releases intraluminal vesicles as exosomes. **(B)** Three-layer framework: EV product information is organized into a payload layer, navigation layer, and manufacturing layer. The payload layer includes miRNAs, mRNAs, proteins, lipids, enzymes, cytokines, and engineered cargo; the navigation layer includes tetraspanins, integrins, adhesion molecules, targeting ligands, and anti-phagocytic modules; the manufacturing layer includes cell source, donor variability, passage number, culture conditions, purification, storage, and release testing. **(C)** Molecular composition and canonical markers: MSC-EVs commonly express CD9, CD63, and CD81 and carry regulatory cargo such as miR-21, miR-146a, let-7 family members, HGF, and VEGF. **(D)** Functional linkage to disease bottlenecks: after uptake, EVs may modulate inflammation, gene expression, angiogenesis, survival, metabolic stress, and repair pathways. **(E)** Product heterogeneity: differences in source and manufacturing explain why similarly named MSC-EV products may exhibit distinct potency and biodistribution.

bottleneck matching and measurable endpoints, not by claims that a pathway is unique to rare diseases.

In immune-mediated rare disorders, the relevant biology is not a generic anti-inflammatory effect, but selective rewiring of pathogenic immune circuits. EVs enriched in miR-146a can suppress inflammatory amplification, lessen microglial activation, and restrain Th17-skewed responses, while MSC-derived vesicles

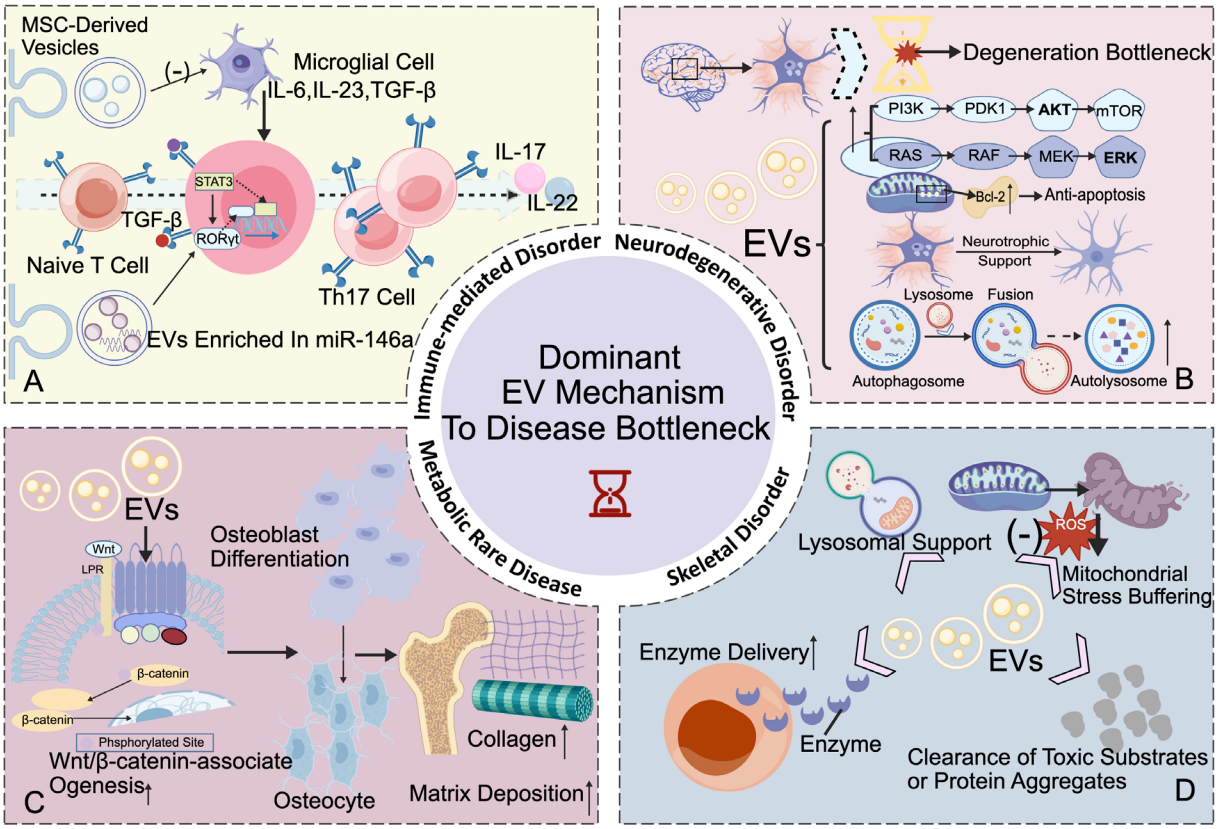


Figure 3. Mechanism-to-bottleneck matching of stem cell-derived EVs in representative rare-disease classes. (A) Immune-mediated rare diseases: MSC-EVs, and especially those enriched in miR-146a, may suppress microglial activation and inflammatory cytokines such as IL-6, IL-23, and TGF-β, thereby reducing STAT3/RORγt-driven Th17 differentiation and downstream IL-17/IL-22 effector responses. **(B)** Neurodegenerative rare diseases: EVs may protect vulnerable neurons by activating PI3K/AKT and RAS/RAF/MEK/ERK signaling, increasing Bcl-2-associated anti-apoptotic activity, reducing glial inflammatory stress, and facilitating autophagy-mediated clearance of toxic proteins through autophagosome–autolysosome flux. **(C)** Skeletal and connective-tissue rare diseases: EVs may enhance Wnt/β-catenin-associated osteogenesis, promote osteoblast differentiation, osteocyte maturation, mineralization, and extracellular-matrix deposition, which is particularly relevant to collagen-defective skeletal fragility. **(D)** Metabolic rare diseases: engineered or selected EVs may deliver enzymes, regulatory RNAs, or proteins that support lysosomal function, substrate clearance, mitochondrial stress buffering, mitophagy, and metabolic rescue. **(E)** Central principle: therapeutic EV development should match the key disease bottleneck with a measurable EV mechanism, including target-cell uptake, pathway engagement, biomarker modulation, and functional rescue.

have also been shown to destabilize RORγt signaling and reduce IL-17-linked effector programs (*33-35*). This logic is especially relevant to autoimmune encephalitis and related rare neuroimmune phenotypes.

In neurodegenerative disorders such as amyotrophic lateral sclerosis (ALS) and Huntington's disease, the central therapeutic priority shifts to preservation of vulnerable neurons and support cells in the presence of a toxic protein/degeneration bottleneck, where AKT/ERK activation, Bcl-2 upregulation, neurotrophic support, and autophagy enhancement are more informative mechanistic anchors than the broad claim of regeneration (*36-38*).

In skeletal disorders such as osteogenesis imperfecta, the key question becomes whether EVs can activate Wnt/β-catenin-associated osteogenesis, improve osteoblast differentiation, and support matrix deposition in a collagen-defective microenvironment (*39,40*).

The mechanistic emphasis changes again in metabolic rare diseases, where enzyme delivery, lysosomal support, mitochondrial stress buffering, and clearance of toxic substrates or protein aggregates may be more relevant than conventional regenerative endpoints (*41,42*). For these disorders, the most persuasive preclinical-to-translational bridge is a potency assay tied to enzyme activity, substrate burden, or organelle stress readouts. Representative cargo-source-target relationships that sharpen this logic are summarized in Table 1.

3. Preclinical advances in stem cell-derived exosomes to treat various rare diseases

Rare-disease preclinical models require critical appraisal. Although encouraging preclinical signals were summarized, the field faces a fundamental translational bottleneck: many monogenic rare-disease animal models only partially reproduce the full human phenotype, organ involvement, and time course, and they may compress or distort clinically relevant progression windows (*43*). For EV therapeutics, this matters because short-

Table 1. Representative cargo-source-target relationships that further define the mechanism-to-disease logic in exosome therapy for rare diseases

Stem cell source	Representative cargo	Rare-disease target/pathway	Example disease	Expected biological effect	Key caveat
Bone marrow MSCs	Osteogenic miRNAs, VEGF/HGF, pro-survival proteins	Wnt/β-catenin, AKT/ERK, COL1A1/2-related osteoblast program	Osteogenesis imperfecta	Osteoblast differentiation, vascular support, anti-apoptotic rescue	Requires osteogenesis-linked potency assay
Adipose MSCs	miR-146a, HGF, anti-inflammatory lipids	RORγt/Th17, NF-kB and NOTCH1 inflammatory circuits	Autoimmune encephalitis, rare immune phenotypes	Immune braking and cytokine reduction	May control phenotype without correcting a mutation
Umbilical cord MSCs	miR-124/miR-21, neurotrophic factors, low-immunogenic secretome	AKT/ERK-Bcl-2 axis, autophagy and CNS target engagement	ALS, Huntington's disease	Neuroprotection and support for BBB/intranasal delivery	Route optimization is decisive
Engineered parental MSCs	Loaded enzymes, siRNA/CRISPR cargo, VEGFC or other defined payloads	GBA/lysosome function, mutant HTT silencing, endothelial or lymphatic repair	Gaucher disease, Huntington's disease, rare lymphatic disorders	Metabolic rescue or precise pathway correction	Highest CMC and comparability burden

lived "phenotypic rescue" can be overestimated if the model's dominant failure mode differs from the human bottleneck. Accordingly, mechanistic endpoints should be treated as translatable only when they exist on a validated causal chain: EV exposure in the relevant tissue → target-cell uptake → pathway engagement → biomarker change → functional readout. We therefore recommend that rare-disease EV evidence be triangulated across complementary model layers (animal models, patient-derived iPSC/organoid systems, and disease-relevant *ex vivo* assays) and anchored to clinically interpretable biomarkers and natural-history knowledge where available (*44*).

3.1. Genetic metabolic rare diseases

In lysosomal and mitochondrial rare diseases, the bottleneck is often a defined metabolic deficit (enzyme deficiency, substrate accumulation, or organelle stress) for which phenotypic rescue may be achieved even without full genetic correction, provided a mechanism-linked axis is engaged.

In Gaucher disease and related lysosomal disorders, the appeal of EV therapy lies less in generalized regeneration than in whether vesicles can restore enzyme-dependent substrate handling in macrophages, glia, or neurons. Emerging evidence suggests that EVs can influence glucosylceramide trafficking, lysosomal function, and inflammatory amplification, but durable correction of glucosylceramidase β deficiency remains a preclinical objective rather than an achieved goal (*41*). Accordingly, translational claims in this area should carefully distinguish direct enzyme replacement from indirect lysosomal support or microenvironmental modulation.

In mitochondrial diseases, stem cell-derived exosomes are better viewed as tools for metabolic reprogramming than as complete genetic cures. Their cargo may modulate oxidative stress, mitophagy, mitochondrial biogenesis, and inflammatory crosstalk, thereby improving bioenergetic resilience in tissues with a high ATP demand (*42*). This distinction matters because partial restoration of stress-response pathways may still yield meaningful symptomatic benefit even when the causal mitochondrial or nuclear mutation is not directly corrected.

For metabolic rare diseases, the most informative preclinical readouts should therefore be mechanism-matched: enzyme activity, substrate burden, ATP production, reactive oxygen species levels, mitophagy markers, lysosome-autophagy flux, and tissue-specific functional rescue. These endpoints are more persuasive than broad histological improvement alone and are also more useful when translating a preclinical signal into a regulatory potency assay.

3.2. Neurodegenerative rare diseases

Central nervous system (CNS) rare diseases are dominated

by two coupled bottlenecks: tissue access and neuronal vulnerability/toxic protein burden, making route selection and target engagement inseparable from the mechanism.

In ALS, the rationale for MSC-EVs is strongest when neurotrophic support, control of neuroinflammation, and the route of administration are considered as a single therapeutic package. Exosomal miR-146a and trophic factors may modulate activated glia while *AKT/ERK-Bcl-2* signaling can protect stressed motor neurons, making the platform more than a passive substitute for the MSC secretome. CNS exposure remains a major bottleneck, so the route of delivery should be treated as part of the therapeutic hypothesis rather than as an aspect of the downstream formulation.

Huntington's disease illustrates why engineered exosomes may be more suitable than unmodified vesicles. Here, the dominant objective is to reduce the toxic huntingtin burden while preserving susceptible neurons, which makes gene-silencing cargo, CRISPR/Cas9-compatible loading strategies, and autophagy-enhancing signals especially relevant (*38,45*). In this context, exosomes function less as generalized anti-inflammatory vesicles and more as programmable nanocarriers for CNS target engagement.

Overall, neurodegenerative rare diseases indicate that the mechanism, tropism, route, dosing interval, and potency cannot be developed independently. Once the target tissue is the brain or spinal cord, surface engineering, intranasal design, blood-brain barrier models, and target-cell uptake assays become central translational variables rather than optional refinements.

3.3. Rare skeletal and connective tissue diseases

For skeletal/connective tissue rare diseases, the bottleneck often lies in matrix fragility and impaired cell-program execution, meaning that "repair" must be framed as program rescue rather than generic regeneration.

In osteogenesis imperfecta, the most persuasive therapeutic use of MSC-EVs is to drive osteoblast differentiation in a collagen-defective setting. Efficacy claims should therefore be linked explicitly to Wnt/β-catenin activation, Runx2/ALP-associated osteogenic programs, and matrix mineralization, rather than to broad regenerative language (*40*). This tighter framing better matches the biology of COL1A1/COL1A2-associated bone fragility and clarifies why osteogenesis-linked potency assays are essential.

For recessive dystrophic epidermolysis bullosa (RDEB) and related connective-tissue fragility syndromes, exosome therapy currently targets the wound-healing phenotype more than the germline defect itself. Near-term goals include local immune control, re-epithelialization, improved extracellular-matrix remodeling, and reduction of the chronic wound burden. That distinction is clinically important because a wound-directed extracellular-vesicle product may still provide meaningful benefit before direct mutation correction becomes feasible.

Evidence for treatment of Ehlers-Danlos syndrome remains limited and should be presented cautiously. At present, Ehlers-Danlos syndrome is best viewed as a hypothesis-generating indication in which exosomes may modulate fibroblast behavior and matrix homeostasis, but disease-specific efficacy data remain sparse. Stating this limitation explicitly strengthens the scientific rigor of this review.

4. Clinical translation status and challenges of stem cell-derived exosome therapy for rare diseases

4.1. Early clinical trials and safety evaluation

As summarized in Supplementary Table S1 (*https://www.biosciencetrends.com/action/getSupplementalData.php?ID=306*), which consolidates the current rare-disease trial landscape from public registries, a consistent pattern emerges from this landscape: stem cell-derived EV/exosome-enriched studies of rare diseases remain in the early phase, have a small sample size, and are highly dependent on the route of administration. Ocular programs rely on subtenon injection, RDEB studies range from topical/local wound dosing to intravenous EV administration, and neuroimmune or neuromuscular programs increasingly favor intranasal delivery.

The congenital myasthenic syndrome study (NCT07226726) is especially instructive because intranasal delivery is treated as part of the therapeutic concept rather than as a secondary formulation choice. Intranasal administration may partly reduce systemic dilution and improve access to neuro-immune interfaces, but it also introduces additional variables, including nasal mucosal integrity, dose reproducibility, device compatibility, and residence time. The MESAE trial in autoimmune encephalitis (NCT07131683) likewise aligns the route, repeated dosing, and neurological outcome scales, illustrating how mechanism–aware trial design is beginning to emerge in the field.

At the same time, the public evidence base remains immature. Several registry entries still lack posted results, and record updates do not always keep pace with estimated completion dates or real-world study progress. At present, the most defensible clinical conclusion is feasibility and early safety rather than definitive disease modification.

4.2. Major challenges in clinical translation

The immediate barrier to clinical translation is not conceptual promise but product definition. For systemic and lifelong rare-disease indications, product definitions also need to anticipate exposure limits (PK/PD and biodistribution) and the possibility that repeat dosing will alter clearance and response. For rare-disease programs, an EV product should be described by a minimum

chemistry, manufacturing, and controls (CMC) package that includes the cell source, donor criteria, passage number, culture medium, conditioning strategy, harvest window, isolation train, storage conditions, and a potency assay explicitly linked to the intended mechanism. This aligns with the broader rare–disease development reality recognized by FDA guidance: small cohorts amplify the impact of manufacturing variability, making comparability and robust endpoints central rather than optional.

The EV dose is not self-evident, so nominal doses should not be compared across studies using the particle number, total protein, producer-cell equivalent, or cargo copy number alone. For rare-disease translation, we recommend a layered dose description: the particle number measured *via* validated single-particle analysis; the total protein and particle-to-protein ratio as purity context; the producer-cell equivalent for manufacturing comparability; and the disease-relevant cargo copy number, enzyme activity, or functional cargo activity when the payload is engineered or mechanism-defining. Release and comparability decisions should prioritize a mechanism-linked potency readout normalized to both the particle number and, when relevant, cargo dose—for example, substrate clearance per particle dose, cytokine suppression per protein-normalized dose, target-gene knockdown per cargo copy, or enzyme activity restored per defined EV dose.

In practical manufacturing terms, this is why scale-out workflows based on ultracentrifugation are increasingly inadequate: tangential flow filtration, usually followed by polishing steps such as size-exclusion chromatography, is better suited for closed, reproducible, and higher-throughput production (*46,47*).

A quality-by-design (QbD) framework is especially valuable for exosome therapeutics. Candidate critical quality attributes (CQAs) include the particle size distribution, particle-to-protein ratio, operational identity-marker panels, sterility/endotoxin, residual host-cell DNA and protein, culture-medium or serum-derived impurities, cargo fingerprints, leakage/stability of externally loaded payloads, and mechanism-linked potency. Critical process parameters (CPPs) include oxygen tension, serum-free adaptation, the cell density, passage number, harvest frequency, buffer composition, tangential flow filtration (TFF) concentration factor, and freeze-thaw history. Without prospectively defining these variables, batch comparability becomes extremely difficult, which is particularly problematic when rare-disease trials enroll only a few patients and every manufacturing lot has outsized clinical influence.

Regulatory strategy must also be rare-disease-specific. Orphan indications often rely on small cohorts, so developers may require biomarker-enriched enrollment, adaptive designs, external or intra-patient controls, and route-specific safety monitoring. And yet orphan-disease flexibility in trial design does not reduce the need for stringent comparability packages: any change in the upstream culture, purification sequence, or loading method can reshape cargo composition and therefore biological activity. In other words, rare-disease development may justify flexible trials, but it also requires stricter analytics.

4.3. PK/PD, biodistribution, and dose-interval design

EV translation in systemic rare diseases is frequently exposure-limited: after intravenous administration, many EV formulations distribute rapidly to mononuclear phagocyte system (MPS)-rich organs such as the liver and spleen, which can reduce bioavailability in harder-to-reach targets. *In vivo* studies show that EV biodistribution depends on the cell source, dose, and route, with prominent accumulation in the liver and spleen after systemic delivery (*48*), and MPS-dominated uptake can contribute to short circulation half-lives in some settings (*49*).

Protein corona and disease state can re-program EV kinetics and cellular uptake. Recent work has indicated that the serum-derived protein corona composition can retarget MSC-EVs away from hepatic macrophages and toward non-phagocytic liver cells, implying that "surface identity" is not fixed at release but is remodeled *in vivo* (*50*).

A practical implication for rare-disease translation is to treat route selection and PK/PD as part of the therapeutic hypothesis: which tissue needs what EV exposure for how long, and what PD biomarker will confirm mechanism engagement. In small-cohort settings, longitudinal, mechanism-linked PD readouts (*e.g.*, enzyme activity, substrate burden, and inflammatory network shifts) are often more informative than single time-point histology.

Dose-interval selection remains a major challenge. Rather than defaulting to weekly or monthly regimens, the interval should be derived from the duration of the PD effect in the target tissue, with the recognition that repeat dosing can also change PK through immune recognition or MPS adaptation. A minimal "PK/PD starter pack" for translation therefore includes: *i*) biodistribution mapping in relevant models, *ii*) target-tissue residence estimates, *iii*) a PD biomarker time course, and *iv*) a pre-specified rule for dose-interval adjustment if PD decay precedes clinical benefit.

4.4. Long-term repeat dosing, immune recognition, and accelerated clearance

Long-term repeat dosing is the default scenario for many rare diseases. Although EVs are often described as having lower immunogenicity than living-cell products, EVs can carry immunologically active surface molecules and can intersect with antigen processing/presentation and adaptive immunity (*51*). For allogeneic stem-cell-derived EVs, repeated administration may

therefore generate anti-product antibodies or functional neutralization, which can manifest as diminishing efficacy or faster clearance—outcomes that regulators and clinical pharmacology frameworks treat as clinically meaningful because it modifies PK, PD, and safety (*52*).

The risk is not merely theoretical: experience from nanomedicines shows that repeated dosing of polyethylene glycol-conjugated (PEGylated) carriers can trigger anti-PEG IgM and complement activation, leading to an accelerated blood clearance phenomenon and altered biodistribution. PEG immunogenicity and anti-PEG antibody prevalence are now recognized as clinically relevant to safety and efficacy for some nanomedicine platforms (*53,54*).

Risk-mitigation principles for rare-disease EV programs include treating immunogenicity as a longitudinal PK/PD modifier, monitoring for anti-EV/anti-excipient antibodies and complement activation signals in repeat-dose studies, minimizing immunogenic impurities (*e.g.*, serum-derived contaminants), and considering dosing-route strategies that reduce systemic exposure when the mechanism allows (*e.g.*, local delivery for wound-dominant phenotypes).

Safety evaluation should extend beyond immunogenicity. EV preparations may expose a phosphatidylserine or tissue factor and thereby increase procoagulant potential; activate a complement; retain host-cell DNA, host-cell proteins, culture-medium contaminants, serum-derived impurities, or adventitious agents; release an exogenously loaded cargo before target-tissue uptake; and accumulate in off-target organs, and especially the MPS-rich liver and spleen after systemic delivery. Repeat-dose studies should therefore include hemocompatibility and thrombin-generation assays, complement split products, residual DNA/protein and media/serum impurity testing, endotoxin/mycoplasma/adventitious-agent release criteria, loaded-cargo leakage and stability assays, and biodistribution panels that quantify off-target accumulation in route-relevant organs.

5. Engineering and functional modification to enhance the therapeutic efficacy of stem cell-derived exosomes in rare diseases

5.1. Cargo engineering modification

Cargo engineering is best discussed as a design trade-off rather than a binary technical choice. Pre-loading strategies, including hypoxia conditioning, cytokine priming, and parental-cell genetic engineering, benefit from biological coherence because the payload is packaged through endogenous vesicle biogenesis and the native membrane architecture is usually better preserved (*17,39,55*). Their main limitation is that the absolute loading dose is less controllable and may drift across donors or batches. This makes pre-loading attractive when the therapeutic goal is systems-level reprogramming, such as amplifying angiogenic or anti-inflammatory tone, but less ideal when a monogenic disorder requires a defined amount of small interfering RNA, messenger RNA, antisense oligonucleotide, or gene-editing cargo.

Post-loading strategies such as electroporation, sonication, extrusion, and chemical transfection offer greater control over the identity and nominal amount of an added therapeutic payload. These approaches are therefore attractive for precision interventions, including siRNA, antisense oligonucleotides, protein cargo, or CRISPR/Cas9-related components (*43,56*). However, higher loading efficiency may come at the cost of vesicle aggregation, RNA precipitation artefacts, membrane injury, altered uptake behavior, or reduced functional potency. For that reason, post-loading workflows should always be paired with assays that assess membrane integrity, retained tropism, and mechanism-linked activity, rather than marker panels alone.

EVs can function as active biologics or as delivery vehicles. A frequent source of conceptual drift in the literature is whether EVs are the active therapeutic entity or whether they are used primarily as delivery vehicles for a defined exogenous payload. This distinction has implications for CMC control, potency testing, and regulatory classification and should be stated explicitly for each rare-disease application.

In rare diseases, the most rational selection rule is mechanism-driven: use pre-loading when the desired product is a biologically enriched secretome, and use post-loading when the therapeutic objective is delivery of a quantifiable mutation-directed payload. Hybrid strategies may be especially relevant when a disorder requires both immune modulation and pathway-specific correction. A concise comparison of these approaches is provided in Table 2.

5.2. Membrane surface engineering modification

Surface engineering marks the transition from passive biodistribution to precision navigation. Classical ligand decoration with arginine-glycine-aspartic acid (RGD) or rabies virus glycoprotein (RVG) peptides remains useful because it operationalizes tissue selectivity-RGD-like motifs for integrin-rich diseased tissues and RVG-like ligands for neuronal targeting. And yet the field is moving beyond fixed peptide tags toward modular navigation systems that combine targeting with triggered release. Magnetic guidance, photo–responsive membranes, and thermos-responsive shells remain largely preclinical, but they are conceptually important because they separate two questions that are often conflated: how to reach the tissue and how to release cargo once the vesicle arrives.

Stealth engineering is equally important. In practice, "stealth" is the engineering response to the MPS-clearance bottleneck described above: without

Table 2. Critical comparison of pre-loading and post-loading strategies for cargo engineering in exosome therapeutics for rare diseases

Strategy Class	Representative methods	Strengths	Limitations	Best-fit rare-disease scenarios
Pre-loading	Hypoxia, IFN-γ or cytokine priming	Preserves endogenous membrane and coordinated biology	Payload dose less controllable, batch drift	Angiogenic or immunomodulatory indications
Pre-loading	Parental-cell gene engineering	Stable enrichment with biologically coherent cargo	Cell-engineering burden, added regulatory complexity	Repeated delivery of defined trophic or miRNA cargo
Post-loading	Electroporation of siRNA/ASO/CRISPR	Direct control of mutation-matched payload	Aggregation, membrane injury, variable encapsulation	Monogenic or toxic-gain-of-function disorders
Post-loading	Sonication, extrusion, chemical transfection	Greater loading for drugs or proteins	May alter native surface proteins and biodistribution	Local delivery or combination products

mitigating opsonization and phagocytic uptake, systemic EV exposure can be dominated by liver-and spleen-associated macrophages rather than the intended target tissue (*49*). Display of CD47 or CD47-mimetic "don't eat me" signals may reduce phagocytic clearance and extend circulation time, whereas PEG-like shielding can improve colloidal stability but may also mask uptake ligands if overused (*18,43*). However, any stealth strategy intended for chronic dosing should be evaluated under repeat-dose conditions for immune recognition and clearance drift rather than assuming a stable single-dose PK profile (*53,54*). A practical design principle is therefore to balance persistence against target-cell internalization rather than maximizing only one of them.

For rare diseases that target the CNS, the next frontier is multicomponent surface design: a brain-penetrating motif, an anti-phagocytic module, and a disease-receptor recognition signal on the same vesicle, ideally paired with a route-specific strategy such as intranasal delivery. At that stage, surface engineering becomes translationally decisive rather than simply elegant.

6. Future perspectives: Exploring the translational pathway from basic research to clinical application

6.1. Integrating multi-omics technologies and artificial intelligence (AI) to decipher mechanisms

AI should not be considered merely as a future accessory; it can define the exosome-discovery workflow itself. A practical pipeline begins with multi-omics characterization of producer cells and exosome batches-proteomics for membrane ligands and soluble effectors, small-RNA sequencing for regulatory cargo, lipidomics for membrane behavior, and single-cell atlases of recipient tissues for receptor availability (*57-59*). These layers can then be integrated using graph-based or multimodal models to predict which vesicle compositions are most likely to bind, enter, and reprogram disease-related target cells.

Rare-disease-specific AI/omics research presents both constraints and opportunities. Rare diseases are defined not only by prevalence but by small cohorts, high heterogeneity, and often a strong genotype-to-phenotype axis; AI methods must therefore address small-N learning and cross-center data barriers. Rare-disease knowledge bases and genome-phenome platforms (*e.g.*, Orphanet/Orphadata and RD-Connect GPAP) provide a structured substrate for standardized phenotypes and gene-disease mapping that can be linked to EV design variables. Methodologically, transfer learning and federated learning are particularly relevant because they help extract a signal from distributed, privacy-constrained datasets without requiring central pooling.

This enables a true in an *in vivo* target-selection paradigm. Rather than manufacturing a vesicle first and only later determining where it reaches, developers can computationally rank membrane-protein/receptor pairs, prioritize candidate targeting motifs, and then validate them experimentally with barcoded vesicle libraries, organ-on-chip blood-brain barrier models, or patient-derived organoids. For rare diseases, where patient material is scarce, this approach is particularly valuable because it reduces wet-lab iteration and concentrates resources on the most biologically plausible candidates.

The long-term objective should be an Exosome Atlas that links the source cell, manufacturing state, cargo composition, biodistribution, potency readouts, and patient phenotype. In rare-disease medicine, such an atlas could serve both diagnostic and therapeutic purposes by identifying disease-associated vesicle signatures while also guiding source-matched or engineering-matched exosome design.

6.2. Establishing regulatory science and industrialization frameworks

Industrial production will depend on whether exosome manufacturing can be made auditable, closed, and digitally traceable. Bioreactor-based upstream culture, TFF/size-exclusion chromatography-based downstream purification, in-line environmental monitoring, and electronic batch records are not simply engineering upgrades; they are prerequisites for lot comparability in geographically distributed rare-disease trials.

A mature regulatory-science package should therefore include reference materials, orthogonal identity assays, route-specific release criteria, and stability data linked to the final container-closure system. Many exosome products are biologically rich but analytically complex, so consensus potency assays—for example, suppression of a Th17 readout, induction of endothelial tube formation, restoration of enzyme activity, or rescue of a disease-relevant reporter cell line—are likely to become the bridge between mechanistic claims and regulatory acceptability.

6.3. Exploring combination therapies and innovative delivery systems

Combination therapy is especially attractive when exosomes cannot fully correct a monogenic defect on their own. In this setting, exosomes may serve as adjuncts to ERT, ASO, AAV gene therapy, small-molecule chaperones, immune biologics, or genome editing by improving tissue access, reducing local inflammation, or prolonging residence time at the target site (*27,39,60*). Biomaterial carriers such as hydrogels, adhesive wound dressings, microneedle arrays, or intranasal mucoadhesive systems should therefore be viewed not as passive containers but as pharmacology-shaping components that influence exposure kinetics and local bioavailability.

The strongest translational candidates are likely to be indication-specific platforms: wound-retentive matrices for RDEB, intranasal systems for neuroimmune rare diseases, and bone-targeting or integrin-targeting vesicles for skeletal disorders. Matching the carrier to the disease context may ultimately matter as much as matching the exosome to the cell type.

7. Conclusion

Stem cell-derived EVs remain one of the most promising cell-free platforms for rare-disease therapeutics, but their future depends on moving from proof-of-concept enthusiasm to matched product-disease design. The central message of this review is that exosome therapy will be far more persuasive when each disease section is anchored to a dominant rare-disease bottleneck, a route-aware delivery strategy, and a potency assay that can travel with the product into clinical development.

Viewed through this lens, the field is shifting from generic regenerative claims toward a more disciplined architecture: source-specific cargo mapping, explicit trade-offs between pre-loading and post-loading, precision surface navigation, TFF-compatible manufacturing, QbD-based control of CQAs and CPPs, and AI-enabled multi-omics pipelines for target selection. EV development for rare diseases is therefore not a smaller version of exosome development for common diseases; it is a stricter version, in which every lot, endpoint, and route decision carries greater weight because patient numbers are limited and heterogeneity is high.

In summary, the most credible path forward lies in integration: integration of the mechanism with disease specificity, engineering with biodistribution, manufacturing with regulatory science, and multi-omics with artificial intelligence. Only by linking these layers can stem cell-derived exosomes evolve from an appealing biological concept into scalable, targetable, and clinically credible therapeutics for patients with rare disorders. This integration should explicitly include PK/PD-aware dosing and proactive management of repeat-dose immunogenicity, procoagulant/complement safety, impurity control, cargo leakage, and off-target organ accumulation because rare-disease programs rarely succeed when assuming single administration.

Funding: None.

Conflict of Interest: The authors have no conflicts of interest to disclose.

References

1. Dawood M, Heavner B, Wheeler MM, *et al*. Genomics research to elucidate the genetics of rare diseases (GREGoR) consortium. GREGoR: Accelerating genomics for rare diseases. Nature. 2025; 647:331-342.
2. Eisfeldt J, Ek M, Nordenskjöld M, Lindstrand A. Toward clinical long-read genome sequencing for rare diseases. Nat Genet. 2025; 57:1334-1343.
3. Tataru EA, Dooms M, Gonzaga-Jauregui C, Pasmooij AMG, O'Connor DJ, Jonker AH. Drug-device combinations in rare diseases: Challenges and opportunities. Drug Discov Today. 2025; 30:104343.
4. Wang X, Pan Z, Liu N, Dai X, Yang Y, Zhang C, Xu Y. Therapeutic potentials of mesenchymal stem cell-derived exosomes for major solid malignancies: A narrative systematic review. Biosci Trends. 2025; 19:521-544.
5. Hwang J, Jang S, Kim C, Lee S, Jeong HS. Role of stem cell-derived exosomes and microRNAs in spinal cord injury. Int J Mol Sci. 2023; 24:13849.
6. Műzes G, Sipos F. Stem cell-based therapies in autoimmune diseases: Current evidence, unmet needs, and future directions-a closing editorial review. Cells. 2026; 15:328.
7. Wang Y, Wang H, Tan J, Cao Z, Wang Q, Wang H, Yue S, Li W, Wang D. Therapeutic effect of mesenchymal stem cells and their derived exosomes in diseases. Mol Biomed. 2025; 6:34.
8. Akbar N, Razzaq SS, Salim A, Haneef K. Mesenchymal stem cell-derived exosomes and their microRNAs in heart repair and regeneration. J Cardiovasc Transl Res. 2024; 17:505-522.
9. Li L, Zhang X, Wu Y, Xing C, Du H. Challenges of mesenchymal stem cells in the clinical treatment of COVID-19. Cell Tissue Res. 2024; 396:293-312.
10. Banerjee D, Bhattacharya A, Puri A, Munde S, Mukerjee N, Mohite P, Kazmi SW, Sharma A, Alqahtani T, Shmrany HA. Innovative approaches in stem cell therapy: Revolutionizing cancer treatment and advancing neurobiology - A

comprehensive review. Int J Surg. 2024; 110:7528-7545.
11. Welsh JA, Goberdhan DCI, O'Driscoll L, *et al*. Minimal information for studies of extracellular vesicles (MISEV2023): From basic to advanced approaches. J Extracell Vesicles. 2024; 13:e12404.
12. Ma ZJ, Yang JJ, Lu YB, Liu ZY, Wang XX. Mesenchymal stem cell-derived exosomes: Toward cell-free therapeutic strategies in regenerative medicine. World J Stem Cells. 2020; 12:814-840.
13. Hade MD, Suire CN, Suo Z. Mesenchymal stem cell-derived exosomes: Applications in regenerative medicine. Cells. 2021; 10:1959.
14. Liu YL, Chen JS, An JH, Cai ZG, Lan JC, Li Y, Kong XW, Zhang MY, Hou R, Wang DH. Characteristics of mesenchymal stem cells and their exosomes derived from giant panda (Ailuropoda melanoleuca) endometrium. *In Vitro* Cell Dev Biol Anim. 2023; 59:550-563.
15. Rau CS, Kuo PJ, Hsieh CH. Adipose-derived stem cell exosomes: Multifaceted therapeutic applications in regenerative medicine. Int J Surg. 2025; 111:7099-7113.
16. Yu H, Zhang J, Yang L, Tian Y, Milne C, Jin P, Li Q, Song R, Wang W. MSC-derived exosomes injectable hyaluronic acid hydrogel for enhanced chronic wound healing. J Control Release. 2025; 385:113985.
17. Wang W, Zhao Y, Li H, Zhang Y, Jia X, Wang C, Zhu P, Wang J, Hou Y. Exosomes secreted from mesenchymal stem cells mediate the regeneration of endothelial cells treated with rapamycin by delivering pro-angiogenic microRNAs. Exp Cell Res. 2021; 399:112449.
18. Lai J, Pan Q, Chen G, Liu Y, Chen C, Pan Y, Liu L, Zeng B, Yu L, Xu Y, Tang J, Yang Y, Rao L. Triple hybrid cellular nanovesicles promote cardiac repair after ischemic reperfusion. ACS Nano. 2024; 18:4443-4455.
19. Sung SE, Seo MS, Kim YI, Kang KK, Choi JH, Lee S, Sung M, Yim SG, Lim JH, Seok HG, Yang SY, Lee GW. Human epidural AD-MSC exosomes improve function recovery after spinal cord injury in rats. Biomedicines. 2022; 10:678.
20. Wang Y, Kong Y, Du J, Qi L, Liu M, Xie S, Hao J, Li M, Cao S, Cui H, Liu A, Ma J, Song Y. Injection of human umbilical cord mesenchymal stem cells exosomes for the treatment of knee osteoarthritis: From preclinical to clinical research. J Transl Med. 2025; 23:641.
21. Barbetta C, Bonomi F, Lepri G, Furst DE, Randone SB, Guiducci S. Mesenchymal stem-cell-derived exosomes and microRNAs: Advancing cell-free therapy in systemic sclerosis. Cells. 2025; 14:1018.
22. Xu K, Ma D, Zhang G, Gao J, Su Y, Liu S, Liu Y, Han J, Tian M, Wei C, Zhang L. Human umbilical cord mesenchymal stem cell-derived small extracellular vesicles ameliorate collagen-induced arthritis *via* immunomodulatory T lymphocytes. Mol Immunol. 2021; 135:36-44.
23. Heydari R, Koohi F, Rasouli M, Rezaei K, Abbasgholinejad E, Bekeschus S, Doroudian M. Exosomes as rheumatoid arthritis diagnostic biomarkers and therapeutic agents. Vaccines (Basel). 2023; 11:687.
24. Wu D, Zhao X, Xie J, Yuan R, Li Y, Yang Q, Cheng X, Wu C, Wu J, Zhu N. Physical modulation of mesenchymal stem cell exosomes: A new perspective for regenerative medicine. Cell Prolif. 2024; 57:e13630.
25. Rezabakhsh A, Sokullu E, Rahbarghazi R. Applications, challenges and prospects of mesenchymal stem cell exosomes in regenerative medicine. Stem Cell Res Ther. 2021; 12:521.
26. Liao HJ, Shu KH, Yu WC, Chiu YL. Engineering mesenchymal stem cell-derived extracellular vesicles for the treatment of chronic kidney diseases. Tissue Eng Regen Med. 2026; 23:1-20.
27. Liu L, Chen S, Song Y, Cui L, Chen Y, Xia J, Fan Y, Yang L, Yang L. Hydrogels empowered mesenchymal stem cells and the derived exosomes for regenerative medicine in age-related musculoskeletal diseases. Pharmacol Res. 2025; 213:107618.
28. Adelipour M, Lubman DM, Kim J. Potential applications of mesenchymal stem cells and their derived exosomes in regenerative medicine. Expert Opin Biol Ther. 2023; 23:491-507.
29. Azizoglu M, Zorba-Yildiz AP, Yilmaz H, Yurtbay G, Catli G, Yavuz G, Yavas AD, Eren M, Arici M, Goken V, Yasar S, Darici H. Regenerative medicine in surgery: Stem cells and exosome applications. Cir Cir. 2025; 93:86-104.
30. Krylova SV, Feng D. The machinery of exosomes: Biogenesis, release, and uptake. Int J Mol Sci. 2023; 24:1337.
31. Liang J, Zhao J, Yang L, Wang Q, Liao J, Li J, Zhuang W, Li F, He J, Tang Y, Chen H, Huang C. MSC-exosomes pretreated by Danshensu extracts pretreating to target the hsa-miR-27a-5p and STAT3-SHANK2 to enhanced antifibrotic therapy. Stem Cell Res Ther. 2025; 16:40.
32. Terstappen GC, Meyer AH, Bell RD, Zhang W. Strategies for delivering therapeutics across the blood-brain barrier. Nat Rev Drug Discov. 2021; 20:362-383.
33. Chen X, Su C, Wei Q, Sun H, Xie J, Nong G. Exosomes derived from human umbilical cord mesenchymal stem cells alleviate diffuse alveolar hemorrhage associated with systemic lupus erythematosus in mice by promoting M2 macrophage polarization *via* the microRNA-146a-5p/NOTCH1 axis. Immunol Invest. 2022; 51:1975-1993.
34. Jung S, Lee S, Kim HJ, Kim S, Moon JH, Chung H, Kang SJ, Park CG. Mesenchymal stem cell-derived extracellular vesicles subvert Th17 cells by destabilizing RORγt through posttranslational modification. Exp Mol Med. 2023; 55:665-679.
35. Tavasolian F, Hosseini AZ, Soudi S, Naderi M. miRNA-146a improves immunomodulatory effects of MSC-derived exosomes in rheumatoid arthritis. Curr Gene Ther. 2020; 20:297-312.
36. Zhu M, Liu M, Guo QL, Zhu CQ, Guo JC. Prolonged DADLE exposure epigenetically promotes Bcl-2 expression and elicits neuroprotection in primary rat cortical neurons *via* the PI3K/Akt/NF-κB pathway. Acta Pharmacol Sin. 2018; 39:1582-1589.
37. Pahlavani HA. Exercise-induced signaling pathways to counteracting cardiac apoptotic processes. Front Cell Dev Biol. 2022; 10:950927.
38. Giovannelli L, Bari E, Jommi C, Tartara F, Armocida D, Garbossa D, Cofano F, Torre ML, Segale L. Mesenchymal stem cell secretome and extracellular vesicles for neurodegenerative diseases: Risk-benefit profile and next steps for the market access. Bioact Mater. 2023; 29:16-35.
39. Li B, Yang J, Wang R, Li J, Li X, Zhou X, Qiu S, Weng R, Wu Z, Tang C, Li P. Delivery of vascular endothelial growth factor (VEGFC) *via* engineered exosomes improves lymphedema. Ann Transl Med. 2020; 8:1498.
40. Youssef El Baradie KB, Hamrick MW. Therapeutic application of extracellular vesicles for musculoskeletal repair & regeneration. Connect Tissue Res. 2021; 62:99-114.
41. Wang L, Lin G, Zuo Z, Li Y, Byeon SK, Pandey A, Bellen

HJ. Neuronal activity induces glucosylceramide that is secreted *via* exosomes for lysosomal degradation in glia. Sci Adv. 2022; 8:eabn3326.
42. Zhang X, Wang Y, Guo X, Xiao Y, Wan W, Zou H, Yang X. Mitochondrial dysfunction in fibrotic diseases: Research progress and MSC-exos therapy. Exp Mol Pathol. 2025; 143:104983.
43. Loewa A, Feng JJ, Hedtrich S. Human disease models in drug development. Nat Rev Bioeng. 2023; 1:545-559.
44. U.S. Food and Drug Administration. Rare diseases: Considerations for the development of drugs and biological products. Guidance for Industry. 2023.
45. Liang Y, Duan L, Lu J, Xia J. Engineering exosomes for targeted drug delivery. Theranostics. 2021; 11:3183-3195.
46. Gimona M, Pachler K, Laner-Plamberger S, Schallmoser K, Rohde E. Manufacturing of human extracellular vesicle-based therapeutics for clinical use. Int J Mol Sci. 2017; 18:1190.
47. Tan F, Li X, Wang Z, Li J, Shahzad K, Zheng J. Clinical applications of stem cell-derived exosomes. Signal Transduct Target Ther. 2024; 9:17.
48. Wiklander OPB, Nordin JZ, O'Loughlin A, *et al*. Extracellular vesicle *in vivo* biodistribution is determined by cell source, route of administration and targeting. J Extracell Vesicles. 2015; 4:26316.
49. Cieślik MC, Bryniarski K, Nazimek K. Biodelivery of therapeutic extracellular vesicles: should mononuclear phagocytes always be feared? Front Cell Dev Biol. 2023; 11:1211833.
50. Liam-Or R, Faruqu FN, Walters A, Han S, Xu L, Wang JT-W, Oberlaender J, Sanchez-Fueyo A, Lombardi G, Dazzi F, Mailaender V, Al-Jamal KT. Cellular uptake and *in vivo* distribution of mesenchymal-stem-cell-derived extracellular vesicles are protein corona dependent. Nat Nanotechnol. 2024; 19:846-855.
51. Xia Y, Zhang J, Liu G, Wolfram J. Immunogenicity of extracellular vesicles. Adv Mater. 2024; 36:e2403199.
52. U.S. Food and Drug Administration. Immunogenicity assessment for therapeutic protein products. Guidance for Industry. 2014.
53. Chen Y, Su YC, Roffler SR. Polyethylene glycol immunogenicity in nanomedicine. Nat Rev Bioeng. 2025; 3:742-760.
54. Ishida T, Kiwada H. Accelerated blood clearance (ABC) phenomenon upon repeated injection of PEGylated liposomes. Int J Pharm. 2008; 354:56-62.
55. Wang X, Chen S, Lu R, Sun Y, Song T, Nie Z, Yu C, Gao Y. Adipose-derived stem cell-secreted exosomes enhance angiogenesis by promoting macrophage M2 polarization in type 2 diabetic mice with limb ischemia *via* the JAK/STAT6 pathway. Heliyon. 2022; 8:e11495.
56. Yamada Y. Nucleic acid drugs-current status, issues, and expectations for exosomes. Cancers (Basel). 2021; 13:5002.
57. Li J, Liu W, Mu Y, Wang X, Zhang H, Tang K, Zhang D. Artificial intelligence-assisted spatial omics-based biomimetic nanoplatform for intelligent and precise intervention in the immunosuppressive core region of ovarian cancer. NPJ Precis Oncol. 2026; 10.
58. Xu M, Chen G, Dong Y, Xiang S, Xue M, Liu Y, Song H, Song H, Wang Y. Stable expression of a truncated TLX variant drives differentiation of induced pluripotent stem cells into self-renewing neural stem cells for production of extracellular vesicles. Stem Cell Res Ther. 2022; 13:436.
59. Patel T, Henna F, Sharif I, Javed I, Mustafa F, Sharif H, Nasir F, Javaid M, Usman SF, Hanani C, Anand N. A narrative review on the therapeutic potential of stem cells in neurodegenerative diseases: Advances, insights, and challenges. Ann Med Surg (Lond). 2025; 88:1441-1453.
60. Liang C, Yi Y, Li J, Aghayants S, Chen X, Cao W, Zhang Q. Unveiling exosomes in combating skin aging: Insights into resources, mechanisms and challenges. Stem Cell Res Ther. 2025; 16:474.

Received May 4, 2026; Revised June 10, 2026; Accepted June 15, 2026.

**Address correspondence to:*
Yanling Chen, Department of Hepatobiliary Surgery, Fujian Institute of Hepatobiliary Surgery, Fujian Medical University Union Hospital, Fuzhou 350001, Fujian China.
E-mail: drchenyl@126.com

Wei Tang, National Center for Global Health and Medicine, Japan Institute for Health Security, Tokyo 162-8655, Japan.
E-mail: politang-tky@umin.ac.jp

Released online in J-STAGE as advance publication June 20, 2026.

Review

DOI: 10.5582/bst.2026.01148

Immunometabolic reprogramming *via* GLP-1 receptor agonists in people with HIV: A multidimensional systemic framework

Liqin Sun[1,2,3,§], Stephane Isnard[2,3,§], Haipeng Zhu[4,§], Jingyi Chen[5,§], Yun He[1,*], Hongzhou Lu[1,*], Jean-Pierre Routy[2,3,*]

[1] Department of Infectious Diseases, National Clinical Research Center for Infectious Diseases, Shenzhen Third People's Hospital, Shenzhen, Guangdong, China;
[2] Research Institute of the McGill University Health Centre, Montréal, QC, Canada;
[3] Chronic Viral Illness Service, McGill University Health Centre, Montréal, QC, Canada;
[4] Department of Infectious Diseases, The Ninth People's Hospital of Dongguan, Dongguan, Guangdong, China;
[5] School of Medicine, Southern University of Science and Technology, Shenzhen, Guangdong, China.

SUMMARY: Antiretroviral therapy (ART) has transformed HIV infection into a manageable chronic condition, but pathological weight gain, adipose dysfunction, and persistent inflammation are increasingly prevalent among aging people with HIV (PWH). Glucagon-like peptide-1 receptor agonists (GLP-1 RAs) and dual GIP/GLP-1 RAs have emerged as transformative therapies, although PWH were underrepresented in pivotal trials. This review integrates randomized trials, observational cohorts, pharmacogenomic studies, and emerging mechanistic evidence within a framework of GLP-1-mediated immunometabolic reprogramming. HIV-specific trials demonstrate reductions in visceral adiposity, body weight, inflammatory biomarkers, and liver fat. Exploratory or preliminary studies suggest possible effects on gut epithelial integrity, immune-cell trafficking, lymphoid pyroptosis, and DNA-methylation aging measures; however, several of these findings remain conference-level, preprint, or post hoc evidence and require prospective validation. We also examine lean-mass loss, weight regain after discontinuation, pharmacogenomic variation, drug access, and research priorities. Overall, GLP-1 RAs are promising components of cardiometabolic care for PWH, but immunologic, gerotherapeutic, and HIV-reservoir applications should currently be considered hypothesis-generating.

Keywords: visceral adiposity, metabolic dysfunction-associated steatotic liver disease, epigenetic clocks, inflammaging, gut barrier, HIV reservoir

1. Introduction

The widespread implementation of combination antiretroviral therapy (ART) has markedly prolonged the life expectancy of people with HIV (PWH), shifting the clinical focus from AIDS-defining opportunistic infections to chronic, non-communicable comorbidities (*1*). Modern antiretroviral regimens, particularly those containing integrase strand transfer inhibitors (INSTIs, such as dolutegravir, bictegravir, or cabotegravir) and tenofovir alafenamide (TAF), while achieving superb rates of virologic suppression, are frequently accompanied by significant weight gain and adipose tissue dysfunction (*2-4*). Although initial post-ART weight gain often represents a physiological "return-to-health" phenomenon in advanced patients, long-term follow-up reveals that aging, polypharmacy including frequent antidepressant use, smoking cessation, and Western lifestyles synergistically drive undesirable, persistent, and pathological obesity, most notably among those with low baseline CD4+ T-cell counts (*3*).

In ART-treated PWH, persistent low-grade systemic inflammation and pathological obesity act synergistically to drive cardiovascular-kidney-metabolic (CKM) syndrome (*5-7*). This clinical entity is characterized by visceral adiposity, type 2 diabetes mellitus (T2DM), metabolic dysfunction-associated steatotic liver disease (MASLD), arterial hypertension, and accelerated atherosclerosis, collectively compromising comorbidity-free healthspan (*5-8*). Consequently, identifying metabolic interventions that combine profound weight-lowering efficacy with systemic anti-inflammatory properties is a premier clinical priority in modern HIV medicine (*1,5*).

Recently, glucagon-like peptide-1 receptor agonists (GLP-1 RAs), including semaglutide, liraglutide, and the

dual GIP/GLP-1 receptor co-agonist tirzepatide, have revolutionized the management of obesity and T2DM (*9,10*). By mimicking endogenous incretin hormones, GLP-1 RAs delay gastric emptying and act directly on the hypothalamic arcuate nucleus to enhance satiety and suppress appetite (*9-11*). In HIV-negative populations, semaglutide achieves a ~15% reduction in body weight (*9*) and reduces the risk of major adverse cardiovascular events (MACE) by 20% in overweight or obese adults without diabetes (*12*). Moreover, the landmark FLOW trial demonstrated a 24% reduction in composite renal outcomes in patients with T2DM and chronic kidney disease (CKD) (*13*).

However, because PWH were systematically excluded from early registrational trials, clinicians have faced a relative dearth of evidence specific to this high-risk population (*12,13*). In reality, the biological impact of the GLP-1 receptor pathway in chronic HIV infection extends far beyond simple weight loss and glucose homeostasis. Recent reviews have begun to synthesize emerging evidence on GLP-1 RAs in PWH, highlighting weight gain mechanisms specific to this population, clinical considerations for GLP-1 RA use, and the potential for cardiometabolic risk reduction (*14,15*). However, these prior clinical studies, including Phase 2b trials (*16*), focused primarily on clinical endpoints without providing an integrated framework linking GLP-1 receptor agonist-mediated immunometabolic reprogramming with geroscience dimensions.

This review develops a translational framework of 'GLP-1-mediated immunometabolic reprogramming' by evaluating clinical trials, real-world cohorts, and emerging mechanistic studies on visceral adipose remodeling, intestinal barrier biology, lymphoid pyroptosis, and epigenetic aging (*16-22*). Evidence maturity varies substantially across these domains; conference abstracts, preprints, and post hoc analyses are identified explicitly. By contrasting GLP-1 RAs with alternative metabolic strategies, we aim to provide a calibrated scientific basis for metabolic management and future research in PWH.

2. Literature Search Strategy

To ensure methodological rigor, we conducted a comprehensive narrative search of PubMed, MEDLINE, EMBASE, and ClinicalTrials.gov databases from inception through April 2026. We utilized combinations of the following Medical Subject Headings (MeSH) terms and free-text keywords: "GLP-1 receptor agonist", "semaglutide", "tirzepatide", "liraglutide", "obesity", "diabetes", "cardiovascular disease", "NAFLD/MASLD", "CKM syndrome", "inflammaging", "epigenetic clocks", "gut barrier", "immune activation" and "people with HIV". Our screening prioritized double-blind, randomized controlled trials (RCTs), prospective and retrospective multi-center clinical cohorts, and established clinical guidelines. To capture the latest advances in this rapidly evolving field, we integrated newly presented oral abstracts and posters from the 2024–2026 Conference on Retroviruses and Opportunistic Infections (CROI) and major national and international hepatology and cardiology symposia, explicitly qualifying these citations as preliminary conference evidence where applicable to maintain scientific transparency.

3. Main findings: Immunometabolic reprogramming *via* GLP-1 receptor agonists in PWH

3.1.1. Adipose tissue pathophysiology and CKM syndrome under ART

The prevalence of obesity (BMI ≥ 30 kg/m²) among ART-treated PWH in North America rose from approximately 14% in 2000 to 28% in 2018 (*23,24*). This rising obesity prevalence has been similarly documented in PWH across Western countries and Southeast Asia (*25*). Women living with HIV bear a disproportionately higher metabolic risk: a pooled analysis of three ART-naive trials demonstrated that women gained a mean BMI of 1.91 kg/m² over 96 weeks, compared with 1.39 kg/m² in men ($P < 0.001$), with the most substantial weight gain occurring within the first year of ART initiation (*2*). Early weight gain typically plateaus approximately two years after treatment initiation, after which weight trajectories parallel those observed in the general population (*26*).

Although population-level obesity trends among PWH mirror those of the general population, African ancestry, advanced age, lower baseline $CD4^+$ T cell counts, and higher pretreatment viral loads represent independent predictors of excessive ART-associated weight gain (*24*). ART-associated weight gain is tightly linked to lipohypertrophy, characterized by disproportionate visceral adipose tissue (VAT) accumulation (*27*). In obese PWH, VAT accounts for nearly one-quarter of total abdominal fat, a pattern strongly associated with insulin resistance and chronic inflammation (*16*). Prior exposure to thymidine analogues (*e.g.*, stavudine) has caused irreversible subcutaneous adipose tissue (SAT) loss (lipoatrophy), resulting in a mixed body composition phenotype characterized by central visceral fat excess and peripheral fat wasting in long-term PWH survivors (*28*).

Visceral fat depots undergo extensive immune cell infiltration, secreting high levels of inflammatory adipokines (*e.g.*, leptin, TNF-α, and IL-6) while suppressing anti-inflammatory adiponectin (*28,29*). Long-term exposure to INSTIs has been shown to exert proadipogenic and profibrotic effects and induce insulin resistance in human and simian adipose tissues (*29*). This localized adipocyte-driven inflammation, superimposed on HIV-mediated persistent systemic immune activation, establishes an "immunometabolic vicious cycle" that accelerates endothelial damage, impairs post-receptor insulin signaling, and induces glomerular sclerosis,

ultimately promoting the full spectrum of CKM syndrome (*5-7*).

3.1.2. Efficacy in VAT and Intrahepatic Triglyceride Clearance

In the phase 2b SLIM LIVER trial evaluating weekly semaglutide (1 mg/week) in PWH with MASLD, semaglutide achieved a 31% relative reduction in intrahepatic triglyceride (IHTG) content over 24 weeks ($P < 0.001$). Complete resolution of hepatic steatosis was observed in 29% of participants. Furthermore, abdominal MRI sub-studies confirmed a significant 15.2% reduction in VAT volume and a 12.4% reduction in SAT (*17*). Tirzepatide, evaluating dual GIP/GLP-1 agonism, demonstrated even greater efficacy in early real-world PWH series, achieving up to 18.5% total body weight loss at 48 weeks (*30*).

3.1.3. Anthropometric Discrepancies and Lean Mass Considerations

While GLP-1 RAs produce substantial body weight reductions in PWH, clinician vigilance is warranted regarding the composition of weight lost. Given that PWH inherently face an elevated baseline risk for sarcopenia, frailty, and sarcopenic obesity due to chronic low-grade inflammation and legacy antiretroviral toxicities, progressive reductions in skeletal muscle mass (SMM) during rapid weight loss may compromise physical function. Thus, clinical implementation of GLP-1 RAs in PWH should routinely incorporate structured resistance exercise regimens and optimized nutritional support (1.2–1.5 g protein/kg/day) to preserve lean mass and functional status (*17,27,37*).

3.2. Efficacy discrepancy: Reconciling RCTs with real-world cohorts

3.2.1. Visceral de-fatting efficacy in clinical trials

The double-blind, randomized, placebo-controlled phase 2b trial led by Eckard *et al*. provides high-quality level-1b evidence on the efficacy of GLP-1 RAs in PWH with central lipohypertrophy (*16*). In this 32-week study, 108 overweight/obese PWH without diabetes received weekly subcutaneous semaglutide (titrated to 1.0 mg) or placebo (*16*). Semaglutide induced a mean weight reduction of 10.4% (versus 2.3% in the placebo group; $P < 0.001$), accompanied by a 30.6% reduction in abdominal VAT area ($P = 0.0017$) and a 9.32 cm reduction in waist circumference ($P < 0.0001$) (*16*). These results demonstrate that under optimal trial conditions, the visceral de-fatting efficacy of GLP-1 RAs in PWH is highly robust and fully comparable to that observed in HIV-negative cohorts (*16*). Additionally, the SLIM LIVER trial corroborated these findings, reporting a 6.7 cm decrease in waist circumference after 24 weeks of semaglutide therapy (*17*). The detailed efficacy outcomes of this landmark trial are summarized in Table 1 (*16*).

Furthermore, subgroup stratifications reveal that PWH with concomitant T2DM achieve more modest weight loss (typically 3–5%) compared to non-diabetic PWH (7–10%) (*10,18*). This efficacy attenuation aligns with general population trends, driven by central GLP-1 resistance and altered receptor desensitization kinetics in diabetic states.

3.2.2. Real-world efficacy dilution: Biological and pharmacogenomic drivers

In contrast, real-world cohort studies reveal lower average effectiveness than tightly controlled trials (*18,30*). In the multicenter CNICS cohort (Haidar *et al*.), 222 PWH achieved a mean weight loss of 5.7% after 12 months of semaglutide (*18*). Similarly, in the UCSD single-center cohort analyzed by Nguyen *et al*. ($N = 225$), GLP-1 RA therapy yielded a mean weight reduction of 5.4 kg, and tirzepatide use was associated with higher odds of achieving at least 5% weight loss than semaglutide use (OR = 5.46) (*30*). Preliminary CROI 2026 data from the Washington, DC cohort (O'Connor *et al*., abstract 695; $N = 362$) showed that 30.4% achieved at least 5% weight loss at 6-12 months; participants with diabetes had lower adjusted odds of reaching the 5% and 10% thresholds. These real-world findings identify three principal biological and clinical considerations (*10,19,29*):

Table 1. Key efficacy outcomes of semaglutide in HIV associated lipohypertrophy (32 Week RCT)

Outcome Endpoint	Semaglutide ($n = 54$)	Placebo ($n = 54$)	Change (95% CI)	P
Body weight change (%)	-10.40%	-2.30%	-8.1% (-10.88, -5.32)	< 0.001
Abdominal VAT area (cm^2)	-30.60%	No significant change	-30.82 cm^2 (-50.13, -11.51)	0.0017
Total body fat (ln kg)*	-18.90%	-	β = -0.21 (-0.34, -0.05)	0.0009
Waist circumference (cm)	-8.30%	-	-9.32 cm (-12.10, -6.54)	< 0.0001
HbA1c (%)	-0.47%	-	-0.47% (-0.67, -0.28)	< 0.0001
HOMA-IR (ln unit)	-43.00%	-	β = -0.56 (-1.04, -0.08)	0.0238

**Note*: β coefficient represents the estimated treatment effect on the natural logarithmic scale (ln kg or ln unit) derived from linear mixed-effects models adjusted for sex and treatment-by-time interactions. CI: confidence interval; VAT: visceral adipose tissue; HOMA-IR: homeostatic model assessment for insulin resistance.

(1). *Confounding by comorbid diabetes*: In a real-world cohort, 82% of patients present with comorbid T2DM (*30*). In diabetic states, target tissue GLP-1 receptor expression is downregulated, and patients exhibit advanced insulin resistance, which blunts central satiety signaling, resulting in significantly lower weight-loss efficacy compared to patients with obesity alone (*10,19*).

(2). Pharmacogenomic and ancestral variations: Real-world data indicate that Black patients achieve less weight loss on GLP-1 RAs than White patients (*19*). A landmark GWAS by Su *et al*. provided a genetic explanation for this disparity, identifying a missense variant in the signal peptide region of GLP1R (rs10305420, p. Pro7Leu) where each additional allele is associated with an extra -0.76 kg of body weight reduction ($P = 2.9 \times 10^{-10}$) (*19*). However, this "booster" allele is highly prevalent in European ancestry populations (~40%) but is found in only 7% of African ancestry populations, predisposing Black patients to a genetically blunted therapeutic response (*19*).

(3). Potential role of adipose tissue fibrosis and remodeling: PWH treated with INSTIs such as dolutegravir or raltegravir can develop a pathologically altered adipose tissue phenotype (*29*). Long-term INSTI exposure has been associated with increased fibrosis in subcutaneous and visceral adipose tissue, periadipocyte collagen deposition, adipocyte hypertrophy, and altered adipogenic and insulin-sensitizing pathways. Whether these histological changes translate into clinically meaningful resistance to GLP-1 RA-mediated fat loss in humans remains an open question and warrants dedicated investigation (*29*).

We also note the combination of GLP-1 RAs with growth hormone-releasing hormone (GHRH) analogs like tesamorelin (*31*) and emerging multi-agent strategy discussions (*32*). A comprehensive summary of key HIV-specific studies, categorized by OCEBM evidence levels and clinical recommendation strengths, is presented in Table 2 (*16-21,30,33*), supported by retrospective CNICS analyses showing liver fibrosis score improvements (*33*).

3.3. Gut mucosal integrity and compartmentalized immune reconstitution

Table 2. Summary of key HIV-specific studies of GLP-1 RAs

Study & Year	Study Design & Sample Size	Evidence Level (OCEBM)	Intervention	Key outcomes and evidence interpretation
Eckard *et al*. 2024 (*16*)	RCT, placebo-controlled, *N* = 108	Level 1b	Semaglutide 1.0 mg SC weekly × 32 wk	VAT -30.6%, weight -10.4%, and hsCRP -39.9%. Randomized phase 2b evidence for body-composition and inflammatory outcomes.
Lake *et al*. (SLIM LIVER) 2024 (*17*)	Single-arm, open-label, *N* = 51	Level 2b	Semaglutide 1.0 mg SC weekly × 24 wk	IHTG -31.3% and 29% MASLD resolution. Single-arm open-label evidence.
Haidar *et al*. (CNICS) 2024 (*18*)	Retrospective cohort, *N* = 222	Level 2b	Semaglutide (real-world practice)	Weight -5.7% at 12 months and HbA1c -1.07% in participants with T2DM. Retrospective cohort evidence.
Nguyen *et al*. (UCSD) 2024 (*30*)	Retrospective cohort, *N* = 225	Level 2b	GLP1 RAs / Tirzepatide	Weight -5.4 kg; tirzepatide associated with higher odds of at least 5% weight loss. Retrospective cohort evidence.
Su *et al*. (GWAS) 2026 (*19*)	Genome-wide association, *N* = 27885	Level 2b (observational association)	GLP1 RAs/ Tirzepatide	GLP1R rs10305420: -0.76 kg/allele; GIPR rs1800437 associated with nausea/ vomiting risk. Research-stage associations; no validated genotype-guided dosing recommendation.
Marin *et al*. (CROI 2026)*(*20*)	Mechanistic pilot substudy (Preliminary conference abstract), *N* = 5	Unrated	Liraglutide SC × 8 mo	Duodenal CD4+ T-cell increase and CD69+ reduction in a small mechanistic substudy. Preliminary conference evidence; hypothesis-generating.
Corley *et al*. (2026) (*21*)	Post hoc analysis of RCT, *N* = 84	Level 2b	Semaglutide *vs* placebo	Exploratory post hoc analysis of a phase 2b RCT; not a clinical treatment recommendation.
Ma *et al*. 2026 (*33*)	Retrospective cohort, *N* = 1850	Level 2b	Semaglutide	FIB-4 score -0.11 in moderate-to-advanced fibrosis and -0.64 in advanced fibrosis. Observational pre/post evidence.

*Preliminary conference evidence applies to Marin *et al*. only; findings await peer-reviewed publication. DM: diabetes mellitus; hsCRP: high-sensitivity C-reactive protein; IHTG: intrahepatic triglyceride; OCEBM: Oxford Centre for Evidence-Based Medicine; OR: odds ratio; RCT: randomized controlled trial; SC: subcutaneous.

3.3.1. The circulating CD_4^+ T-cell paradox

A multi-center clinical cohort study in Germany evaluating PWH treated with dulaglutide or semaglutide reported a statistically significant, non-time-dependent decrease in circulating CD4+ T-cell counts, with a median decline of approximately -60 cells/μL ($P = 0.035$) (*34*). Crucially, this decline was restricted to the CD4+ T-cell compartment, as circulating CD8+ T-cell counts, plasma cytokines, and viral suppression remained entirely unaffected (*34*), most notably among individuals with low baseline CD4+ counts. While this initial finding raised concerns regarding potential incretin-mediated immunosuppression, tissue-level investigations suggest a possible compartmentalized mucosal phenomenon rather than cell depletion (*20,34*).

3.3.2. Preliminary signals of mucosal barrier repair and immune modulation

In a preliminary pilot mechanistic study presented at CROI 2026 (Marin *et al*., oral abstract 115, preliminary conference evidence; $N = 5$), paired duodenal and colonic mucosal biopsies were evaluated in PWH before and after liraglutide therapy (*20*):

Physical Barrier Repair: Liraglutide therapy induced progressive reconstruction of duodenal microvilli, accompanied by the significant upregulation of genes governing epithelial differentiation (CDX2, VIL1) and tight junction integrity (OCLN, TJP1) (*20*). This exploratory finding suggests potential mitigation of the "leaky gut" pathology that persists in PWH despite suppressive ART (*35,36*).

Exploratory mucosal T-Cell dynamics: Duodenal CD4+ T-cell frequency increased from 12% at baseline to 24% post-treatment ($P < 0.01$), while the proportion of highly activated CD69+ mucosal T-cells dropped from 74% to 13% (*20*). Given the unblinded pilot design and extremely small sample size ($N = 5$), these quantitative shifts represent early mechanistic signals rather than definitive proof of tissue-level immune reconstitution (*20,34*).

3.3.3. Hypothesis-generating nature of mucosal homing dynamics

The observation of declining peripheral CD4+ T-cell counts alongside preliminary signals of increased mucosal CD4+ T cells in a small pilot cohort supports a speculative hypothesis of compartmental redistribution (*20,34*). Given that chronic HIV infection persistently compromises the intestinal barrier and promotes microbial translocation despite suppressive ART (*35,36*), it is hypothesized that GLP-1 RAs may modulate gut endothelial adhesion molecules (such as MAdCAM-1), encouraging α4β7+CCR9+ CD4+ T-cell recruitment into the lamina propria. However, because this model relies on a pilot conference abstract ($N = 5$), the α4β7/CCR9 homing axis must be strictly categorized as a hypothesis-generating concept (*20,34,37*). Well-powered, prospective clinical trials with expanded tissue-biopsy cohorts are required to validate these mucosal dynamics.

3.4. Cardio-kidney-metabolic (CKM) protection and inflammatory decay

3.4.1. Anti-inflammatory decay and endothelial preservation

Persistent chronic inflammation is a key driver of accelerated cardiovascular disease in PWH on suppressive ART (*5,6*). In the Eckard RCT, 32 weeks of once-weekly semaglutide led to a dramatic and statistically significant reduction in systemic and vascular inflammatory biomarkers (*16*):

High-Sensitivity C-Reactive Protein (hsCRP): Percent change of -39.92% ($P = 0.01$, 95% CI: -0.87 to -0.15), dropping the median baseline hsCRP from a high-cardiovascular-risk state (4.04 μg/mL) toward a safer target (*16*).

Soluble CD163 (sCD163): Percent change of -12.10% ($P = 0.05$, 95% CI: -0.26 to 0.001), indicating a substantial cooling of vascular macrophage activation (*16*).

Interleukin-6 (IL-6): Percent change of -18.84% ($P = 0.07$, 95% CI: -0.44 to 0.02) (*16*).

These findings were corroborated by Funderburg *et al*., confirming that the anti-inflammatory effects of semaglutide were weight-independent, pointing to a direct, receptor-mediated immunomodulatory action of GLP-1 RAs (*38*). In terms of calculated risk, semaglutide treatment resulted in a 33% reduction in the 10-year ASCVD risk score ($P = 0.026$) (*16*).

3.4.2. Cardiorenal and hepatic protection

In the prospective, single-arm, open-label phase 2b SLIM LIVER pilot trial (ACTG A5371, Lake *et al*.), 24 weeks of dose-escalated semaglutide led to a -31.3% relative reduction in intrahepatic triglyceride (IHTG) content, with complete MASLD resolution (defined as IHTG < 5%) achieved in 29% of participants ($P < 0.0001$) (*17*). This hepatic clearance was accompanied by a 5.8% decrease in waist circumference and a 10.5% decrease in plasma triglycerides (*17*). Key endpoints of the SLIM LIVER study are summarized in Table 3 (*17*).

In a general-population systematic review and meta-analysis, GLP-1 RA therapy was associated with a slower annual decline in eGFR and a 24% reduction in microalbuminuria; HIV-specific renal outcome data remain limited (*39*). These findings are directionally consistent with cardiorenal benefits reported in large general-population trials (*13,40,41*). In PWH, cardiovascular risk-score changes should be interpreted cautiously (*16,42*). Preliminary CROI 2026 findings from Ross Eckard *et*

Table 3. Key endpoints of the SLIM LIVER study (24 weeks of semaglutide)

Outcome Endpoint	Baseline	Week 24	Absolute change (95% CI)	Relative change	*P*
IHTG (%)	12.7 ± 6.1%	8.5 ± 4.7%	-4.2% (-5.4, -3.1)	-31.30%	< 0.0001
Body weight (kg)	103.0 ± 20.8kg	95.1 ± 22.8kg	-7.8kg (-9.5, -6.1)	-8.10%	< 0.0001
Waist circumference (cm)	115.0 ± 11.8cm	108.0 ± 12.9cm	-6.7cm (-8.2, -5.1)	-5.80%	< 0.0001
HOMA-IR	5.4 ± 5.1	3.9 ± 3.9	-1.5 (-3.2, 0.2)	-27.70%	0.086
Triglycerides (mg/dL)	150.0 ± 87.9	131.0 ± 75.8	-26.8 (-46.1, -7.5)	-10.50%	0.007
ALT (IU/L)	30.7 ± 13.4	24.8 ± 11.9	-6.1 (-9.7, -2.5)	-15.30%	0.001
MASLD resolution (IHTG < 5%)	0%	29%	+29.00%		< 0.001

**Note*: Baseline and Week 24 values are raw observed means ± standard deviations (SD). Absolute and relative changes are modeled estimates accounting for baseline covariates. ALT elevation defined as > 19 IU/L in females and >30 IU/L in males. ALT: alanine aminotransferase; HOMA-IR: homeostatic model assessment for insulin resistance; IHTG: intrahepatic triglyceride; MASLD: metabolic dysfunction-associated steatotic liver disease.

al. (abstract 699) reported improvement in calculated 10-year ASCVD risk but no significant 32-week change in flow-mediated dilation, pulse-wave velocity, or coronary calcium (*42*). Thus, short-term changes in risk scores may reflect metabolic and inflammatory improvement rather than established structural vascular remodeling.

3.5. Epigenetic rejuvenation and gerotherapeutic potential

3.5.1. Multi-Tissue and Systems-Based DNA Methylation Clocks

Corley *et al*. reported an exploratory post hoc DNA-methylation analysis of the randomized phase 2b trial of semaglutide in HIV-associated lipohypertrophy. Epigenetic aging was not a prespecified endpoint, but adjusted analyses identified significant between-group decelerations across multiple biological aging clocks (*21*):

PCGrimAge (High-precision mortality and healthspan clock) Decreased by -3.08 years ($P = 0.007$) (*21*).

GrimAge V2 (Multisystem chronic disease clock): Decreased by -2.26 years ($P = 0.009$) (*21*).

PhenoAge (Physiological aging clock): Decreased by -4.90 years ($P = 0.004$) (*21*).

DunedinPACE (Rate of aging clock): Decreased by -0.09 units/year, slowing the biological pace of aging by 9% ($P = 0.01$) (*21*).

OMICmAge (Multi-omic clock) & RetroAge (Transposable elements clock): Decreased by -2.20 years ($P = 0.009$) and -2.20 years ($P = 0.030$), respectively, demonstrating enhanced multi-omic healthspan optimization and transposable element heterochromatin stability (*21*).

Systems-Based Organ Clocks: Evaluation of 11 organ-system clocks demonstrated concordant decelerations across tissue compartments, highlighted by a significant reduction in composite SystemsAge (-4.17 years, $P = 0.009$), with the most prominent system-specific decelerations observed in inflammation, brain, and heart systems clocks ($P < 0.05$), highlighting multi-organ gerotherapeutic protection in PWH (*21*).

3.5.2. Organ-specific biological age deceleration

To eliminate confounding variables (*e.g.*, weight loss and baseline inflammation), deconvoluted organ-system epigenetic clocks were evaluated (*21*). In fully adjusted ANCOVA models (controlling for age, sex, BMI, hsCRP, and sCD163), semaglutide demonstrated highly significant, localized epigenetic rejuvenation (*21*):

Inflammation Clock: Decreased by -5.01 years ($P = 0.0056$), reflecting profound molecular "cooling" (*21*).

Brain Clock: Decreased by -4.99 years ($P = 0.0049$), establishing a molecular basis for evaluating GLP-1 RAs in HIV-associated neurocognitive disorders (HAND) (*21*).

Metabolic Clock: Decreased by -4.72 years ($P = 0.0090$), indicating comprehensive resetting of insulin sensitivity pathways (*21*).

Cardiovascular, Renal, and Hepatic Clocks: Decreased by -4.34 years ($P = 0.0088$), -4.20 years ($P = 0.014$), and -4.19 years ($P = 0.042$), respectively (*21*).

In exploratory analyses, 49% of semaglutide-treated participants showed an increase in epigenetic telomere-length estimates, and changes in selected aging measures were associated with 4.5-meter walk velocity (*21*). These findings do not establish cellular rejuvenation or frailty reversal and require prospective validation. Haidar and Delaney discussed the clinical implications of GLP-1 RAs in aging PWH (*15*), while Kim and Dixit reviewed the broader metabolic regulation of immunological aging (*43*). The reported biological-age measures are summarized in Table 4 (*21*).

3.6. Neurobehavioral regulation and substance use reduction

3.6.1. Central nervous system satiety and reward modulation

Tobacco and alcohol use are important behavioral treatment targets in PWH. The molecular rationale for incretin-mediated behavioral regulation involves central nervous system pathways (*44*). GLP-1 receptors are expressed in the hypothalamic arcuate nucleus and area

Table 4. Effects of semaglutide on epigenetic clocks in PWH (32-week RCT)

DNA Methylation Clock	Core Physiological Relevance	Change with Semaglutide	*P*
PCGrimAge	High-precision mortality and healthspan clock	-3.08 years	0.007
GrimAge V2	Multisystem chronic disease, mortality risk clock	-2.26 years	0.009
PhenoAge	Composite physiological aging clock	-4.90 years	0.004
DunedinPACE	Current pace/velocity of biological aging	-0.09 units/year (~9% deceleration)	0.010
OMICmAge	Multi-omics integrated biological age clock	-2.20 years	0.009
SystemsAge	Multisystem organ biological age clock	-4.17 years	0.009
RetroAge	Transposable element epigenetic clock	-2.20 years	0.030

**Note*: All clocks measure absolute biological age in years, except DunedinPACE, which is a rate-of-aging metric expressed in units per year.

Table 5. Studies evaluating GLP-1 RAs for substance use reduction in PWH

Trial Name / Reference	Drug	Target Study Population	Primary Endpoint	Status / Key Findings
GL1DER HIV RCT (NCT06351163)	Semaglutide SC	PWH with unhealthy alcohol use (*N* = 120)	Reduction in alcohol consumption, cardiovascular risk markers	Ongoing
Comprehensive Trial (NCT07221214)	Semaglutide SC	PWH with AUD (*N* = 80)	Weekly drinking days and heavy drinking days	Ongoing
CNICS cohort, Ruderman *et al.* 2026 (*45*)	Semaglutide SC	PWH who smoked cigarettes (*N* = 123)	Daily cigarette consumption reduction in PWH smokers	Published: 24% reduction in smoking intensity; 21% reported no smoking at end of follow-up

AUD: alcohol use disorder; PWH: people with HIV; SC: subcutaneous.

postrema, and GLP-1 signaling can modulate mesolimbic reward pathways involving the ventral tegmental area and nucleus accumbens (*44*).

3.6.2. Clinical real-world evidence

Clinical real-world evidence strongly supports this model:

Tobacco use: In the final peer-reviewed CNICS analysis, 123 PWH who smoked reported a mean baseline intensity of 10.5 cigarettes/day. After semaglutide initiation, smoking intensity decreased by 2.5 cigarettes/day (24%), and 21% reported no smoking at the end of follow-up (*45*).

Alcohol Use Disorder (AUD): In a nationwide registry analysis by Wang *et al*., semaglutide exposure was associated with a 36% reduction in the risk of hospitalization for alcohol use disorder (*46*).

Neuropsychiatric safety: Preliminary CROI 2026 findings from Haidar *et al*. (abstract 447) reported improvement in depressive symptoms among PWH receiving semaglutide. Because this evidence remains conference-level, it should not be interpreted as proof of an antidepressant effect.

Ongoing and reported clinical trials of GLP-1 RAs for substance use reduction in PWH are summarized in Table 5 (*45*):

3.7. Lymphoid sanctuary pyroptosis (GSDMD) and GLP-1 counter-regulation

The persistence of chronic low-grade inflammation in PWH under suppressive ART has historically lacked a unified tissue-level explanation (*22*). A landmark study by Crawford *et al*. analyzed lymph node and ileal biopsies from 20 ART-suppressed PWH (*22*). Using high-sensitivity RNAscope, they detected transcriptionally active, latent HIV vRNA+ cells in all lymph node germinal centers, despite complete plasma viral suppression (*22*). Crucially, the frequency of these tissue-resident HIV vRNA+ cells correlated directly with markers of cell-intrinsic pyroptosis—specifically cleaved gasdermin D (GSDMD+)—in lymph nodes (*22*). This suggests that low-level transcription of latent HIV in tissue sanctuaries continually drives GSDMD-mediated cell death, perpetuating chronic localized inflammation (*22*).

Crawford *et al*. also observed more GLP-1-positive enteroendocrine L cells in the ileum of PWH than in HIV-negative controls (*22*). Ileal GLP-1-positive cell density correlated directly with systemic inflammatory cytokines and inversely with lymph-node pyroptosis (*22*). These cross-sectional associations support a compensatory counter-regulatory model, but they do not demonstrate that exogenous GLP-1 RAs suppress GSDMD cleavage in PWH. Therapeutic enhancement of GLP-1 signaling should therefore be framed as a testable hypothesis rather than an established HIV-cure intervention (*22,47,48*).

3.8. Unified multi-organ topological signaling network

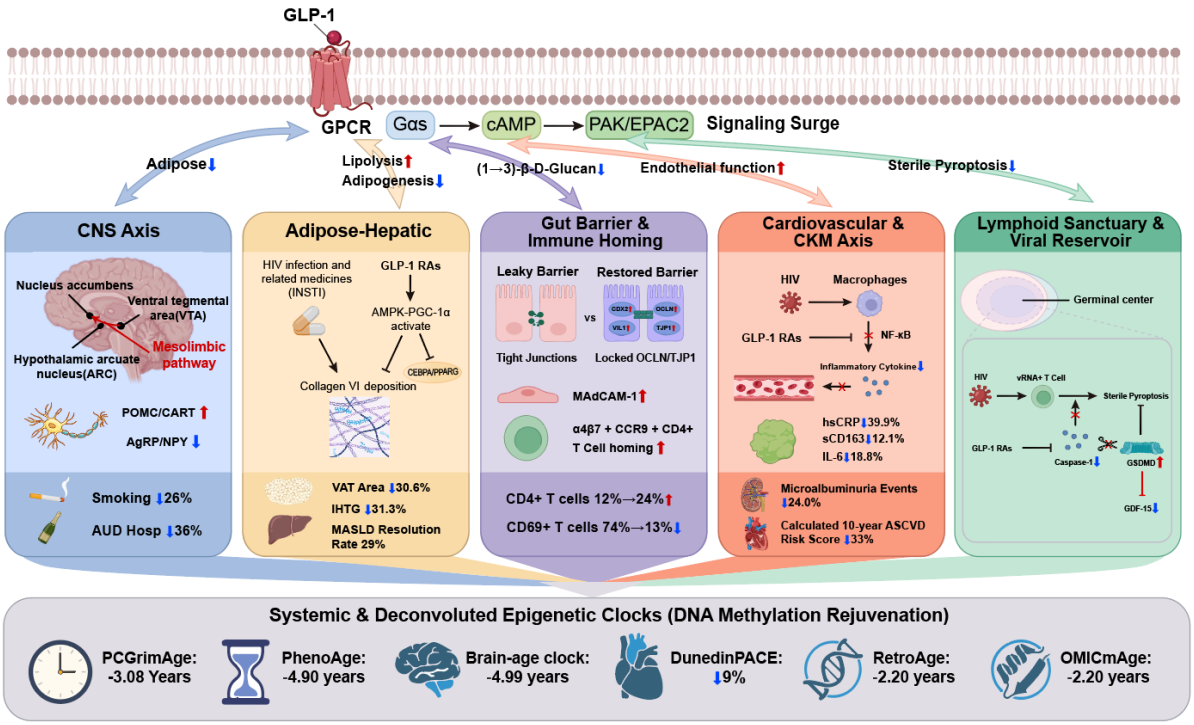


Figure 1. Multidimensional systemic framework of GLP-1 RA-mediated immunometabolic reprogramming in PWH. *Note*: Figure 1 is structured as a dual-layer topological signaling diagram depicting molecular cascades and organ-system clinical endpoints.

GLP-1 receptor agonists and dual GIP/GLP-1 receptor agonists engage canonical Gαs-coupled receptor signaling and downstream cAMP-dependent pathways (*10*). Direct immunoregulatory signaling through GLP-1R on T cells has been demonstrated mainly in preclinical alloimmune models (*48*). Together, these findings motivate—but do not yet prove—a multi-system immunometabolic model across the following compartments in ART-suppressed PWH (Figure 1):

(A) Central nervous system (CNS reward & neurobehavioral reset): Direct activation of hypothalamic arcuate nucleus (ARC) neurons (POMC/CART↑, AgRP/NPY↓) suppresses hunger, while modulation of mesolimbic dopaminergic projections from the ventral tegmental area (VTA) to the nucleus accumbens resets reward circuitry (*44*). This behavioral reset drives a 26.0% reduction in daily cigarette consumption (*45*), a 21.0% complete tobacco cessation rate (*45*), and a 36.0% drop in alcohol use disorder (AUD)-related hospitalizations (*46*).

(B) *Adipose and hepatic tissue (Immunometabolic fat remodeling)*: Activation of the cellular AMPK/PGC-1α metabolic axis stimulates lipophagy (*49*) and blocks integrase strand transfer inhibitor (INSTI)-induced Collagen VI matrix deposition and profibrotic transcription (CEBPA/PPARG↓) (*29*). This converts fibrotic, hyper-hypertrophic fat depots into beiged adipocytes, reducing VAT area by 30.6% (*16*) and IHTG content by 31.3% (achieving complete MASLD resolution in 29.0% of participants) (*17*).

(C) *Gut mucosal barrier preservation & immune compartmentalization*: Incretin signaling upregulates epithelial differentiation genes (*CDX2*, *VIL1*) and tight junction assembly (*OCLN*, *TJP1*), repairing leaky intestinal breaches and halting systemic lipopolysaccharide (LPS) endotoxemia (*35,36*) (Hypothesized pathway based on preliminary pilot data, $N = 5$). Concurrently, mucosal endothelial MAdCAM-1 induction recruits circulating $\alpha_4\beta_7^+CCR9^+CD4^+$ T cells back into the lamina propria, doubling mucosal $CD4^+$ T-cell density (12% to 24%) and extinguishing pathologically activated $CD69^+$ mucosal T cells (74% to 13%) (*20*).

(D) *Cardiovascular-kidney-metabolic (CKM) pathogenesis decay*: Negative regulation of vascular macrophage NF-κB pathways cools systemic endothelial inflammation, reducing hsCRP by 39.92% and sCD163 by 12.10% (*16,38*). This translates into arterial microvascular protection, lowering computed 10-year ASCVD risk scores by 33% (*16*) and reducing composite renal/microalbuminuria events by 24.0% (*39*).

(E) Lymphoid sanctuary and epigenetic aging: Persistent lymphoid HIV transcription is associated with GSDMD-mediated pyroptosis, while ileal GLP-1 upregulation may represent compensatory counter-regulation (*22*). Plasma GDF-15 is associated with HIV reservoir markers and mitochondrial stress, but a GLP-1 RA-mediated reduction in GDF-15 has not been established (*50*). Separately, an exploratory post hoc randomized-trial analysis found reductions in several DNA-methylation aging measures, including PCGrimAge and DunedinPACE (*21*).

3.9. Cross-therapeutic comparison: GLP-1 RAs *vs*. alternative metabolic interventions

Optimizing clinical decision-making for aging PWH INSTI-induced obesity and CKM syndrome mandates a head-to-head comparison between incretin mimetics and alternative therapeutic regimens (*27,28*). A "one-size-fits-all" approach is inadequate given post-ART adipose accumulation heterogeneity, legacy NRTI-induced subcutaneous lipoatrophy, and prevalent anabolic resistance (*27,28*).

Lifestyle intervention remains the nonpharmacological foundation (*27*), while metformin offers low cost and exploratory mTOR-related reservoir effects (*37,47*). In HIV-specific studies, GLP-1 RAs have shown substantial reductions in VAT and inflammatory biomarkers (*16,38*); liver-fat, epigenetic, and gut outcomes derive from open-label, post hoc, or preliminary studies and should be interpreted accordingly (*17,20,21*). Key clinical boundaries include:

Sarcopenia Mitigation: GLP-1 RA-mediated weight loss involves skeletal muscle mass reduction, mandating concurrent resistance exercise (*17,27*).

Legacy Adipose Protection: For PWH with extensive historical NRTI lipoatrophy, the depot-specificity of tesamorelin remains valuable for visceral fat reduction without worsening subcutaneous fat loss (*28,31*).

Adjuvant Reservoir Blunting: Metformin's capacity to suppress intracellular mTOR-driven proliferation provides unique utility (*37,47*).

PK/PD integrity: Bariatric surgery can alter gastric volume, pH, emptying, intestinal exposure, and bile-acid handling, which may change antiretroviral exposure in a drug-specific manner (*51-53*). Regimen review and therapeutic monitoring should be considered rather than assuming a uniform loss of absorption (*53*).

A comprehensive multidimensional comparison is detailed in Table 6 (*16,17,27,31,37,39,47,51,52*):

3.10. Discussion: Unresolved biology, clinical implementation & translational frontiers

3.10.1. Gastrointestinal tolerability and stepped titration

Gastrointestinal adverse events such as nausea, vomiting, diarrhea, and constipation are common during dose escalation (*16*). Clinical implementation considerations are reviewed by Patoulias *et al.* (*54*). Recent observational analyses have not established an overall increase in thyroid-cancer risk (*55,56*). Current semaglutide labeling contraindicates use in patients with a personal or family history of medullary thyroid carcinoma or multiple endocrine neoplasia syndrome type 2 and recommends initiation at 0.25 mg once weekly with titration at 4-week intervals (*57*).

3.10.2. Sarcopenia prevention and muscle mass preservation

PWH are predisposed to sarcopenia and osteopenia due to the pro-inflammatory milieu of chronic infection, legacy antiretroviral toxicities, and aging (*27*). Clinical trials show that GLP-1 RA induced weight loss includes a significant reduction in skeletal muscle mass and psoas muscle volume (*17*). Consequently, clinicians should mandate structured resistance training (2–3 sessions weekly) and adequate protein intake (1.2–1.5 g/kg/day) during therapy (*17,27,37*).

3.10.3. Post-discontinuation metabolic rebound ("Bounce-back effect")

Obesity and CKM syndrome are chronic conditions (*58*). Discontinuing GLP-1 RA leads to rapid appetite recovery, with most individuals regaining lost weight within 1.5 years (*58*). Follow-up data from the SLIM LIVER cohort (Erlandson *et al*.) confirmed that 24 weeks after stopping semaglutide, participants experienced rapid weight regain and reversal of cardiometabolic, lipidomic, and blood pressure benefits (*59*). Real-world database analyses (Sarpatwari *et al*.) revealed that up to 75% of patients discontinue GLP-1 RAs within 12 months, influenced by out-of-pocket costs and access barriers (*60*). Short-term use is insufficient; long-term behavioral, dietary, and financial maintenance strategies are essential (*58-60*).

3.10.4. Pharmacogenomic precision medicine strategy

The GLP1R rs10305420 (p.Pro7Leu) association with treatment response and the GIPR rs1800437 (p.Glu354Gln) association with nausea or vomiting provide hypotheses for precision pharmacotherapy (*19*). However, these associations require external validation and prospective clinical-utility studies; genotype-guided drug selection, avoidance, or dose titration is not currently validated. Table 7 therefore presents these variants as research-stage companion-diagnostic candidates rather than clinical recommendations (*19*).

3.10.5. GLP-1 RAs in HIV cure and reservoir eradication strategies

The association between persistent lymphoid HIV transcription, GSDMD-mediated pyroptosis, and compensatory ileal GLP-1 production suggests new mechanistic questions for HIV-cure research (*22*). Localized lymphoid inflammation and ongoing antigen expression may contribute to reservoir persistence (*22,47,61,62*). Whether exogenous GLP-1 RAs can safely modulate these pathways or improve reservoir outcomes remains untested; their role in 'shock and kill' or 'block and lock' strategies should be considered hypothesis-generating (*22,48*). Four prospective research blueprints

Table 6. Multidimensional comparison of therapeutic strategies for weight gain and CKM syndrome in PWH

Therapeutic Strategy	Clinical Indications	Primary Molecular & Physiological Mechanisms	Distinct Immunometabolic Benefits for PWH	Core Biological Boundaries & Limitations	Evidence interpretation
GLP-1 RAs (*e.g.*, Semaglutide) (*16,17*)	Overweight/Obesity (BMI ≥ 27 kg/m^2 with comorbidities or ≥ 30 kg/m^2). CKM, MASLD under ART (*16,17*).	Central satiety and delayed gastric emptying; reductions in inflammatory biomarkers in PWH (*16,38*).	HIV-specific randomized and open-label studies show reductions in VAT and IHTG; epigenetic and gut findings remain exploratory or preliminary (*16,17,20,21*).	Gastrointestinal adverse events; lean-mass loss; weight regain after discontinuation (*59); and access/cost barriers (60*).	Randomized phase 2b evidence for body composition; other outcomes are exploratory. Grade A Recommendation (*16,17*)
Metformin (*37,47*)	T2DM. Off-label use for insulin resistance and MetD in PWH (*37*).	Hepatic AMPK activation. Mitochondrial Complex I inhibition. GDF-15 mitokine upregulation (*37*).	Low-cost therapy; HIV pilot data suggest mTOR-related reservoir effects but do not establish clinical reservoir reduction (*47*).	Negligible weight loss (<1.0 kg) (*37*). Lactic acidosis risk in advanced CKD (*37*). Vitamin B12 depletion (*37*).	Small pilot/observational evidence; not established for weight management in nondiabetic PWH. Grade B Recommendation (*37,47*)
SGLT2 inhibitors (*e.g.*, empagliflozin) (*63*)	T2DM with guideline-based cardiorenal indications (*63*).	Renal SGLT2 inhibition with glucosuria and natriuresis.	HIV-specific evidence is limited to observational use and safety; no HIV-specific cardiorenal efficacy trial was identified (*63*).	Mycotic genitourinary infections occurred in 5% versus 1% with GLP-1 agonists ($P = 0.17$); uptake was 8.8% among eligible PWH with T2DM (*63*).	Limited observational safety and utilization evidence in PWH. Grade B/C Recommendation (*39*)
Tesamorelin (*31,64*)	Targeted reduction of excess visceral abdominal fat (EVAF) in PWH with lipodystrophy (*31*).	Synthetic GHRH analog. Stimulates pituitary synthesis and release of endogenous IGF-1 (*31*).	Randomized HIV studies demonstrate selective VAT reduction without loss of subcutaneous fat (*64*).	Daily SC injection; IGF-1 elevation and glycemic monitoring; benefits diminish after discontinuation (*64*).	Randomized placebo-controlled evidence for VAT reduction in HIV-associated abdominal adiposity. Grade A Recommendation (*31*)
Lifestyle Intervention (*27*)	Universal baseline therapy for all overweight/obese PWH (*27*).	Negative caloric balance. Mechanical muscle-stretch induction. Preserves muscle mass (*27*).	Foundational nonpharmacological therapy; resistance exercise is advisable to mitigate loss of muscle mass during weight reduction (*17,27*).	Adherence can be challenging; whether lifestyle therapy reverses INSTI-associated adipose fibrosis is unknown (*29*).	Foundational therapy; HIV-specific evidence for preventing GLP-1-related lean-mass loss remains limited. Grade A Recommendation (*27*)
Bariatric Surgery (*51,52*)	Severe Class II/III obesity (BMI ≥ 35 with progressive cardiorenal collapse) (*51,52*).	Restrictive and/or malabsorptive anatomical change with endocrine and bile-acid effects.	Retrospective studies suggest acceptable short-term safety in PWH (*51,52*).	ART exposure may change after surgery; regimen-specific review and therapeutic monitoring are recommended (*53*).	Retrospective safety data; no randomized comparison in PWH. Grade B Recommendation (*51,52*)

MetD: metabolic dysfunction; SMM: skeletal muscle mass; T2DM: type 2 diabetes mellitus.

Table 7. Research-stage pharmacogenomic associations requiring clinical validation

Screening target	Genotype and reported association	Evidence status	Clinical implication
GLP1R rs10305420 (*19*)	GLP1R p. Pro7Leu effect allele associated with an additional -0.76 kg weight loss per allele; ancestry frequencies were reported (*19*).	Genome-wide association; requires external validation and prospective clinical-utility studies.	Do not alter standard semaglutide titration solely on genotype outside a research protocol.
GLP1R rs10305420 (*19*)	Absence of the GLP1R effect allele was associated with less average weight loss at the population level (*19*).	Population-level association; not a validated definition of an individual nonresponder.	Assess response using standard clinical criteria; no validated genotype-based switching threshold exists.
GIPR rs1800437 (*19*)	GIPR p. Glu354Gln variant associated with tirzepatide-related nausea or vomiting risk (*19*).	Genome-wide association; prospective validation is required.	Use product labeling and symptom-guided titration; genotype-guided dose reduction or avoidance is not validated.

Table 8. High-priority clinical trial blueprints for future HIV-metabolic research

Project Codename	Study Design & Arm Allocation	Target Study Population	Primary Scientific Hypothesis and Mechanism	Anticipated Clinical Endpoints
PRO-MUSCLE HIV	Prospective, multi-center, randomized open-label RCT: Arm A: Semaglutide + resistance training + protein; Arm B: Semaglutide monotherapy; Arm C: Lifestyle control	Sarcopenic or elderly (> 65 years) PWH on stable ART with central obesity (*27*)	Resistance exercise and high-protein intake prevent semaglutide induced lean mass loss, mitigating sarcopenia and frailty (*17,27*)	48-week change in skeletal muscle mass index (DXA); handgrip strength; Short Physical Performance Battery (SPPB) score (*17,27*)
CURE-MET HIV	Multi-center double-blind RCT: Arm A: Tirzepatide weekly (15 mg); Arm B: Semaglutide weekly (2.4 mg); Arm C: Placebo control (*16*)	Virologically suppressed PWH with high baseline inflammation (hsCRP > 3 μg/mL) (*16*)	Test whether tirzepatide or semaglutide changes inflammatory and mitochondrial-stress markers, including GDF-15, and whether those changes correlate with reservoir measures (*22,50*).	72-week change in cell-associated HIV-1 RNA/DNA ratio; Intact Proviral DNA Assay (IPDA); plasma GDF-15 level (*22,50*)
GENO-GUIDE PWH	Prospective validation study comparing standard care with a prespecified genotype-stratified research algorithm; no unvalidated dose changes outside protocol (*19*).	High-risk overweight PWH initiating GLP-1 RA therapy (*19*)	Determine whether GLP1R/GIPR variants improve prediction of response or tolerability beyond clinical factors (*19*).	12-month treatment discontinuation (dropout) rate; incidence of Grade 3/4 gastrointestinal adverse events; mean weight loss (*19*)
DUAL-MET CARDIO	Exploratory randomized trial: semaglutide plus an SGLT2 inhibitor versus semaglutide alone versus placebo (*13,39,63*).	High-cardiovascular-risk PWH with T2DM, established ASCVD, or CKD (*13,16,39*).	Test additive cardiorenal effects and safety in PWH; HIV-specific combination efficacy is not established (*13,39,63*).	96-week composite of major adverse cardiovascular events (MACE) and CKD progression; rate of genital mycotic infections (*13,16,39*)

are outlined in Table 8 (*13,16,17,19,22,27,39,50*).

4. Conclusions

GLP-1 RAs and dual co-agonists are promising options for obesity and cardiometabolic risk management in PWH. HIV-specific clinical studies support reductions in body weight, visceral adiposity, liver fat, and selected inflammatory biomarkers, while evidence for gut immune remodeling, biological-aging effects, and HIV-reservoir modification remains preliminary, exploratory, or mechanistic. Treatment should be individualized using established clinical indications, standard dose titration, resistance exercise and adequate protein intake, and long-term plans for weight maintenance. Pharmacogenomic dosing and HIV-cure applications should remain within research protocols until prospectively validated.

Acknowledgements

The authors are grateful to the study participants of the clinical trials presented in this review. The authors

would like to thank Angie Massicotte for administrative assistance.

Funding: This work was supported by National Science and Technology Major Project for Prevention and Control of Emerging, Re emerging and Major Infectious Diseases (No. 2025ZD01904500), Shenzhen Clinical Research Center for Emerging Infectious Diseases (No. LCYSSQ20220823091203007), the National Natural Science Foundation of China (No. 82574171), the project of the Guangdong Basic and Applied Basic Research Foundation (No. 2024A1515012118), the Guangdong Provincial Medical Science and Technology Research Fund Project (No. A2025250), National Key Research and Development Program of China (No. 2024YFC2311105), The high-level medical specialist team introduction training project of Dongguan, and Sanming Project of Medicine in Shenzhen (SZSM202311033).

Conflict of Interest: The authors have no conflicts of interest to disclose.

References

1. Marcus JL, Leyden WA, Alexeeff SE, Anderson AN, Hechter RC, Hu H, Lam JO, Towner WJ, Yuan Q, Horberg MA, Silverberg MJ. Comparison of Overall and Comorbidity-Free Life Expectancy Between Insured Adults With and Without HIV Infection, 2000-2016. JAMA Netw Open. 2020; 3:e207954.
2. Bares SH, Smeaton LM, Xu A, Godfrey C, McComsey GA. HIV-Infected Women Gain More Weight than HIV-Infected Men Following the Initiation of Antiretroviral Therapy. J Womens Health (Larchmt). 2018; 27:1162-1169.
3. Sax PE, Erlandson KM, Lake JE, *et al*. Weight Gain Following Initiation of Antiretroviral Therapy: Risk Factors in Randomized Comparative Clinical Trials. Clin Infect Dis. 2020; 71:1379-1389.
4. Wohl DA, Koethe JR, Sax PE, McComsey GA, Kuritzkes DR, Moyle G, Kaplan L, van Wyk J, Campo RE, Cohen C. Antiretrovirals and Weight Change: Weighing the Evidence. Clin Infect Dis. 2024; 79:999-1005.
5. Bares SH, Wu X, Tassiopoulos K, Lake JE, Koletar SL, Kalayjian R, Erlandson KM. Weight Gain After Antiretroviral Therapy Initiation and Subsequent Risk of Metabolic and Cardiovascular Disease. Clin Infect Dis. 2024; 78:395-401.
6. Shah ASV, Stelzle D, Lee KK, *et al*. Global Burden of Atherosclerotic Cardiovascular Disease in People Living With HIV: Systematic Review and Meta-Analysis. Circulation. 2018; 138:1100-1112.
7. Ndumele CE, Rangaswami J, Chow SL, *et al*. Cardiovascular-Kidney-Metabolic Health: A Presidential Advisory From the American Heart Association. Circulation. 2023; 148:1606-1635.
8. Liu C, Sun L, Xiao X, He Y, Zhao F, Luo Y, Zhao D, Jiang Y, Gao K, Gong W, Li X, Kong T, Lu H, Liu J. Longitudinal evolution and risk profiles of comorbidity among people with HIV in China: a retrospective cohort study. Front Public Health. 2025; 13:1753514.
9. Wilding JPH, Batterham RL, Calanna S, Davies M, Van Gaal LF, Lingvay I, McGowan BM, Rosenstock J, Tran MTD, Wadden TA, Wharton S, Yokote K, Zeuthen N, Kushner RF, STEP 1 Study Group. Once-Weekly Semaglutide in Adults with Overweight or Obesity. N Engl J Med. 2021; 384:989-1002.
10. Drucker DJ. The expanding landscape of GLP-1 medicines. Nat Med. 2026; 32:47-57.
11. Jastreboff AM, Aronne LJ, Ahmad NN, Wharton S, Connery L, Alves B, Kiyosue A, Zhang S, Liu B, Bunck MC, Stefanski A, SURMOUNT-1 Investigators. Tirzepatide Once Weekly for the Treatment of Obesity. N Engl J Med. 2022; 387:205-216.
12. Lincoff AM, Brown-Frandsen K, Colhoun HM, *et al*. Semaglutide and Cardiovascular Outcomes in Obesity without Diabetes. N Engl J Med. 2023; 389:2221-2232.
13. Perkovic V, Tuttle KR, Rossing P, Mahaffey KW, Mann JFE, Bakris G, Baeres FMM, Idorn T, Bosch-Traberg H, Lausvig NL, Pratley R, FLOW Trial Committees and Investigators. Effects of Semaglutide on Chronic Kidney Disease in Patients with Type 2 Diabetes. N Engl J Med. 2024; 391:109-121.
14. Thomas TS, Srinivasa S. Weighing In: Glucagon-Like Peptide-1 Receptor Agonism for Persons With HIV. Top Antivir Med. 2024; 32:579-588.
15. Haidar L, Delaney JAC. Glucagon-like peptide-1 receptor agonists in the aging population of people with HIV: emerging evidence and clinical implications. Curr Opin HIV AIDS. 2026; 21:355-361.
16. Eckard AR, Wu Q, Sattar A, Ansari-Gilani K, Labbato D, Foster T, Fletcher AA, Adekunle RO, McComsey GA. Once-weekly semaglutide in people with HIV-associated lipohypertrophy: a randomised, double-blind, placebo-controlled phase 2b single-centre clinical trial. Lancet Diabetes Endocrinol. 2024; 12:523-534.
17. Lake JE, Kitch DW, Kantor A, Muthupillai R, Klingman KL, Vernon C, Belaunzaran-Zamudio PF, Fichtenbaum CJ, Heath S, Perazzo H, Corey K, Brown TT, Landay A, Sattler F, Erlandson KM. The Effect of Open-Label Semaglutide on Metabolic Dysfunction-Associated Steatotic Liver Disease in People With HIV. Ann Intern Med. 2024; 177:835-838.
18. Haidar L, Crane HM, Nance RM, *et al*. Weight loss associated with semaglutide treatment among people with HIV. AIDS. 2024; 38:531-535.
19. Su QJ, Ashenhurst JR, Xu W, Tran V, Ryanne Wu R, Weldon CH, Shi J, Hicks B, 23andMe Research Team, Abul-Husn NS, Aslibekyan S, Holmes MV, Koelsch BL, Auton A. Genetic predictors of GLP1 receptor agonist weight loss and side effects. Nature. 2026; 653:770-775.
20. Marin M, Mfusi S, Gopee K, *et al*. GLP-1 RA Induces Gut T-Cell and Epithelial Remodeling in PWH From a Clinical Trial in South Africa. In: Conference on Retroviruses and Opportunistic Infections (CROI); 2026; Abstract 115.
21. Corley MJ, Dwaraka VB, Pang AP, Labbato D, Smith R, Ross Eckard A, McComsey GA. Semaglutide slows epigenetic aging in a randomized trial of HIV-associated lipohypertrophy. Nat Commun. 2026; 17:6606.
22. Crawford PA, Rhein J, Chipman JG, *et al*. Ongoing lymphoid HIV production drives pyroptosis and GLP-1 counter-regulation in ART-suppressed infection. bioRxiv [Preprint]. 2026:2026.01.09.698696. doi: 10.64898/2026.01.09.698696.
23. Koethe JR, Jenkins CA, Lau B, *et al*. Rising Obesity Prevalence and Weight Gain Among Adults Starting Antiretroviral Therapy in the United States and Canada.

AIDS Res Hum Retroviruses. 2016; 32:50-8.
24. Bourgi K, Rebeiro PF, Turner M, Castilho JL, Hulgan T, Raffanti SP, Koethe JR, Sterling TR. Greater Weight Gain in Treatment-naive Persons Starting Dolutegravir-based Antiretroviral Therapy. Clin Infect Dis. 2020; 70:1267-1274.
25. Li T, Sun L, He Y, Zhou Y, Xu L, Zhao F, Hu D, Wang H, Lu H, Liu J. Increasing trends of overweight and obesity in treatment-naive people living with HIV in Shenzhen from 2014 to 2020: an emerging health concern. Front Public Health. 2023; 11:1186838.
26. Sun L, Jiang Y, Isnard S, *et al*. Comparative safety and efficacy of BIC/FTC/TAF versus DTG+3TC in antiretroviral treatment-naive patients with HIV as first-line regimens: A real-world cohort study. Biosci Trends. 2026; 20:205-216.
27. Hawkins KL, Zhang L, Ng DK, Althoff KN, Palella FJ Jr, Kingsley LA, Jacobson LP, Margolick JB, Lake JE, Brown TT, Erlandson KM. Abdominal obesity, sarcopenia, and osteoporosis are associated with frailty in men living with and without HIV. AIDS. 2018; 32:1257-1266.
28. Koethe JR, Lagathu C, Lake JE, Domingo P, Calmy A, Falutz J, Brown TT, Capeau J. HIV and antiretroviral therapy-related fat alterations. Nat Rev Dis Primers. 2020; 6:48.
29. Gorwood J, Bourgeois C, Pourcher V, *et al*. The Integrase Inhibitors Dolutegravir and Raltegravir Exert Proadipogenic and Profibrotic Effects and Induce Insulin Resistance in Human/Simian Adipose Tissue and Human Adipocytes. Clin Infect Dis. 2020; 71:e549-e560.
30. Nguyen Q, Wooten D, Lee D, Moreno M, Promer K, Rajagopal A, Tan M, Tang M, Duren K, Yin J, Hill L. Glucagon-like Peptide 1 Receptor Agonists Promote Weight Loss Among People With HIV. Clin Infect Dis. 2024; 79:978-982.
31. Beach R, Tims-Cook Z, McGary CS, Thote T. Differing Presentations of Excess Visceral Abdominal Fat in People Living With HIV: Two Clinical Cases Highlighting Distinct Therapeutic Pathways With Tesamorelin and Glucagon-Like Peptide-1 Receptor Agonists. Clin Infect Dis. 2026; 82:S87-S91.
32. Pryke L, Koethe JR, Bailin S. Obesity and Weight Management in HIV: Epidemiology, Complications, and Emerging Treatments. Curr HIV/AIDS Rep. 2026; 23:6.
33. Ma J, Ruderman SA, Haidar L, *et al*. Impact of semaglutide on liver fibrosis score in people with HIV: findings from the CNICS cohort. AIDS. 2026; doi: 10.1097/QAD.0000000000004544.
34. Noe S, Ivanova A, Johnsson-Oldenbüttel C, Schäfer G, Schewe K, Hoffmann C. Immunological alterations with GLP-1 agonists in people living with HIV. HIV Med. 2024; 25:893-894.
35. Ramendra R, Isnard S, Mehraj V, Chen J, Zhang Y, Finkelman M, Routy JP. Circulating LPS and (1→3)-β-D-Glucan: A Folie à Deux Contributing to HIV-Associated Immune Activation. Front Immunol. 2019; 10:465.
36. Ouyang J, Yan J, Zhou X, Isnard S, Harypursat V, Cui H, Routy JP, Chen Y. Relevance of biomarkers indicating gut damage and microbial translocation in people living with HIV. Front Immunol. 2023; 14:1173956.
37. Isnard S, Lin J, Fombuena B, *et al*. Repurposing Metformin in Nondiabetic People With HIV: Influence on Weight and Gut Microbiota. Open Forum Infect Dis. 2020; 7:ofaa338.
38. Funderburg NT, Ross Eckard A, Wu Q, Sattar A, Ailstock K, Cummings M, Labbato D, McComsey GA. The Effects of Semaglutide on Inflammation and Immune Activation in HIV-associated Lipohypertrophy. Open Forum Infect Dis. 2025; 12:ofaf152.
39. Sasaki T, Giang SM, Wu J, Yokoo T, Gallagher M, Bellomo R, Wang AY. The effect of GLP-1 receptor agonists on renal outcomes: a systematic review and meta-analysis. Nephrol Dial Transplant. 2026; 41:681-691.
40. Kosiborod MN, Abildstrøm SZ, Borlaug BA, *et al*. Semaglutide in Patients with Heart Failure with Preserved Ejection Fraction and Obesity. N Engl J Med. 2023; 389:1069-1084.
41. Packer M, Zile MR, Kramer CM, Baum SJ, Litwin SE, Menon V, Ge J, Weerakkody GJ, Ou Y, Bunck MC, Hurt KC, Murakami M, Borlaug BA, SUMMIT Trial Study Group. Tirzepatide for Heart Failure with Preserved Ejection Fraction and Obesity. N Engl J Med. 2025; 392:427-437.
42. Ross Eckard A, Wu Q, Sattar A, Labbato D, Koberssy Z, Daher J, McComsey GA. Effects of semaglutide on subclinical cardiovascular health in people with HIV. In: Conference on Retroviruses and Opportunistic Infections (CROI); 2026; Abstract 699.
43. Kim HH, Dixit VD. Metabolic regulation of immunological aging. Nat Aging. 2025; 5:1425-1440.
44. Klausen MK, Thomsen M, Wortwein G, Fink-Jensen A. The role of glucagon-like peptide 1 (GLP-1) in addictive disorders. Br J Pharmacol. 2022; 179:625-641.
45. Ruderman SA, Crane HM, Haidar L, *et al*. Initiating semaglutide therapy reduces tobacco cigarette smoking intensity among people with HIV. AIDS. 2026; doi: 10.1097/QAD.0000000000004596.
46. Wang W, Volkow ND, Berger NA, Davis PB, Kaelber DC, Xu R. Associations of semaglutide with incidence and recurrence of alcohol use disorder in real-world population. Nat Commun. 2024; 15:4548.
47. Planas D, Pagliuzza A, Ponte R, *et al*. LILAC pilot study: Effects of metformin on mTOR activation and HIV reservoir persistence during antiretroviral therapy. EBioMedicine. 2021; 65:103270.
48. Ben Nasr M, Usuelli V, Dellepiane S, *et al*. Glucagon-like peptide 1 receptor is a T cell-negative costimulatory molecule. Cell Metab. 2024; 36:1302-1319.e12.
49. Ghahari N, Telittchenko R, Loucif H, Isnard S, Routy JP, Olagnier D, van Grevenynghe J. Harnessing Autophagy to Overcome Antigen-Specific T-Cell Dysfunction: Implication for People Living with HIV-1. Int J Mol Sci. 2023; 24:11018.
50. Isnard S, Royston L, Berini CA, *et al*. Plasma GDF-15 levels are associated with HIV reservoir markers independently of inflammation in people with HIV on antiretroviral therapy. J Infect Dis. 2026; jiag202.
51. Sierra L, Aitharaju V, Prado R, Cymbal M, Chaterjee A, Khurana A, Patel R, Firkins S, Simons-Linares R. In-Hospital Outcomes of Bariatric Surgery in People Living with HIV: A Nationwide Analysis. Obes Surg. 2025; 35:3111-3119.
52. Aitharaju V, Sierra L, Syed A, Flora B, Staneff E, Chatterjee A, Khurana A, Patel R, Firkins S, Simons-Linares R. Safety of bariatric surgery in HIV-positive patients on antiretroviral therapy. Surg Obes Relat Dis. 2025; 21:1126-1130.
53. Zino L, Kingma JS, Marzolini C, Richel O, Burger DM, Colbers A. Implications of Bariatric Surgery on the Pharmacokinetics of Antiretrovirals in People Living with

HIV. Clin Pharmacokinet. 2022; 61:619-635.
54. Patoulias D, Karakasis P, Ruža I, El-Tanani M, Rizzo M. Unraveling the safety and efficacy of semaglutide for people living with HIV and metabolic co-morbidities. Expert Opin Drug Saf. 2025; 24:121-124.
55. Vilsbøll T, Stellfeld M, Aroda VR, Dandanell S, David JP, Kristiansen CTP, Rasmussen S, Roberts FL, Hegedüs L. Assessment of thyroid cancer risk associated with glucagon-like peptide 1 receptor agonist use. Diabetes Obes Metab. 2026; 28:1499-1507.
56. Brito JP, Herrin J, Swarna KS, Singh Ospina NM, Montori VM, Toro-Tobon D, Umpierrez GE, Galindo RJ, Deng Y, Mickelson MM, Shao H, Polley EC, McCoy RG. GLP-1RA Use and Thyroid Cancer Risk. JAMA Otolaryngol Head Neck Surg. 2025; 151:243-252.
57. U.S. Food and Drug Administration. WEGOVY (semaglutide) prescribing information. Revised May 2026. *https://www.accessdata.fda.gov/drugsatfda_docs/label/2026/215256s031lbl218316s003lbl.pdf* (accessed August 10, 2026).
58. West S, Scragg J, Aveyard P, Oke JL, Willis L, Haffner SJP, Knight H, Wang D, Morrow S, Heath L, Jebb SA, Koutoukidis DA. Weight regain after cessation of medication for weight management: systematic review and meta-analysis. BMJ. 2026; 392:e085304.
59. Erlandson KM, Kitch DW, Kantor A, Belaunzaran-Zamudio PF, Brown TT, Fichtenbaum CJ, Heath SL, Sattler FR, Lake JE. The Bounce-back Effect: What Happens After Cessation of Low-dose Semaglutide in People With HIV. Clin Infect Dis. 2026; 82:e544-e548.
60. Sarpatwari A, Soto MJ, Ganguli I, Sloan CE, Goss F, Sinaiko AD. Glucagon-Like Peptide-1 Receptor Agonist Order Fills and Out-of-Pocket Costs by Race, Ethnicity, and Indication. JAMA Health Forum. 2025; 6:e254258.
61. Takata H, Mitchell JL, Pacheco J, *et al*. An active HIV reservoir during ART is associated with maintenance of HIV-specific CD8+ T cell magnitude and short-lived differentiation status. Cell Host Microbe. 2023; 31:1494-1506.e4.
62. Dubé M, Tastet O, Dufour C, Sannier G, Brassard N, Delgado GG, Pagliuzza A, Richard C, Nayrac M, Routy JP, Prat A, Estes JD, Fromentin R, Chomont N, Kaufmann DE. Spontaneous HIV expression during suppressive ART is associated with the magnitude and function of HIV-specific CD4+ and CD8+ T cells. Cell Host Microbe. 2023; 31:1507-1522.e5.
63. Sise ME, Katz-Agranov N, Strohbehn IA, Harden D, Moreno D, Durbin C, Toribio M, Neilan TG, Zanni MV. Brief Report: Use and Side Effects of Sodium-Glucose Transporter 2 Inhibitors Among US People With HIV With Clinical Indications. J Acquir Immune Defic Syndr. 2023; 94:53-56.
64. Falutz J, Allas S, Mamputu JC, Potvin D, Kotler D, Somero M, Berger D, Brown S, Richmond G, Fessel J, Turner R, Grinspoon S. Long-term safety and effects of tesamorelin, a growth hormone-releasing factor analogue, in HIV patients with abdominal fat accumulation. AIDS. 2008; 22:1719-1728.

Received June 6, 2026; Revised August 9, 2026; Accepted August 17, 2026.

[§]These authors contributed equally to this work.
**Address correspondence to:*
Jean-Pierre Routy, Division of Hematology, Chronic Viral Illness Service, and Research Institute of the McGill University Health Centre, Montreal, QC, Canada.
E-mail: jean-pierre.routy@mcgill.ca

Hongzhou Lu and Yun He, Department of Infectious Diseases, National Clinical Research Center for Infectious Diseases, Shenzhen Third People's Hospital, Shenzhen, Guangdong, China.
E-mail: luhongzhou@fudan.edu.cn (HL), yuer-he@163.com (YH)

Released online in J-STAGE as advance publication August 21, 2026.

Original Article

DOI: 10.5582/bst.2026.01000

PRXL2B facilitates the progression of hepatocellular carcinoma and the therapeutic efficacy of oncolytic adenovirus H101 through the PI3K/AKT/PD-L1 axis

Ziqi Zhang[1,§], Hongli Chen[2,§], Yangming Liu[3,§], Hao Wang[1], You Yan[1,4], Yanxi Yu[1], Zuotian Huang[1], Yanyao Liu[1], Wei Li[1], Zhongjun Wu[1], Meiqing Kang[1], Xiaoyong Luo[5], Ping Che[6,*], Rui Liao[1,*]

[1] Department of Hepatobiliary Surgery, The First Affiliated Hospital of Chongqing Medical University, Chongqing, China;
[2] Nanchuan District Maternal and Child Health Care Hospital, Chongqing, China;
[3] Department of Obstetric, The Affiliated Banan Hospital of Chongqing Medical University, Chongqing, China;
[4] Department of Pathology, The Second Affiliated Hospital of Chongqing Medical University, Chongqing, China;
[5] Department of Gastrointestinal Surgery, Chongqing Jiulongpo People's Hospital, Chongqing, China;
[6] Department of Hepatobiliary Surgery, Shapingba Hospital affiliated to Chongqing University (Shapingba District People's Hospital of Chongqing), Chongqing, China.

SUMMARY: Oncolytic adenovirus H101 has shown antitumor activity in hepatocellular carcinoma (HCC), but the molecular determinants of treatment response remain unclear. In this study, a Hepa1-6 subcutaneous tumor model was established in C57BL/6 mice and treated with intratumoral H101, followed by integrated transcriptomic and proteomic analyses to identify candidate genes associated with H101 response. PRXL2B was selected for further investigation using public multi-omics datasets, tissue microarray-based immunohistochemistry, *in vitro* functional assays, mechanistic analyses, and *in vivo* validation experiments. Integrated multi-omics analyses identified PRXL2B as a candidate gene downregulated after H101 treatment. Public datasets and tissue-based validation further showed that PRXL2B was upregulated in HCC tissues. In MHCC97H and HCCLM3 cells, PRXL2B knockdown inhibited proliferation, migration, and invasion, promoted apoptosis and cell-cycle arrest, and enhanced the antitumor effect of H101. Mechanistically, PRXL2B silencing reduced AKT phosphorylation and PD-L1 expression. *In vivo*, PRXL2B knockdown suppressed tumor growth, and the combination of PRXL2B knockdown and H101 produced the strongest antitumor effect. These findings indicate that PRXL2B promotes malignant phenotypes in HCC and may modulate H101 efficacy through the PI3K/AKT/PD-L1 axis. Targeting PRXL2B may therefore represent a potential strategy to enhance the therapeutic efficacy of oncolytic virus therapy in HCC.

Keywords: hepatocellular carcinoma, oncolytic adenovirus, H101, PRXL2B, PD-L1

1. Introduction

Hepatocellular carcinoma (HCC), as the most prevalent subtype of primary liver cancer, persists as a primary cause of cancer-related mortality globally. Curative treatments, such as resection, local ablative procedures, and transplantation, can improve survival rates among carefully selected early-stage patients (*1*). Nevertheless, due to the asymptomatic progression and delayed detection, a substantial number of patients are diagnosed with advanced-stage disease, precluding the application of potentially curative therapies. For these patients, targeted therapy and immune checkpoint inhibitors (ICIs) have the potential to enhance overall survival. However, their efficacy is still constrained by tumor heterogeneity, immune microenvironment suppression, and acquired resistance (*2*). Consequently, exploring novel strategies that integrate "direct tumor cell killing" with "immune remodeling" remains a critical direction for HCC treatment.

Oncolytic virus (OV) therapy exerts its effects *via* dual mechanisms. Firstly, it selectively replicates within tumor cells and causes their lysis (*3*). Secondly, it induces immunogenic cell death, facilitates the release of tumor antigens, and activates both innate and adaptive immune responses (*4*). This therapeutic approach has gained increasing attention since the early studies in the 1950s, where the first viral agents were used in cancer treatment, and has since evolved with the development of genetically modified oncolytic viruses that can

selectively target cancer cells. H101, a recombinant adenoviral oncolytic agent, has demonstrated clinical potential in several tumor types, such as non-small cell lung cancer, head and neck squamous cell carcinoma, glioblastoma, and HCC (*5-7*). In particular, its use in HCC has shown promise in preclinical and clinical trials, offering a new strategy to target both tumor cells and the immune microenvironment (*8*). Nevertheless, the efficacy of OV varies significantly across different tumor types and among individuals. This variability is partly due to differences in the tumor microenvironment and the immune system's ability to recognize and respond to the viral infection (*9*). The key molecules and predictive biomarkers related to its response remain unclear. Recent studies suggest that immune checkpoint proteins, such as PD-L1, and tumor-intrinsic factors, like mutations in the PI3K/AKT pathway, may influence OV therapy efficacy in HCC (*10*). In particular, the tumor-intrinsic factors and downstream immune regulation mechanisms that influence the sensitivity and tolerance of oncolytic adenovirus therapy in HCC require further clarification (*11*).

Multi-omics investigations, encompassing transcriptomics and proteomics, have emerged as potent methodologies to characterize alterations in tumor molecular profiles subsequent to therapeutic interventions. These studies contribute to surmounting the limitations of single-omics approaches, which frequently encounter discrepancies between transcriptional and protein-level data. Through the integration of transcriptomic and proteomic data, more robust candidate molecules can be identified, thereby furnishing a more reliable foundation for comprehending molecular mechanisms and translating research findings into clinical applications (*12*). In recent years, multi-omics has been applied in HCC research to uncover novel therapeutic targets and biomarkers. For instance, studies have amalgamated genomic, transcriptomic, and proteomic data to identify pivotal signaling pathways implicated in HCC progression. A study demonstrated that the integration of proteomic and transcriptomic profiles could assist in identifying potential therapeutic targets such as PD-L1 and VEGF in HCC, offering insights into immune evasion mechanisms and tumor vascularization (*13*). Furthermore, a study in employed multi-omics approaches to analyze alterations in the tumor microenvironment (TME) in HCC, revealing novel perspectives on how metabolic shifts in the TME influence tumorigenesis. By integrating metabolomics with transcriptomics and proteomics, the researchers were able to uncover novel biomarkers associated with a poor prognosis in HCC patients (*14*). This approach underscored the crucial role of metabolic reprogramming in the development and progression of liver cancer. Another study in utilized multi-omics to explore the role of long non-coding RNAs (lncRNAs) in HCC, integrating RNA sequencing, proteomics, and epigenomics to delineate lncRNA-associated pathways in HCC. The integration of these data provided a more in-depth understanding of epigenetic regulation in liver cancer progression, presenting potential lncRNA targets for therapeutic intervention (*15*). These examples illustrate the substantial potential of multi-omics in understanding HCC biology and in the development of personalized medicine strategies for liver cancer (*16*).

In the present study, an immunocompetent Hepa1-6 subcutaneous tumor model was employed to assess the effects of intratumoral H101 treatment. Transcriptomic and proteomic data were integrated to identify response-related genes, and PRXL2B was selected as a key target. The findings were further validated using multi-omics data, immunohistochemistry of HCC tissue microarrays, *in vitro* functional assays, and mechanistic studies (PI3K/AKT-PD-L1 axis), along with *in vivo* combination therapy experiments, to clarify the role of PRXL2B in HCC progression and the efficacy of H101.

2. Materials and Methods

2.1. Cells and culture

Mouse Hepa1-6 cells, Hepatic progenitor cells (derived from mouse liver), Telomerase-immortalized human liver epithelial cells, Human hepatocellular carcinoma cells, and human liver cancer cell lines MHCC97H and HCCLM3 were purchased from Sevier (China). Animal experiments were approved by the Ethics Committee of Chongqing Medical University (IACUC-CQMU-2024-11061). Cells were cultured in DMEM supplemented with 10% fetal bovine serum (FBS, Procell) and 1% penicillin-streptomycin at 37°C in a 5% CO_2 incubator. Cells were passaged at a ratio of 1:3 to 1:5 and used for experiments during the logarithmic growth phase. H101 was purchased from Ankerui. *In vitro* infection was performed at a multiplicity of infection (MOI) of 0.05 for 96 hours, as previously described in Song *et al*., 2025 (*17*). The experimental groups were NC, shPRXL2B, and shPRXL2B + H101.

2.2. Clinical sample collection

The animal experiments were approved by the Ethics Committee of Chongqing Medical University (Approval No: IACUC-CQMU-2024-11061). The tissue microarray study was approved by the Ethics Committee of the First Affiliated Hospital of Chongqing Medical University (Approval No: 2024-607-01). A total of 84 pathological paraffin-embedded samples (including 84 HCC samples and 83 adjacent normal liver tissue samples) were collected from patients who underwent surgery at Chongqing Medical University between 2020 and 2023. Survival data from 84 patients who participated in postoperative follow-up were also included. These samples were used for tissue microarray preparation and

subsequent immunohistochemistry (IHC) and in situ hybridization analysis. All participants provided written informed consent. The samples were pathologically confirmed as HCC after surgery. All studies were conducted in accordance with the principles of the Declaration of Helsinki and the Istanbul Declaration.

2.3. Subcutaneous tumor implantation and treatment

Female C57BL/6 mice (7–8 weeks old) were used to establish subcutaneous Hepa1-6 tumor models. The mice were inoculated subcutaneously with 2×10^6 Hepa1-6 cells in PBS. When the tumor volume reached approximately 80 mm^3, intratumoral injections of H101 (1×10^8 PFU per dose, diluted in PBS, 80–120 μL per dose) were administered daily for 3 consecutive days, starting on day 9. The tumors were harvested on day 14. The tumor volume was calculated using the formula $V = 0.5 \times \text{length} \times \text{width}^2$. The experiment included 4 mice per group. All animal experiments were approved by the Ethics Committee of Chongqing Medical University (IACUC-CQMU-2024-11061).

2.4. Virus/plasmid construction and PRXL2B knockdown

PRXL2B expression was knocked down using shRNA. Human-shRNA-1 (h-sh1) and mouse-shRNA-1 (m-sh1) were used for *in vitro* and *in vivo* experiments, respectively. The shRNA vector was pLVX-shRNA2-Puro (BamHI/EcoRI cloning). The sequences are as follows (suggested for inclusion in the supplementary materials):

h-shPRXL2B-1 (insert sequence):
GATCGGGATGAGAGCAAGCAGCTTTACTCGAGT
AAAGCTGCTTGCTCTCATCCTTTTTT
M-shPRXL2B-1 (insert sequence):
GATCGATGAGAGCAAGCAAATCTATACTCGAGTA
TAGATTTGCTTGCTCTCATTTTTTT

Stable cell lines were selected using puromycin. Sensitivity for shRNA screening was optimized by titrating concentrations in pilot experiments, typically ranging from 1–3 μg/mL for 3–5 days.

2.5. Transcriptomics, proteomics analysis and multi-omics integration

Total RNA was extracted from tumor tissues using TRIzol reagent (Thermo Fisher Scientific, USA). cDNA libraries were constructed using SuperScript™ II Reverse Transcriptase (Invitrogen, USA). Paired-end sequencing (2 × 150 bp) was carried out using the Illumina NovaSeq™ 6000 platform. Differentially expressed genes (DEGs) were identified using DESeq2 with thresholds of $|\log2 \text{ - fold change}| \geq 1$ and FDR < 0.05. GO and KEGG enrichment analyses were conducted on DEGs. For proteomics, the raw data were processed using the Thermo Orbitrap Fusion Lumos platform and analyzed using Proteome Discoverer. Protein quantification was normalized using row means and column medians. Differential protein analysis was conducted with a p-value < 0.05 and FC > 1.2 or FC < 0.83. Pathway enrichment was carried out using standard enrichment factor calculations and presented as bubble plots. We integrated transcriptomic DEGs and proteomic differential proteins to identify robust candidate genes. Directionally consistent genes were selected for further validation based on their biological significance.

2.6. Immunohistochemistry and scoring

Immunohistochemical analysis was performed on a tissue microarray (TMA) cohort of 84 HCC samples to assess PRXL2B expression. This tissue microarray study was approved by the Ethics Committee of the First Affiliated Hospital of Chongqing Medical University (Approval No: 2024-607-01). The antibody used for PRXL2B detection was the C1orf93 polyclonal antibody (Proteintech, Catalog No: 26304-1-AP, Rabbit, IgG isotype), which was applied at the recommended dilution of 1:600. The H-score was calculated based on the staining intensity and the percentage of positive cells, classifying PRXL2B expression into high and low groups for subsequent survival analysis. The immunohistochemical procedure involved deparaffinization and rehydration of tissue sections, followed by antigen retrieval. The sections were incubated with the primary antibody (C1orf93, diluted 1:600) at room temperature for 1.5 hours. After incubation, the sections were washed and treated with a secondary antibody, followed by appropriate substrate development for visualization. The stained tissue sections were then evaluated by two independent pathologists to determine the staining intensity and the percentage of positively stained cells.

2.7. Western blot and antibodies

Cells were lysed in RIPA lysis buffer (Beyotime, China) for 10 minutes at 4°C. The supernatant was collected and centrifuged at 15,000 rpm for 15 minutes at 4°C. Protein concentration was measured using the BCA protein assay kit (Solarbio, Beijing, China). A total of 20 μg of protein was boiled and separated by 12.5% SDS-PAGE, then transferred to a PVDF membrane (Millipore, USA). The membrane was blocked with 5% non-fat milk for 1 hour, followed by incubation with primary antibodies at 4°C: PRXL2B (1:500, Proteintech #26304-1-AP, China), AKT (1:5000, Proteintech 10176-2-AP, China), p-AKT (1:2000; Proteintech #66444-1-Ig, China), PD-L1 (1:2000; 66248-1-Ig, Proteintech, China), and GAPDH (1:2000; #60004-1-Ig, Proteintech, China). Protease/phosphatase inhibitor cocktail (Beyotime, Catalog No. P1081, 50X) was added during the protein

extraction process to prevent protein degradation and dephosphorylation.

2.8. Cell migration and invasion assays

A wound healing assay was conducted to evaluate cell migration. Cells (5×10^6 cells per well) were seeded in 6-well plates. Once the cells reached 100% confluence, a 200 μl pipette tip was employed to create a scratch in the cell monolayer. The wounds were infected with H101 at a multiplicity of infection (MOI) of 0.05. Wound healing was monitored at designated intervals over 48 hours. Images were captured from five distinct angles per well and analyzed using ImageJ software (version 1.52) to measure the wound area. The percentage of wound healing was quantified using the following formula: [1-(Wound Area at Tt/Wound Area at T0)]×100%. Transwell assays were used to evaluate cell migration and invasion. For the migration assay, 10^4 cells were plated in 100 μl of serum-free medium in 24-well inserts (Corning, USA). For the invasion assay, cells were plated on Matrigel-coated inserts (Beyotime, China). To each insert, 100 μL of medium with H101 (MOI = 0.05) or serum-free medium was added. In the lower chamber, 500 μL of medium with 10% FBS was used as a chemoattractant. After 24 hours of incubation, non-migrating or non-invading cells in the upper chamber were removed using a cotton swab. Cells that had migrated or invaded through the insert were fixed with 4% paraformaldehyde and stained with 0.1% crystal violet. The number of migrating or invading cells in three random fields was quantified under an inverted microscope (Leica, Germany).

2.9. Cell apoptosis detection

Cells were harvested from one well of a 6-well plate. Floating cells were collected in a centrifuge tube, and adherent cells were digested with 0.25% trypsin to obtain single cells, ensuring not to over-digest. The cells were washed twice with PBS at 1000 rpm for 5 minutes. Cells (1×10^6) were resuspended in 500 μL of PBS (PH = 7.2) and stored in 1.5 mL EP tubes for apoptosis detection.

2.10. Cell cycle detection

Cells were harvested from one well of a 6-well plate. Floating cells were collected in a centrifuge tube. The adherent cells were digested with 0.25% trypsin to obtain single cells, again ensuring to avoid over-digestion. The cells were washed twice with PBS at 1000 rpm for 5 minutes and resuspended in 100 μL of PBS. Slowly, 900 μL of pre-chilled 75% ethanol was added while gently shaking to prevent cell aggregation. The cells were stored at 4°C for 2-3 weeks. Flow cytometry analysis of cell cycle and apoptosis was performed using a Attune NxT flow cytometer (Thermo Fisher Scientific, USA), and data were analyzed using Modfit software (version 4.1).

2.11. Cell proliferation assay

According to the manufacturer's instructions, the Cell Count Kit-8 (CCK-8) (Topscience, China) was used to conduct cell proliferation assays. 1×10^4 HCC97-H and HCC-LM3 cells were seeded in 96-well plates and infected with the virus as described in the virus growth assays. At various time points (0, 24, 48, 72, and 96 hours), 10 μL of CCK-8 solution (mixed with 100 μL DMEM medium) was added to each well and incubated at 37°C for 1 hour. The optical density (OD) was measured using a microplate reader (Bio-Rad, USA) at 450 nm.

2.12. Statistical analysis

Statistical comparisons were conducted using Student's *t*-test for two-group Statistical comparisons were conducted using Student's *t*-test for two-group comparisons (with normality tested). One-way ANOVA with post-hoc testing was employed for multiple group comparisons. Survival analysis was carried out using Kaplan-Meier curves and log-rank tests. Cox regression analysis was performed for both univariate and multivariate models. Statistical analyses were performed using GraphPad Prism version 9.0 (GraphPad Software, USA) for *t*-test and ANOVA, and SPSS version 26.0 (IBM, USA) for Kaplan–Meier survival analysis and Cox regression.

3. Results

3.1. H101 inhibition of tumor growth and identification of response-related genes

To assess the impact of oncolytic adenovirus H101 on liver cancer growth, a subcutaneous Hepa1-6 tumor model was established in immunocompetent female C57BL/6 mice. When the tumor volume approximated 80 mm^3, H101 (1×10^8 PFU per dose, diluted in PBS) was administered *via* intratumoral injection once daily for three consecutive days, commencing on day 9. Tumors were excised on day 14 for subsequent omics analysis (n = 4 per group) (Figure 1a). In comparison with the control group, the tumors in the H101-treated group exhibited a substantial reduction in size at the experimental endpoint (Figure 1b). Tumor growth curves demonstrated that H101 treatment significantly impeded tumor volume expansion (Figure 1c), and the tumor weight at the endpoint was also significantly decreased (Figure 1d, two-tailed Student's *t*-test, p = 0.027). To analyze the molecular characteristics of the tumors subsequent to H101 treatment, RNA-seq and proteomics analyses were conducted on tumor tissues (log2FC of Transcriptomic = -0.9300, P-value of Transcriptomic

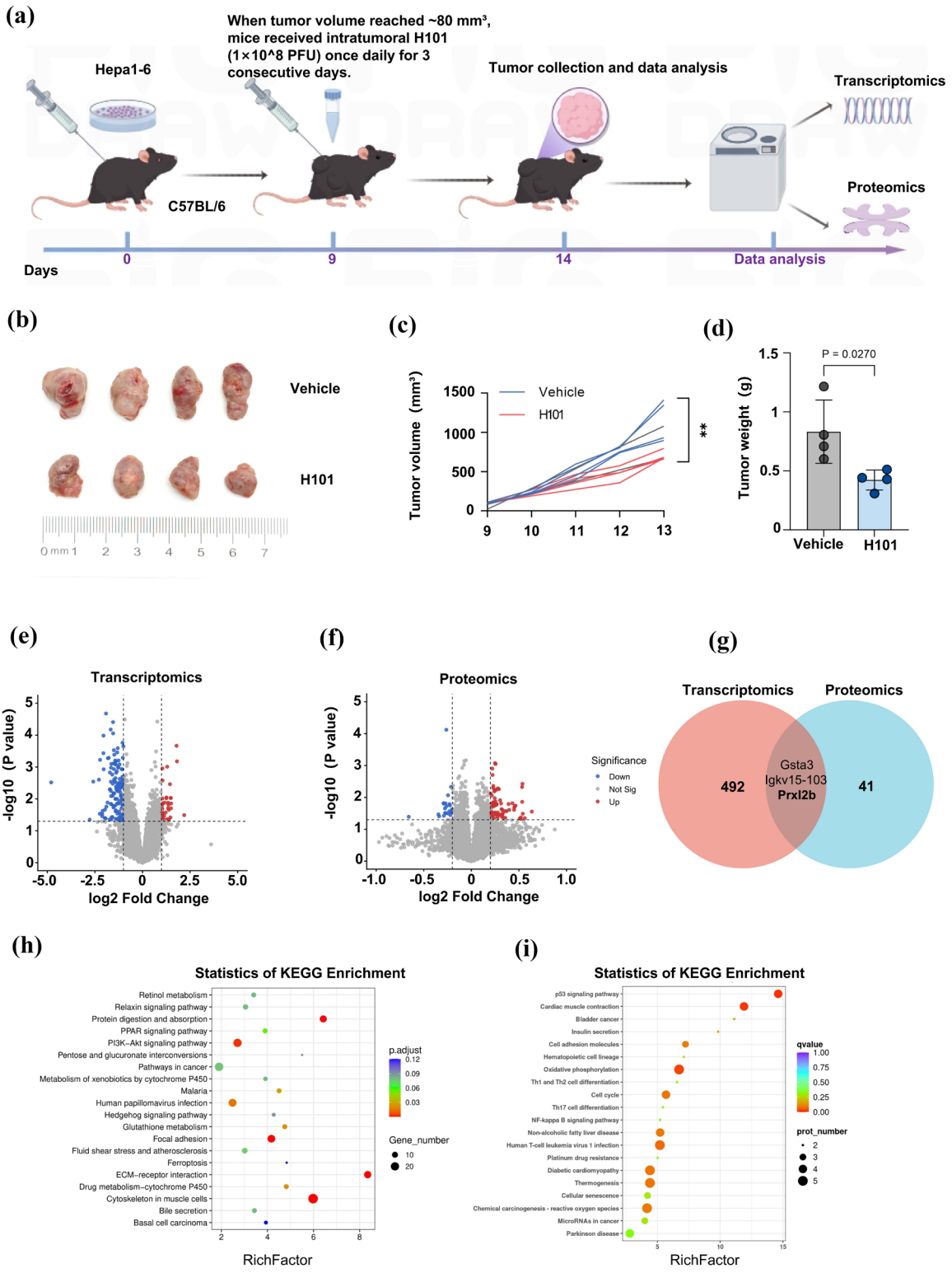


Figure 1. Intratumoral H101 suppresses Hepa1-6 subcutaneous tumor growth and identifies PRXL2B through integrated transcriptomic and proteomic analyses. (a) Schematic illustration of the experimental design. Female C57BL/6 mice were subcutaneously inoculated with Hepa1-6 cells (2×10^6). When tumors reached approximately 80 mm^3, mice received intratumoral H101 injections (1×10^8 PFU) once daily for 3 consecutive days beginning on day 9. Tumors were collected on day 14 for transcriptomic and proteomic analyses ($n = 4$ per group). **(b)** Representative images of excised tumors collected at day 14. **(c)** Tumor growth curves. Tumor volume was calculated as V = 0.5 × length × $width^2$. **(d)** Tumor weights at day 14. Data are presented as mean ± SD with individual values. Statistical significance was determined using a two-tailed Student's *t*-test. **(e)** Volcano plot of differentially expressed genes (DEGs) identified by RNA-seq analysis in H101-treated and PBS-treated tumors. **(f)** Volcano plot of differentially expressed proteins identified by proteomic analysis in H101-treated and PBS-treated tumors. **(g)** Venn diagram showing the overlap between transcriptomic and proteomic analyses, with PRXL2B highlighted. **(h)** KEGG pathway enrichment analysis of transcriptomic DEGs **(h)** and differentially expressed proteins **(i)** The x-axis indicates the enrichment factor (GeneRatio). Dot size represents gene/protein counts, and dot color indicates adjusted P values.

= 0.0200 and log2FC of Proteomic = -1.5327, *p*-value of Proteomic = 0.0038). Volcano plots revealed a considerable number of differentially expressed genes (DEGs), with two genes being upregulated and one gene being downregulated (Figure 1e). Significant differential proteins were also detected through proteomics analysis (Figure 1f). Further integration of RNA-seq DEGs with differential proteins from proteomics yielded three common candidate molecules (Figure 1g), suggesting that these molecules could serve as stable core nodes involved in the H101 response. Pathway enrichment analysis indicated that the differential molecules were predominantly enriched in tumor-associated signaling pathways, with the PI3K/AKT pathway being one of the significantly enriched pathways (Figure 1h–i). This implies that the antitumor effects of H101 may be regulated by this classical oncogenic pathway. Based on the expression direction and potential biological significance of the intersecting candidate molecules, PRXL2B (C1orf93), which was downregulated following H101 treatment, was selected as the key target for further investigation. Integrated transcriptomic and proteomic analyses identified PRXL2B as a candidate gene associated with H101 treatment. Because PRXL2B was consistently downregulated after H101 treatment and showed potential biological relevance, it was selected for further investigation.To further explore the role of PI3K/AKT pathway in HCC progression, Gene Set Enrichment Analysis (GSEA) was conducted on the transcriptomic and proteomic data. The PI3K/AKT pathway was significantly enriched, with high NES values and low P-values, indicating its important role in tumor progression and potential modulation by H101 therapy (Supplementary Figure S1, *https://www.biosciencetrends.com/action/getSupplementalData.php?ID=303*).

3.2. Multi-omics analysis reveals PRXL2B upregulation in HCC and its correlation with prognosis and PI3K/AKT pathway activity

To explore the expression pattern and potential clinical implications of PRXL2B in HCC, we initially analyzed data from the TCGA database. Pan-cancer analysis indicated that PRXL2B exhibited abnormal expression across diverse cancer types, and a notable differential expression was detected in the hepatocellular carcinoma (LIHC/HCC) cohort (Figure 2a). In independent GEO datasets (GSE54236, GSE144269), the expression of PRXL2B was consistently elevated in HCC tissues compared to non-tumor tissues (Figure 2b), suggesting that PRXL2B may exert a promotional effect on HCC development. We further assessed the relationship between PRXL2B expression and disease progression, as well as the activity of the PI3K/AKT pathway. Stage-associated analysis revealed disparities in PRXL2B expression among different clinical stages (Figure 2c). Moreover, PRXL2B expression was significantly correlated with the PI3K/AKT pathway activity score (Figure 2c), which was in line with the observed enrichment of the PI3K/AKT pathway in tumor omics analysis. Kaplan–Meier survival analysis demonstrated a significant association between PRXL2B expression and overall survival (OS), disease-specific survival (DSS), progression-free interval (PFI), and disease-free interval (DFI) (Figure 2d). Spatial transcriptomics data further indicated that PRXL2B signals were predominantly localized in tumor regions rather than non-malignant regions (Figure 2e-f), corroborating its expression profile associated with tumor cells.

3.3. Clinical validation of PRXL2B upregulation and its prognostic significance in HCC

To validate the expression of PRXL2B in clinical HCC samples, an IHC analysis was conducted on a TMA cohort comprising 84 paired tumor and adjacent non-tumor tissue samples. The relationship between PRXL2B expression and clinicopathologic features in 84 HCC patients is presented in Table 1. The H-score of PRXL2B was correlated with various clinical characteristics, including age, gender, HBsAg status, AFP level, vascular invasion, tumor size, differentiation, and stage (Figure 3a).The expression of PRXL2B was high in tumor tissues, as evidenced by representative IHC images (Figure 3b).The correlation between PRXL2B expression and clinicopathological features was also analyzed. In the clinical cohort, PRXL2B expression was associated with overall survival; however, the statistical significance of this correlation may vary depending on the selected cutoff and follow-up duration (Figure 3c). When compared with paired adjacent tissues, the H-scores of PRXL2B were significantly higher in tumor tissues (Figure 3d), indicating an upregulation of PRXL2B in HCC tissues. Additionally, Western blotting of paired tumor and adjacent tissue samples corroborated the upregulation of PRXL2B protein expression in tumors (Figure 3e). These clinical findings, in conjunction with bioinformatics analysis, suggest that PRXL2B is upregulated in HCC and may be associated with disease progression and prognosis.

3.4. PRXL2B knockdown inhibits malignant phenotypes and enhances H101 efficacy *in vitro*

To investigate the functional role of PRXL2B in HCC cells, the protein expression of PRXL2B was initially quantified in various liver cancer cell lines. Differential expression of PRXL2B was detected among the HCC cell lines (Figure 4a). MHCC97H and HCCLM3 cells were chosen for subsequent functional studies. After establishing PRXL2B knockdown models, the cells were divided into the negative control (NC), shPRXL2B, and shPRXL2B + H101 groups. The cells in these groups were infected with H101 at a multiplicity of infection

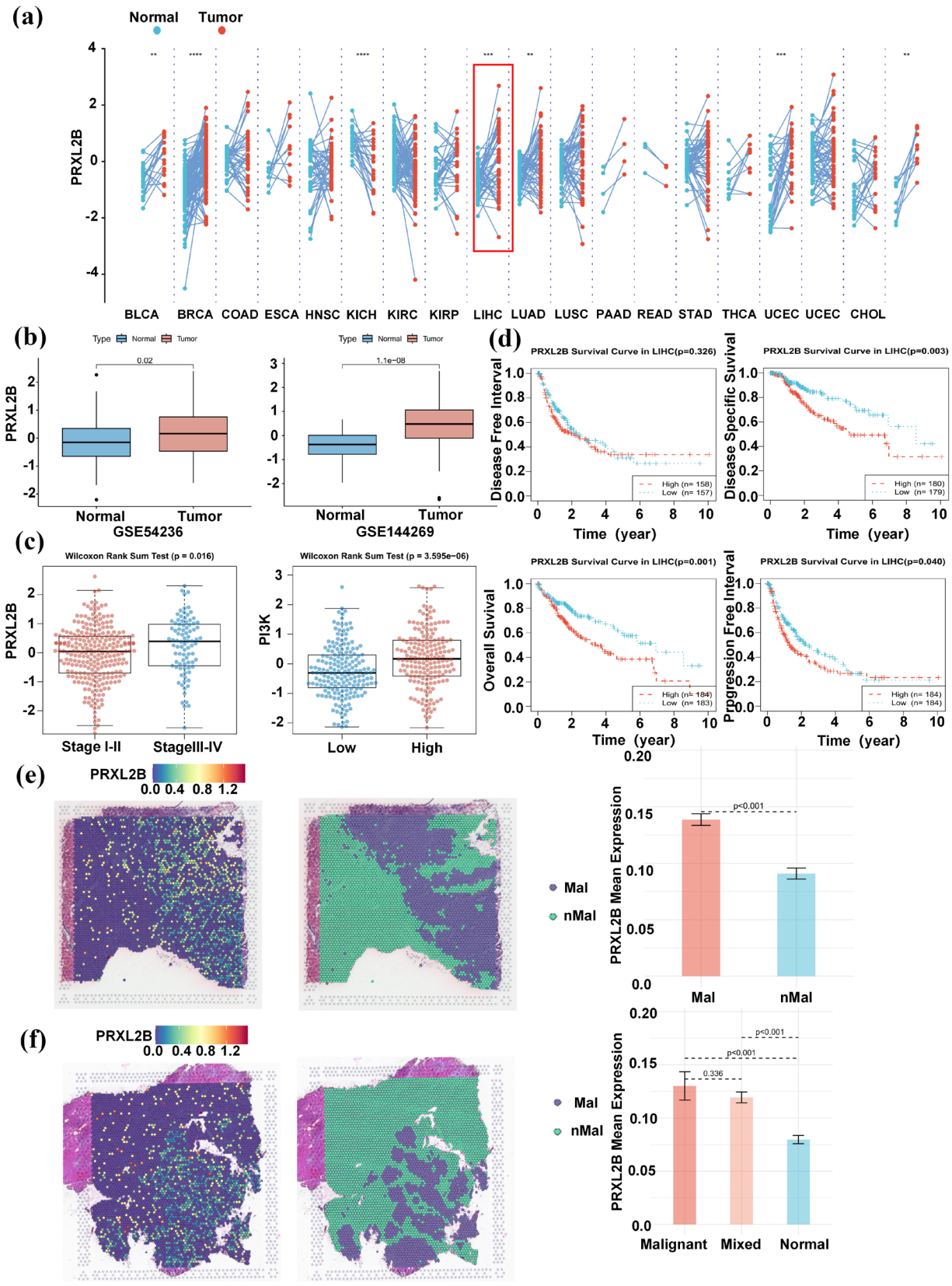


Figure 2. Multi-omics analyses support PRXL2B upregulation in HCC and its association with prognosis and PI3K/AKT pathway activity. **(a)** Pan-cancer analysis of PRXL2B expression in tumor and normal tissues, with the LIHC cohort highlighted. **(b)** Differential expression analysis of PRXL2B in HCC and non-tumor tissues across multiple GEO datasets. **(c)** Correlation analysis of PRXL2B expression with clinical stage and PI3K/AKT pathway activity. **(d)** Kaplan–Meier survival analysis of PRXL2B expression in the TCGA-LIHC cohort. **(e–f)** Spatial transcriptomic analysis of PRXL2B expression, including spatial distribution patterns and comparisons between different tissue regions/groups.

Table 1. The relationship of PRXL2B expression with clinicopathologic features in 84 HCC patients

Variables	Number of patients		
	PRXL2B low expression	PRXL2B high expression	*p*
Gender			ns
Mele	38	28	
Female	8	9	
Age (Years)			ns
> 60	9	12	
≦ 60	37	25	
Differentiatation			0.029
Well/moderate	33	25	
poor	12	12	
AFP			0.035
≧ 25	11	9	
< 25	34	28	
Vascular Invasion			0.040
MVI (+)	18	14	
MVI (-)	27	23	
HBsAg			ns
Positive	41	31	
Negative	4	6	
Cirrhosis			ns
yes	29	29	
no	16	8	
Tumor size (cm)			0.032
≧ 5	9	9	
< 5	36	28	
BCLC stage			0.025
0/A	35	35	
B/C/D	10	2	

(MOI) of 0.05 for 96 hours. CCK-8 assays indicated that the knockdown of PRXL2B significantly diminished cell viability in both MHCC97H and HCCLM3 cells, and the combined treatment with H101 further augmented this inhibitory effect (Figure 4b–c). Transwell migration and invasion assays additionally demonstrated that the knockdown of PRXL2B significantly curtailed cell migration and invasion in both cell lines (Figure 4d,f). Wound healing assays presented consistent findings (Figure 4e,g). Regarding mechanistic phenotypes, flow cytometry revealed that the knockdown of PRXL2B elevated the apoptosis rate (Figure 4h) and modified cell cycle distribution, with G2 - phase arrest being observed in HCCLM3 cells (Figure 4i). These *in vitro* results illustrate that the knockdown of PRXL2B significantly suppresses the malignant phenotypes of HCC cells and potentiates the antitumor effects of H101.

3.5. PRXL2B regulates AKT phosphorylation and PD-L1 expression, enhancing *in vivo* antitumor efficacy

To further clarify the molecular mechanisms underpinning PRXL2B knockdown, RNA-seq analysis was performed on MHCC97H cells (biological replicates3) under normal control (NC) and short hairpin RNA targeting PRXL2B (shPRXL2B) conditions. Differential analysis and volcano plots indicated the presence of significant differentially expressed genes (DEGs) subsequent to PRXL2B knockdown (Figure 5a). Enrichment analysis demonstrated that these DEGs were significantly enriched in immune-related and tumor signaling pathways (Figure 5b-c), and the programmed death-ligand 1 (PD-L1) axis, which participates in immune evasion, was identified as a potential target. In light of the observed enrichment of the PI3K/AKT pathway in our murine tumor data, we conducted further investigations into the phosphorylation status of AKT and the expression of PD-L1. Western blot analysis demonstrated that knockdown of PRXL2B led to a substantial reduction in p-AKT levels and down-regulated PD-L1 expression, as compared with the negative control (NC) group. The combined treatment with H101 further augmented these effects (Figure 5d). Densitometric quantification verified the consistent decline in PD-L1 (normalized to GAPDH), PRXL2B (normalized to GAPDH and expressed relative to NC), and the p-AKT/AKT ratio (relative to NC) (Figure 5e–g). These findings suggest that PRXL2B modulates the PI3K/AKT pathway and PD-L1 expression, which is associated with immune evasion and influences the response to H101 treatment. Finally, the *in-vivo* antitumor effects of PRXL2B knockdown in combination with H101 were validated within the Hepa1-6 subcutaneous tumor model. In comparison to the NC group, the growth rate of tumors in the shPRXL2B group was notably slower. Furthermore, the combination of PRXL2B knockdown and H101 resulted in the most substantial reduction in tumor volume and weight at the experimental endpoint (Figure 5h–j). These *in-vivo* results, when integrated with the *in-vitro* findings, imply that PRXL2B plays a pivotal role in regulating the malignancy of HCC, and its inhibition may augment the efficacy of oncolytic virus therapy. To further validate the involvement of the PI3K/AKT pathway and immune evasion *in vivo*, immunohistochemical (IHC) staining was performed on tumor tissues. As shown in Figure 5k, the expression levels of p-AKT and PD-L1 were significantly decreased in the shPRXL2B group compared with the NC group. Quantitative analysis confirmed a consistent reduction in both markers. These findings are consistent with the *in vitro* Western blot results and further support that PRXL2B regulates the PI3K/AKT pathway and PD-L1 expression *in vivo* (Figure 5k).

4. Discussion

This study identifies PRXL2B as a potential regulator of hepatocellular carcinoma progression and the antitumor efficacy of oncolytic adenovirus H101. Using integrated transcriptomic and proteomic analyses, we found that PRXL2B was consistently downregulated after H101 treatment in the murine tumor model, suggesting that it may be involved in the tumor response to oncolytic virotherapy. Functional assays further demonstrated that PRXL2B knockdown inhibited HCC cell proliferation,

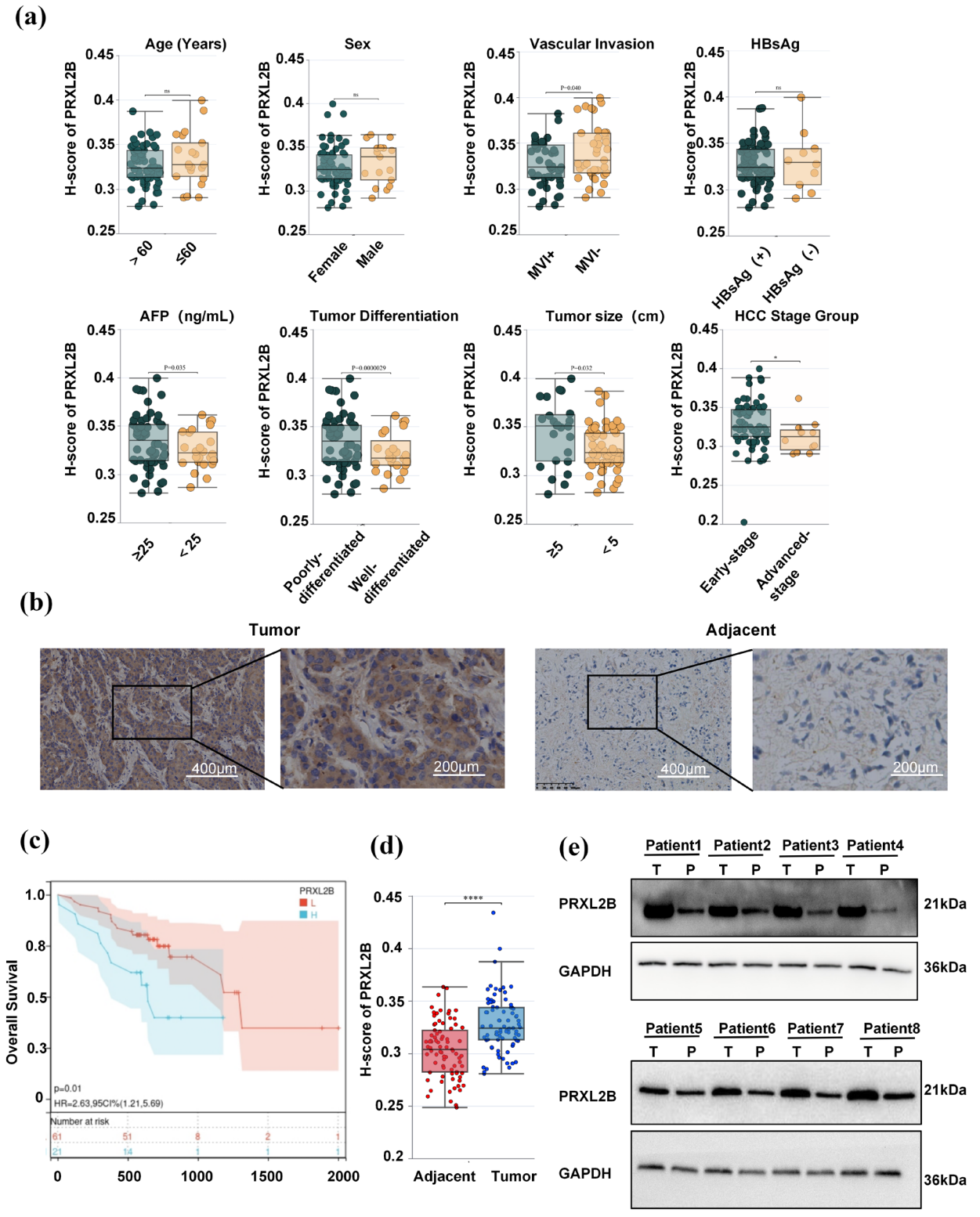


Figure 3. Clinical validation of PRXL2B expression in HCC tissue microarrays and its association with clinicopathological features and prognosis. (a) Correlation analysis between PRXL2B immunohistochemical staining (H-score) and clinicopathological characteristics in the HCC tissue microarray cohort (n = 84). **(b)** Representative immunohistochemical staining images of PRXL2B expression in tumor and paired adjacent tissues. Scale bars are indicated. **(c)** Kaplan–Meier overall survival analysis of PRXL2B expression in the LIHC cohort. **(d)** Comparison of PRXL2B H-scores between tumor and paired adjacent tissues. **(e)** Western blot analysis of PRXL2B protein expression in paired tumor **(T)** and adjacent **(P)** tissues, with GAPDH as a loading control.

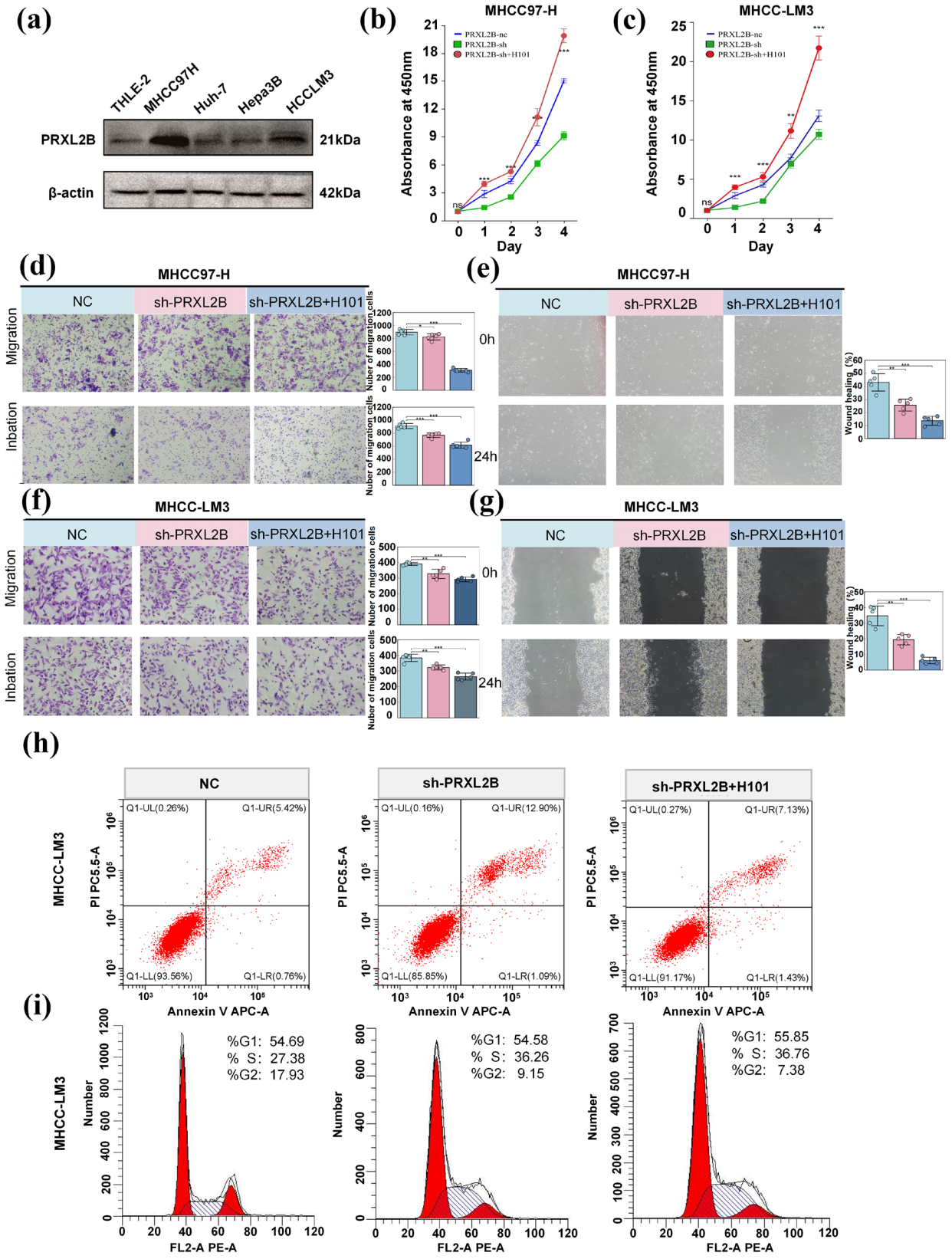


Figure 4. PRXL2B knockdown suppresses malignant phenotypes of HCC cells and enhances the effects of H101 *in vitro*. **(a)** Western blot analysis of PRXL2B expression in liver cancer cell lines, with GAPDH as a loading control. **(b–c)** CCK-8 assays of cell viability in MHCC97H **(b)** and HCCLM3 **(c)** cells under NC, shPRXL2B, and shPRXL2B + H101 conditions. Cells were infected with H101 (MOI = 0.05) for 96 h. **(d)** Transwell migration and invasion assays in MHCC97H cells. **(e)** Wound healing assays in MHCC97H cells at 0 h and 24 h, with quantification of wound closure. **(f)** Transwell migration and invasion assays in HCCLM3 cells. **(g)** Wound healing assays in HCCLM3 cells at 0 h and 24 h, with quantification of wound closure. **(h)** Flow cytometric analysis of apoptosis in HCCLM3 cells using Annexin V/PI staining. **(i)** Cell cycle distribution analysis of HCCLM3 cells using PI staining. Data are presented as mean ± SD. Statistical significance was determined using one-way ANOVA with post hoc testing.

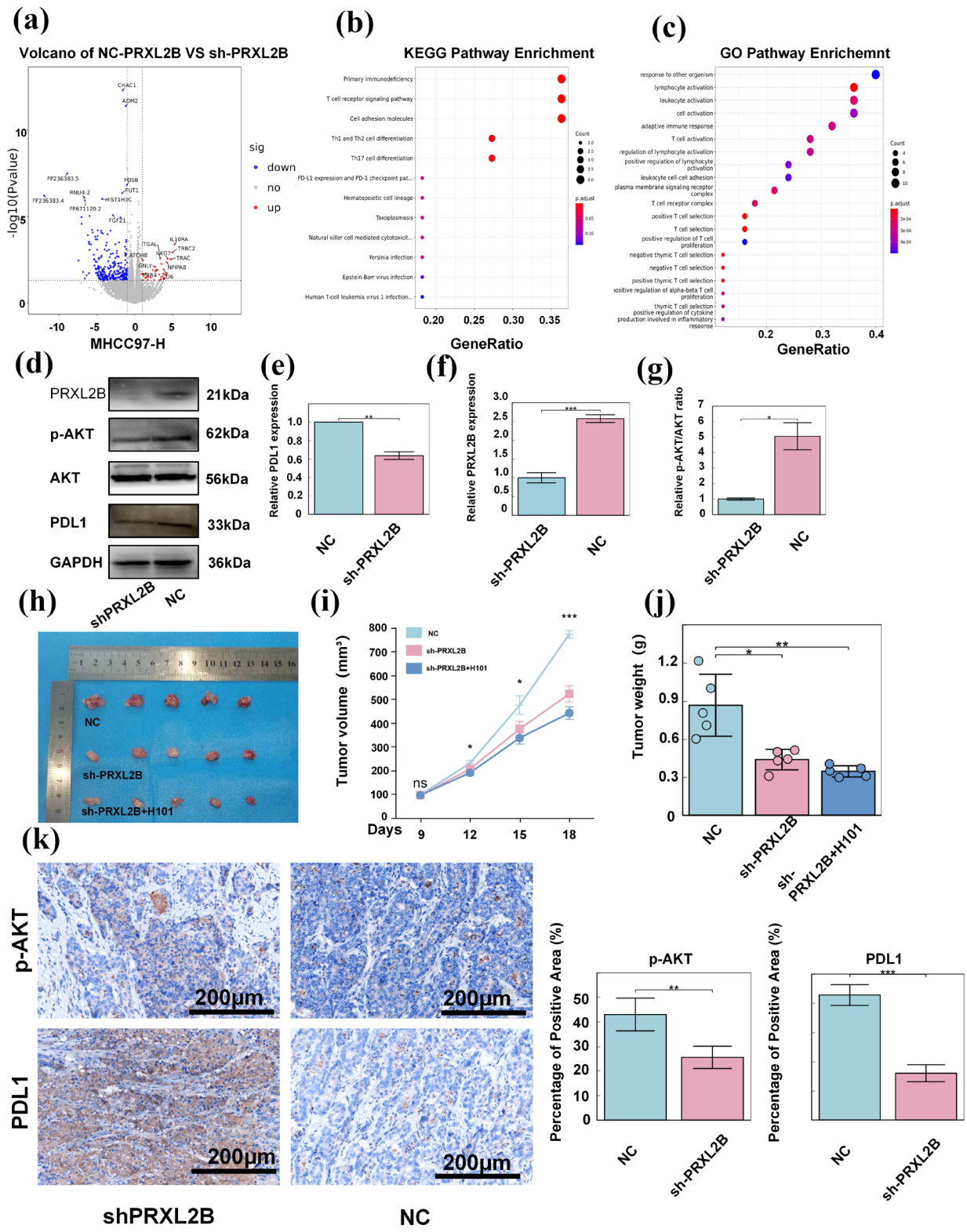


Figure 5. PRXL2B knockdown suppresses AKT signaling and PD-L1 expression and enhances the antitumor activity of H101. (a) Volcano plot of DEGs identified by RNA-seq analysis in NC and shPRXL2B MHCC97H cells. **(b)** KEGG pathway enrichment analysis of DEGs following PRXL2B knockdown. The x-axis indicates GeneRatio. Dot size represents gene counts, and dot color indicates adjusted *p* values. **(c)** GO enrichment analysis of DEGs following PRXL2B knockdown. **(d)** Representative Western blots of PRXL2B, PD-L1, p-AKT, total AKT, and GAPDH in MHCC97H cells under NC, shPRXL2B, and shPRXL2B + H101 conditions. Cells were infected with H101 (MOI = 0.05) for 96 h. **(e–g)** Densitometric quantification of PD-L1, PRXL2B, and p-AKT/AKT levels. **(h)** Representative images of excised tumors from Hepa1-6 subcutaneous tumor models in the NC, shPRXL2B, and shPRXL2B + H101 groups. Solid line = NC (negative control) and dashed line = shPRXL2B (PRXL2B knockdown). **(i–j)** Tumor growth curves **(i)** and tumor weights at the experimental endpoint **(j)**. Data are presented as mean ± SD with individual values. Statistical significance was determined using one-way ANOVA with post hoc testing. **(k)** Representative immunohistochemical staining images of p-AKT and PD-L1 in tumor tissues, with quantification shown on the right. Data are presented as mean ± SD.

migration, and invasion, promoted apoptosis, and enhanced the antitumor effect of H101 both *in vitro* and *in vivo*. These findings support a tumor-promoting role of PRXL2B in HCC and suggest that PRXL2B may represent a promising target for combination therapy with oncolytic viruses.

In addition to PRXL2B-mediated effects, our study highlights the therapeutic potential of H101 as an oncolytic adenovirus in HCC. Oncolytic viruses selectively replicate in tumor cells and induce tumor lysis while stimulating antitumor immunity (*18*). H101 treatment alone can trigger immunogenic cell death, recruit immune effector cells, and enhance tumor antigen presentation, which may synergize with immune checkpoint modulation (*19*). The observed downregulation of PRXL2B after H101 treatment suggests that viral replication and the host response may directly or indirectly modulate oncogenic signaling pathways (*20*). These findings imply that combining H101 with molecularly targeted interventions, such as PRXL2B inhibition, could enhance tumor cell killing and overcome intrinsic resistance mechanisms (*21*). Future studies should further investigate the impact of H101 on the tumor microenvironment, including innate and adaptive immune responses, and explore combination strategies with immune checkpoint inhibitors to improve therapeutic efficacy in HCC.

Our tissue-based validation and public dataset analyses consistently showed that PRXL2B was upregulated in HCC tissues. This finding is in line with a potential oncogenic role of PRXL2B in liver cancer. However, although PRXL2B expression was elevated in tumors, its associations with clinicopathological features and survival were not consistently significant in our tissue microarray cohort. This discrepancy between public dataset-based analyses and our clinical validation cohort may be attributed to differences in sample size, patient heterogeneity, cutoff selection, and follow-up duration (*22*). Therefore, while PRXL2B appears to be involved in HCC progression, its value as an independent prognostic biomarker remains inconclusive and requires further validation in larger and well-characterized clinical cohorts.

Mechanistically, our data suggest that PRXL2B may exert its effects through the PI3K/AKT/PD-L1 axis. PRXL2B knockdown reduced p-AKT and PD-L1 expression in HCC cells, indicating that PRXL2B may contribute not only to tumor cell survival but also to immune evasion. Because the PI3K/AKT pathway plays a central role in tumor growth, survival, and therapeutic resistance, its suppression after PRXL2B silencing provides a plausible mechanistic basis for the observed antitumor effects (*23*). In addition, the reduction in PD-L1 expression suggests that PRXL2B may influence the immunosuppressive phenotype of HCC, thereby affecting responsiveness to oncolytic virus therapy. To further support the *in vivo* relevance of this mechanism, we supplemented immunohistochemical staining of tumor tissues from the animal experiments. The results showed that p-AKT and PD-L1 expression were decreased in the shPRXL2B group compared with the NC group, and were further reduced in the combination treatment group, which was consistent with our Western blot findings. These data strengthen the evidence that PRXL2B regulates the PI3K/AKT/PD-L1 axis *in vivo* and further support its involvement in tumor progression and therapeutic response (*24*).

The combination of PRXL2B knockdown and H101 produced the strongest antitumor effect *in vivo*, suggesting that PRXL2B inhibition may enhance the efficacy of oncolytic virotherapy (*25*). This combinational strategy warrants further investigation. Nevertheless, several limitations of this study should be acknowledged. First, although PRXL2B was upregulated in HCC, its clinical significance was not consistently confirmed in our tissue microarray cohort. Second, an H101-alone treatment group was not included in the current study, which limits our ability to fully distinguish the independent effect of H101 from its interaction with PRXL2B knockdown. Third, although our data support the involvement of the PI3K/AKT/PD-L1 axis, other signaling pathways, such as NF-kB or JAK/STAT, may also participate in PRXL2B-mediated regulation and deserve further study (*26*). Overall, our findings indicate that PRXL2B contributes to HCC malignant progression and may modulate the therapeutic response to H101. Future studies should focus on validating PRXL2B in larger clinical cohorts, clarifying its predictive value for oncolytic virus therapy, and exploring whether PRXL2B-targeted interventions can improve the efficacy of combination treatment strategies in HCC.

Funding: This work was supported by the National Natural Science Foundation of China (No. 82170666 and 82572988), the First-Class Discipline-Mentoring Team (No. 030102050401CYYY-DSTDXM-202411), and the Key Project of Nutrition and Health Special Fund of Chongqing Maternal and Child Health Association Research Fund Management Committee (No. CQMCHA-NH2025-03).

Conflict of Interest: The authors have no conflicts of interest to disclose.

Data Availability: The RNA-seq and proteomics datasets generated and/or analyzed during the current study are available from the corresponding author upon reasonable request. The clinical information from the tissue microarray cohort contains sensitive patient-related data and is therefore available only upon reasonable request and with appropriate ethical approval. All other data supporting the findings of this study are included in the manuscript and Supplementary Information.

References

1. Anwanwan D, Singh SK, Singh S, Saikam V, Singh R. Challenges in liver cancer and possible treatment approaches. Biochim Biophys Acta Rev Cancer. 2020; 1873:188314.
2. Raja J, Ludwig JM, Gettinger SN, Schalper KA, Kim HS. Oncolytic virus immunotherapy: future prospects for oncology. J Immunother Cancer. 2018; 6:140.
3. Abudoureyimu M, Lai Y, Tian C, Wang T, Wang R, Chu X. Corrigendum: Oncolytic Adenovirus-A Nova for Gene-Targeted Oncolytic Viral Therapy in HCC. Front Oncol. 2020; 10:701.
4. Mantwill K, Klein FG, Wang D, Hindupur SV, Ehrenfeld M, Holm PS, Nawroth R. Concepts in Oncolytic Adenovirus Therapy. Int J Mol Sci. 2021; 22:10522.
5. Duan Y, Bai H, Li X, Wang D, Wang Y, Cao M, Zhang N, Chen H, Wang Y. Oncolytic Adenovirus H101 Synergizes with Radiation in Cervical Cancer Cells. Curr Cancer Drug Targets. 2021; 21:619-630.
6. Qiao C, Xu Y, He Y, Cai Z, Wang H. Oncolytic adenovirus H101 enhances the anti-tumor effects of PD-1 blockade *via* CD47 downregulation in tumor cells. Oncol Res. 2025; 33:1161-1172.
7. Xi P, Zeng D, Chen M, Jiang L, Zhang Y, Qin D, Yao Z, He C. Enhancing pancreatic cancer treatment: The role of H101 oncolytic virus in irreversible electroporation. Front Immunol. 2025; 16:1546242.
8. Santos Apolonio J, Lima de Souza Gonçalves V, Cordeiro Santos ML, Silva Luz M, Silva Souza JV, Rocha Pinheiro SL, de Souza WR, Sande Loureiro M, de Melo FF. Oncolytic virus therapy in cancer: A current review. World J Virol. 2021; 10:229-255.
9. Kaufman HL, Kohlhapp FJ, Zloza A. Oncolytic viruses: a new class of immunotherapy drugs. Nat Rev Drug Discov. 2015; 14:642-662.
10. van Lieshout L, van de Stolpe A, van der Ploeg P, Bowtell D, de Hullu J, Piek J. Signal Transduction Pathway Activity in High-Grade, Serous Ovarian Carcinoma Reveals a More Favorable Prognosis in Tumors with Low PI3K and High NF-κB Pathway Activity: A Novel Approach to a Long-Standing Enigma. Cancers (Basel). 2020; 12:2660.
11. Song D, Jia X, Liu X, *et al*. Identification of the receptor of oncolytic virus M1 as a therapeutic predictor for multiple solid tumors. Signal Transduct Target Ther. 2022; 7:100.
12. Shi ZR, Duan YX, Cui F, Wu ZJ, Li MP, Song PP, Peng QL, Ye WT, Yin KL, Kang MQ, Yu YX, Yang J, Tang W, Liao R. Integrated proteogenomic characterization reveals an imbalanced hepatocellular carcinoma microenvironment after incomplete radiofrequency ablation. J Exp Clin Cancer Res. 2023; 42:133.
13. Cheng AL, Hsu C, Chan SL, Choo SP, Kudo M. Challenges of combination therapy with immune checkpoint inhibitors for hepatocellular carcinoma. J Hepatol. 2020; 72:307-319.
14. Budhu A, Roessler S, Zhao X, Yu Z, Forgues M, Ji J, Karoly E, Qin LX, Ye QH, Jia HL, Fan J, Sun HC, Tang ZY, Wang XW. Integrated metabolite and gene expression profiles identify lipid biomarkers associated with progression of hepatocellular carcinoma and patient outcomes. Gastroenterology. 2013; 144:1066-1075. e1061.
15. Amicone L, Citarella F, Cicchini C. Epigenetic regulation in hepatocellular carcinoma requires long noncoding RNAs. Biomed Res Int. 2015; 2015:473942.
16. Gao Q, Zhu H, Dong L, *et al*. Integrated Proteogenomic Characterization of HBV-Related Hepatocellular Carcinoma. Cell. 2019; 179:561-577.e522.
17. Song W, Yuan Y, Cao F, Pan H, Liu Y. The key pathways and genes related to oncolytic Newcastle disease virus-induced phenotypic changes in ovarian cancer cells. J Microbiol. 2025; 63:e2411018.
18. Marchini A, Ilkow CS, Melcher A. Oncolytic Virus Immunotherapy. Cancers (Basel). 2021; 13:3672.
19. Ghasemi Darestani N, Gilmanova AI, Al-Gazally ME, Zekiy AO, Ansari MJ, Zabibah RS, Jawad MA, Al-Shalah SAJ, Rizaev JA, Alnassar YS, Mohammed NM, Mustafa YF, Darvishi M, Akhavan-Sigari R. Mesenchymal stem cell-released oncolytic virus: an innovative strategy for cancer treatment. Cell Commun Signal. 2023; 21:43.
20. Kaufman HL, Maciorowski D. Advancing oncolytic virus therapy by understanding the biology. Nat Rev Clin Oncol. 2021; 18:197-198.
21. Wang Z, Sun P, Li Z, Xiao S. Clinical Advances and Future Directions of Oncolytic Virotherapy for Head and Neck Cancer. Cancers (Basel). 2023; 15:5291.
22. Kui X, Wang Y, Zhang C, Li H, Li Q, Ke Y, Wang L. Prognostic value of SH3PXD2B (Tks4) in human hepatocellular carcinoma: a combined multi-omics and experimental study. BMC Med Genomics. 2021; 14:115.
23. He Y, Sun MM, Zhang GG, Yang J, Chen KS, Xu WW, Li B. Targeting PI3K/Akt signal transduction for cancer therapy. Signal Transduct Target Ther. 2021; 6:425.
24. Nishida N, Sakai K, Morita M, Aoki T, Takita M, Hagiwara S, Komeda Y, Takenaka M, Minami Y, Ida H, Ueshima K, Nishio K, Kudo M. Association between Genetic and Immunological Background of Hepatocellular Carcinoma and Expression of Programmed Cell Death-1. Liver Cancer. 2020; 9:426-439.
25. Samson A, Bentham MJ, Scott K, *et al*. Oncolytic reovirus as a combined antiviral and anti-tumour agent for the treatment of liver cancer. Gut. 2018; 67:562-573.
26. Hin Tang JJ, Hao Thng DK, Lim JJ, Toh TB. JAK/STAT signaling in hepatocellular carcinoma. Hepat Oncol. 2020; 7:HEP18.

Received January 5, 2026; Revised May 2, 2026; Accepted May 18, 2026.

[§]These authors contributed equally to this work.
**Address correspondence to:*
Ping Che, Department of Hepatobiliary Surgery, Shapingba Hospital affiliated to Chongqing University (Shapingba District People's Hospital of Chongqing), No. 2, Jialang Road, Shapingba District, Chongqing 400030, China.
E-mail: dr.che@cqu.edu.cn

Rui Liao, Department of Hepatobiliary Surgery, The First Affiliated Hospital, Chongqing Medical University, No.1, Youyi Road, Yuzhong District, Chongqing 400016, China.
E-mail: liaorui99@163.com

Released online in J-STAGE as advance publication May 21, 2026.

Original Article

DOI: 10.5582/bst.2026.01202

ATP6L impairs vascular stability in colorectal cancer *via* PDGFB/PDGFRβ signaling

Xiangdong Tian[1,§,*], Dandan Chen[1,2,§], Jiaqi Duo[1,§], Shi Zhang[1], Lisha Qi[1,*]

[1] Tianjin Medical University Cancer Institute and Hospital, National Clinical Research Center for Cancer, Tianjin Key Laboratory of Digestive Cancer, Tianjin's Clinical Research Center for Cancer, State Key Laboratory of Druggability Evaluation and Systematic Translational Medicine, Tianjin, China;
[2] Department of Pathology, Cangzhou People's Hospital, Cangzhou, Hebei, China.

SUMMARY: Vascular instability, characterized by impaired pericyte coverage, is a hallmark of tumor progression. ATP6L is highly expressed in colorectal cancer (CRC) tissues and promotes tumor progression by enhancing the tumor microvasculature; however, its direct impact on vascular stability remains unclear. ATP6L expression, microvascular morphology, and pericyte coverage were analyzed by immunohistochemistry in a cohort of 179 CRC specimens, and the role of ATP6L in vascular stability was further investigated by modulating its expression both *in vitro* and *in vivo*. *In vitro*, MC38 and CT26 cells with ATP6L overexpression or knockdown were co-cultured with mouse vascular smooth muscle cells (MOVAS), and MOVAS proliferation, migration, and apoptosis were evaluated using EdU incorporation, transwell migration, and TUNEL staining assays, respectively. PDGFB secretion and PDGFRβ expression were assessed by ELISA, Western blotting, and immunofluorescence. Along the normal colorectal mucosa–adenoma–adenocarcinoma sequence, ATP6L upregulation was closely associated with progressive vascular instability, characterized by loss of pericyte coverage and increasing vascular morphological heterogeneity. Mechanistically, ATP6L overexpression promoted extracellular acidification, suppressed PDGFB secretion, and subsequently reduced PDGFRβ expression in pericytes, thereby impairing their recruitment and survival. Conversely, ATP6L knockdown attenuated extracellular acidification, restored PDGFB/PDGFRβ signaling, and rescued pericyte proliferation, migration, and survival. These findings identify ATP6L as a key mediator of perivascular dysfunction in CRC and demonstrate that ATP6L-induced extracellular acidification disrupts vascular stability by suppressing the PDGFB/PDGFRβ signaling axis and impairing pericyte function.

Keywords: colorectal cancer, ATP6L, vascular stability, pericytes, PDGFB/PDGFRβ signaling

1. Introduction

Abnormal tumor vasculature, characterized by structural fragility and functional inefficiency, is a critical hallmark of cancer (*1,2*). Beyond the mere formation of new blood vessels (angiogenesis), the stability and maturation of these vessels are essential for efficient perfusion and drug delivery (*3,4*). Conversely, vascular instability—marked by chaotic architecture, high permeability, and poor pericyte coverage (*1,5,6*)—promotes hypoxia, immune evasion, and metastasis. This understanding has shifted the therapeutic focus towards vascular normalization, a strategy aimed at restoring vessel integrity. In this context, pericytes, the mural cells that envelop capillaries, are crucial gatekeepers of vascular stability (*7,8*). Their recruitment, adhesion, and function are tightly regulated, and their depletion is a hallmark of the immature, dysfunctional tumor vasculature (*5,9*).

A principal driver of the hostile tumor microenvironment is extracellular acidosis (*10,11*), predominantly mediated by the vacuolar H+-ATPase (V-ATPase) proton pump (*12*). As a key functional subunit of the V-ATPase complex, ATP6L is commonly upregulated in malignancies (*13*). Through its promotion of extracellular acidification, ATP6L has been firmly implicated in promoting aggressive tumor behaviors, including enhanced invasiveness and acquired chemoresistance, underscoring its multifaceted pro-tumorigenic functions (*14-16*). However, despite the well-recognized role of ATP6L-driven acidosis in remodeling the tumor microenvironment, its direct impact on the tumor vasculature—particularly on pericyte function and vascular stability—remains largely unexplored. Although the acidic niche is known to broadly influence stromal cells (*10,17*), the specific molecular mechanisms by which cancer cell-derived

ATP6L compromises pericyte integrity and disrupts vascular homeostasis in colorectal cancer (CRC) remain to be elucidated.

In this study, we identify ATP6L as a critical driver of perivascular dysfunction in CRC. The normal–adenoma–carcinoma progression in colorectal cancer is accompanied by a progressive upregulation of ATP6L, which closely parallels a spectrum of vascular abnormalities, including microvessel shrinkage, lumen narrowing, and pericyte dropout. Mechanistically, ATP6L overexpression appears to instigate pericyte dysfunction through an acidification-driven PDGFB/PDGFRβ signaling axis: ATP6L overexpression promotes an acidic microenvironment that suppresses PDGFB secretion, leading to reduced PDGFRβ expression on pericytes and consequently impairing their recruitment and survival. Conversely, ATP6L depletion reverses this deleterious cascade, restoring pericyte proliferation, migration, and survival. This work seeks to identify ATP6L as a novel modulator of the tumor vasculature, revealing a direct link between tumor acidification and vascular dysfunction. Together, these findings identify a novel link between tumor microenvironmental acidification and vascular abnormalities, suggesting ATP6L as a potential therapeutic target to normalize tumor vasculature and improve treatment efficacy.

2. Materials and Methods

2.1. Patient tissue specimens and clinical data

A total of 179 cases of surgically resected, pathologically confirmed colorectal cancer (CRC) specimens, along with corresponding clinicopathological data, were retrospectively collected from the Department of Pathology at Tianjin Medical University Cancer Institute and Hospital between July 2014 and February 2015. Additionally, 29 cases of matched normal colorectal mucosa, adjacent adenoma, and primary adenocarcinoma tissue samples were included for serial analysis. The study was approved by the Institutional Review Board of Tianjin Medical University Cancer Institute and Hospital (Approval No. bc2020073), and informed consent was obtained from all participants. Patient demographics and clinical characteristics are summarized in Table 1.

2.2. Immunohistochemistry (IHC) and immunofluorescence (IF)

Formalin-fixed, paraffin-embedded tissue sections (4 μm thick) were processed for IHC and IF staining following standard protocols. The primary antibodies used included: anti-ATP6L (1:200, Abcam plc, America), anti-CD31 (1:100, Zsbio, Beijing, China), anti-α-SMA (1:200, Abcam plc, America), anti-PDGFB (1:150, Abcam plc, America), and anti-PDGFRβ (1:150, Abcam plc, America). Appropriate secondary antibodies and detection systems (DAB for IHC, Alexa Fluor-conjugated for IF) were applied. Hematoxylin was used for counterstaining.

ATP6L expression in tumor cells was evaluated independently by two experienced pathologists blinded to clinical outcomes. For each specimen, two representative fields at 200× magnification were selected from the tumor-normal mucosal interface where active angiogenesis was evident. ATP6L staining was considered positive when brown cytoplasmic granules were present. Staining intensity was graded on a scale of 0 to 2 (0: no staining; 1: weak; 2: strong). The percentage of immunoreactive tumor cells was scored on a scale of 1 to 3 (1: < 30%; 2: 30–80%; 3: > 80%). A composite score for each field was calculated by multiplying the intensity score by the percentage score. The final ATP6L expression score for each case was the average of the two field scores. Tumors were then classified as having low expression (average score 1–3) or high expression (average score 4–6). Please refer to the previously published literature for specific evaluation details (*18*).

For each IHC/IF-stained section, five representative fields of view (200x magnification) in the tumor invasive front were captured to quantify vascular parameters. All quantifications were performed using ImageJ software (National Institutes of Health, USA). Microvessel Density (MVD) was determined by counting CD31-positive endothelial cell clusters or single cells in each field (*19*). Any brown-stained endothelial cell or cell cluster clearly separated from adjacent vessels was counted as a single microvessel. The mean count per field was calculated. The lumen area (μm²) of each CD31+

Table 1. Clinicopathological characteristics of colorectal cancer patients

Characteristics	Number of patients (%)
Age	
< 50	35 (19.6)
≥ 50	144 (80.4)
Gender	
Male	102 (57.0)
Female	77 (43.0)
Size	
< 5cm	124 (69.3)
≥ 5cm	55 (30.7)
Differentiation	
Poor	48 (26.8)
High/ Moderate	131 (73.2)
Clinical stage	
I/II	93 (52.0)
III/IV	86 (48.0)
Lymph Node Metastasis	
Present	73 (40.8)
Absent	106 (59.2)
Distant Metastasis	
Present	34 (19.0)
Absent	145 (81.0)
ATP6L expression level	
Low	46 (25.7)
High	133 (74.3)

vessel was measured, and the equivalent diameter was calculated. Pericyte Coverage Index was defined as the percentage of CD31-positive vascular perimeter that was co-localized with α-SMA-positive staining. Automated co-localization analysis was performed on CD31/α-SMA double-IF images. The cutoff of 96.10% for dichotomizing pericyte coverage as "High" or "Low" was derived from the cohort mean.

2.3. Cell culture and transfection

Mouse colorectal cancer cell lines MC38 and CT26, and mouse vascular smooth muscle cells (MOVAS) were obtained from ATCC. All cell lines were authenticated *via* short tandem repeat profiling and tested regularly for mycoplasma contamination. CRC cells were cultured in DMEM supplemented with 10% FBS. MOVAS cells were cultured in smooth muscle cell growth medium. Stable cell lines of MC38 and CT26, including sh-control (Ctrl), sh-ATP6L (KD), empty Vector, and ATP6L overexpression (OE), were generated by lentiviral transduction and selected with puromycin (2 μg/mL) for two weeks.

2.4. *In vitro* co-culture and functional assays

An indirect co-culture system was employed. Stably transfected MC38 and CT26 cells were seeded in the lower chamber of 6-well plates. MOVAS cells were seeded on Transwell inserts (0.4 μm pore, Corning) placed in the same well, allowing the sharing of conditioned medium without direct cell-cell contact. After 48 hours of co-culture, MOVAS cells were collected for analysis.

MOVAS cell proliferation was assessed using the 5-ethynyl-2′-deoxyuridine (EdU) incorporation assay kit according to the manufacturer's protocol. The proliferation rate was expressed as the percentage of EdU-positive nuclei.

The migratory ability of MOVAS cells was evaluated using 24-well Transwell chambers (8 μm pore size). MOVAS cells (2×10^4) suspended in serum-free medium were seeded into the upper chamber, while the lower chamber contained conditioned medium from CRC cultures. After 24 hours, migrated cells on the lower membrane surface were fixed, stained with 0.1% crystal violet, and counted in five random fields (200x).

Apoptosis of MOVAS cells was detected using a TUNEL assay kit. The apoptotic index was calculated as the percentage of TUNEL-positive nuclei. Additionally, expression levels of cleaved caspase-3, Bax and Bcl-2 were analyzed by Western blot.

2.5. Extracellular acidification detection

Extracellular acidification was assessed using the P61 fluorescent pH probe. Cells were seeded in black, clear-bottom 96-well plates at 4×10^4 cells/well and cultured overnight. Before staining, cells were washed twice with dilution buffer and then incubated with P61 working solution in the dark at 37°C for 30 min. Fluorescence intensity was measured at excitation/emission wavelengths of 488/580 nm and normalized to the control group. Three replicate wells were analyzed per condition, and the mean values were plotted using GraphPad Prism.

2.6. Lactic acid treatment for MOVAS

Following cell attachment, the culture medium was removed, and the cell monolayer was rinsed once or twice with PBS. Subsequently, the cells were incubated with culture medium containing 5 mM lactic acid. After incubation for 24–48 hours at 37°C in a humidified atmosphere of 5% CO_2, MOVAS were collected, and total protein was extracted for Western blot analysis.

2.7. Animal Experiments

All animal procedures were approved by the Institutional Animal Care and Use Committee of Tianjin Medical University Cancer Institute and Hospital (Protocol No. AE-2022216). Six-week-old female nude mice were subcutaneously inoculated in the right dorsal flank with MC38-vector or MC38-ATP6L-overexpressing cells (5×10^6 cells in 100 μL PBS per mouse) to induce tumor development. When tumors reached an average volume of 200 mm^3, tumor-bearing mice were randomly divided into three groups (n=6 per group): (a) Vector control, (b) ATP6L-overexpressing (OE), and (c) ATP6L-OE treated with Baf A1. Baf A1 was dissolved in a vehicle consisting of 10% DMSO, 40% PEG300, 5% Tween-80, and 45% saline, prepared fresh before each injection and sonicated to clarity (final concentration 2.5 mg/mL). Mice in the Baf A1 treatment group received intratumoral injections of Baf A1 at 5 mg/kg body weight (40 μL per injection) three times per week, while mice in the Vector and OE groups received equal-volume vehicle injections on the same schedule. This locally administered dose was chosen based on the reported anti-tumor efficacy of systemically delivered Baf A1 at 0.1–1 mg/kg and precedent for intratumoral Baf A1 administration in xenograft models, with local delivery adjusted to maximize target engagement while reducing off-target effects. Four weeks after treatment initiation, tumor tissue samples from each group were collected and subjected to histological evaluation. Tumor volume was measured twice weekly and calculated using the formula: Volume = (Length × $Width^2$)/2.

2.8. Analysis of *in vivo* vascular function and architecture

To evaluate functional vessel density and vascular permeability, we intravenously administered DyLight 594-conjugated lectin, which binds to the endothelial

glycocalyx to label perfused vessels, and FITC-dextran, which extravasates through leaky vessels. Vascular permeability and perfusion were assessed one day before euthanasia. Mice were intravenously injected with 100 μL of 2 mg/mL FITC-dextran (70 kDa). After 30 minutes, mice were anesthetized, and a subset (n = 3 per group) received an intracardiac injection of 100 μL of DyLight 594-conjugated Lycopersicon esculentum lectin to label perfused vessels. Tumor vessels were imaged using a two-photon microscope. Vessel permeability was quantified as the ratio of FITC-dextran intensity in the perivascular area to that within the vessel lumen. Perfused vessel density was calculated from lectin-positive areas. For immunofluorescence analysis of tumor sections, the pericyte coverage index was determined as described above.

2.9. Statistical analysis

Statistical analyses were performed using SPSS 25.0 (IBM) and GraphPad Prism 9.0. The distribution of data was assessed for normality using the Shapiro-Wilk test; for comparisons between two groups, an unpaired two-tailed Student's t-test (for normally distributed data) or the Mann-Whitney U test (for non-normally distributed data) was used. For comparisons among multiple groups, one-way ANOVA followed by Tukey's post-hoc test or the Kruskal-Wallis test with Dunn's post-hoc test was applied, as appropriate. Correlation analyses were performed using Pearson's or Spearman's correlation coefficient. Categorical data were analyzed using the Chi-square test. Data are presented as mean ± standard deviation (SD). A p-value < 0.05 was considered statistically significant. The "n" for each experiment indicates the number of biological replicates, as detailed in the figure legends.

3. Results

3.1. Vascular instability increases during normal mucosa-adenoma-adenocarcinoma sequence in CRC

To investigate the evolution of vascular morphology during CRC development, we performed double immunofluorescence staining for CD31 (endothelial marker) and α-SMA (pericyte/smooth muscle cell marker) on 29 matched tissue sets containing normal mucosa, adenoma and adenocarcinoma. Normal mucosa exhibited regular microvessels with a circular or oval shape and uniform thin walls, in adenoma, vascular morphology remained relatively regular, in contrast, adenocarcinoma tissue displayed vessels with impaired integrity, irregular shapes, variable diameters, and uneven wall thickness (Figure 1A). Quantitative analysis of the 29 paired samples showed a significant progressive decrease in pericyte coverage from normal mucosa to adenoma to adenocarcinoma (Normal mucosa: 96.8% ± 2.1%; Adenoma: 92.5% ± 4.3%; Adenocarcinoma: 76.4% ± 9.8%) (Figure 1B). While the mean microvessel density (MVD), lumen diameter, and lumen area did not differ significantly among the three groups, the distribution of these parameters was markedly more heterogeneous in adenoma and adenocarcinoma tissues (Supplementary Figure S1A-C, *https://www.biosciencetrends.com/action/getSupplementalData.php?ID=317*). Across the entire cohort of 179 CRC cases, poorly differentiated tumors showed significantly lower pericyte coverage than well/moderately-differentiated tumors (Figure 1D).

These observations indicate that vascular instability, characterized by immature morphology and reduced pericyte attachment, progressively increases during CRC development and correlates with poorer histological differentiation.

3.2. ATP6L expression negatively correlates with vascular stability and PDGFRβ signaling in human CRC tissues

Given the established role of ATP6L in promoting tumor malignancy, we next examined its relationship with vascular stability. In the matched tissue sequence, ATP6L expression, assessed by IHC score, progressively increased from normal mucosa to adenocarcinoma (Table 2). In the 179 CRC tissues, tumors with high ATP6L expression exhibited significantly larger microvascular luminal diameters and cross-sectional areas compared with their ATP6L-low counterparts (Figures 2B,2C), indicative of a dilated and aberrant vascular phenotype. Representative images of double CD31/α-SMA staining revealed scattered pericyte distribution and lower pericyte coverage in ATP6L-high tumors (Figure 2D). A significant negative correlation was confirmed between ATP6L expression and pericyte coverage index across the cohort (Figure 2E).

The interaction between PDGFB and PDGFRβ is a critical determinant of vascular stability. While PDGFB/PDGFRβ signaling is known to play a role in pericyte recruitment and vascular maturation, its precise contribution to tumor angiogenesis and vascular remodeling across different tumor contexts remains incompletely understood (*20,21*). IHC staining was then performed to examine the correlation between ATP6L expression and the protein levels of PDGFB and PDGFRβ in CRC specimens. Interestingly, CRC tissues with low ATP6L expression exhibited markedly elevated PDGFB levels alongside reduced stromal PDGFRβ expression. In contrast, tissues with high ATP6L expression showed significantly decreased PDGFB levels and increased stromal PDGFRβ levels (Figure 2F). This inverse relationship between ATP6L and PDGFRβ suggests a potential disruption in the crucial PDGFB/PDGFRβ signaling axis required for pericyte recruitment and maintenance.

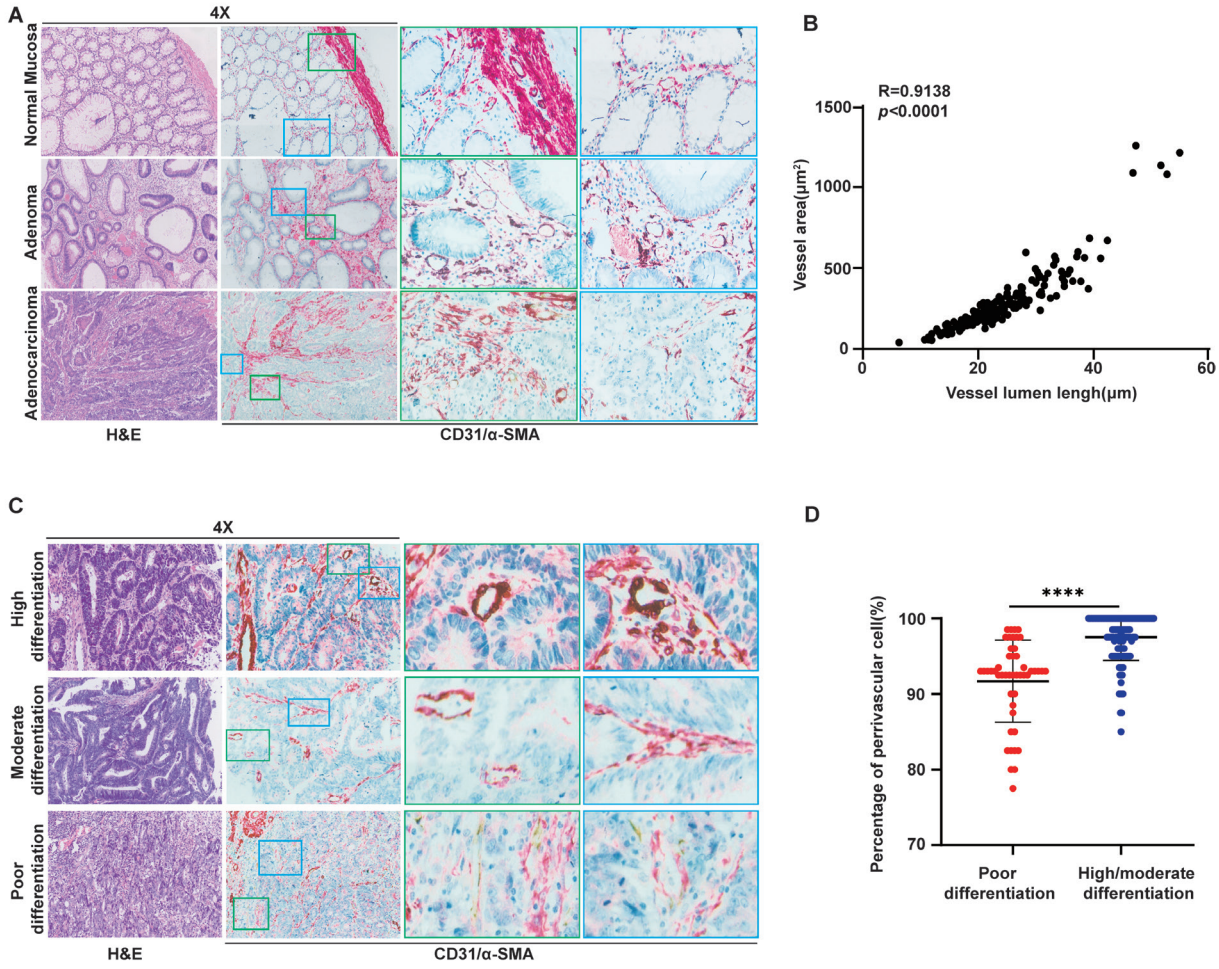


Figure 1. Vascular instability increases during colorectal cancer progression and correlates with tumor differentiation. (A). HE staining and representative immunofluorescence images of human colonic tissues stained for the endothelial cell marker CD31 (brown) and the pericyte marker α-SMA (red) in normal colonic mucosa, adenoma and adenocarcinoma. Insets 1 and 2 show higher-magnification images of the vessels (boxed areas). **(B).** Quantitative analysis of pericyte coverage in 29 matched normal mucosa-adenoma-adenocarcinoma tissue trios. Data are presented as mean ± SD. $P < 0.001$; one-way ANOVA with Tukey's post-hoc test. **(C).** HE staining and α-SMA/CD31 double staining to assess the relationship between differentiation grade and perivascular cell coverage in 179 cases. **(D).** Comparison of pericyte coverage between poorly differentiated (n = 48) and high/moderate differentiated (n = 131) tumors in the 179-case cohort. Data are presented as mean ± SD. ****, $p < 0.0001$.

Table 2. ATP6L expression during the colorectal normal mucosa-adenoma–adenocarcinoma sequence

	ATP6L expression *n* (%)			X^2	*p* value
	Total	Low expression	High expression		
Normal mucosa	29	27 (93.1)	2 (6.9)	39.518	$P < 0.001$
Adenoma	29	20 (67.0)	9 (33.0)		
Adenocarcinoma	29	4 (13.8)	25 (86.2)		
Total	87	51 (58.6)	36 (41.4)		

3.3. ATP6L overexpression in CRC cells inhibits pericyte function and disrupts PDGFB/PDGFRβ signaling *in vitro*

To establish causality, we generated stable MC38 and CT26 cell lines with ATP6L overexpression (OE) and corresponding Vector controls, respectively (Figure 3A). Using an indirect co-culture system (Figure 3B), we found that the conditioned medium from ATP6L-OE cells significantly increased extracellular H^+ concentration, confirming enhanced acidification (Figure 3C). Conditioned medium from ATP6L-OE cells not only potently inhibited the proliferation and migration of MOVAS, a pericyte model (Figures 3D,3E), but also promoted its apoptosis. This pro-apoptotic effect was supported by both molecular changes—increased Bax/Bcl-2 ratio and cleaved Caspase-3 (Figure 3F)—and a

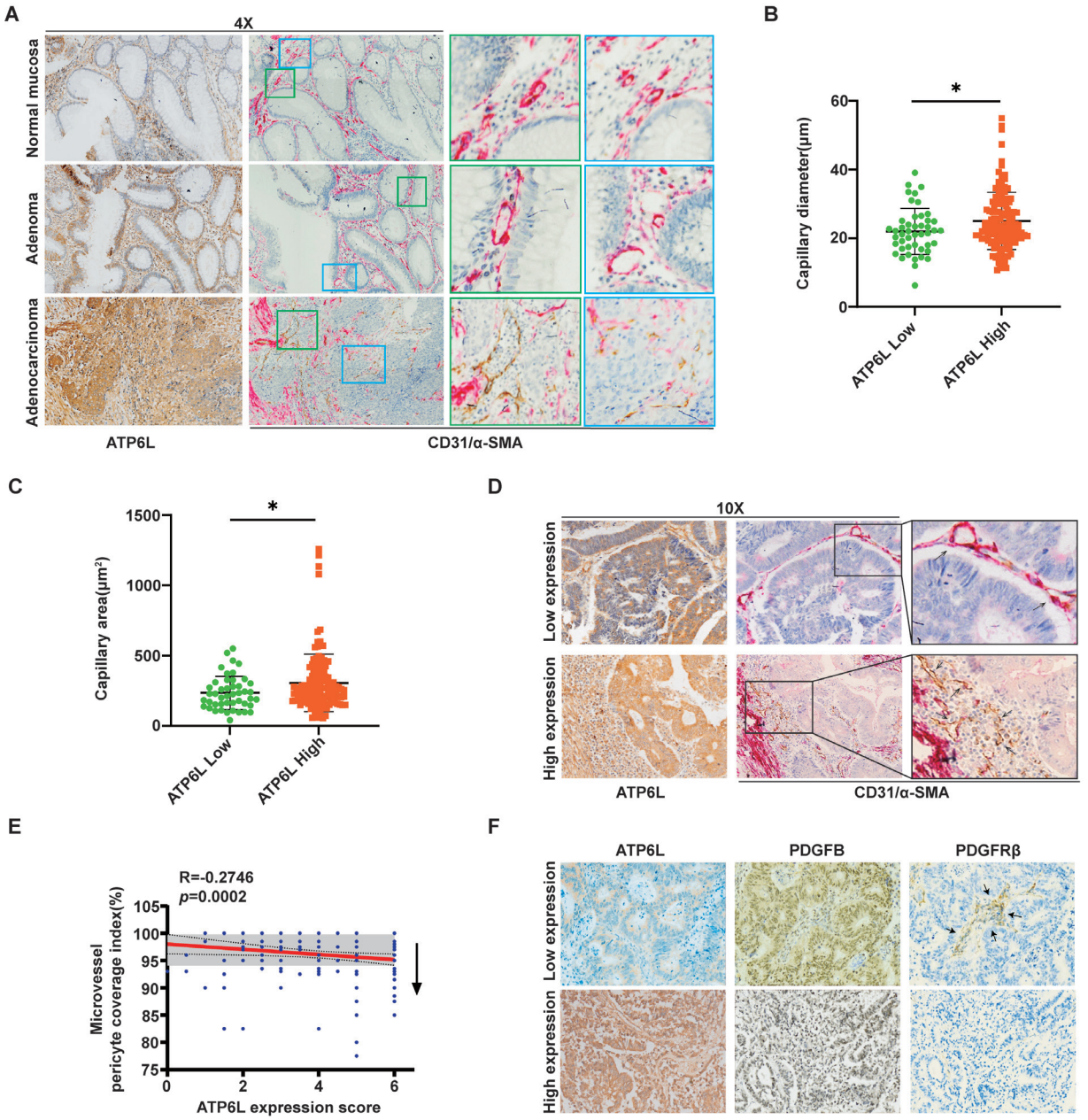


Figure 2. ATP6L expression is associated with vascular instability and PDGFRβ signaling dysregulation in human CRC. (A). Representative images of ATP6L immunohistochemistry and CD31/α-SMA double immunohistochemistry staining in normal mucosa and adenocarcinoma tissues, showing samples labeled as "normal mucosa," "adenoma," and "adenocarcinoma," respectively. **(B)**, **(C)**. Quantification of microvascular lumen diameter **(B)** and lumen area **(C)** in CRC tissues with ATP6L high expression *vs.* ATP6L low expression. **(D).** Representative images of CD31/α-SMA double immunofluorescence staining in colorectal cancer tissues with different ATP6L expression levels. **(E).** Correlation between ATP6L expression and pericyte coverage index (%) in 179 CRC tissues. Spearman's correlation analysis. **(F).** Representative immunohistochemical staining images showing ATP6L, PDGFB and PDGFRβ expression in serial sections of CRC tissues. *, $p < 0.05$.

2.8-fold increase in TUNEL-positive cells (Figure 3G).

Recapitulating the observations from CRC specimens, our mechanistic investigations revealed a significant reduction in PDGFRβ concentration in the co-culture medium of ATP6L-OE cells (Figure 3H). It has been reported that lactate can be taken up and utilized by pericytes for energy generation and various biogenic processes, which are critical for normal pericyte function (*22,23*). Given that ATP6L-OE cells markedly increased extracellular H^+ concentration, we hypothesized that ATP6L overexpression in CRC cells creates an acidic extracellular milieu that in turn suppresses PDGFB secretion. To test this hypothesis, we sought to block the acidic environment induced by ATP6L-OE using Bafilomycin A1 (Baf A1), a specific and reversible inhibitor of V-ATPase that prevents intracellular acidification (*24*). Concurrently, ELISA results demonstrated that the PDGFB protein concentration in the co-culture supernatant was significantly reduced in MOVAS cells co-cultured with MC38/

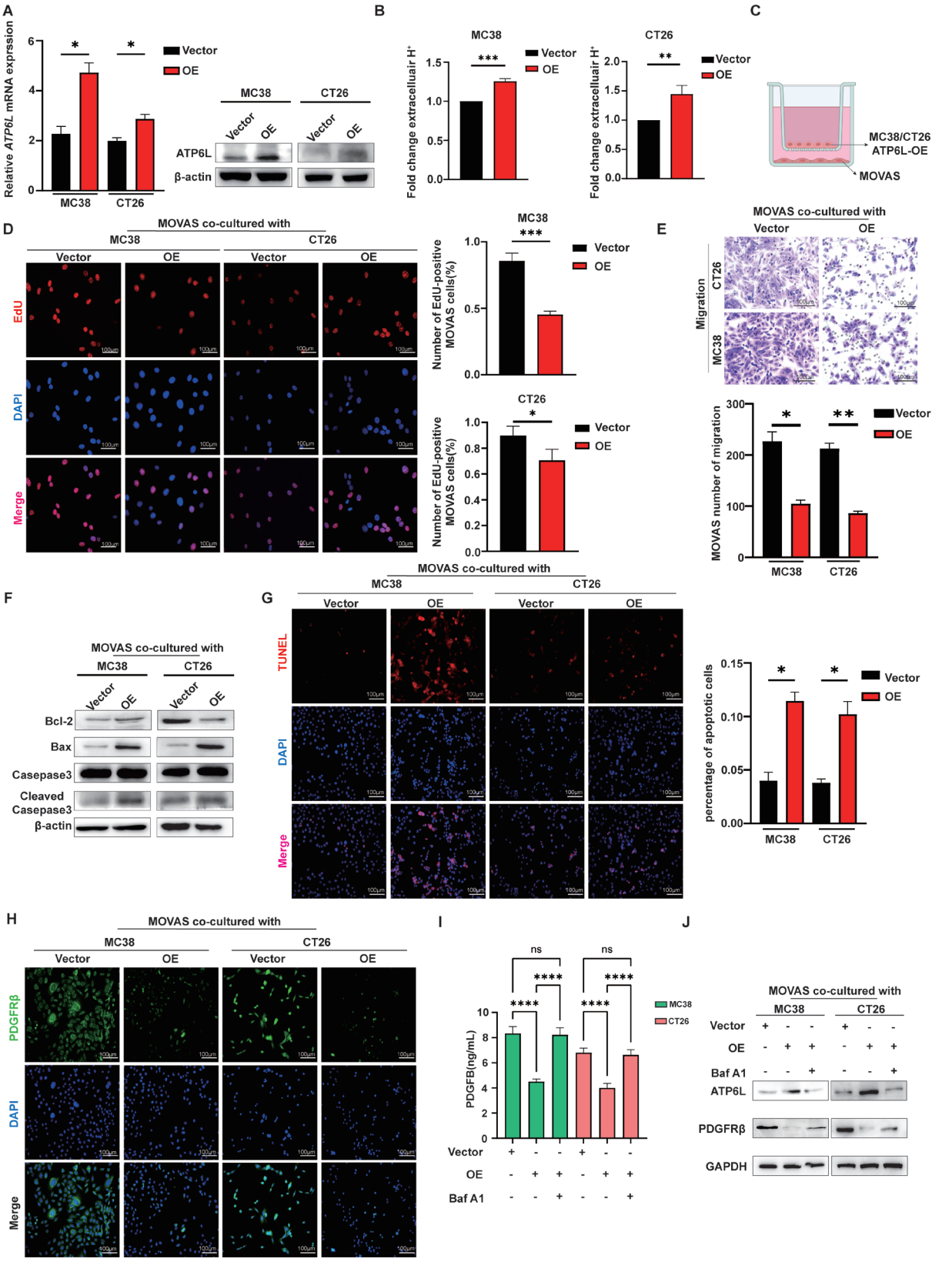


Figure 3. ATP6L overexpression in CRC cells impairs pericyte function and dysregulates PDGFB/PDGFRβ signaling *in vitro*. **(A).** Validation of ATP6L overexpression in MC38 and CT26 cell lines at the mRNA and protein levels. **(B).** Extracellular acidification rate detected by the P61 pH-sensitive fluorescent probe in conditioned medium from Vector and ATP6L-overexpressing (ATP6L-OE) CRC cells. **(C).** Co-culture of MOVAS cells with MC38/CT26. **(D).** Proliferation of mouse vascular smooth muscle cells (MOVAS) after 24-hour co-culture with CRC cells, assessed by EdU incorporation assay—representative images and quantification for MC38 and CT26 co-cultures. **(E).** Migration of MOVAS cells assessed by Transwell assay after co-culture. Representative images and quantification. F&G. Apoptosis of MOVAS cells. Western blot analysis of apoptosis-related proteins **(F).** and representative TUNEL staining images, quantification of TUNEL-positive cells **(G)**. **(H).** Expression of PDGFRβ in MOVAS cells after co-culture, detected by immunofluorescence. **(I).** Quantification of PDGFB concentration in co-culture medium by ELISA. **(J).** Western blot analysis of PDGFRβ expression in different co-culture systems. Data are presented as mean ± SD from at least three independent experiments. Scale bars, 100 μm.*, $p < 0.05$; **, $p < 0.01$; ***, $p < 0.001$; ****, $p < 0.0001$; ns, not significant. Unpaired two-tailed *t*-test.

CT26 ATP6L-OE cells, relative to the Vector control group. Correspondingly, PDGFRβ protein expression in MOVAS cells was markedly downregulated in both ATP6L-OE co-culture groups. Importantly, pre-treatment of ATP6L-OE cells with Baf A1 partially restored both the supernatant PDGFB concentration and the PDGFRβ expression level in MOVAS cells (Figures 3I,3J).

To further explore the mechanistic link between ATP6L and the PDGFB/PDGFRβ axis in the context of CRC pericyte function and vascular stability, we generated ATP6L-knockdown (ATP6L-KD) MC38 and CT26 cell lines (Figure 4A) and carried out parallel experiments. Compared with the control group, MOVAS cells co-cultured with ATP6L-KD MC38/CT26 cells (Figure 4B) exhibited enhanced proliferation and migration and reduced apoptosis (Figures 4C–F). We found conditioned medium from ATP6L-KD cells significantly decreased extracellular H^+ concentration, indicating attenuated acidification (Figure 4G). ELISA showed that co-culture with ATP6L-KD cells elvated supernatant PDGFB secretion (Figure 4H), while Western blot analysis revealed that PDGFRβ protein levels were inversely correlated with ATP6L expression. To assess the functional contribution of ATP6L's proton-pumping activity, we treated ATP6L-KD cells with lactate, which partially reversed the reduction in PDGFB secretion. Consistently, this exogenous H^+ supplementation also abrogated the ATP6L-KD-induced alterations in PDGFRβ expression (Figure 4I). These pH fluctuations, in turn, may serve as a regulatory mechanism for the PDGFB/PDGFRβ axis.

Collectively, these *in vitro* data support a model in which ATP6L regulates the PDGFB/PDGFRβ signaling axis by modulating extracellular H+ levels, thereby influencing pericyte function and vascular stability.

3.4. ATP6L overexpression compromises vascular stability and perfusion *in vivo*

We sought to verify these *in vitro* findings in an *in vivo* model with MC-38 cells. The mouse tumor xenograft model was established by subcutaneously implanting either ATP6L-OE or Vector MC38 cells into the groins of each nude mouse. ATP6L-OE tumors exhibited significantly larger volumes than Vector controls, and intratumoral Baf A1 administration effectively inhibited their *in vivo* growth (Figure 5A). Upon tumor dissection, the subcutaneous tumorigenic active area in the ATP6L-OE group was found to be significantly larger than that in the Vector group. Notably, intratumoral injection of Baf A1 effectively promoted apoptosis within the tumors (Figure 5B). Meanwhile, lectin perfusion and FITC-dextran extravasation assays revealed that ATP6L-OE tumors exhibited a 30% reduction in functional vessel density and a 2.1-fold increase in permeability. Notably, these vascular abnormalities were partially reversed upon intratumoral administration of Baf A1 (Figure 5C).

To address pericyte heterogeneity and avoid marker-specific bias, we assessed pericyte coverage using three markers—α-SMA, NG2 and PDGFRβ—in combination with CD31. All three markers exhibited significantly reduced co-localization with CD31 in ATP6L-OE tumors, confirming global pericyte dysfunction. Notably, this vascular defect was partially rescued by intratumoral administration of Baf A1, which effectively reversed the vascular dysfunction induced by ATP6L overexpression (Figure 5D). Collectively, these findings confirm that ATP6L overexpression in tumor cells is sufficient to drive vascular instability and dysfunction *in vivo.*

4. Discussion

The role of ATP6L in promoting tumor malignancy has been confirmed in studies of other cancer types, including hepatocellular carcinoma (*14*), breast cancer (*15*), and pancreatic cancer (*16*). Our group has previously demonstrated that ATP6L is highly expressed in poorly differentiated CRC and promotes tumor cell mesenchymal-epithelial transition (*17*). However, the relationship between ATP6L and angiogenesis or vascular stability remains poorly understood. Here, we identify a novel role for ATP6L, a key subunit of the V-ATPase proton pump, in driving vascular instability in CRC. Specifically, we found that high ATP6L expression in CRC cells is both clinically correlated with and functionally sufficient to reduce pericyte coverage and disrupt normal vascular architecture, culminating in a dysfunctional and hyperpermeable tumor vasculature.

Our analysis of the adenoma–adenocarcinoma sequence corroborates the notion of progressive vascular maladaptation accompanying colorectal tumorigenesis (*1,25,26*). Specifically, we observed a marked reduction in pericyte coverage along the normal mucosa–adenoma–adenocarcinoma continuum, reflecting progressive vessel immaturity. This vascular instability was further exacerbated in poorly differentiated tumors, implying a close relationship between aggressive cancer phenotypes and a compromised stromal microenvironment (*1,2,27*). Importantly, the selective association of high ATP6L expression with enlarged, tortuous vessels and diminished pericyte coverage in human CRC specimens implicates ATP6L as a key mediator that bridges tumor-intrinsic acidification and perivascular dysfunction.

Mechanistically, our functional data support a model linking tumor cell acidification to pericyte dysfunction and vascular instability *via* the PDGFB/PDGFRβ signaling axis. PDGFB/PDGFRβ signaling is a critical determinant of vascular stability (28,29), yet in tumors, pericytes are typically sparse and form loose associations with endothelial cells (*30,31*). This may partly arise from tumor-derived PDGFB, which disrupts the physiological PDGFB/PDGFRβ gradient (*32*). Although this signaling axis has been implicated in pericyte

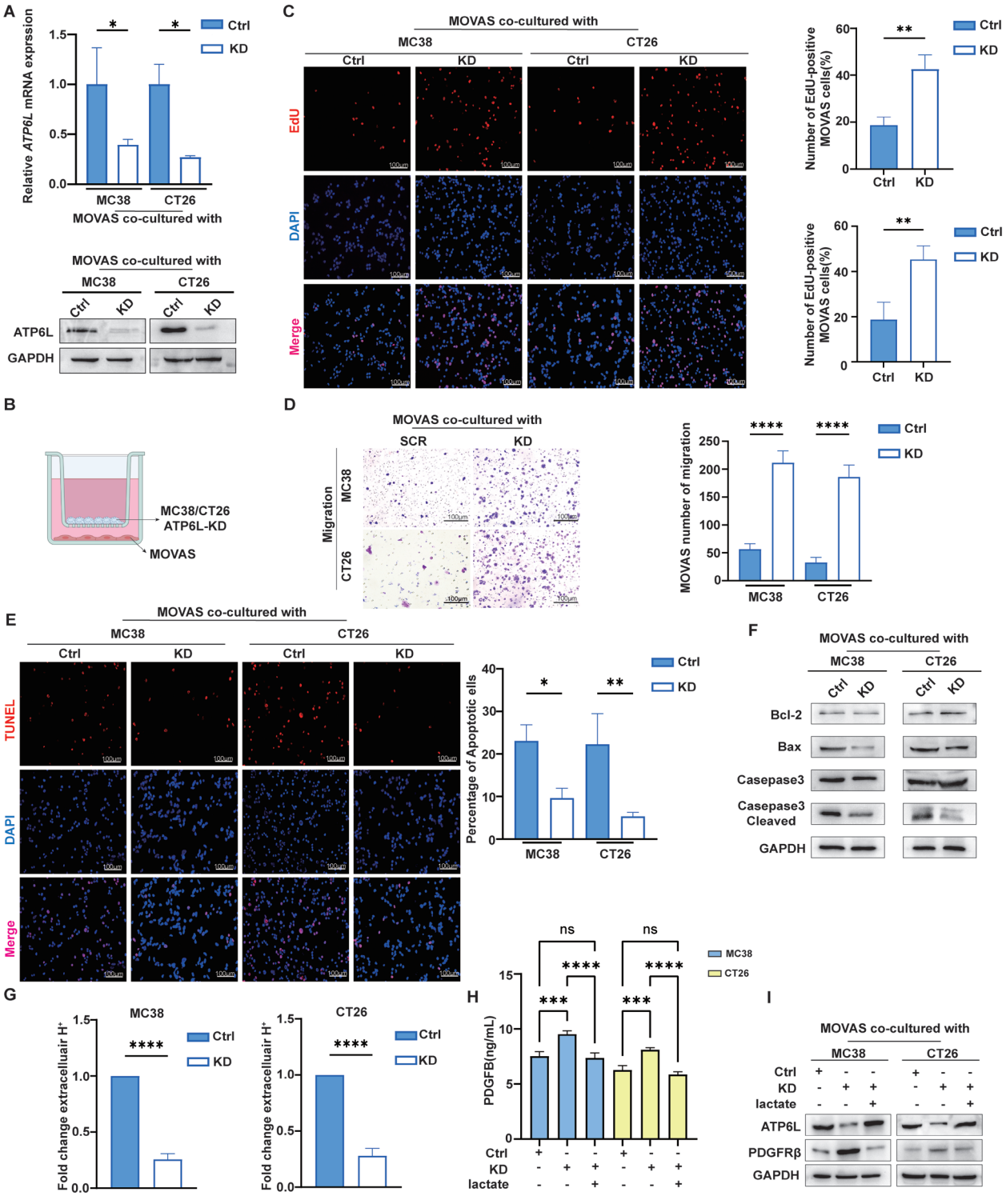


Figure 4. ATP6L knockdown in CRC cells enhances pericyte function and activates PDGFB/PDGFRβ signaling *in vitro*. (A). Validation of ATP6L knockdown in MC38 and CT26 cell lines at the mRNA and protein levels. **(B).** Co-culture of MOVAS cells with MC38/CT26. **(C).** Proliferation of mouse vascular smooth muscle cells (MOVAS) after 24-hour co-culture with CRC cells, assessed by EdU incorporation assay—representative images and quantification for MC38 and CT26 co-cultures. **(D).** Migration of MOVAS cells assessed by Transwell assay after co-culture. Representative images and quantification. E&F. Apoptosis of MOVAS cells. Western blot analysis of apoptosis-related proteins **(E)** and representative TUNEL staining images, quantification of TUNEL-positive cells **(F)**. **(G).** Extracellular acidification rate detected by the P61 pH-sensitive fluorescent probe in conditioned medium from control (Ctrl) and ATP6L-knockdown (ATP6L-KD) CRC cells. **(H).** Quantification of PDGFB concentration in co-culture medium by ELISA. **(I).** Western blot analysis of PDGFRβ expression in different co-culture systems. Data are presented as mean ± SD from at least three independent experiments. Scale bars, 100 μm.*, $p < 0.05$; **, $p < 0.01$; ***, $p < 0.001$; ****, $p < 0.0001$; ns, not significant. Unpaired two-tailed *t*-test.

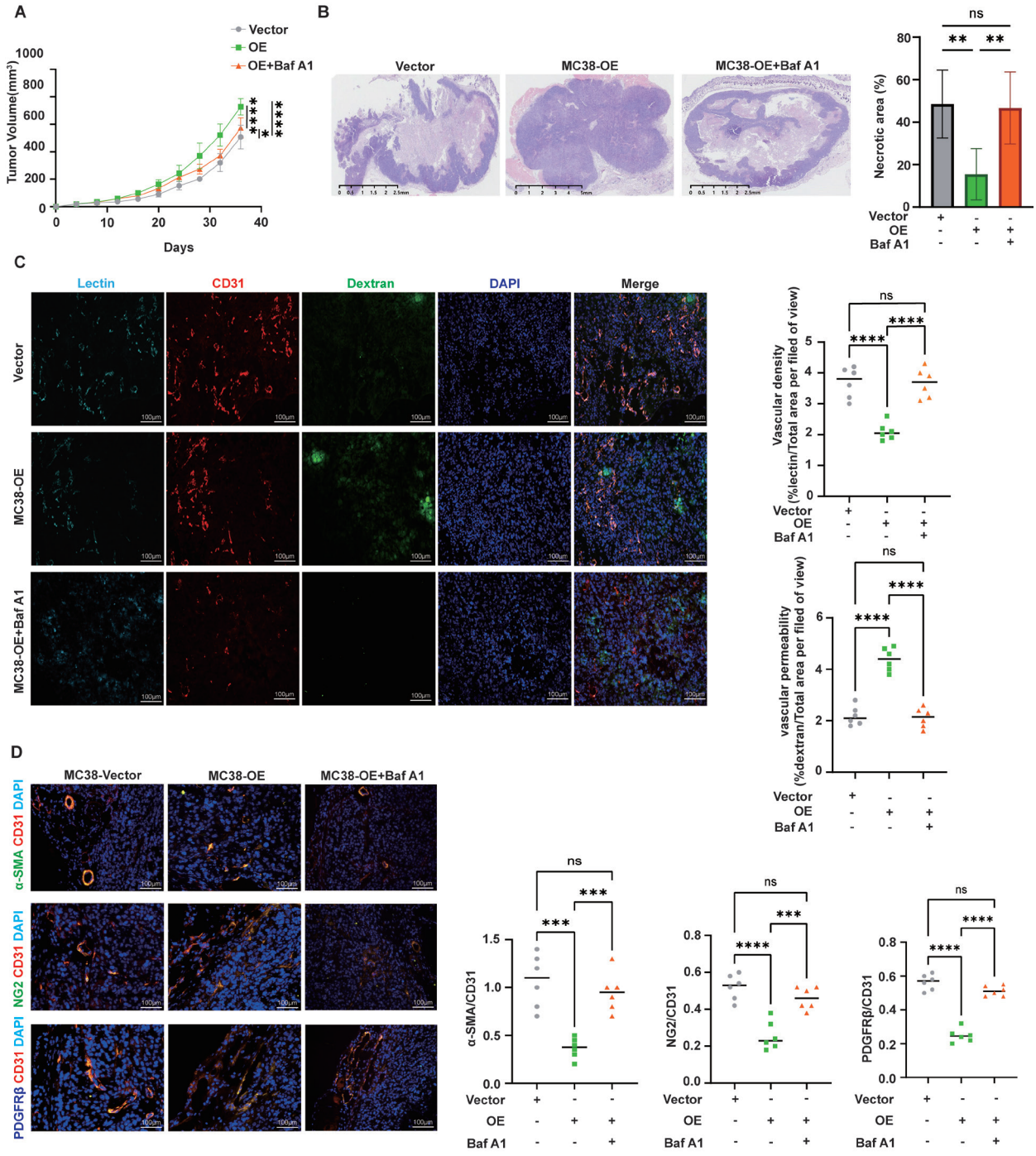


Figure 5. ATP6L overexpression compromises vascular stability and perfusion *in vivo*. (A). *In vivo* tumor growth curves. **(B).** Tumor necrosis under different conditions, H&E staining and quantification. **(C).** Analysis of tumor vasculature in MC38 xenograft models. Representative merged images of perfused vessels (Lectin, blue), endothelial marker CD31 (red), and permeable vasculature (FITC-dextran, green). Quantification of perfused vessel density and vascular permeability index. **(D).** Assessment of pericyte coverage in tumor xenografts. Representative immunofluorescence images showing co-localization of the endothelial marker CD31 (red) with pericyte markers α-SMA, NG2 and PDGFRβ (green). Scale bars, 100μm. Quantification of pericyte coverage for each marker.*, $p < 0.05$;**, $p < 0.01$;***, $p < 0.001$; ****, $p < 0.0001$; ns, not significant.

recruitment and vascular maturation, its precise role in tumor angiogenesis and vascular remodeling remains incompletely understood and appears to be context-dependent (*1,30,33*).

We find that ATP6L overexpression in CRC cells acidifies the extracellular space and suppresses PDGFB secretion. This reduction in PDGFB, acting paracrinally, downregulates PDGFRβ expression on pericytes, thereby disrupting a signaling cascade critical for their recruitment and survival. The resultant pericyte dysfunction—manifested as reduced proliferation, impaired migration, and heightened apoptosis—is consistent with our phenotypic observations. Moreover, ATP6L expression levels directly correlate with changes

in intracellular pH, which in turn modulate PDGFB/PDGFRβ signaling. *In vivo*, ATP6L-overexpressing tumors exhibit a dysfunctional vasculature with poor perfusion, elevated permeability, and sparse pericyte coverage. Together, these findings support a model in which ATP6L regulates the PDGFB/PDGFRβ axis *via* extracellular H^+, thereby regulating pericyte function and vascular stability. A schematic representation of the proposed ATP6L–extracellular acidification–PDGFB/PDGFRβ–pericyte axis is shown in Figure 6.

In our model, ATP6L overexpression creates an acidic microenvironment that suppresses PDGFB secretion, thereby reducing PDGFRβ expression on pericytes and impairing vascular stability. Of note, a previous study by Hosaka *et al*. has shown that in tumors with high PDGFB expression, sustained exposure to elevated PDGFB levels can also cause pericyte loss through PDGFRβ internalization and degradation (*34*). Thus, insufficient PDGFRβ signaling, arising from either decreased ligand availability or receptor downregulation, underlies pericyte dysfunction and vascular instability in both contexts. These observations underscore that the integrity of PDGFRβ signaling is essential for maintaining vascular stability, while the upstream regulatory mechanisms may vary by tumor type and microenvironmental context.

Translationally, our findings suggest that ATP6L could serve as both a biomarker for metastasis-prone unstable vasculature and a therapeutic target for vascular normalization. Targeting ATP6L may reverse PDGFB/PDGFRβ dysregulation, stabilize tumor vessels, and improve drug delivery, potentially overcoming the hypoxia-driven invasiveness associated with current anti-angiogenic therapies. However, limitations include the observational nature of human tissue correlations, the preliminary mechanistic data, and the use of murine cell models—all of which warrant cautious interpretation.

In conclusion, we demonstrate that ATP6L is a critical driver of vascular instability in colorectal cancer. By promoting a tumor-acidified microenvironment that disrupts the PDGFB/PDGFRβ signaling axis, ATP6L undermines pericyte function, leading to a leaky, immature vasculature. Targeting this axis may offer a novel strategy to normalize the tumor vasculature and improve therapeutic outcomes.

Funding: This work was supported by grants from the National Natural Science Foundation of China

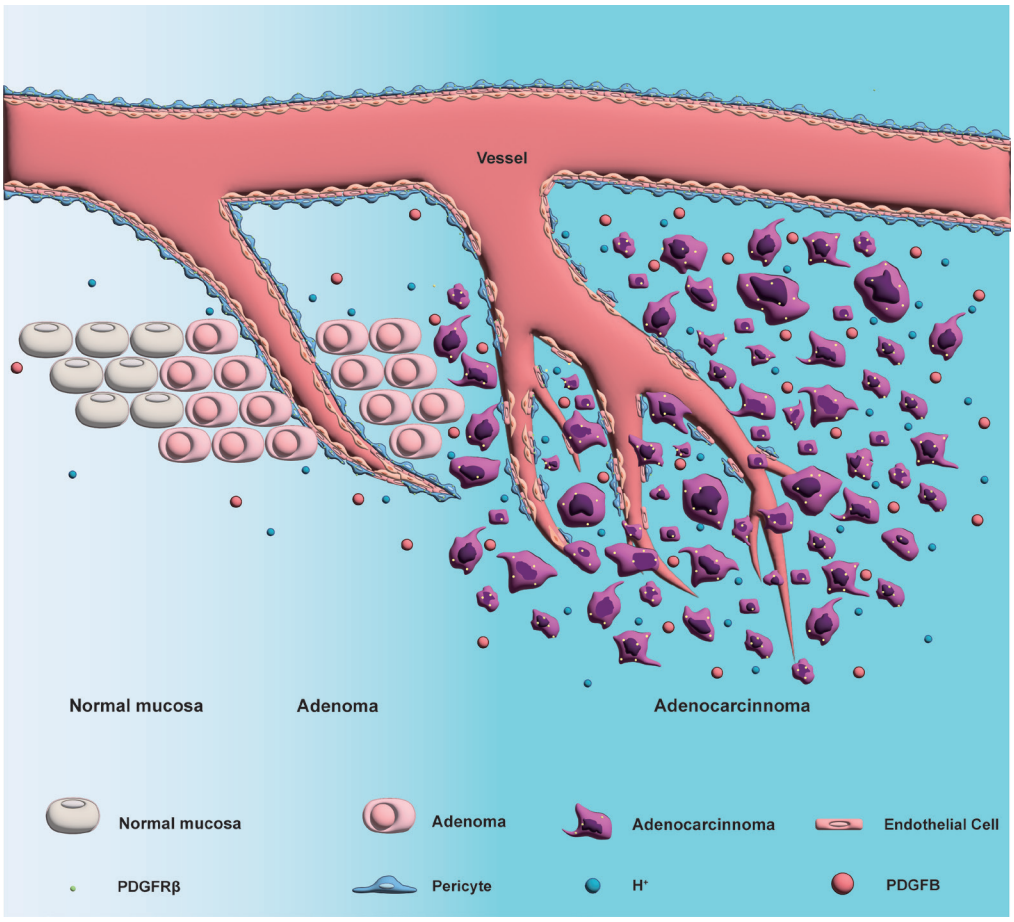


Figure 6. Proposed model of ATP6L-mediated vascular destabilization through extracellular acidification and dysregulation of the PDGFB/PDGFRβ axis in colorectal cancer.

(82472991), Natural Science Foundation of Tianjin (23JCYBJC00600), and Tianjin Key Medical Discipline Construction Project (TJYXZDXK-3-016C).

Conflict of Interest: The authors have no conflicts of interest to disclose.

Ethics approval: The human component of this study involving patient participation was approved by the Ethics Committee of Tianjin Medical University Cancer Institute and Hospital (Approval No. bc2020073) in accordance with the Declaration of Helsinki. The animal experiments were approved by the same ethics committee (Approval No. AE-2022216) in accordance with NIH Guidelines for Animal Research.

References

1. Guelfi S, Hodivala-Dilke K, Bergers G. Targeting the tumour vasculature: from vessel destruction to promotion. Nat Rev Cancer. 2024; 24:655-675.
2. Martin JD, Seano G, Jain RK. Normalizing Function of Tumor Vessels: Progress, Opportunities, and Challenges. Annu Rev Physiol. 2019; 81:505-534.
3. Magnussen AL, Mills IG. Vascular normalisation as the stepping stone into tumour microenvironment transformation. Br J Cancer. 2021; 125:324-336.
4. Jain RK. Normalization of tumor vasculature: an emerging concept in antiangiogenic therapy. Science. 2005; 307:58-62.
5. Jordan AM, Drake RJG, Hodivala-Dilke KM. Angiocrine and pericrine signaling: how endothelial cells and pericytes drive cancer progression and therapy resistance. Physiol Rev. 2026; 106:87-119.
6. Tian L, Goldstein A, Wang H, *et al*. Mutual regulation of tumour vessel normalization and immunostimulatory reprogramming. Nature. 2017; 544:250-254.
7. Zhu J, Yang W, Ma J, He H, Liu Z, Zhu X, He X, He J, Chen Z, Jin X, Wang X, He K, Wei W, Hu J. Pericyte signaling *via* soluble guanylate cyclase shapes the vascular niche and microenvironment of tumors. EMBO J. 2024; 43:1519-1544.
8. Gomez D, Owens GK. Smooth muscle cell phenotypic switching in atherosclerosis. Cardiovasc Res. 2012; 95:156-164.
9. Pan X, Li X, Dong L, *et al*. Tumour vasculature at single-cell resolution. Nature. 2024; 632:429-436.
10. Swietach P, Boedtkjer E, Pedersen SF. How protons pave the way to aggressive cancers. Nat Rev Cancer. 2023; 23:825-841.
11. Corbet C, Feron O. Tumour acidosis: from the passenger to the driver's seat. Nat Rev Cancer. 2017; 17:577-593.
12. Forgac M. Vacuolar ATPases: rotary proton pumps in physiology and pathophysiology. Nat Rev Mol Cell Biol. 2007; 8:917-929.
13. Cotter K, Capecci J, Sennoune S, Huss M, Maier M, Martinez-Zaguilan R, Forgac M. Activity of plasma membrane V-ATPases is critical for the invasion of MDA-MB231 breast cancer cells. J Biol Chem. 2015; 290:3680-3692.
14. Zeng S, Chen J, Ren Y, *et al*. Multiscale imaging on proton pump-driven acidity for assessing tumor progression and metastasis. Nat Commun. 2026; 17:1785.
15. You H, Jin J, Shu H, Yu B, Milito AD, Lozupone F, Deng Y, Tang N, Yao G, Fais S, Gu J, Qin W. Small interfering RNA targeting the subunit ATP6L of proton pump V-ATPase overcomes chemoresistance of breast cancer cells. Cancer Lett. 2009; 280:110-119.
16. Stransky L, Cotter K, Forgac M. The Function of V-ATPases in Cancer. Physiol Rev. 2016; 96:1071-1091.
17. Wang J, Chen D, Song W, Liu Z, Ma W, Li X, Zhang C, Wang X, Wang Y, Yang Y, Cao W, Qi L. ATP6L promotes metastasis of colorectal cancer by inducing epithelial-mesenchymal transition. Cancer Sci. 2020; 111:477-488.
18. Tian X, Xia Y, Gong W, Zhu K, Yang Y, Han Z, Liu Y, Li J, Li X, He Y, Gao M, Chen L, Guo H, Zhao Q. PLK4 as a Key Regulator of Neuroblastoma Differentiation and a Promising Therapeutic Target. Int J Biol Sci. 2025; 21:4979-4996.
19. Qin Y, Zhao W. The Modeling Analysis and Effect of CHI3L1 and CD31-Marked Microvessel Density in the Occurrence and Development of Cervical Squamous Cell Carcinoma. Comput Math Methods Med. 2022; 2022:3516335.
20. Guo Z, Cao Y. Mechanisms of Pericyte-Mediated Cancer Metastasis. Adv Sci (Weinh). 2026; 13:e00031.
21. Lee SJ, Kim S, Jo DH, Cho CS, Kim SR, Kang D, Chae J, Yoo DK, Ha S, Chung J, Kim JH. Specific ablation of PDGFRβ-overexpressing pericytes with antibody-drug conjugate potently inhibits pathologic ocular neovascularization in mouse models. Commun Med (Lond). 2021; 1:58.
22. Lee HW, Xu Y, Zhu X, Jang C, Choi W, Bae H, Wang W, He L, Jin SW, Arany Z, Simons M. Endothelium-derived lactate is required for pericyte function and blood-brain barrier maintenance. EMBO J. 2022; 41:e109890.
23. Zou MZ, Liu WL, Chen HS, Bai XF, Gao F, Ye JJ, Cheng H, Zhang XZ. Advances in nanomaterials for treatment of hypoxic tumor. Natl Sci Rev. 2021; 8:nwaa160.
24. Wang R, Wang J, Hassan A, Lee CH, Xie XS, Li X. Molecular basis of V-ATPase inhibition by bafilomycin A1. Nat Commun. 2021; 12:1782.
25. Liu Z, Sun B, Qi L, Li Y, Zhao X, Zhang D, Zhang Y. Dickkopf-1 expression is down-regulated during the colorectal adenoma-carcinoma sequence and correlates with reduced microvessel density and VEGF expression. Histopathology. 2015; 67:158-166.
26. Staton CA, Chetwood AS, Cameron IC, Cross SS, Brown NJ, Reed MW. The angiogenic switch occurs at the adenoma stage of the adenoma carcinoma sequence in colorectal cancer. Gut. 2007; 56:1426-1432.
27. Suvac A, Ashton J, Bristow RG. Tumour hypoxia in driving genomic instability and tumour evolution. Nat Rev Cancer. 2025; 25:167-188.
28. Abramsson A, Lindblom P, Betsholtz C. Endothelial and nonendothelial sources of PDGF-B regulate pericyte recruitment and influence vascular pattern formation in tumors. J Clin Invest. 2003; 112:1142-1151.
29. Lindahl P, Johansson BR, Levéen P, Betsholtz C. Pericyte loss and microaneurysm formation in PDGF-B-deficient mice. Science. 1997; 277:242-245.
30. Sun R, Kong X, Qiu X, Huang C, Wong PP. The Emerging Roles of Pericytes in Modulating Tumor Microenvironment. Front Cell Dev Biol. 2021; 9:676342.
31. Kasurinen JH, Hagström J, Kaprio T, Jalkanen S, Salmi M, Böckelman C, Haglund C. Prognostic Values of

Tissue and Serum Angiogenic Growth Factors Depend on the Phenotypic Subtypes of Colorectal Cancer. Cancers (Basel). 2023; 15.
32. Zhang Y, Cedervall J, Hamidi A, *et al*. Platelet-Specific PDGFB Ablation Impairs Tumor Vessel Integrity and Promotes Metastasis. Cancer Res. 2020; 80:3345-3358.
33. Huinen ZR, Huijbers EJM, van Beijnum JR, Nowak-Sliwinska P, Griffioen AW. Anti-angiogenic agents—overcoming tumour endothelial cell anergy and improving immunotherapy outcomes. Nat Rev Clin Oncol. 2021; 18:527-540.
34. Hosaka K, Yang Y, Seki T, *et al*. Tumour PDGF-BB expression levels determine dual effects of anti-PDGF drugs on vascular remodelling and metastasis. Nat Commun. 2013; 4:2129.

Received August 4, 2026; Revised August 25, 2026; Accepted August 27, 2026.

[§]These authors contributed equally to this work.
**Address correspondence to:*
Xiangdong Tian and Lisha Qi, Tianjin Medical University Cancer Institute and Hospital, West HuanHu Road, Ti Yuan Bei, Hexi District, Tianjin 300060, China.
E-mail: xiangdongtian@tmu.edu.cn; lqi01@tmu.edu.cn

Released online in J-STAGE as advance publication August 28, 2026.

Original Article

DOI: 10.5582/bst.2026.01126

Underrecognized cardiovascular complications after hepatectomy: population-level mortality burden from a multicentre population-attributable fraction (PAF) analysis

Junlong Dai[1,2,3,§], Zhancheng Qiu[1,§], Jimmy Che-To Lai[2,3,4,5], Yu Zhang[6], Fei Xie[7], Yu Yu[8], Kangyi Jiang[9], Tinghao Chen[10], Vincent Wai-Sun Wong[2,4,5], Tianfu Wen[1], Chuan Li[1,*]

[1] Division of Liver Surgery, Department of General Surgery, West China Hospital, Sichuan University, Chengdu, Sichuan, China;
[2] Medical Data Analytics Centre, The Chinese University of Hong Kong, Hong Kong SAR, China;
[3] Department of Medicine and Therapeutics, CUHK, Hong Kong SAR, China;
[4] State Key Laboratory of Digestive Disease, CUHK, Hong Kong SAR, China;
[5] Li Ka Shing Institute of Health Sciences, CUHK, Hong Kong SAR, China;
[6] Department of Hepatopancreatobiliary Surgery, Sichuan Academy of Medical Sciences (Sichuan Provincial People's Hospital), Chinese Academy of Sciences, Chengdu, Sichuan, China;
[7] Department of Hepatobiliary and Pancreatic Surgery, the First People's Hospital of Neijiang City, Neijiang, Sichuan, China;
[8] Department of Hepatopancreatobiliary Surgery, the Second People's Hospital of Yibin City, Yibin, Sichuan, China;
[9] Department of Hepatobiliary Surgery, People's Hospital of Leshan, Leshan, Sichuan, China;
[10] Department of General Surgery, Ziyang Central Hospital, Ziyang, Sichuan, China.

SUMMARY: Postoperative complications remain major determinants of outcomes after hepatectomy for hepatocellular carcinoma (HCC), but whether complications that prolong hospitalization are also those that contribute most to mortality remains unclear. This multicentre cohort study included 1,883 patients undergoing curative-intent hepatectomy for HCC across seven tertiary centers. Postoperative complications were categorized by organ system, and adjusted population-attributable fractions (PAFs) were calculated to estimate their contributions to 90-day mortality and prolonged hospital stay. Multivariable Cox models were used to assess associations with overall survival and recurrence-free survival. A divergence between hospitalization burden and mortality burden was observed. Liver surgery-specific complications accounted for the largest population-level burden of prolonged hospitalization (PAF 11.0%) and 90-day mortality (PAF 10.0%). Cardiovascular complications were the leading non-liver contributor to 90-day mortality (PAF 9.4%), despite a smaller contribution to prolonged hospitalization (PAF 4.1%). Pulmonary complications, cardiovascular complications, renal complications, and glucose dysregulation were independently associated with worse overall survival, whereas no complication domain was independently associated with recurrence-free survival. These findings show that postoperative recovery burden and mortality burden are not interchangeable after hepatectomy. Liver surgery-specific complications dominated hospitalization burden, whereas cardiovascular complications represented an underrecognized non-liver contributor to early mortality and worse long-term survival. An integrated perioperative framework incorporating systematic cardiovascular risk assessment may improve risk prioritization after hepatectomy for HCC.

Keywords: hepatocellular carcinoma, hepatectomy, postoperative complications, population-attributable fraction, overall survival

1. Introduction

Hepatectomy remains the cornerstone curative treatment for hepatocellular carcinoma (HCC) and offers the possibility of long-term survival (*1*). Despite advances in surgical techniques and increasing adoption of minimally invasive approaches, postoperative morbidity remains substantial, with complications continuing to compromise recovery, resource utilization, and long-term outcomes (*2*). Improving perioperative outcomes therefore remains a central objective in modern liver surgery.

Previous studies have described the incidence of postoperative complications and their associations with short- and long-term outcomes in patients undergoing hepatectomy for HCC (*2-4*). However, most analyses have focused on individual complication rates, relative risks, or conventional severity grading,

without accounting for their overall impact at the population level. For surgical outcome prioritization, neither complication incidence nor relative risk alone is sufficient. A rare complication with a high relative risk may be clinically serious but contribute less to the overall burden of adverse outcomes than a more common complication with a moderate relative risk. Conversely, a frequent complication may consume substantial postoperative resources even if its individual-level risk is modest.

In clinical practice of liver surgery, complications that prolong hospitalization or require direct surgical management, such as liver surgery-specific complications, may receive greater attention (*5-7*). By contrast, systemic complications, including cardiovascular events, may be less visible in routine surgical outcome assessment but may still contribute substantially to early postoperative mortality. The population-attributable fraction (PAF), widely used in epidemiological research, integrates exposure prevalence and relative risk to estimate the proportion of outcome burden associated with a given factor at the population level (*8*). Applied to postoperative complications, PAF may help distinguish complications that primarily increase healthcare burden, such as prolonged length of stay, from those that contribute disproportionately to mortality. This distinction is particularly relevant after hepatectomy, where postoperative risk reflects both liver-specific injury and systemic perioperative vulnerability (*9*).

In this multicentre cohort study, we systematically categorized postoperative complications following hepatectomy for HCC by organ system and applied PAF-based analyses to quantify their relative contributions to short- and long-term outcomes. Through this approach, we aimed to refine risk stratification and provide a population-level framework to prioritize perioperative interventions.

2. Materials and Methods

2.1. Study design and data source

This multicentre retrospective cohort study included consecutive adult patients undergoing curative-intent hepatectomy for HCC at seven high-volume tertiary hepatobiliary centers in China between January 2014 and December 2019.

Curative intent was defined as complete macroscopic tumor removal without radiologic or intraoperative evidence of distant metastasis. Only patients who achieved R0 resection, confirmed by histopathological examination demonstrating microscopically negative margins, were eligible for inclusion. Patients undergoing palliative or non-curative procedures were excluded.

Clinical data were extracted from institutional electronic medical record systems using predefined case report forms. Collected variables included demographic characteristics, comorbidities, preoperative laboratory parameters, tumor burden and pathological features, operative details, and postoperative outcomes. Postoperative complications were identified through systematic review of inpatient medical and nursing records and were adjudicated according to uniform predefined criteria across centers to ensure inter-institutional consistency.

2.2. Participants

The date of hepatic resection was defined as the index date. Inclusion criteria were age ≥ 18 years, first liver resection, histologically confirmed HCC, R0 resection, and availability of complete medical and nursing records for postoperative complication assessment. Exclusion criteria included non-curative or palliative procedures, concomitant major resection of other organs, insufficient data for complication adjudication, unreliable follow-up, and Barcelona Clinic Liver Cancer (BCLC) stage C disease.

Only patients with HCC were included to ensure population homogeneity, as intrahepatic cholangiocarcinoma and combined tumors differ substantially in tumor biology, prognostic determinants, and postoperative management, particularly regarding the use of adjuvant chemotherapy (*e.g.*, ABC-02 regimen), which may confound long-term outcomes.

A total of 2,457 patients were screened. After applying predefined inclusion and exclusion criteria, 1,883 patients were included in the final analysis (Figure 1). Patients were followed from the index date until death, tumor recurrence, loss to follow-up, or the administrative censoring date of 30 June 2023, whichever occurred first.

The study was conducted in accordance with the Declaration of Helsinki (2013) and was approved by the Biomedical Ethics Committee of West China Hospital (approval number: 2026-758), with informed consent waived owing to the retrospective nature of the study.

2.3. HCC diagnosis and management

HCC diagnosis and management followed contemporary national guidelines (*1*). Diagnosis was established by characteristic radiologic findings on multiphasic contrast-enhanced CT or MRI or confirmed histologically when necessary. All patients underwent standardized preoperative evaluation, including assessment of liver function reserve (Child–Pugh class and MELD score), viral hepatitis status, and tumor burden using contrast-enhanced imaging. Surgical candidacy was determined through multidisciplinary discussion, taking into account liver reserve, tumor stage, and overall fitness for major hepatectomy. Perioperative management followed institutional

standardized protocols, including intraoperative blood loss control strategies and structured postoperative monitoring. Antiviral therapy was administered to patients with active hepatitis B virus infection according to guidelines. Postoperative surveillance consisted of clinical evaluation, serum AFP testing, and imaging every 3–6 months during the first 2 years and every 6 months thereafter. Recurrence was defined radiologically or histologically.

2.4. Outcome and post-surgery complications definitions

The primary outcome was 90-day all-cause mortality. Secondary outcomes included prolonged length of hospital stay, overall survival, and recurrence-free survival. Prolonged length of hospital stay was defined as hospitalization duration above the 75th percentile of the cohort distribution. Overall survival and recurrence-free survival were calculated from the date of surgery to death and tumor recurrence, respectively.

Postoperative complications were defined and categorized according to standardized criteria summarized in Supplementary Table S1 (*https://www.biosciencetrends.com/action/getSupplementalData.php?ID=310*). Complication events were assessed during the index hospitalization and were independently reviewed by two investigators. Any discrepancies were resolved through discussion and consensus. Complications were classified using the Clavien–Dindo classification (*10*). Severe complications were defined as grade ≥ III. In addition, the Comprehensive Complication Index (CCI) was calculated to quantify the cumulative burden of postoperative morbidity (*11*).

Liver surgery-specific complications were defined in accordance with the framework proposed by the International Study Group of Liver Surgery (ISGLS), including post-hepatectomy liver failure (PHLF), bile leakage, postoperative ascites, postoperative blood transfusion, and reoperation. PHLF and bile leakage were defined according to ISGLS consensus criteria (Supplementary Figure S1, *https://www.biosciencetrends.com/action/getSupplementalData.php?ID=310*) (*12,13*).

Other postoperative complications were categorized into cardiovascular, pulmonary, renal, infection-related, metabolic and electrolyte, and gastrointestinal complications based on predefined clinical criteria. Cardiovascular complications were restricted to primary cardiovascular events, including new-onset or clinically significant arrhythmia and acute cardiac events. Instead, postoperative hemodynamic instability was recorded separately as an indicator of postoperative severity. Composite complication groups were constructed to reflect organ-system morbidity, while individual components were also analyzed where appropriate.

2.5. Statistical analysis

2.5.1. Descriptive statistics

Continuous variables were summarized as mean ± standard deviation or median with interquartile range, as appropriate. Categorical variables were presented as counts and percentages. Between-group comparisons were performed using Student's *t*-test or Wilcoxon rank-sum test for continuous variables and chi-square or Fisher's exact test for categorical variables, as appropriate. Statistical significance was defined as a two-sided p-value < 0.05. All analyses were conducted using R software (version 4.3.1; R Foundation for Statistical Computing, Vienna, Austria).

2.5.2. Missing data and multiple imputations

Missing data patterns were evaluated prior to analysis (Supplementary Figure S2, *https://www.biosciencetrends.com/action/getSupplementalData.php?ID=310*). Variables with missing values were imputed using multiple imputations by chained equations under the missing-at-random assumption. Five imputed datasets were generated with 20 iterations per dataset (*14*). Imputation diagnostics demonstrated good agreement between observed and imputed values (Supplementary Figure S3 and S4, *https://www.biosciencetrends.com/action/getSupplementalData.php?ID=310*). Exposure variables, outcomes, and derived composite indices were not imputed. Estimates from imputed datasets were combined using Rubin's rules.

2.5.3. Risk estimation for short-term outcomes

For binary outcomes (90-day mortality and prolonged length of stay), adjusted relative risks (RRs) with 95% confidence intervals (CIs) were estimated using Poisson regression models with log link and robust variance estimators. Each organ system–specific complication group was modeled independently as the exposure variable to minimize collinearity between complication domains and adjusted for predefined demographic characteristics, comorbidities, liver function parameters, tumor stage, and surgical factors. Restricted cubic spline functions were applied to assess potential non-linear associations between selected continuous covariates and binary outcomes (Supplementary Table S2, *https://www.biosciencetrends.com/action/getSupplementalData.php?ID=310*).

Pairwise correlations among complication domains were assessed using Phi coefficients to evaluate clustering and potential collinearity (Supplementary Figure S5, *https://www.biosciencetrends.com/action/getSupplementalData.php?ID=310*). The number of complication domains per patient was also calculated to describe the extent of co-occurrence. Although co-occurrence of postoperative complications was clinically relevant, most patients had no complication

domain or only a single complication domain, indicating that extensive overlap across domains was not the predominant pattern. Because postoperative complications may still co-occur or arise sequentially within shared clinical cascades, simultaneous inclusion of multiple complication domains in the same model could yield unstable estimates and obscure the total burden associated with each domain. Therefore, each complication domain was modeled separately. These models were intended to estimate total population-level association and attributable burden of each domain, rather than to partition mutually exclusive causal effects among competing complications.

2.5.4. Population-attributable fraction

To quantify the population-level impact of each complication, adjusted PAFs were calculated using a counterfactual approach. PAF was calculated using the formula below:

$$PAF = \frac{Risk_{observed} - Risk_{counter\ factual}}{Risk_{observed}}$$

For each complication, predicted outcome risks were estimated under observed exposure and under a hypothetical scenario in which the complication was absent. Bootstrap resampling (200 replications within each imputed dataset) was performed to derive 95% confidence intervals and P values (*8*).

2.5.5. Survival analysis for long-term outcomes

OS and recurrence-free survival RFS were estimated using the Kaplan–Meier method and compared using the log-rank test. Patients with unavailable long-term followup (n = 2, 0.1%) and recurrence status (n = 73, 3.9%) were excluded from recurrence-free survival analyses. Multivariable Cox proportional hazards models were constructed to estimate adjusted hazard ratios (HRs) with 95% CIs. Each complication was entered separately as an exposure variable and adjusted for predefined demographic characteristics, liver function parameters, tumor burden, and surgical factors. Cox models were fitted within each imputed dataset and pooled using Rubin's rules. The proportional hazards assumption was evaluated using Schoenfeld residuals.

2.5.6. Sensitivity analyses

Three predefined sensitivity strategies were implemented to evaluate the robustness of the findings. First, alternative multivariable adjustment strategies were applied to assess stability of RR and PAF estimates (Supplementary Table S3, *https://www.biosciencetrends.com/action/getSupplementalData.php?ID=310*). Model A served as the primary model; Model B (tumor-burden–focused) was additionally adjusted for pathological aggressiveness; Model C (comorbidity-focused) was additionally adjusted for comorbidities; and Model D (surgery-focused) emphasized surgery details and prior abdominal surgery. Covariate selection in each model was constrained according to the events-per-variable (EPV) principle, maintaining EPV ≥ 10. Second, analyses were repeated after excluding patients with BCLC stage B disease. Third, PAF estimates were recalculated under alternative adjustment strategies to evaluate the robustness of the counterfactual approach (Supplementary Figure S6, *https://www.biosciencetrends.com/action/getSupplementalData.php?ID=310*).

3. Results

3.1. Study population and baseline characteristics

A total of 1,883 patients undergoing curative-intent hepatectomy for HCC were included in the analysis (Figure 1). The cohort was predominantly male (84.6%), with a mean age of 53.5 ± 11.6 years and a mean BMI of 23.2 ± 3.2 kg/m². Hypertension and diabetes mellitus were present in 20.1% and 12.3% of patients, respectively, while preoperative documented cardiovascular disease was uncommon (1.9%). Chronic hepatitis B infection was the predominant underlying liver disease, with 85.3% of patients positive for HBsAg and 49.4% having HBV DNA > 10^3 IU/mL (Supplementary Table S4, *https://www.biosciencetrends.com/action/getSupplementalData.php?ID=310*).

Overall liver function was relatively preserved. The mean Child-Pugh score was 5.1 ± 0.3, the median ALBI score was −2.8 (IQR, −3.1 to −2.6), and the mean MELD score was 7.6 ± 1.3. Cirrhosis was present in 57.0% of patients. The median tumor size was 5.0 cm (IQR, 3.0–7.5), single tumors were present in 85.2%, and microvascular invasion was identified in 28.6%. Most patients had BCLC stage 0 or A disease, while 7.3% had BCLC stage B disease (Supplementary Tables S4–S5, *https://www.biosciencetrends.com/action/getSupplementalData.php?ID=310*).

Regarding surgical characteristics, 25.0% of patients underwent major hepatectomy, 37.8% underwent anatomic hepatectomy, and 20.2% underwent laparoscopic hepatectomy. The median surgical duration was 205 minutes (IQR, 165–255), and the median intraoperative blood loss was 200 mL (IQR, 100–400). Hepatic inflow occlusion was performed in 82.9% of patients, with a median occlusion time of 34 minutes (IQR, 20–46) among those with available data (Supplementary Table S5, *https://www.biosciencetrends.com/action/getSupplementalData.php?ID=310*).

During the index hospitalization, 55.5% of patients experienced at least one postoperative complication, whereas 7.4% developed severe complications (Clavien-Dindo grade ≥ III). The median Comprehensive

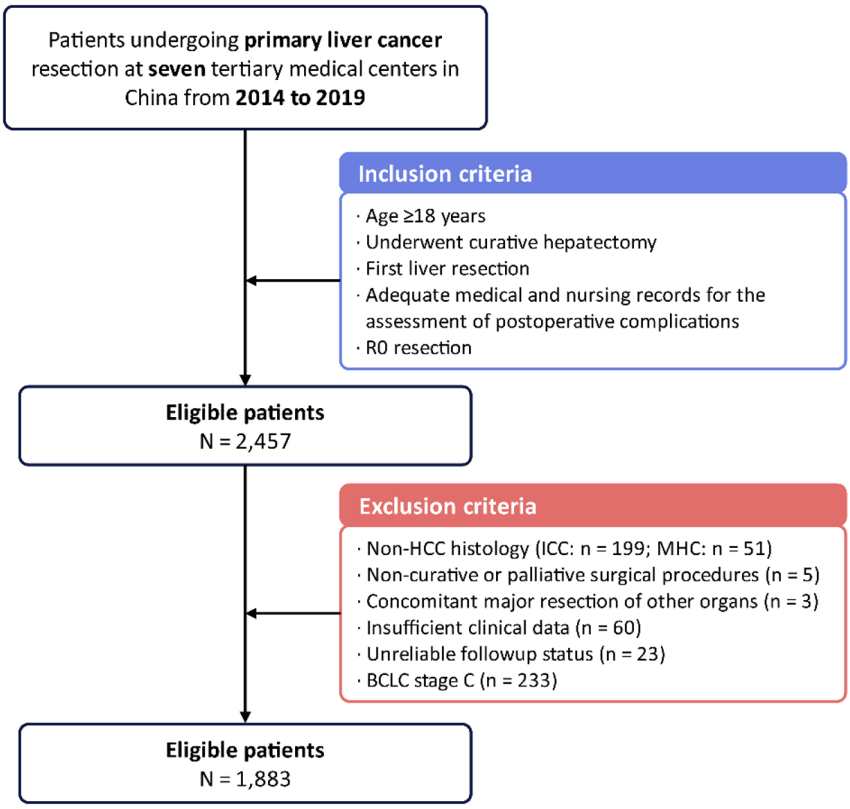


Figure 1. Patient selection and study design. Flowchart illustrates the inclusion and exclusion of patients undergoing primary liver cancer resection, resulting in the final study cohort.

Complication Index (CCI) was 8.7 (IQR, 0.0–17.4) (Table 1; Supplementary Figure S7, *https://www.biosciencetrends.com/action/getSupplementalData.php?ID=310*). Liver surgery-specific complications included bile leakage in 124 patients (6.6%), postoperative blood transfusion in 147 patients (7.8%), postoperative ascites in 48 patients (2.5%), PHLF in 46 patients (2.4%), and reoperation in 5 patients (0.3%). Cardiovascular complications included clinically significant arrhythmia in 120 patients (6.4%) and acute cardiac events in 45 patients (2.4%). Postoperative hemodynamic instability occurred in 126 patients (6.7%) and was recorded separately as an indicator of postoperative severity rather than as part of the cardiovascular complication composite. Thirty-day mortality occurred in 52 patients (2.8%), and 90-day mortality occurred in 118 patients (6.3%). The median length of hospital stay was 11 days (IQR, 8–16), with 505 patients (26.9%) classified as having prolonged hospitalization.

3.2. Postoperative complications and short-term clinical outcomes

Co-occurrence of postoperative complication domains was observed. At the domain level, 515 patients (27.3%) had one complication domain and 246 patients (13.1%) had two or more complication domains. Pairwise correlation analysis showed limited-to-moderate correlations among most postoperative complications, without evidence of strong collinearity across major domains (Supplementary Figure S5, *https://www.biosciencetrends.com/action/getSupplementalData.php?ID=310*). Therefore, subsequent PAF estimates were interpreted as domain-specific total burdens rather than mutually exclusive causal fractions. In multivariable analyses adjusting for demographic characteristics, comorbidities, liver function, tumor burden, and surgical factors (Model A), several postoperative complication domains were associated with adverse short-term outcomes. However, their relative contributions differed between 90-day mortality and prolonged hospitalization.

For 90-day mortality (Table 2; Supplementary Table S6, *https://www.biosciencetrends.com/action/getSupplementalData.php?ID=310*), liver surgery-specific complications accounted for the largest population-level burden (adjusted RR 1.61, 95% CI 1.08–2.40; adjusted PAF 10.0%, 95% CI 1.1–20.0). Cardiovascular complications were also strongly associated with 90-day mortality and represented the leading non-liver complication domain contributing to mortality at the population level (adjusted RR 2.21, 95% CI 1.40–3.50; adjusted PAF 9.4%, 95% CI 2.5–16.9). Renal complications (adjusted RR 3.00, 95% CI 1.51–5.94; adjusted PAF 4.0%, 95% CI 0.3–8.3) and pulmonary complications (adjusted RR 2.47, 95%

Table 1. Postoperative complications and adverse outcomes

Variables	No. (%)
Liver surgery-specific complications	
PHLF	46 (2.4%)
Bile leakage	124 (6.6%)
Postoperative ascites	48 (2.5%)
Postoperative blood transfusion	147 (7.8%)
Reoperation	5 (0.3%)
Cardiovascular complications	
Arrhythmia	120 (6.4%)
Acute cardiac events	45 (2.4%)
Pulmonary complications	63 (3.3%)
Renal complications	36 (1.9%)
Infection-related complications	
Incision infection	61 (3.2%)
Pulmonary infection	18 (1.0%)
Systemic infection	25 (1.3%)
Metabolic and electrolyte disorder	
Hypokalemia	7 (0.4%)
Hyperkalemia	51 (2.7%)
Hypoglycemia	278 (14.8%)
Hyperglycemia	30 (1.6%)
Gastrointestinal dysfunction	
Nausea and vomiting	93 (4.9%)
Diarrhea and constipation	20 (1.1%)
Indication of severity	
Escalation of care	22 (1.2%)
Postoperative hemodynamic instability	126 (6.7%)
Parenteral nutrition	3 (0.2%)
Mortality	
30-day	52 (2.8%)
90-day	118 (6.3%)
Hospitalization	
LOS (day)	11.0 [8.0, 16.0]
Prolonged hospital stay	505 (26.9%)
Clavien-Dindo grade	
0	838 (44.5%)
I	661 (35.1%)
II	245 (13.0%)
III	97 (5.2%)
IV	29 (1.5%)
V	13 (0.7%)
CCI	8.7 [0.0, 17.4]

Abbreviations: MASLD = Metabolic dysfunction-associated steatotic liver disease; PHLF = post-hepatectomy liver failure; CCI = Comprehensive complication index; LOS = Length of hospital stay.

CI 1.39–4.38; adjusted PAF 5.0%, 95% CI 0.2–10.1) were also associated with increased early mortality. In contrast, potassium imbalance, glucose dysregulation, and gastrointestinal dysfunction were not independently associated with 90-day mortality.

For prolonged hospitalization (Table 2; Supplementary Table S6, *https://www.biosciencetrends.com/action/getSupplementalData.php?ID=310*), liver surgery-specific complications had the greatest population-level impact (adjusted RR 1.65, 95% CI 1.41–1.93; adjusted PAF 11.0%, 95% CI 7.0–14.7). Among individual liver surgery-specific components, postoperative blood transfusion, postoperative ascites, and PHLF contributed meaningfully to prolonged length of stay. Several non-liver complications were also associated with prolonged hospitalization, including pulmonary complications (adjusted RR 2.29, 95% CI 1.88–2.78; adjusted PAF 4.8%, 95% CI 3.1–6.8), cardiovascular complications (adjusted RR 1.50, 95% CI 1.22–1.86; adjusted PAF 4.1%, 95% CI 1.5–6.7), renal complications (adjusted RR 1.78, 95% CI 1.29–2.46; adjusted PAF 1.9%, 95% CI 0.5–3.4), potassium imbalance (adjusted RR 2.22, 95% CI 1.80–2.75; adjusted PAF 4.3%, 95% CI 2.6–6.1), and glucose dysregulation (adjusted RR 1.26, 95% CI 1.04–1.53; adjusted PAF 4.5%, 95% CI 0.7–8.5).

Taken together, these findings indicate a divergence between hospitalization burden and mortality burden. This pattern was further illustrated in the population-level burden map (Figure 2), which integrated complication incidence, adjusted relative risk, and adjusted PAF for each complication domain. Liver surgery-specific complications showed the greatest population-level burden for prolonged hospitalization, whereas cardiovascular complications, despite a smaller contribution to prolonged length of stay, remained a major contributor to 90-day mortality.

3.3. Sensitivity analyses for short-term outcomes

Sensitivity analyses generally supported robustness of the main findings. For 90-day mortality, cardiovascular complications remained significantly associated with increased mortality across the tumor-burden-focused model, comorbidity-focused model, and surgery-focused model, with adjusted RRs ranging from 1.85 to 2.30 and adjusted PAFs ranging from 7.9% to 9.4%. Similar findings were observed after excluding patients with BCLC stage B disease, in whom cardiovascular complications remained associated with 90-day mortality, with an adjusted RR of 2.23 and an adjusted PAF of 8.7% (Supplementary Tables S7-S10, *https://www.biosciencetrends.com/action/getSupplementalData.php?ID=310*).

For prolonged hospitalization, liver surgery-specific complications consistently showed the greatest population-level burden across sensitivity analyses, with adjusted PAFs ranging from 10.9% to 12.2%. Cardiovascular complications were also consistently associated with prolonged hospitalization, but their adjusted PAFs were lower, ranging from 3.5% to 4.6% (Supplementary Tables S11-S14, *https://www.biosciencetrends.com/action/getSupplementalData.php?ID=310*).

3.4. Postoperative complications and long-term outcomes

The median follow-up duration, estimated using the reverse Kaplan–Meier method, was 36.4 months (IQR, 19.5–55.4 months). Recurrence-free survival analyses were conducted among 1,811 patients after exclusion of 72 individuals with missing recurrence data. During follow-up, 659 patients (35.0%) died, and 992 of 1,811 evaluable patients (54.8%) developed tumor

Table 2. Adjusted relative risks and population-attributable fractions of postoperative complications for 90-day mortality and prolonged length of stay

Variables	90-day mortality Relative Risk (95% CI)	90-day mortality Adjusted PAF (95% CI), %	P value	Prolonged LOS Relative Risk (95% CI)	Prolonged LOS Adjusted PAF (95% CI), %	P value
Liver surgery-specific complications	1.610 (1.082, 2.396)	10.0 (1.1, 20.0)	0.026	1.653 (1.413, 1.934)	11.0 (7.0, 14.7)	< 0.001
PHLF	2.341 (1.110, 4.938)	3.5 (-0.5, 7.8)	0.088	2.219 (1.766, 2.787)	3.5 (2.0, 5.1)	< 0.001
Bile leakage	1.578 (0.893, 2.788)	4.0 (-1.5, 10.2)	0.178	0.997 (0.754, 1.319)	-0.0 (-1.8, 2.0)	0.942
Postoperative ascites	1.737 (0.828, 3.646)	2.2 (-1.4, 6.2)	0.280	2.073 (1.664, 2.582)	3.6 (2.1, 5.3)	< 0.001
Postoperative blood transfusion	1.294 (0.759, 2.206)	2.6 (-3.1, 9.1)	0.414	1.730 (1.447, 2.067)	6.4 (3.8, 9.1)	< 0.001
Reoperation	2.472 (0.410, 14.917)	0.5 (-0.6, 2.3)	0.722	2.401 (1.493, 3.863)	0.5 (0.0, 1.1)	0.046
Other organs' complications						
Cardiovascular complications	2.209 (1.397, 3.495)	9.4 (2.5, 16.9)	0.008	1.504 (1.216, 1.860)	4.1 (1.5, 6.7)	< 0.001
Renal complications	2.998 (1.513, 5.940)	4.0 (0.3, 8.3)	0.030	1.780 (1.290, 2.456)	1.9 (0.5, 3.4)	0.010
Pulmonary complications	2.466 (1.389, 4.378)	5.0 (0.2, 10.1)	0.036	2.287 (1.883, 2.777)	4.8 (3.1, 6.8)	< 0.001
Infection-related complications						
Incision infection	1.609 (0.778, 3.329)	2.2 (-1.4, 6.8)	0.316	1.835 (1.440, 2.338)	2.9 (1.5, 4.6)	< 0.001
Pulmonary infection	3.236 (1.162, 9.013)	1.8 (-0.7, 4.9)	0.170	2.266 (1.652, 3.109)	1.3 (0.4, 2.5)	0.002
Systemic infection	1.726 (0.604, 4.934)	1.1 (-1.4, 4.2)	0.446	1.989 (1.306, 3.029)	1.3 (0.2, 2.4)	0.018
Metabolic and electrolyte disorder						
Potassium imbalance	0.736 (0.247, 2.189)	-1.0 (-3.5, 2.1)	0.492	2.223 (1.798, 2.748)	4.3 (2.6, 6.1)	< 0.001
Glucose dysregulation	1.196 (0.761, 1.881)	3.2 (-5.3, 12.0)	0.448	1.262 (1.044, 1.526)	4.5 (0.7, 8.5)	0.022
Gastrointestinal dysfunction	0.705 (0.292, 1.698)	-1.8 (-5.2, 2.6)	0.358	1.124 (0.838, 1.508)	0.7 (-1.2, 2.7)	0.492

Abbreviations: CI = Confidence Interval, PHLF = post hepatectomy liver failure. *Notes*: Models were adjusted for patient demographics (age, sex, BMI), comorbidities (diabetes, hypertension), liver disease severity (MELD score, cirrhosis), tumor burden (BCLC stage), and surgical characteristics (major resection, laparoscopic approach). Negative PAF estimates indicate no positive population-attributable burden under the fitted model and should not be interpreted as a protective effect.

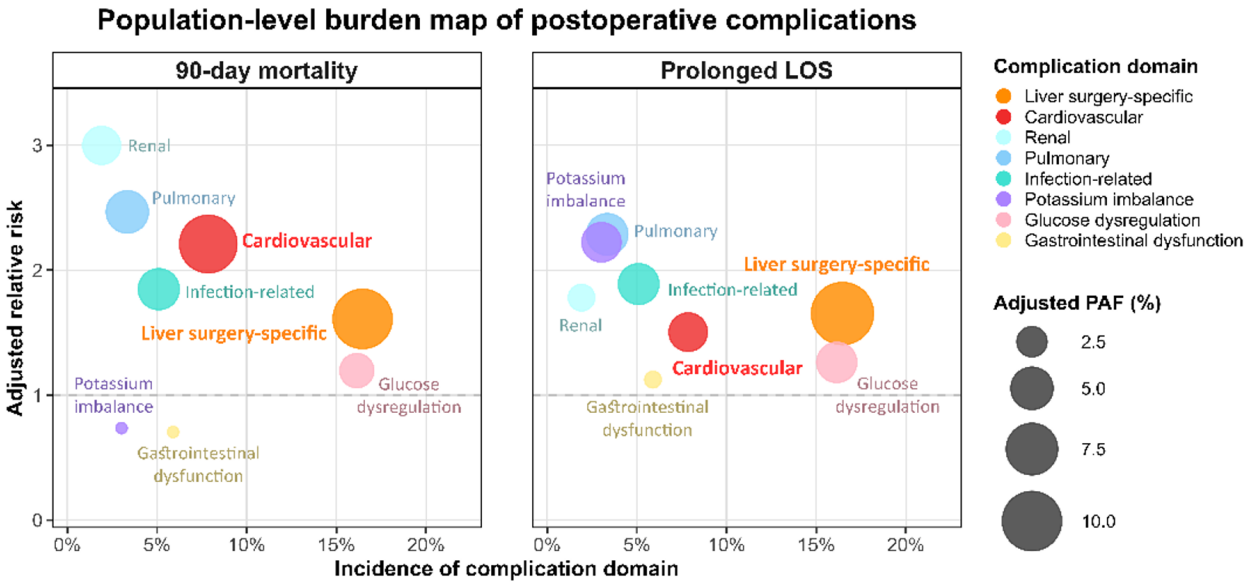


Figure 2. Population-level burden map of postoperative complications. Bubble plots showing the relationship between complication-domain incidence, adjusted relative risk, and adjusted population-attributable fraction (PAF) for 90-day mortality and prolonged length of stay. The x-axis represents the incidence of each complication domain, the y-axis represents adjusted relative risk, and bubble size represents adjusted PAF. Colors indicate complication domains. PAF estimates should be interpreted as domain-specific population-level burdens rather than mutually exclusive causal fractions.

recurrence. The 1-, 3-, and 5-year overall survival rates were 82.7%, 64.3%, and 45.5%, respectively, whereas the corresponding recurrence-free survival rates were 68.5%, 47.4%, and 38.3%. Kaplan–Meier curves stratified by BCLC stage are shown in Supplementary Figure S8 (*https://www.biosciencetrends.com/action/getSupplementalData.php?ID=310*).

Kaplan–Meier analyses demonstrated poorer overall survival among patients with postoperative complications, whereas recurrence-free survival showed less pronounced separation between complication groups (Figure 3). In multivariable Cox models, several postoperative complication domains were independently associated with reduced overall survival, but no complication domain was independently associated with recurrence after adjustment (Figure 4; Supplementary Tables S15–S18, *https://www.biosciencetrends.com/action/getSupplementalData.php?ID=310*).

Specifically, pulmonary complications (adjusted HR 1.83, 95% CI 1.30–2.56), cardiovascular complications (adjusted HR 1.59, 95% CI 1.24–2.03), renal complications (adjusted HR 1.67, 95% CI 1.06–2.63), and glucose dysregulation (adjusted HR 1.34, 95% CI 1.09–1.65) were independently associated with worse overall survival. In contrast, no complication domain was independently associated with recurrence-free survival after adjustment.

4. Discussion

In this multicentre study of patients undergoing curative-intent hepatectomy for HCC, we applied a population-attributable fraction (PAF) framework to evaluate population-level impact of postoperative complications. The principal finding was a divergence between hospitalization burden and mortality burden. Liver surgery-specific complications contributed the greatest population-level burden of prolonged hospitalization, and also accounted for the largest PAF for 90-day mortality. However, cardiovascular complications represented the leading non-liver complication domain for 90-day mortality and remained strongly associated with worse long-term overall survival, despite contributing less to prolonged length of stay. No complication domain was independently associated with recurrence after adjustment. These findings suggest that postoperative complications may influence prognosis through distinct pathways, with liver surgery-specific complications mainly driving recovery burden, whereas cardiovascular complications may represent an underrecognized contributor to mortality risk.

Postoperative morbidity after hepatectomy has traditionally been evaluated using complication incidence, Clavien–Dindo grade, or individual relative risks. While these measures are clinically useful, they do not fully capture the population-level impact of different complication domains. A complication with a high relative risk but low incidence may contribute less to overall outcome burden than a more common complication with a moderate relative risk (*15*). The PAF framework provides a complementary perspective by integrating exposure frequency and relative risk, thereby helping prioritize complications according to their expected contribution to adverse outcomes at the

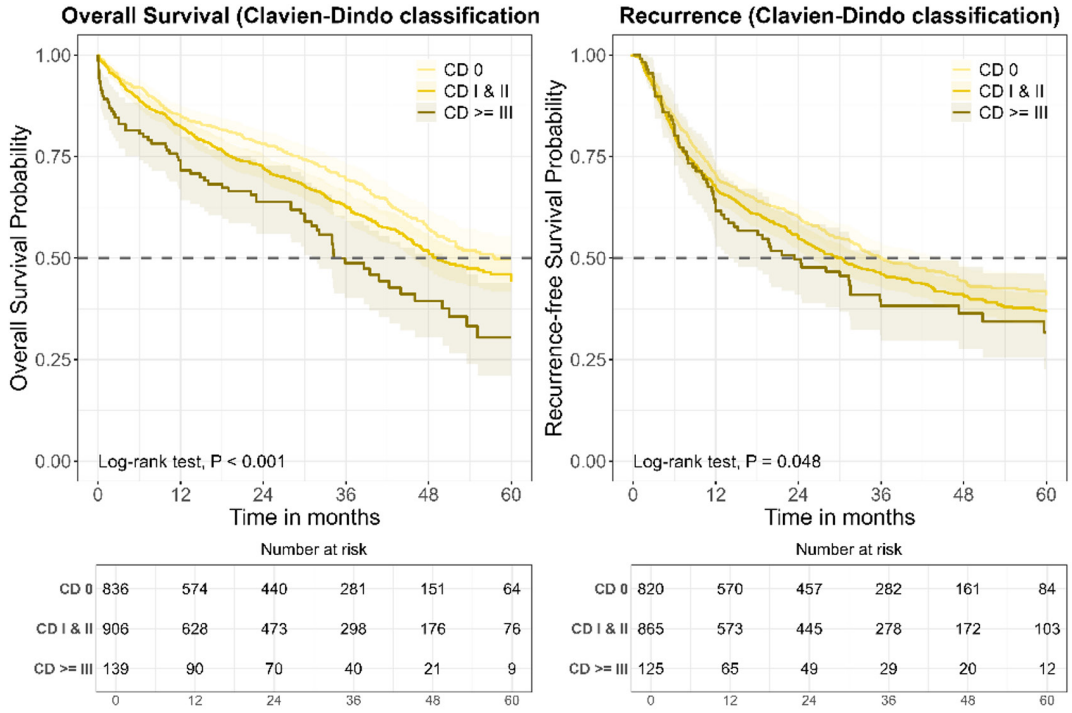


Figure 3. Overall survival and recurrence according to Clavien-Dindo classification. Kaplan-Meier curves showing overall survival (left panel) and recurrence-free survival probability (right panel) stratified by Clavien-Dindo post-operation complication classification (no complication, mild complication, and severe complication). Shaded areas represent 95% confidence intervals. The dashed horizontal line indicates the 50% probability level. Numbers at risk are shown below each plot. Differences between groups were assessed using the log-rank test.

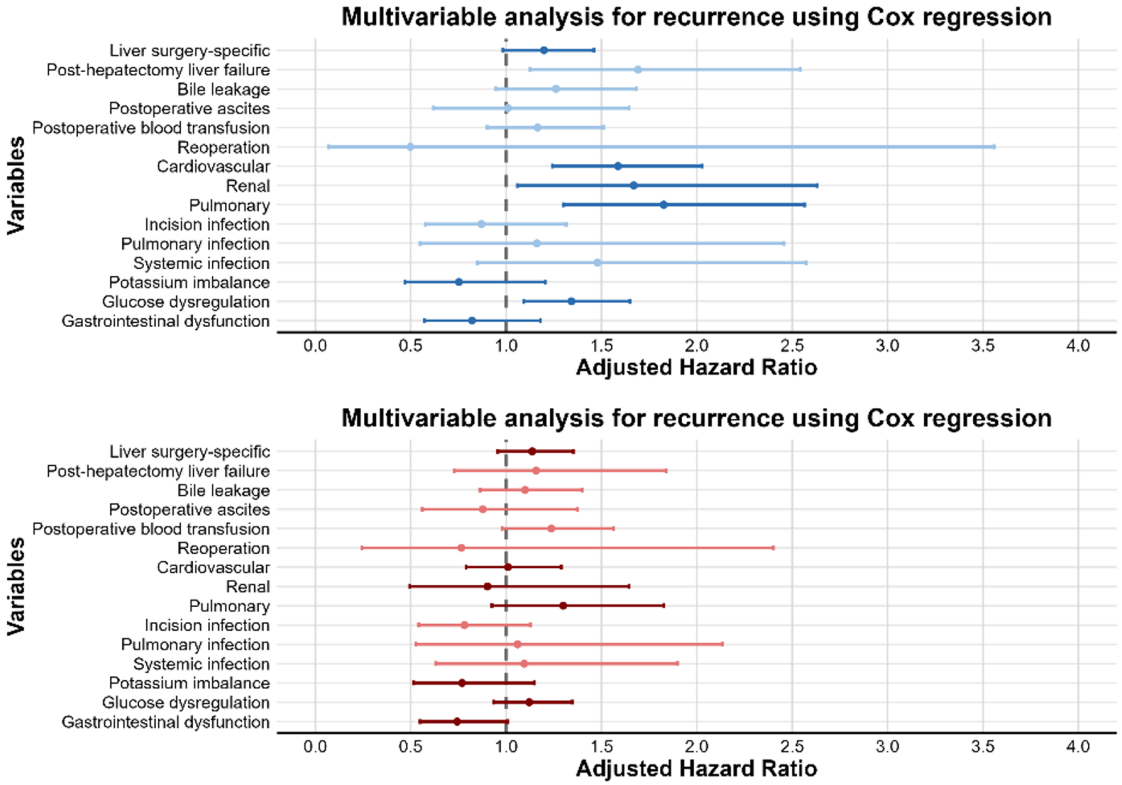


Figure 4. Adjusted associations between postoperative complications and long-term outcomes. Multivariable Cox regression analyses of postoperative complications in relation to overall survival (upper panel, blue) and recurrence (lower panel, red). Adjusted hazard ratios (HRs) with 95% confidence intervals (CIs) are shown. The vertical dashed line indicates an HR of 1.0. All models were adjusted for predefined clinically relevant covariates to minimize confounding. Based on prior literature and clinical relevance, models were adjusted for patient demographics (age, sex, body mass index), comorbidities (diabetes, hypertension), liver disease severity (MELD score and presence of cirrhosis), tumor burden (BCLC stage), and surgical characteristics (major resection and laparoscopic approach).

population level (*16-18*). In this study, this approach revealed that the apparent importance of complication domains depended on the outcome being considered: liver surgery-specific complications dominated prolonged hospitalization, whereas cardiovascular complications carried a substantial mortality burden despite a smaller impact on hospital stay.

This distinction has important clinical implications. Liver surgery-specific complications, such as PHLF, bile leakage, postoperative ascites, blood transfusion, and reoperation, are highly visible to hepatobiliary surgeons because they often require direct procedural, interventional, or liver-focused management and substantially prolong hospitalization (*19-21*). In contrast, cardiovascular complications may be less prominent in routine surgical outcome assessment if postoperative morbidity is judged mainly by length of stay or liver-specific adverse events (*22,23*). Nevertheless, our findings indicate that cardiovascular complications were the leading non-liver contributor to 90-day mortality and were independently associated with worse overall survival. This suggests a potential mismatch between clinical visibility and prognostic relevance: complications that most prolong hospital stay may not fully capture those most relevant to mortality risk.

The association between cardiovascular complications and mortality is biologically plausible, but should be interpreted within a broader perioperative vulnerability framework. Hepatectomy exposes patients to substantial physiological stress, including hemodynamic shifts, blood loss, fluid redistribution, inflammatory activation, sympathetic stimulation, and metabolic disturbance (*24-26*). In patients with limited cardiometabolic reserve, these stressors may precipitate clinically significant arrhythmia or acute cardiac events. Importantly, postoperative complications may not occur as isolated events. Some cardiovascular complications may develop secondary to other severe postoperative insults or share upstream causes such as bleeding, infection, liver dysfunction, inflammation, or systemic physiological stress (*27*). Therefore, the present findings should not be interpreted as proving a direct causal pathway from cardiovascular complications to mortality. Rather, cardiovascular complications may serve as clinically observable warning signals of systemic vulnerability and adverse postoperative trajectory.

This interpretation is clinically relevant because attention and resource allocation in surgical practice often follow complications that visibly require direct procedure-related management. In high-volume and highly specialized hepatobiliary centers, postoperative pathways are frequently oriented toward surgical recovery and bed turnover. Under such conditions, non-liver complications may be less visible within liver surgery-centered outcome assessment, even when they carry important prognostic implications. Our findings suggest that cardiovascular complications, despite contributing less to hospitalization burden than liver surgery-specific complications, identify a subgroup of patients with increased early mortality risk and worse long-term survival. The discordance between overall survival and recurrence-free survival is also informative. Absence of an independent association with recurrence-free survival further suggests that the long-term impact of postoperative complications may be driven more by systemic recovery and non-oncologic survival pathways than by tumor recurrence (*30*).

Our findings also support a broader shift from a purely technical liver surgery framework toward an integrated perioperative medicine framework. Modern hepatectomy outcomes are not determined solely by operative technique or liver-specific injury. They also reflect systemic vulnerability, including cardiometabolic reserve, renal function, pulmonary reserve, and the capacity to tolerate surgical stress (*28,29*). This is particularly relevant as the surgical population ages and the burden of metabolic and cardiovascular comorbidities increases. From this perspective, cardiovascular complications should not be viewed as peripheral events after hepatectomy, but as part of the systemic risk profile that shapes early mortality and long-term survival. Multidisciplinary perioperative pathways incorporating cardiovascular evaluation, intraoperative hemodynamic optimization, postoperative monitoring, and early recognition of cardiac events may therefore complement conventional liver-focused strategies.

Several strengths of this study deserve emphasis. First, this was a large multicentre cohort with detailed perioperative data and clinically meaningful short- and long-term endpoints. Second, complications were categorized using a predefined organ-system framework, allowing comparison of liver surgery-specific and non-liver complications within a unified analytic structure. Third, multiple imputations, robust regression models, bootstrap-based PAF estimation, and several sensitivity analyses were used to examine stability of the findings. The main results were generally consistent across tumor-burden-focused, comorbidity-focused, and surgery-focused adjustment strategies, as well as after excluding patients with BCLC stage B disease.

This study also has limitations. First, its retrospective design may introduce misclassification and residual confounding, although complications were adjudicated using predefined criteria and medical and nursing records. Second, organ-system grouping inevitably involves clinical judgment, and complications within the same domain may differ in severity, mechanism, and preventability. We, therefore, interpreted composite complication domains as indicators of system-level morbidity rather than as homogeneous biological entities. Third, PAF estimates rely on model-based counterfactual assumptions and should not be interpreted as proof that the corresponding complication could be fully eliminated in clinical practice. Instead, PAF was

used to compare relative population-level burden and to inform prioritization. Fourth, temporal relationships among postoperative complications could not be fully disentangled. Some complications may occur sequentially or share upstream causes, and future studies incorporating time-dependent or causal pathway analyses may further clarify these mechanisms. Finally, the cohort was derived from mainland China and was dominated by HBV-related HCC, so external validation in more diverse etiologic and healthcare settings is warranted.

In conclusion, this multicentre study shows that postoperative complications after hepatectomy exert distinct population-level effects on recovery and survival. Liver surgery-specific complications dominated prolonged hospitalization, but cardiovascular complications, despite being less prominent as drivers of hospital stay, emerged as the leading non-liver contributor to 90-day mortality and were independently associated with worse overall survival. These findings expose a blind spot in conventional liver surgery outcome assessment: complications that most visibly delay discharge are not necessarily those that carry greatest mortality relevance. Perioperative care after hepatectomy should therefore move beyond a liver-centric complication framework and incorporate systematic cardiovascular risk assessment and monitoring into routine surgical pathways for HCC.

Acknowledgements

The authors thank all participating centers, clinicians, and research staff for their contributions to data collection, clinical coordination, and patient care throughout this multicentre study.

Funding: This study was supported by grants from the Natural Science Foundation of Sichuan Province (2024NSFSC0637), the National Natural Science Foundation of China (82572143/82100650), and the National Key R&D Program of China (2022YFC2503701). The funding agency was not involved in the study design, data collection, analysis and interpretation, or writing of the manuscript and the decision to submit it for publication.

Conflict of Interest: The authors have no conflicts of interest to disclose.

Data Availability Statement: Datasets generated during and/or analyzed during the current study are not publicly available due to patient privacy and institutional restrictions, but are available from the corresponding author on reasonable request.

References

1. Zhou J, Sun H, Wang Z, *et al*. China Liver Cancer Guidelines for the Diagnosis and Treatment of Hepatocellular Carcinoma (2024 Edition). Liver Cancer. 2025; 14:779-835.
2. Kong J, Li G, Chai J, Yu G, Liu Y, Liu J. Impact of Postoperative Complications on Long-Term Survival After Resection of Hepatocellular Carcinoma: A Systematic Review and Meta-Analysis. Ann Surg Oncol. 2021; 28:8221-8233.
3. Kabir T, Syn NL, Tan ZZX, *et al*. Predictors of post-operative complications after surgical resection of hepatocellular carcinoma and their prognostic effects on outcome and survival: A propensity-score matched and structural equation modelling study. Eur J Surg Oncol. 2020; 46:1756-1765.
4. Famularo S, Russolillo N, Donadon M, *et al*. Benchmarking postoperative outcomes after open liver surgery for cirrhotic patients with hepatocellular carcinoma in a national cohort. HPB (Oxford). 2022; 24:1365-1375.
5. Zhu S, Gu LH, Shen Y, *et al*. Clinical features, risk factors, outcomes, and prediction model for intrahepatic and perihepatic abscess following hepatectomy for hepatocellular carcinoma. HPB (Oxford). 2025; 27:352-361.
6. Rajakannu M, Cherqui D, Cunha AS, Castaing D, Adam R, Vibert E. Predictive nomograms for postoperative 90-day morbidity and mortality in patients undergoing liver resection for various hepatobiliary diseases. Surgery. 2023; 173:993-1000.
7. Yang T, Liu K, Liu CF, *et al*. Impact of postoperative infective complications on long-term survival after liver resection for hepatocellular carcinoma. Br J Surg. 2019; 106:1228-1236.
8. Northridge ME. Public health methods--attributable risk as a link between causality and public health action. Am J Public Health. 1995; 85:1202-1204.
9. van Hootegem SJM, van der Linde M, Schneider MA, *et al*. Impact of postoperative complications on clinical outcomes after gastrectomy for cancer: multicentre study. Br J Surg. 2025; 112.
10. Clavien PA, Barkun J, de Oliveira ML, *et al*. The Clavien-Dindo classification of surgical complications: five-year experience. Ann Surg. 2009; 250:187-196.
11. Slankamenac K, Graf R, Barkun J, Puhan MA, Clavien PA. The comprehensive complication index: a novel continuous scale to measure surgical morbidity. Ann Surg. 2013; 258:1-7.
12. Rahbari NN, Garden OJ, Padbury R, *et al*. Posthepatectomy liver failure: a definition and grading by the International Study Group of Liver Surgery (ISGLS). Surgery. 2011; 149:713-724.
13. Koch M, Garden OJ, Padbury R, *et al*. Bile leakage after hepatobiliary and pancreatic surgery: a definition and grading of severity by the International Study Group of Liver Surgery. Surgery. 2011; 149:680-688.
14. Sterne JA, White IR, Carlin JB, Spratt M, Royston P, Kenward MG, Wood AM, Carpenter JR. Multiple imputations for missing data in epidemiological and clinical research: potential and pitfalls. Bmj. 2009; 338:b2393.
15. Görgec B, Benedetti Cacciaguerra A, Lanari J, *et al*. Assessment of Textbook Outcome in Laparoscopic and Open Liver Surgery. JAMA Surg. 2021; 156:e212064.
16. Goense L, Meziani J, Ruurda JP, van Hillegersberg R. Impact of postoperative complications on outcomes after oesophagectomy for cancer. Br J Surg. 2019; 106:111-119.
17. Crnovrsanin N, Giring S, Oppel A, Rompen IF, Schiefer S,

Jorek N, Schmidt T, Müller-Stich BP, Sisic L, Nienhüser H. Effects of postoperative complications in oesophageal cancer on survival, hospital outcomes, and long-term quality of life: retrospective cohort study. BJS Open. 2025; 9.
18. Smits FJ, Verweij ME, Daamen LA, *et al*. Impact of Complications After Pancreatoduodenectomy on Mortality, Organ Failure, Hospital Stay, and Readmission: Analysis of a Nationwide Audit. Ann Surg. 2022; 275:e222-e228.
19. Sellers D, Srinivas C, Djaiani G. Cardiovascular complications after non-cardiac surgery. Anaesthesia. 2018; 73 Suppl 1:34-42.
20. Wilcox T, Smilowitz NR, Xia Y, Beckman JA, Berger JS. Cardiovascular Risk Factors and Perioperative Myocardial Infarction After Noncardiac Surgery. Can J Cardiol. 2021; 37:224-231.
21. Lyu Z, Ji Y, Ji Y. Association between stress hyperglycemia ratio and postoperative major adverse cardiovascular and cerebrovascular events in noncardiac surgeries: a large perioperative cohort study. Cardiovasc Diabetol. 2024; 23:392.
22. Zhao BC, Lei SH, Zhuang PP, Yang X, Feng WJ, Qiu SD, Yang H, Liu KX. Preoperative N-terminal Pro-B-type Natriuretic Peptide and High-sensitivity Cardiac Troponin T and Outcomes after Major Noncardiac Surgery: A Prospective Cohort Study. Anesthesiology. 2024; 141:475-488.
23. Duceppe E, Parlow J, MacDonald P, Lyons K, McMullen M, Srinathan S, Graham M, Tandon V, Styles K, Bessissow A, Sessler DI, Bryson G, Devereaux PJ. Canadian Cardiovascular Society Guidelines on Perioperative Cardiac Risk Assessment and Management for Patients Who Undergo Noncardiac Surgery. Can J Cardiol. 2017; 33:17-32.
24. Yoshikawa T, Nomi T, Hokuto D, Yasuda S, Kawaguchi C, Yamada T, Kanehiro H, Nakajima Y. Risk Factors for Postoperative Ascites in Patients Undergoing Liver Resection for Hepatocellular Carcinoma. World J Surg. 2017; 41:2095-2100.
25. Shen Y, Hu YL, Xu JH, *et al*. Incidence, risk factors, outcomes, and prediction model of surgical site infection after hepatectomy for hepatocellular carcinoma: A multicenter cohort study. Eur J Surg Oncol. 2025; 51:109486.
26. Huang H, Zhou P, Li J, Luo H, Yu L. Enhanced recovery after surgery in primary liver cancer patients undergoing hepatectomy: experience from a large tertiary hospital in China. BMC Surg. 2023; 23:185.
27. Society for Hepato-pancreato-biliary Surgery of Chinese Research Hospital A, Editorial Board of Chinese Journal of Digestive S, Yang S, Zeng Y, Chen M, Dong J. Expert consensus on perioperative assessment of hepatic reserve function (2025 edition). Chinese Journal of Digestive Surgery. 2025; 24:1383-1396.
28. Puelacher C, Lurati Buse G, Seeberger D, *et al*. Perioperative Myocardial Injury After Noncardiac Surgery: Incidence, Mortality, and Characterization. Circulation. 2018; 137:1221-1232.
29. Glance LG, Joynt Maddox KE, Cavanaugh S, Knight PA, Mazzeffi M, Shang J, Stone PW, Lustik SJ, Panda K, Kreso M, Pyne S, Dick AW. Association of the cardiovascular-kidney-metabolic syndrome and adverse outcomes after noncardiac surgery. Br J Anaesth. 2026; 136:507-515.
30. Fuster-Anglada C, Mauro E, Ferrer-Fàbrega J, Caballol B, Sanduzzi-Zamparelli M, Bruix J, Fuster J, Reig M, Díaz A, Forner A. Histological predictors of aggressive recurrence of hepatocellular carcinoma after liver resection. J Hepatol. 2024; 81:995-1004.

Received May 20, 2026; Revised July 10, 2026; Accepted July 24, 2026.

[§]These authors contributed equally to this work.
**Address correspondence to:*
Chuan Li, Division of Liver Surgery, Department of General Surgery, West China Hospital, Sichuan University, Chengdu, Sichuan, China.
E-mail: lichuan@scu.edu.cn

Released online in J-STAGE as advance publication July 31, 2026.

Brief Report

DOI: 10.5582/bst.2026.01083

Gene expression profiling of the L4-stage nematode *Caenorhabditis elegans* following ethanol exposure

Masaki Miyazawa[1,2], Ching Ouyang[3], Mariko Sezaki[1], Kayo Yasuda[2], Naoaki Ishii[2], Yoko Fujita-Yamaguchi[1,4,*]

[1] Department of Applied Biochemistry, Tokai University School of Engineering, Hiratsuka, Kanagawa, Japan;
[2] Department of Health Management, School of Health Studies, Tokai University, Hiratsuka, Kanagawa, Japan;
[3] Integrative Genomics Core, City of Hope Comprehensive Cancer Center, Duarte, CA, USA;
[4] Arthur Riggs Diabetes & Metabolism Research Institute, Beckman Research Institute of City of Hope, Duarte, CA, USA.

SUMMARY: Previous studies have suggested that low to moderate alcohol exposure can extend *Caenorhabditis elegans* (*C. elegans*) lifespan, but early molecular mechanisms linking ethanol exposure to longevity have not been fully characterized. Here, we investigated how ethanol treatment affects transcriptional networks in L4-stage *C. elegans* by time-resolved RNA-seq. L4-stage *C. elegans* were exposed to 5% ethanol and time-resolved RNA-seq was performed after 1, 4, and 20 hours in solution cultures, followed by differential gene expression and KEGG pathway-based Gene Set Enrichment Analysis. At 1 hour, GSEA analysis showed significant enrichment of genes in the Longevity regulating pathway (worm) with elevated expression. Core-enrichment genes exhibited coordinated upregulation of redox-defense modules, including glutathione S-transferases (*gst*) and p38 MAPK components (*pmk-2/pmk-3*), consistent with upregulation of SKN-1/Nrf2-related stress-response genes. Detoxification (*gpx* and *fmo* families) and lipid-remodeling genes were enriched at 1 hour. By 4 hours, *sod-3*, a canonical DAF-16/FOXO target, was clearly upregulated, suggesting engagement of DAF-16-associated antioxidant responses, whereas Peroxisome and TGF-β signaling pathways were significantly downregulated. Together, these findings provide transcriptomic insights into a temporally structured longevity-associated response to ethanol exposure, in which early detoxification and antioxidant programs, together with membrane-lipid remodeling, are followed by DAF-16-associated gene induction and repression of peroxisome- and development-related signaling. These pathway-level changes highlight candidate biological processes potentially associated with ethanol-linked lifespan modulation in *C. elegans*.

Keywords: *Caenorhabditis elegans*, ethanol exposure, gene expression, signaling pathways, metabolic homeostasis

1. Introduction

The nematode *C. elegans* has long been a powerful model organism for investigating conserved biological processes across species, owing to its highly preserved functional pathways and ease of experimentation. Approximately 40% of *C. elegans* genes have human orthologs, making it an invaluable system for studying mechanisms relevant to human health, including aging (*1-4*).

Research on aging in *C. elegans* has provided significant insights into the molecular pathways that govern lifespan. Key mechanisms identified include the insulin/insulin-like growth factor 1 (IGF-1) signaling (IIS) pathway, TOR signaling, mitochondrial function, and oxidative stress responses. Among these, the IIS pathway has been extensively studied for its conserved role in lifespan regulation. In *C. elegans*, activation of DAF-2, the insulin/IGF-1 receptor, negatively regulates the FOXO transcription factor DAF-16, thereby modulating gene expression related to stress resistance, metabolism, and longevity (*5,6*). Mutations in *daf-2* or its downstream effectors extend lifespan, underscoring the central role of this pathway in aging.

Similarly, mitochondrial function and oxidative stress have emerged as critical determinants of aging. For example, the *mev-1* mutant, which harbors a defect in mitochondrial complex II, produces excessive reactive oxygen species (ROS) and exhibits a markedly shortened lifespan (*7*). Likewise, mutations in genes encoding antioxidant enzymes, such as superoxide dismutase (SOD), exacerbate oxidative damage and reduce longevity (*7*). These foundational findings emphasize the importance of balancing ROS production and antioxidant defense mechanisms to promote cellular health and longevity.

Alcohol consumption presents a complex relationship

with human health, demonstrating both beneficial and detrimental effects. Moderate alcohol intake has been associated with a reduced risk of cardiovascular diseases (*8*) and type 2 diabetes (*9*). In contrast, chronic or excessive alcohol consumption is linked to an increased risk of liver damage, cancer, and neurodegenerative disorders (*10*). At the molecular level, alcohol can influence gene expression, epigenetic landscapes, and metabolic pathways, with effects that may either support health or contribute to disease progression.

C. elegans serves as a useful system for examining the effects of alcohol exposure in a controlled environment. Previous studies have shown that ethanol's impact on lifespan depends on its concentration. Low ethanol concentrations, ranging from 0.005% (1 mM) to 2%, have generally been linked to lifespan extension (*11-13*), whereas higher concentrations (3–5% or ≥ 4%) tend to reduce lifespan (*11,13*). Furthermore, developmental timing plays a crucial role, with varying effects observed when ethanol is administered at the L1 larval stage, during embryonic development, or in young adults.

In our earlier studies, we investigated the effects of ethanol exposure on *C. elegans* lifespan by treating L4-stage worms with 5% ethanol, a concentration modestly higher than that used in most prior reports. Under these conditions, we observed a reproducible, statistically significant extension of lifespan. At that time, mechanistic analyses relied on classical candidate-gene approaches (*e.g.*, RT-PCR and lifespan measurements in selected mutant strains) and were therefore limited in scope, precluding definitive conclusions. Building on this long-standing experimental framework, the present study re-examined the 5% ethanol response using time-resolved RNA-seq to obtain transcriptomic and pathway-level insights into ethanol-associated longevity responses in *C. elegans*.

2. Materials and Methods

2.1. Culture and maintenance of *C. elegans* strains

The wild-type *C. elegans* used throughout this study was the N2 strain obtained from the Caenorhabditis Genetics Center (University of Minnesota). *C. elegans* worms were cultured and maintained as previously described (*7*). All experiments were conducted at 20–22°C unless otherwise stated. *C. elegans* were maintained on nematode growth medium (NGM) agar plates (9 cm) covered with *Escherichia coli* (*E. coli*) OP50 cells as a food source. To obtain synchronized *C. elegans* cultures, reproductive adults bearing eggs were collected by washing with S-buffer (50 mM potassium phosphate buffer, pH 6.0, containing 0.1M NaCl) into 15 mL tubes. After allowing worms to settle for 5 min, the supernatant was aspirated, and the collected worms were suspended in 4.5 mL of S-buffer to which 0.5 mL of 5% sodium hypochlorite and 0.1 mL of 10N NaOH were added and vigorously mixed. After confirming that the worms were dissolved under a stereo microscope, eggs were collected and washed three times with 10 mL of S-buffer by centrifugation at 1300 × g for 30 sec. Collected eggs were then suspended in 3-4 mL of S-buffer in 15 mL tubes and incubated flat at 20°C overnight to allow fertilization of eggs. L1-stage worms were precipitated by centrifugation at 1,300 × g for 30 sec., resuspended in 2-3 mL of S-buffer, and subjected to counting. Approximately 1,500 of them were plated on NGM agar plates (9 cm) covered with *E. coli* OP50 cells (Day 1).

2.2. Administration of Ethanol for Lifespan Experiment

Experimental methods are summarized in Figure 1A. On Day 3, *C. elegans* worms were treated with 200 µL of 1.25 mg/mL fluorodeoxyuridine (FUdR) per 9 cm petri dish to inhibit reproduction by blocking embryo development with FUdR. On Day 4, ten 4-day-old worms were carefully placed on NGM agar covered with *E. coli* OP50 cells in 3 cm petri dishes. A total of ten dishes (100 worms) were used per lifespan experiment. Prior to transferring worms, 180 µL of either 5% ethanol containing 1.25 mg/mL FUdR for ethanol treatments or 180 µL of S-buffer containing 1.25 mg/mL FUdR for controls was added to each dish, and the worms were then transferred into this liquid. The effects of chronic ethanol exposure on *C. elegans* longevity were determined by recording the day each worm died. Worms were classified as dead when they no longer responded to touch with a platinum wire pick. The effects of ethanol on *C. elegans* lifespan were quantified as the ratio of the mean ± SEM of the 50% survival day for ethanol-treated worms to the mean ± SEM of the 50% survival day for control worms. Statistical comparisons between ethanol-treated and control groups were performed using an unpaired Student's *t*-test.

2.3. Total RNA isolation

On Day 3, *C. elegans* worms were exposed to ethanol concentrations of 0% or 5% in S-buffer for 1, 4, or 20 hours at 20°C. Approximately 1,500 *C. elegans* worms at the L4 larval stage that had been cultured on agar plates covered with *E. coli* OP50 cells were harvested by washing the plates with S-buffer, followed by centrifugation. The collected worms were washed with S-buffer to remove residual bacteria. After washing thoroughly, the worms were resuspended in 1 mL of S-buffer and exposed to either 0% or 5% ethanol for 1, 4, or 20 hours at 20°C. After treatment, worms were collected for RNA extraction using TRI Reagent® (Molecular Research Center, Inc., OH, USA), according to the manufacturer's protocol. Collected worms were homogenized in 0.5 mL of TRI Reagent® using a plastic homogenizer. After homogenization, 50 µL of 1-bromo-3-chloropropane (Molecular Research Center, Inc., OH,

USA) was added to each sample, followed by vigorous shaking for 15 seconds. Samples were incubated at room temperature for 15 minutes and centrifuged at 12,000 × g for 15 minutes at 4°C. The RNA-containing aqueous layer was transferred to a new tube and precipitated with 0.5 mL of isopropanol (FUJIFILM Wako Pure Chemical Corporation, Osaka, Japan), incubated for 30 minutes at room temperature, followed by centrifugation at 12,000 × g for 10 minutes at 4°C. The resulting RNA pellet was washed with 75% ethanol, air-dried, and dissolved in RNase-free water (Ambion, TX, USA).

2.4. RNA-seq analysis

RNA quality and quantity were assessed using the Bioanalyzer System (Agilent Technologies, Inc., CA, USA). Sample pairs that passed the RNA Integrity Number (RIN) evaluation were selected for sequencing library preparation using the KAPA mRNA HyperPrep Kit (Roche, MA, USA). Sequencing was performed on the Illumina NovaSeq 6000 using the S4 Reagent Kit v1.5 (Illumina, CA, USA) in paired-end mode of 2×151 cycles, with the base calling conducted using Real-time Analysis (RTA) software v3.4.4.

For RNA-seq data analysis, sequence reads passing quality check were preprocessed for adaptor and polyA removal using trimmomatic v.0.39 (*14*) and fastp v.0.23.2 (*15*). Reads were then mapped to the *C. elegans* reference genome ce10 using STAR v.2.7.9a (*16*), with an index for gene and transcript annotations. Strand-specific paired-end fragment counts of each gene annotated in RefGene were calculated using the featureCounts function in the Subread package v.2.0.3 (*17*). To enhance accuracy of the gene expression estimates, a total of 15,060 genes with counts per million (CPM) > 1 in at least three samples were selected for downstream analysis. The Bioconductor package edgeR v.3.32.1 (*18*) was applied with a design matrix for testing differential expression between sample groups with different conditions based on quasi-likelihood F-tests. Statistical p-values were adjusted using the Benjamini and Hochberg method. Pre-ranked Gene Set Enrichment Analysis (GSEA) (*19*) was conducted for functional enrichment analysis with gene sets obtained from the Kyoto Encyclopedia of Genes and Genomes (KEGG) (*20*). Genes from edgeR results were ranked by the sign of log fold-change (logFC) in combination with $-\log_{10}$ of the p-value for this analysis. GSEA results were visualized using R (v4.4.1) with clusterProfiler v4.12.6 and enrichplot v1.24.4 packages (*21*).

3. Results and Discussion

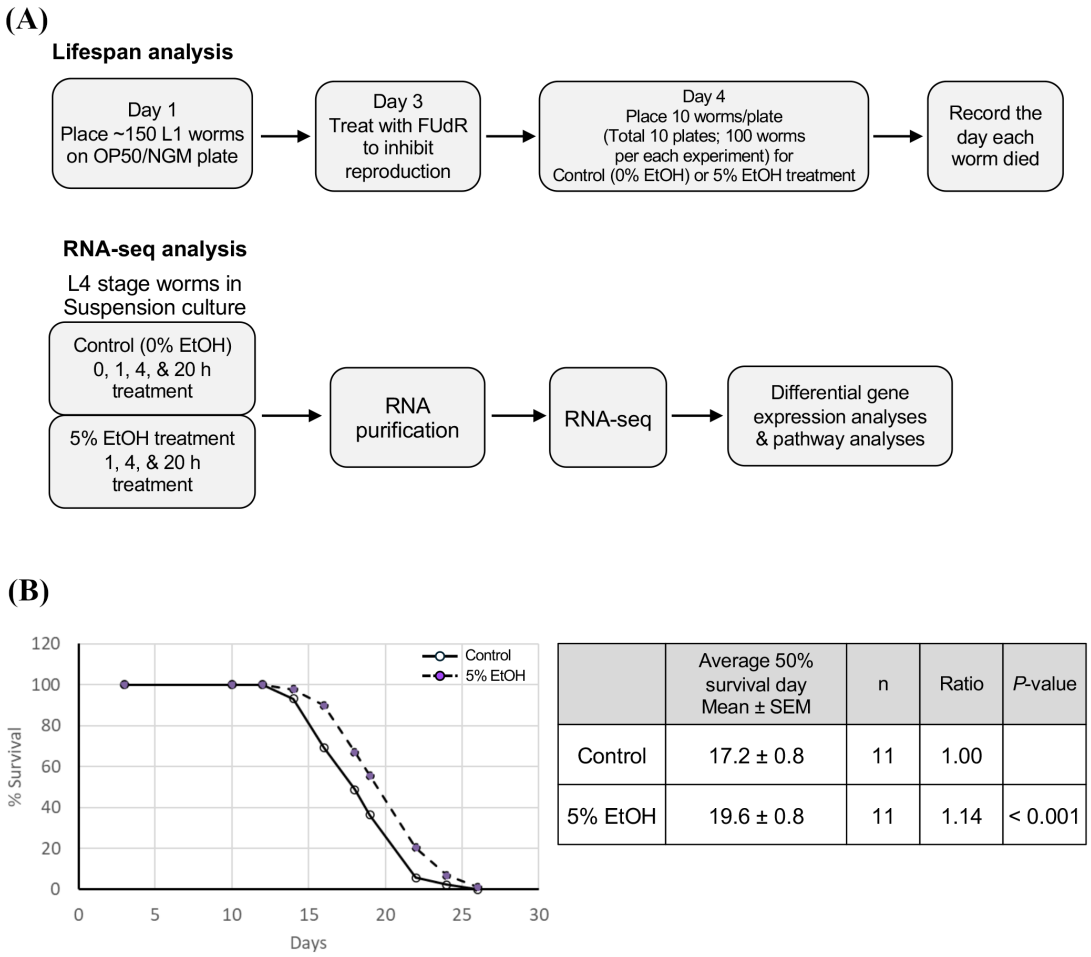
3.1. Observed lifespan extension following 5% ethanol exposure

Figure 1A shows experimental schemes for the lifespan as well as RNA-seq analyses. Lifespan experiments revealed that 5% ethanol treatment extended the lifespan compared with controls as shown in Figure 1B, which presents a representative result showing lifespan extension in 4-day-old wild-type *C. elegans* treated with 5% ethanol. The mean 50% survival day was 17.2 ± 0.8 and 19.6 ± 0.8 (means ± SEM, $n = 11$, $p < 0.001$) for control and ethanol-treated worms, respectively, indicating a 1.14-fold increase in lifespan in response to ethanol treatment (Figure 1B). To minimize food limitation during the lifespan assay, *E. coli* OP50 was allowed to grow to a non-limiting density before the assay. The protocol was also designed so that the ethanol solution covered the worms on the agar for at least 1 hour, thereby maintaining continuous ethanol exposure during the initial treatment period.

Previous studies have reported both beneficial and harmful effects of ethanol exposure on *C. elegans* lifespan, depending on ethanol concentration and the developmental stage at which treatment is administered (*11-13*). In our study, 4-day-old young adults treated with 5% ethanol exhibited a significant increase in lifespan (Figure 1B). As mentioned in the Introduction, low ethanol concentrations have generally been linked to lifespan extension (*11-13*), whereas higher concentrations tend to reduce lifespan (*11,13*). Based on those previous studies, 5% ethanol might have been expected to shorten lifespan; however, we observed a significant lifespan extension under this condition. While we used 5% ethanol (approximately 860 mM), which approaches the ED50 level reported (*22*), we did not observe rapid lethality within the 4-hour exposure time point. To assess whether the *E. coli* food supply may have been affected by the ethanol treatment, *E. coli* OP50 cells were cultured in LB broth containing 5, 10, 15, or 20% ethanol for 2 hours, and OD600 was then measured to estimate surviving *E. coli* cells, which showed a slight reduction to 70%, 65%, 63%, and 58% of the control level, respectively (Data not shown). These data indicate that 5% ethanol did not deplete the food supply and strongly suggest that the observed lifespan extension is not a starvation-mediated effect.

Based on the observed lifespan extension in young adult worms after 5% ethanol exposure (Figure 1B), we next used RNA-seq to explore transcriptomic responses and pathway changes potentially associated with this phenotype. At first, differences in the actual ethanol concentration and exposure time between agar plate culture and solution culture should be carefully considered, as summarized in Table 1. We confirmed that the 5% ethanol solution remained on the agar for more than 1 hour but did not persist overnight, suggesting that the ethanol effect observed in the agar plate assay is most comparable to the 1- to 4-hour exposure period used in the solution-based RNA-seq assay.

3.2. Gene expression patterns following 5% ethanol



	Average 50% survival day Mean ± SEM	n	Ratio	*P*-value
Control	17.2 ± 0.8	11	1.00	
5% EtOH	19.6 ± 0.8	11	1.14	< 0.001

Figure 1. Experimental design and lifespan analysis of wild-type *C. elegans* following 5% ethanol exposure. The effects of ethanol exposure on lifespan and gene expression profiles of *C. elegans* were assessed as described in the Methods. (**A**) Experimental schemes for the lifespan and RNA-seq analyses. For lifespan analysis, 4-day-old wild-type worms were cultured on agar plates in the presence or absence of 5% ethanol, and survival was monitored over time. For RNA-seq analysis, L4-stage worms were incubated in S-buffer under 5% ethanol or ethanol-free control conditions for 0, 1, 4, and 20 hours, followed by RNA extraction and gene expression analysis. **(B)** Representative results on wild-type *C. elegans* N2 strain, showing the observed lifespan extension following 5% ethanol exposure. The survival curves are shown on the left, and the result summary from 11 independent experiment sets is shown on the right.

Table 1. Comparison of two phases of experiment

Aim of experiment	Effects of ethanol on lifespan	Effects of ethanol on gene expression profiles
Culture conditions	On E. coli OP50-covered agar plates under 5% ethanol and FUdR treatment	In S-buffer in the presence or absence of 5% ethanol (no food, no FUdR treatment)
Culture length	27 days	1, 4, and 20* hours
Fully exposed to 5% ethanol	At least 1 hour	1, 4, and 20** hours
Lifespan measurements	Ethanol treatment started on Day 4, then live worms were counted every 2 days	-
RNA-seq experiments	-	RNA was prepared after 1, 4, and 20 hours culture

*At 20 hours in solution culture, eggs were observed in non-ethanol control culture, indicating that despite starvation, worms continued to develop.
**At 20 hours of exposure to 5% ethanol in solution culture, the worms showed retardation of development and weakness most likely due to the toxic effects caused by ethanol exposure.

exposure

In the present study, we re-examined, using RNA-seq profiling, the transcriptomic responses associated with the lifespan phenotype observed in our earlier 5% ethanol studies conducted more than two decades ago. The experimental design is schematically illustrated in Figure 1A. L4-stage *C. elegans* were treated with 5% ethanol or without ethanol (0% control) in S-buffer for 1, 4, and 20 hours, after which total RNA was extracted for sequencing.

First, we generated a Multidimensional Scaling (MDS) plot to visualize similarities and differences in transcriptomic profiles between ethanol-treated and control samples, as well as variation among biological replicates (Figure 2A). The MDS plot revealed distinct clustering of the 0% and 5% ethanol-treated samples, with clear shifts corresponding to treatment duration. For example, in the control group (blue points), the 0-, 1-, and 4-hour samples clustered in close proximity, indicating minimal changes in gene expression. In contrast, the 5% ethanol group (red points) exhibited progressive divergence over time. While the 1-hour sample remained near the untreated control group, the 4-hour and 20-hour samples shifted toward the lower right of the plot, suggesting substantial transcriptomic reprogramming with prolonged ethanol exposure. Notably, the 20-hour sample was positioned furthest from all other samples, indicating extensive gene expression changes. This separation likely reflects starvation and physiological stress, which became more pronounced after more than 4 hours of solution culture. Although worms in the control group laid eggs which were observed at 20 hours solution culture, no eggs were observed in the ethanol-treated group, and the worms showed retardation of development and weakness most likely due to the toxic effects of ethanol exposure.

Volcano plots were used to visualize differentially expressed genes in the ethanol-free time-course analysis (Figure 2B) and in comparisons between 5% ethanol-treated and ethanol-free samples at each time point (Figure 2C). These plots depict statistical significance relative to the magnitude of change (fold change). Consistent with the MDS plot, the number of significantly up- or downregulated genes increased over time. Subsequently, Gene Set Enrichment Analysis (GSEA) was conducted to identify functionally relevant pathways affected by ethanol treatment.

3.3. Time-dependent gene expression changes in the ethanol-free control group

Because the RNA-seq experiments were performed in S-buffer without food, time-dependent effects caused by food deprivation had to be considered when evaluating ethanol-associated gene expression changes. Therefore, we first examined gene expression changes over time in the ethanol-free control group to identify starvation-responsive genes and distinguish them from ethanol-associated changes. To this end, we examined gene expression changes in worms cultured for 1, 4, and 20 hours in the absence of ethanol (Figure 2A; blue diamond, circle and triangle shapes) as compared to the 0-hour control (Figure 2A; black diamond).

We then applied GSEA using the Kyoto Encyclopedia of Genes and Genomes (KEGG) database to evaluate whether a specific pathway was significantly altered under the experimental conditions. As a result, GSEA of ethanol-free worms revealed pronounced early starvation responses at 1 and 4 hours (*vs.* the 0-hour control), with several canonical stress pathways significantly enriched (FDR < 0.05) (Figure 3A). At 1 hour, results showed a strong activation of autophagy, mitophagy, the ubiquitin-proteasome system, and efferocytosis pathways (Figure 3A). These pathways facilitate degradation of unnecessary cellular components and play a crucial role under conditions with limited energy sources. Conversely, metabolic pathways such as fatty acid and amino acid metabolism were downregulated, indicating an adaptive response to reduced energy intake. At 4 hours, pathways related to growth and differentiation, such as TGF-β and Wnt signaling, were activated, suggesting their involvement in worm development (Figure 3A). Notably, autophagy-related pathways exhibited even stronger activation than at 1 hour, consistent with the notion that starvation drives increased cellular breakdown and recycling to conserve energy and resources.

3.4. Transcriptomic pathway changes potentially associated with lifespan modulation after 5% ethanol exposure

To understand the transcriptomic landscape potentially associated with ethanol-linked lifespan modulation, we analyzed RNA-seq data from L4-stage *C. elegans* cultured in S-buffer without food supply at 1, 4, and 20 hours in the presence of 5% ethanol.

First, we performed KEGG-based GSEA (5% ethanol *vs.* time-matched 0% controls; significance defined as FDR < 0.05) to identify early pathway changes following ethanol exposure. At the 1-hour time point, multiple stress-resistance and detoxification programs were significantly upregulated, including the Longevity regulating pathway (worm), Glutathione metabolism, Drug metabolism—cytochrome P450, Metabolism of xenobiotics by cytochrome P450, and Drug metabolism—other enzymes (Figure 3B). Among lipid pathways, Sphingolipid metabolism was also significantly enriched at 1 hour. In contrast, Peroxisome, TGF-β signaling, and Wnt signaling showed downward trends at 1 hour but did not meet the FDR < 0.05 threshold. At 4 hours, Peroxisome, TGF-β signaling, and Wnt signaling were significantly downregulated (FDR

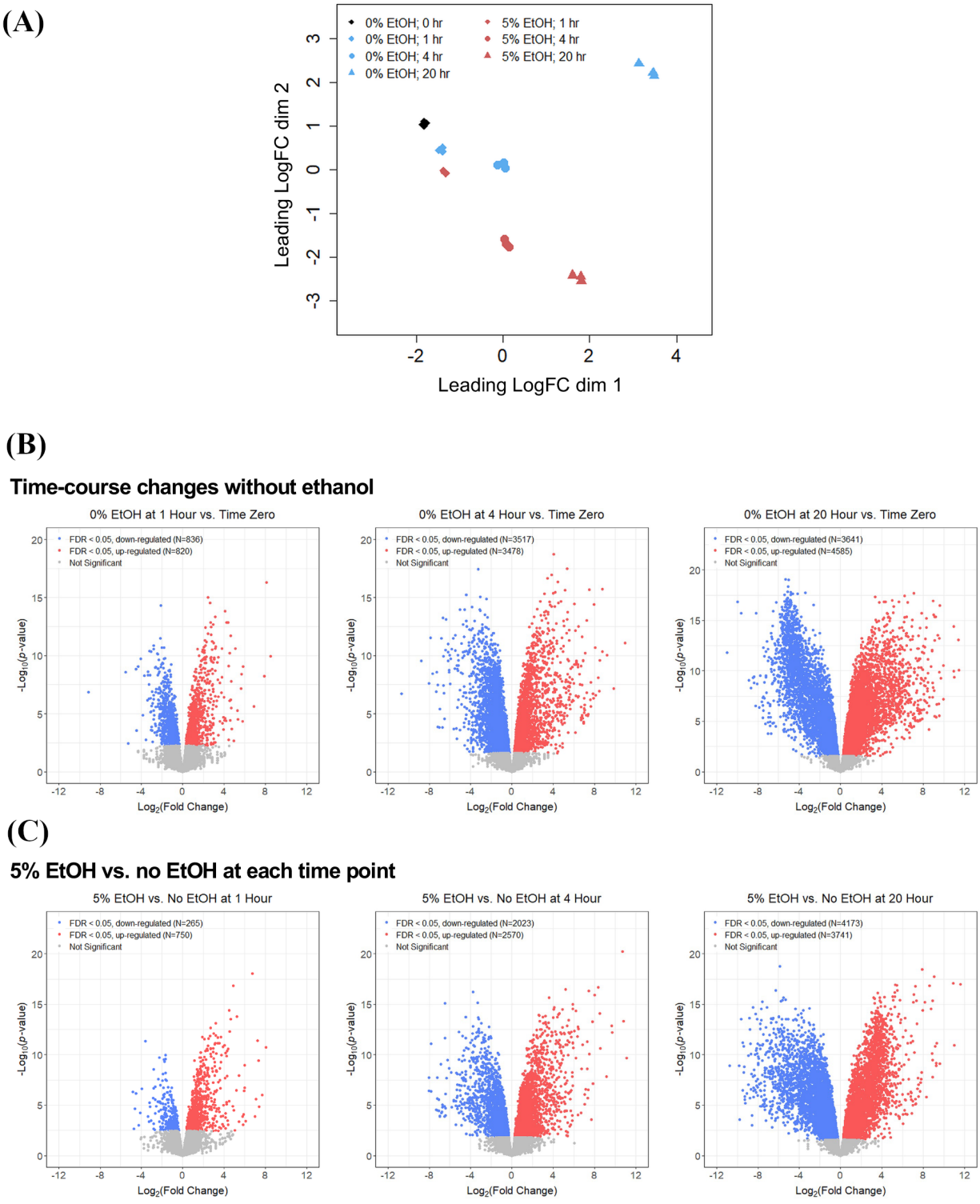
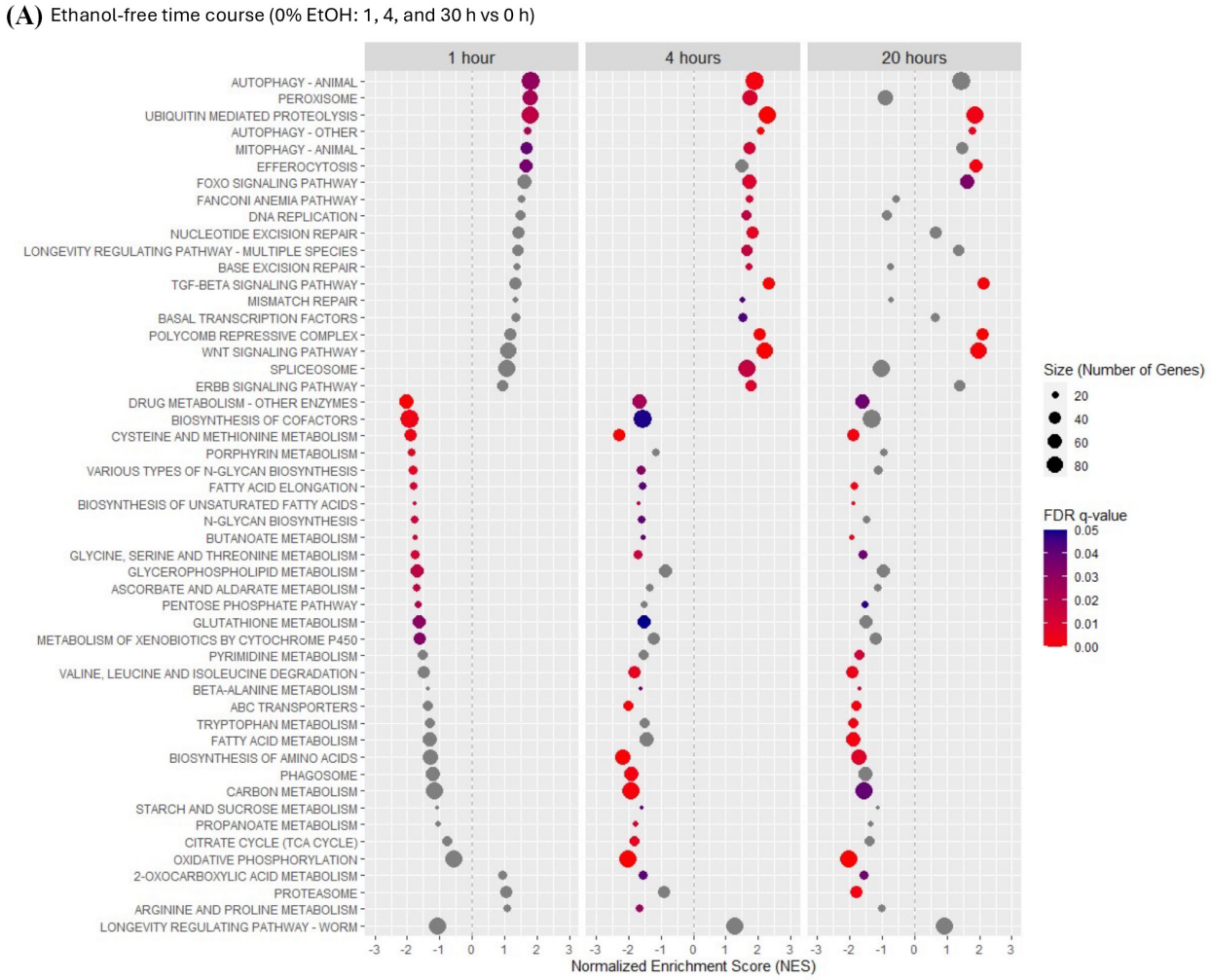


Figure 2. Multidimensional Scaling (MDS) Plot and differential expression analysis (volcano plots). (**A**) MDS plot of distances between gene expression profiles comparing the transcriptional responses of worms under 0% ethanol (control; blue) and worms cultured in the presence of 5% ethanol (treatment; red). Each point represents a sample, differentiated by color or shape according to the designated ethanol treatment throughout time-course experiments. The distance between points reflects the leading log-fold change (logFC) between each pair of samples. Time points are shown at 0 hr (♦, $n = 4$), 1 hr (◊, $n = 3$), 4 hr (○, $n = 3$), 20 hr (Δ, $n = 3$). (**B**) Volcano plots showing differentially expressed genes in the time-course analysis under ethanol-free conditions, in which gene expression at 1, 4, and 20 hours was compared with that at 0 h. (**C**) Volcano plots showing differentially expressed genes between 5% ethanol-treated and ethanol-free samples at 1, 4, and 20 hours. Genes with statistically significant changes are highlighted according to FDR < 0.05 (red, significantly upregulated; blue, significantly downregulated; gray, not significant).



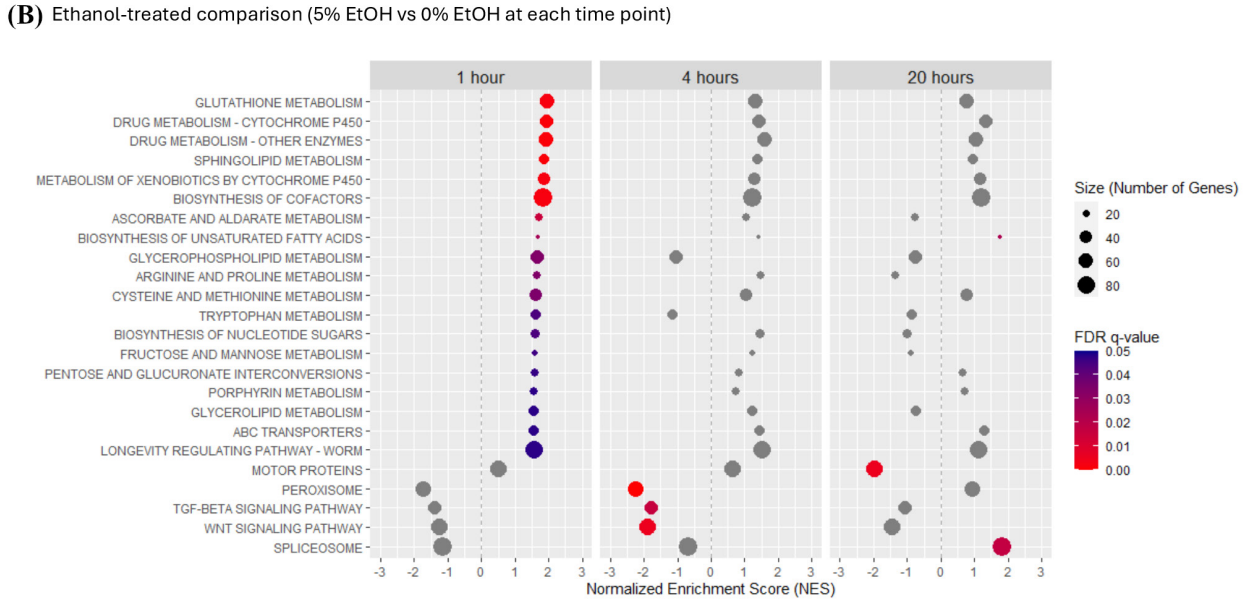
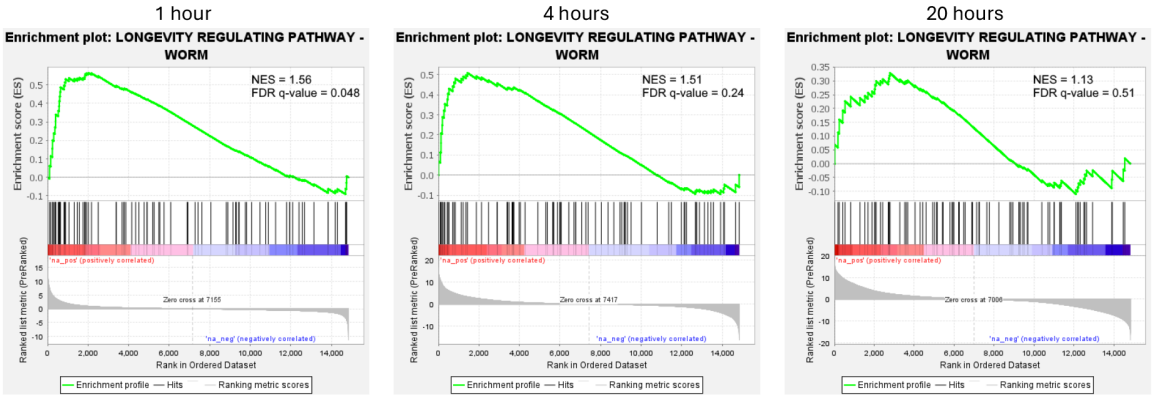
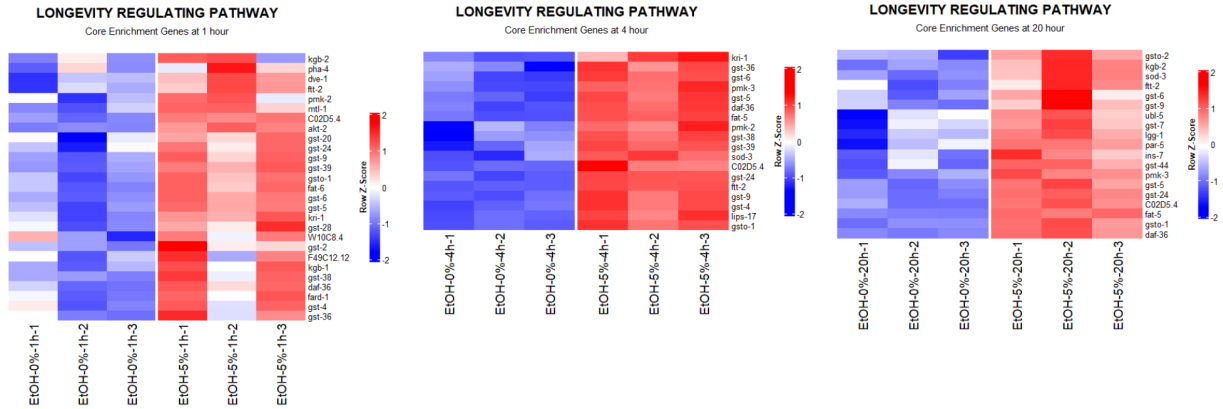


Figure 3. Gene Set Enrichment Analysis (Pathway analysis). (**A**) *C. elegans* functional pathways were analyzed as described in the Methods. Transcripts from worms cultured under ethanol-free conditions for 1, 4, and 20 hours were compared to those at time zero. Functional pathways showing statistical significance (FDR < 0.05) are color-coded as indicated in the legend. (**B**) Transcripts under ethanol conditions (5% *vs.* 0%) were compared at 1, 4, and 20 hours. Functional pathways showing statistical significance (FDR < 0.05) are color-coded as indicated in the legend. Enrichment Plots of the Longevity Regulating pathway generated by two different analyses are shown in (**C**) and (**D**).

(C) Enrichment Plots : Longevity Regulating Pathway



(D) Core enrichment genes: 1, 4, and 20 h



List of Genes upregulated by 5% EtOH treatment

Only at 1h	At 1, 4, & 20h	At 1h & 4h	Only at 4 h	At 4h & 20h	Only at 20h
kgb-2	C02D5.4	gst-36	lips-17	fat-5	gsto-2
pha-4	daf-36	gst-38		pmk-3	kgb-2
dve-1	ftt-2	gst-39		sod-3	ubl-5
mtl-1	gst-24	gst-4			gst-7
akt-2	gst-6	pmk-2			lgg-1
gst-20	gst-5	kri-1			par-5
fat-6	gst-9				ins-7
gst-28	gsto-1				gst-44
W10C8.4					
gst-2					
F49C12.12					
kgb-1					
fard-1					

Figure 3 (continued). Gene Set Enrichment Analysis (Pathway analysis). (**A**) *C. elegans* functional pathways were analyzed as described in the Methods. Transcripts from worms cultured under ethanol-free conditions for 1, 4, and 20 hours were compared to those at time zero. Functional pathways showing statistical significance (FDR < 0.05) are color-coded as indicated in the legend. (**B**) Transcripts under ethanol conditions (5% *vs.* 0%) were compared at 1, 4, and 20 hours. Functional pathways showing statistical significance (FDR < 0.05) are color-coded as indicated in the legend. Enrichment Plots of the Longevity Regulating pathway generated by two different analyses are shown in (**C**) and (**D**).

< 0.05), indicating sustained repression of peroxisomal fatty-acid functions and growth/differentiation signals beyond the acute phase. Pathways that were significant at 1 hour, namely the Longevity regulating pathway, Glutathione metabolism, and P450/drug-metabolism pathways, did not cross the FDR < 0.05 threshold at 4 hours yet remained directionally concordant with their 1-hour profiles. Lipid-associated pathways likewise maintained concordant trends at 4 hours without reaching significance. Taken together, these results show that ethanol exposure is associated with an early, significant activation of longevity-related and detoxification pathways (with accompanying sphingolipid remodeling), followed by significant suppression of peroxisomal and developmental signaling at 4 hours. These pathway-level patterns suggest a time-dependent shift toward

somatic maintenance and energy sparing at the expense of growth, and identify candidate processes that may be related to the observed lifespan phenotype.

3.5 Gene expression and network analyses of longevity-associated and stress-response pathways after 5% ethanol exposure

The longevity-regulating pathway was enriched at 1 hour of 5% ethanol exposure and remained upregulated for up to 20 hours, providing transcriptomic clues to longevity-associated responses after ethanol exposure (Figure 3B). Further examination of the longevity-regulating pathway (Figure 3C and D) revealed that gene activation at 1 hour was the most significant in terms of the number of upregulated genes involved in this pathway, with distinct expression patterns emerging as ethanol exposure duration increased. As shown in the Enrichment plots for ethanol treatment at 1 hour, 4 hours, and 20 hours (Figure 3C), dynamic changes in longevity-regulating pathway activation over time can be observed. Specifically, the plots indicate that the normalized enrichment score (NES) remained positive at all time points, indicating upregulation of genes annotated within longevity-related pathways in response to ethanol treatment. Although the NES value declined at 20 hours, most genes involved in lifespan extension remained elevated. Figure 3D presents gene expression changes for core enrichment genes in the longevity-regulating pathway.

In *C. elegans* treated with 5% ethanol, multiple genes associated with antioxidant and stress responses were significantly upregulated (Figure 3D). Notably, genes within the *gst* family (*gst-6*, *gst-9*, *gst-36*, *etc*.), which encode glutathione S-transferases involved in detoxification of harmful metabolites and toxins generated by oxidative stress within cells, were upregulated at 1 hour ethanol exposure and remained upregulated for up to 20 hours. This indicates rapid activation of cellular detoxification mechanisms in response to ethanol-associated mild oxidative stress. The *sod-3* gene, a canonical DAF-16/FOXO target involved in antioxidant defense, was not significantly induced at 1 hour but was robustly upregulated after 4 and 20 hours of ethanol exposure. Another stress-responsive pathway affected by ethanol treatment was the p38 MAP kinase pathway, including genes exemplified by *pmk-2* and *pmk-3*. These genes regulate cellular defense mechanisms against environmental stressors and infections. Their increased expression following 1 hour of ethanol treatment suggests an ethanol-associated cellular adaptive stress response. After 4 hours of ethanol treatment, these antioxidant and detoxification-related genes were further upregulated. This sequential pattern suggests that initial detoxification responses may be followed by engagement of classical longevity effectors. Such a timeline fits previous models where transient stress activates SKN-1 and DAF-16 pathways to enhance stress resistance and extend lifespan (*23*). In our case, early induction of detoxification genes may prevent oxidative damage, while later DAF-16-mediated antioxidant gene activation (*e.g.*, *sod-3*) may further strengthen cellular resilience.

To further visualize the relationships between ethanol-regulated genes and KEGG pathways, we generated cnetplots for genes altered after 1 hour of 5% ethanol exposure (Figure 4). This analysis was focused on the early phase of ethanol response, because 1 hour represented the most prominent activation of the longevity-related pathway.

The cnetplot analysis revealed a network in which the Longevity regulating pathway (worm) was closely associated with antioxidant, detoxification, and drug metabolism pathways, including cytochrome P450 metabolism, glutathione metabolism, and xenobiotic metabolism (Figure 4A). Genes associated with the upregulated pathways are shown in Figure 4B, whereas downregulated pathways and their associated genes are shown in Figure 4C and D, respectively.

Short-term (1 hour) ethanol treatment notably upregulated genes encoding detoxification enzymes including cytochrome P450s and glutathione S-transferases, consistent with previous findings that mild ethanol exposure induces stress-protective metabolic responses (*13*). The close clustering of longevity-associated and stress response pathways implies coordinated regulation, potentially mediated by conserved transcription factors such as SKN-1/Nrf2 and DAF-16/FOXO. In *C. elegans*, SKN-1 drives detoxification gene expression and extends lifespan under stress, while DAF-16 promotes antioxidant defenses (*23*). Thus, the network topology observed in Figure 4 supports the interpretation that ethanol exposure is associated with a hormetic-like transcriptomic response, in which mild cellular stress may activate cytoprotective longevity programs. Our study provides transcriptomic insights after ethanol exposure and extends previous studies (*24-26*), offering time-resolved pathway-level data that complement the recent study by Sterken *et al*. (*26*), who examined transcriptional responses of *C. elegans* across a time course of ethanol exposure to determine which genes and genetic pathways are regulated in response to ethanol.

Growth-promoting and developmental pathways, including TGF-β signaling, showed downward trends at 1 hour and were significantly downregulated at 4 hours. In *C. elegans*, inhibition of the DAF-7/TGF-β pathway promotes dauer formation and extends lifespan under adverse conditions (*27*), suggesting that downregulation of TGF-β signaling after ethanol exposure may be one candidate pathway associated with a stress-resistant metabolic state and lifespan modulation.

Altogether, these findings indicate that brief ethanol exposure, particularly within the 1- to 4-hour period, is associated with a coordinated transcriptomic response characterized by activation of cytoprotective pathways

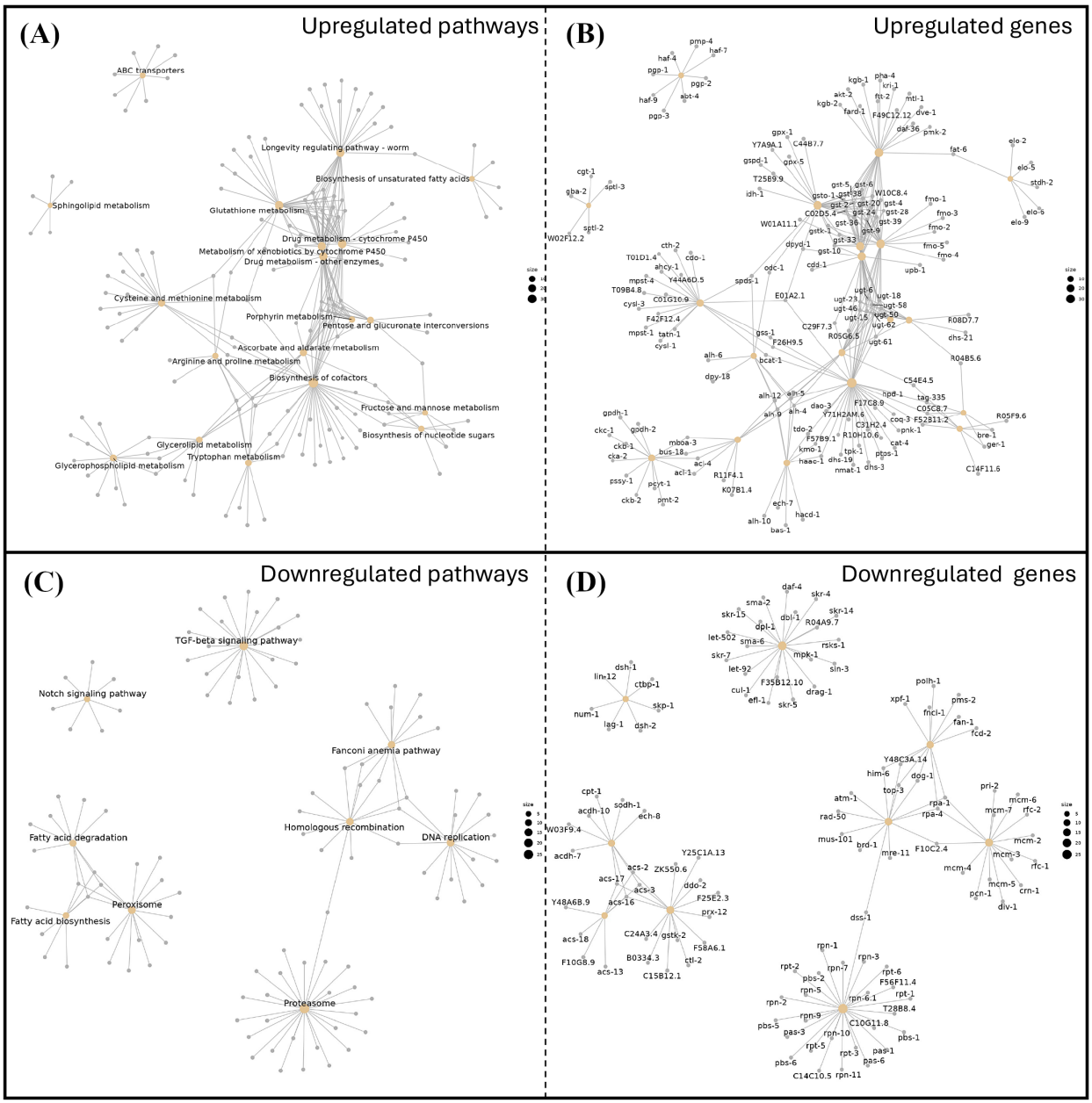


Figure 4. Gene-concept network (cnetplot) of KEGG pathways altered after 1 hour of 5% ethanol exposure in *C. elegans*. The cnetplot depicts linkages of genes and biological concepts (KEGG pathways) as a network. Networks of upregulated pathways (**A**) and corresponding gene names (**B**) as well as networks of downregulated pathways (**C**) and corresponding gene names (**D**) are shown. KEGG pathways (larger yellow nodes) are connected to nodes representing genes (smaller gray nodes) that contribute to each pathway's enrichment.

and suppression of growth-promoting processes. This shift toward stress resistance and metabolic conservation may contribute to, or occur in parallel with, the observed lifespan extension and is consistent with the concept of hormesis, in which mild stress activates protective mechanisms that promote longevity (*23,27*). Future studies are warranted to clarify the mechanistic links between ethanol-induced stress responses and aging.

Acknowledgements

Research reported in this publication included work performed in the Integrative Genomics Core supported by the National Cancer Institute of the National Institutes of Health under grant number P30CA033572. The authors also acknowledge the Life Science Support Center, Tokai University, for providing research facilities. The authors thank Drs. Masayuki Tanaka and Akinori Takase for their technical assistance.

Funding: This study was supported by the Japan Health Sciences Foundation (Health Sciences Basic Project and Integrated Study Project in Drug Innovation Science, to YFY).

Conflict of Interest: The authors have no conflicts of

interest to disclose.

Data Availability: The data discussed in this publication have been deposited in NCBI's Gene Expression Omnibus (GEO) and are accessible through GEO Series accession number GSE296436.

References

1. Lai CH, Chou CY, Ch'ang LY, Liu CS, Lin W. Identification of novel human genes evolutionarily conserved in Caenorhabditis elegans by comparative proteomics. Genome Res. 2000; 10:703-713.
2. Shaye DD, Greenwald I. OrthoList: a compendium of C. elegans genes with human orthologs. PLoS One. 2011; 6:e20085.
3. Kim W, Underwood RS, Greenwald I, Shaye DD. OrthoList 2: A New Comparative Genomic Analysis of Human and Caenorhabditis elegans Genes. Genetics. 2018; 210:445-461.
4. Kwon HC, Lee SV. Brief guide to Caenorhabditis elegans survival assays. Mol Cells. 2025; 48:100232.
5. Honda Y, Honda S. Oxidative stress and life span determination in the nematode Caenorhabditis elegans. Ann N Y Acad Sci. 2002; 959:466-474.
6. Murphy CT, McCarroll SA, Bargmann CI, Fraser A, Kamath RS, Ahringer J, Li H, Kenyon C. Genes that act downstream of DAF-16 to influence the lifespan of Caenorhabditis elegans. Nature. 2003; 424:277-283.
7. Ishii N, Fujii M, Hartman PS, Tsuda M, Yasuda K, Senoo-Matsuda N, Yanase S, Ayusawa D, Suzuki K. A mutation in succinate dehydrogenase cytochrome b causes oxidative stress and ageing in nematodes. Nature. 1998; 394:694-697.
8. Ronksley PE, Brien SE, Turner BJ, Mukamal KJ, Ghali WA. Association of alcohol consumption with selected cardiovascular disease outcomes: a systematic review and meta-analysis. BMJ. 2011; 342:d671.
9. Koppes LL, Dekker JM, Hendriks HF, Bouter LM, Heine RJ. Moderate alcohol consumption lowers the risk of type 2 diabetes: a meta-analysis of prospective observational studies. Diabetes Care. 2005; 28:719-725.
10. Rehm J, Baliunas D, Borges GL, Graham K, Irving H, Kehoe T, Parry CD, Patra J, Popova S, Poznyak V, Roerecke M, Room R, Samokhvalov AV, Taylor B. The relation between different dimensions of alcohol consumption and burden of disease: an overview. Addiction. 2010; 105:817-843.
11. Yu X, Zhao W, Ma J, Fu X, Zhao ZJ. Beneficial and harmful effects of alcohol exposure on Caenorhabditis elegans worms. Biochem Biophys Res Commun. 2011; 412:757-762.
12. Castro PV, Khare S, Young BD, Clarke SG. Caenorhabditis elegans battling starvation stress: low levels of ethanol prolong lifespan in L1 larvae. PLoS One. 2012; 7:e29984.
13. Wu Z-Q, Li K, Ma J-K, Li Z-J. Effects of ethanol intake on anti-oxidant responses and the lifespan of Caenorhabditis elegans. CyTA - Journal of Food. 2019; 17:288-296.
14. Bolger AM, Lohse M, Usadel B. Trimmomatic: a flexible trimmer for Illumina sequence data. Bioinformatics. 2014; 30:2114-2120.
15. Chen S, Zhou Y, Chen Y, Gu J. fastp: an ultra-fast all-in-one FASTQ preprocessor. Bioinformatics. 2018; 34:i884-i890.
16. Dobin A, Davis CA, Schlesinger F, Drenkow J, Zaleski C, Jha S, Batut P, Chaisson M, Gingeras TR. STAR: ultrafast universal RNA-seq aligner. Bioinformatics. 2013; 29:15-21.
17. Liao Y, Smyth GK, Shi W. featureCounts: an efficient general purpose program for assigning sequence reads to genomic features. Bioinformatics. 2014; 30:923-930.
18. Robinson MD, McCarthy DJ, Smyth GK. edgeR: a Bioconductor package for differential expression analysis of digital gene expression data. Bioinformatics. 2010; 26:139-140.
19. Subramanian A, Tamayo P, Mootha VK, Mukherjee S, Ebert BL, Gillette MA, Paulovich A, Pomeroy SL, Golub TR, Lander ES, Mesirov JP. Gene set enrichment analysis: a knowledge-based approach for interpreting genome-wide expression profiles. Proc Natl Acad Sci U S A. 2005; 102:15545-15550.
20. Kanehisa M, Furumichi M, Sato Y, Matsuura Y, Ishiguro-Watanabe M. KEGG: biological systems database as a model of the real world. Nucleic Acids Res. 2025; 53:D672-D677.
21. Wu T, Hu E, Xu S, Chen M, Guo P, Dai Z, Feng T, Zhou L, Tang W, Zhan L, Fu X, Liu S, Bo X, Yu G. clusterProfiler 4.0: A universal enrichment tool for interpreting omics data. Innovation (Camb). 2021; 2:100141.
22. Morgan PG, Sedensky MM. Mutations affecting sensitivity to ethanol in the nematode, Caenorhabditis elegans. Alcohol Clin Exp Res. 1995; 19:1423-1429.
23. Blackwell TK, Steinbaugh MJ, Hourihan JM, Ewald CY, Isik M. SKN-1/Nrf, stress responses, and aging in Caenorhabditis elegans. Free Radic Biol Med. 2015; 88:290-301.
24. Kwon JY, Hong M, Choi MS, Kang S, Duke K, Kim S, Lee S, Lee J. Ethanol-response genes and their regulation analyzed by a microarray and comparative genomic approach in the nematode Caenorhabditis elegans. Genomics. 2004; 83:600-614.
25. Patananan AN, Budenholzer LM, Eskin A, Torres ER, Clarke SG. Ethanol-induced differential gene expression and acetyl-CoA metabolism in a longevity model of the nematode Caenorhabditis elegans. Exp Gerontol. 2015; 61:20-30.
26. Sterken MG, van Wijk MH, Quamme EC, Riksen JAG, Carnell L, Mathies LD, Davies AG, Kammenga JE, Bettinger JC. Transcriptional analysis of the response of C. elegans to ethanol exposure. Sci Rep. 2021; 11:10993.
27. Shaw WM, Luo S, Landis J, Ashraf J, Murphy CT. The C. elegans TGF-beta Dauer pathway regulates longevity *via* insulin signaling. Curr Biol. 2007; 17:1635-1645.

Received March 28, 2026; Revised May 14, 2026; Accepted May 19, 2026.

**Address correspondence to:*
Yoko Fujita-Yamaguchi, Arthur Riggs Diabetes & Metabolism Research Institute, Beckman Research Institute of City of Hope, Duarte, CA 91010, USA.
E-mail: yyamaguchi@coh.org

Released online in J-STAGE as advance publication June 2, 2026.

BST
BioScience Trends

Guide for Authors

1. Scope of Articles

BioScience Trends (Print ISSN 1881-7815, Online ISSN 1881-7823) is an international peer-reviewed journal. *BioScience Trends* devotes to publishing the latest and most exciting advances in scientific research. Articles cover fields of life science such as biochemistry, molecular biology, clinical research, public health, medical care system, and social science in order to encourage cooperation and exchange among scientists and clinical researchers.

2. Submission Types

Original Articles should be well-documented, novel, and significant to the field as a whole. An Original Article should be arranged into the following sections: Title page, Abstract, Introduction, Materials and Methods, Results, Discussion, Acknowledgments, and References. Original articles should not exceed 5,000 words in length (excluding references) and should be limited to a maximum of 50 references. Articles may contain a maximum of 10 figures and/or tables. Supplementary Data are permitted but should be limited to information that is not essential to the general understanding of the research presented in the main text, such as unaltered blots and source data as well as other file types.

Brief Reports definitively documenting either experimental results or informative clinical observations will be considered for publication in this category. Brief Reports are not intended for publication of incomplete or preliminary findings. Brief Reports should not exceed 3,000 words in length (excluding references) and should be limited to a maximum of 4 figures and/or tables and 30 references. A Brief Report contains the same sections as an Original Article, but the Results and Discussion sections should be combined.

Reviews should present a full and up-to-date account of recent developments within an area of research. Normally, reviews should not exceed 8,000 words in length (excluding references) and should be limited to a maximum of 10 figures and/or tables and 100 references. Mini reviews are also accepted, which should not exceed 4,000 words in length (excluding references) and should be limited to a maximum of 5 figures and/or tables and 50 references.

Policy Forum articles discuss research and policy issues in areas related to life science such as public health, the medical care system, and social science and may address governmental issues at district, national, and international levels of discourse. Policy Forum articles should not exceed 3,000 words in length (excluding references) and should be limited to a maximum of 5 figures and/or tables and 30 references.

Communications are short, timely pieces that spotlight new research findings or policy issues of interest to the field of global health and medical practice that are of immediate importance. Depending on their content, Communications will be published as "Comments" or "Correspondence". Communications should not exceed 1,500 words in length (excluding references) and should be limited to a maximum of 2 figures and/or tables and 20 references.

Editorials are short, invited opinion pieces that discuss an issue of immediate importance to the fields of global health, medical practice, and basic science oriented for clinical application. Editorials should not exceed 1,000 words in length (excluding references) and should be limited to a maximum of 10 references. Editorials may contain one figure or table.

News articles should report the latest events in health sciences and medical research from around the world. News should not exceed 500 words in length.

Letters should present considered opinions in response to articles published in *BioScience Trends* in the last 6 months or issues of general interest. Letters should not exceed 800 words in length and may contain a maximum of 10 references. Letters may contain one figure or table.

3. Editorial Policies

For publishing and ethical standards, *BioScience Trends* follows the Recommendations for the Conduct, Reporting, Editing, and Publication of Scholarly Work in Medical Journals issued by the International Committee of Medical Journal Editors (ICMJE, *https://icmje.org/recommendations*), and the Principles of Transparency and Best Practice in Scholarly Publishing jointly issued by the Committee on Publication Ethics (COPE, *https://publicationethics.org/resources/guidelines-new/principles-transparency-and-best-practice-scholarly-publishing*), the Directory of Open Access Journals (DOAJ, *https://doaj.org/apply/transparency*), the Open Access Scholarly Publishers Association (OASPA, *https://oaspa.org/principles-of-transparency-and-best-practice-in-scholarly-publishing-4*), and the World Association of Medical Editors (WAME, *https://wame.org/principles-of-transparency-and-best-practice-in-scholarly-publishing*).

BioScience Trends will perform an especially prompt review to encourage innovative work. All original research will be subjected to a rigorous standard of peer review and will be edited by experienced copy editors to the highest standards.

Ethical Approval of Studies and Informed Consent: For all manuscripts reporting data from studies involving human participants or animals, formal review and approval, or formal review and waiver, by an appropriate institutional review board or ethics committee is required and should be described in the Methods section. When your manuscript contains any case details, personal information and/or images of patients or other individuals, authors must obtain appropriate written consent, permission and release in order to comply with all applicable laws and regulations concerning privacy and/or security of personal information. The consent form needs to comply with the relevant legal requirements of your particular jurisdiction, and please do not send signed consent form to *BioScience Trends* to respect your patient's and any other individual's privacy. Please instead describe the information clearly in the Methods (patient consent) section of your manuscript while retaining copies of the signed forms in the event they should be needed. Authors should also state that the study conformed to the provisions of the Declaration of Helsinki (as revised in 2013, *https://wma.net/what-we-do/medical-ethics/declaration-of-helsinki*). When reporting experiments on animals, authors should indicate whether the institutional and national guide for the care and use of laboratory animals was followed.

Reporting Clinical Trials: The ICMJE (*https:// icmje.org/recommendations/browse/publishing-and-editorial-issues/clinical-trial-registration.html*) defines a clinical trial as any research project that prospectively assigns people or a group of people to an intervention, with or without concurrent comparison or control groups, to study the relationship between a health-related intervention and a health outcome. Registration of clinical trials in a public trial registry at or before the time of first patient enrollment is a condition of consideration for publication in *BioScience Trends*, and the trial registration number will be published at the end of the Abstract. The registry must be independent of for-profit interest and publicly accessible. Reports of trials must conform to CONSORT 2010 guidelines (*https://consort-statement.org/consort-2010*). Articles reporting the results of randomized trials must include the CONSORT flow diagram showing the progress of patients throughout the trial.

Conflict of Interest: All authors are required to disclose any actual or potential conflict of interest including financial interests or relationships with other people or organizations that might raise questions of bias

in the work reported. If no conflict of interest exists for each author, please state "There is no conflict of interest to disclose".

Submission Declaration: When a manuscript is considered for submission to *BioScience Trends*, the authors should confirm that 1) no part of this manuscript is currently under consideration for publication elsewhere; 2) this manuscript does not contain the same information in whole or in part as manuscripts that have been published, accepted, or are under review elsewhere, except in the form of an abstract, a letter to the editor, or part of a published lecture or academic thesis; 3) authorization for publication has been obtained from the authors' employer or institution; and 4) all contributing authors have agreed to submit this manuscript.

Initial Editorial Check: Immediately after submission, the journal's managing editor will perform an initial check of the manuscript. A suitable academic editor will be notified of the submission and invited to check the manuscript and recommend reviewers. Academic editors will check for plagiarism and duplicate publication at this stage. The journal has a formal recusal process in place to help manage potential conflicts of interest of editors. In the event that an editor has a conflict of interest with a submitted manuscript or with the authors, the manuscript, review, and editorial decisions are managed by another designated editor without a conflict of interest related to the manuscript.

Peer Review: *BioScience Trends* operates a single-anonymized review process, which means that reviewers know the names of the authors, but the authors do not know who reviewed their manuscript. All articles are evaluated objectively based on academic content. External peer review of research articles is performed by at least two reviewers, and sometimes the opinions of more reviewers are sought. Peer reviewers are selected based on their expertise and ability to provide quality, constructive, and fair reviews. For research manuscripts, the editors may, in addition, seek the opinion of a statistical reviewer. Every reviewer is expected to evaluate the manuscript in a timely, transparent, and ethical manner, following the COPE guidelines (*https://publicationethics.org/files/cope-ethical-guidelines-peer-reviewers-v2_0.pdf*). We ask authors for sufficient revisions (with a second round of peer review, when necessary) before a final decision is made. Consideration for publication is based on the article's originality, novelty, and scientific soundness, and the appropriateness of its analysis.

Suggested Reviewers: A list of up to 3 reviewers who are qualified to assess the scientific merit of the study is welcomed. Reviewer information including names, affiliations, addresses, and e-mail should be provided at the same time the manuscript is submitted online. Please do not suggest reviewers with known conflicts of interest, including participants or anyone with a stake in the proposed research; anyone from the same institution; former students, advisors, or research collaborators (within the last three years); or close personal contacts. Please note that the Editor-in-Chief may accept one or more of the proposed reviewers or may request a review by other qualified persons.

Language Editing: Manuscripts prepared by authors whose native language is not English should have their work proofread by a native English speaker before submission. If not, this might delay the publication of your manuscript in *BioScience Trends*.

The Editing Support Organization can provide English proofreading, Japanese-English translation, and Chinese-English translation services to authors who want to publish in *BioScience Trends* and need assistance before submitting a manuscript. Authors can visit this organization directly at *https://www.iacmhr.com/iac-eso/support.php?lang=en*. IAC-ESO was established to facilitate manuscript preparation by researchers whose native language is not English and to help edit works intended for international academic journals.

Copyright and Reuse: Before a manuscript is accepted for publication in *BioScience Trends*, authors will be asked to sign a transfer of copyright agreement, which recognizes the common interest that both the journal and author(s) have in the protection of copyright. We accept that some authors (*e.g.*, government employees in some countries) are unable to transfer copyright. A JOURNAL PUBLISHING AGREEMENT (JPA) form will be e-mailed to the authors by the Editorial Office and must be returned by the authors by mail, fax, or as a scan. Only forms with a hand-written signature from the corresponding author are accepted. This copyright will ensure the widest possible dissemination of information. Please note that the manuscript will not proceed to the next step in publication until the JPA Form is received. In addition, if excerpts from other copyrighted works are included, the author(s) must obtain written permission from the copyright owners and credit the source(s) in the article.

4. Cover Letter

The manuscript must be accompanied by a cover letter prepared by the corresponding author on behalf of all authors. The letter should indicate the basic findings of the work and their significance. The letter should also include a statement affirming that all authors concur with the submission and that the material submitted for publication has not been published previously or is not under consideration for publication elsewhere. The cover letter should be submitted in PDF format. For an example of Cover Letter, please visit: *https://www.biosciencetrends.com/downcentre* (Download Centre).

5. Submission Checklist

The Submission Checklist should be submitted when submitting a manuscript through the Online Submission System. Please visit Download Centre (*https://www.biosciencetrends.com/downcentre*) and download the Submission Checklist file. We recommend that authors use this checklist when preparing your manuscript to check that all the necessary information is included in your article (if applicable), especially with regard to Ethics Statements.

6. Manuscript Preparation

Manuscripts are suggested to be prepared in accordance with the "Recommendations for the Conduct, Reporting, Editing, and Publication of Scholarly Work in Medical Journals", as presented at *https://www.ICMJE.org*.

Manuscripts should be written in clear, grammatically correct English and submitted as a Microsoft Word file in a single-column format. Manuscripts must be paginated and typed in 12-point Times New Roman font with 24-point line spacing. Please do not embed figures in the text. Abbreviations should be used as little as possible and should be explained at first mention unless the term is a well-known abbreviation (*e.g.* DNA). Single words should not be abbreviated.

Title page: The title page must include 1) the title of the paper (Please note the title should be short, informative, and contain the major key words); 2) full name(s) and affiliation(s) of the author(s), 3) abbreviated names of the author(s), 4) full name, mailing address, telephone/fax numbers, and e-mail address of the corresponding author; 5) author contribution statements to specify the individual contributions of all authors to this manuscript, and 6) conflicts of interest (if you have an actual or potential conflict of interest to disclose, it must be included as a footnote on the title page of the manuscript; if no conflict of interest exists for each author, please state "There is no conflict of interest to disclose").

Abstract: The abstract should briefly state the purpose of the study, methods, main findings, and conclusions. For articles that are Original Articles, Brief Reports, Reviews, or Policy Forum articles, a one-paragraph abstract consisting of no more than 250 words must be included in the manuscript. For Communications, Editorials, News, or Letters, a brief summary of main content in 150 words or fewer should be included in the manuscript. For articles reporting clinical trials, the trial registration number should be stated at the end of the Abstract. Abbreviations must be kept to a minimum and non-standard

abbreviations explained in brackets at first mention. References should be avoided in the abstract. Three to six key words or phrases that do not occur in the title should be included in the Abstract page.

Introduction: The introduction should provide sufficient background information to make the article intelligible to readers in other disciplines and sufficient context clarifying the significance of the experimental findings

Materials/Patients and Methods: The description should be brief but with sufficient detail to enable others to reproduce the experiments. Procedures that have been published previously should not be described in detail but appropriate references should simply be cited. Only new and significant modifications of previously published procedures require complete description. Names of products and manufacturers with their locations (city and state/country) should be given and sources of animals and cell lines should always be indicated. All clinical investigations must have been conducted in accordance Materials/ Patients and Methods.

Results: The description of the experimental results should be succinct but in sufficient detail to allow the experiments to be analyzed and interpreted by an independent reader. If necessary, subheadings may be used for an orderly presentation. All Figures and Tables should be referred to in the text in order, including those in the Supplementary Data.

Discussion: The data should be interpreted concisely without repeating material already presented in the Results section. Speculation is permissible, but it must be well-founded, and discussion of the wider implications of the findings is encouraged. Conclusions derived from the study should be included in this section.

Acknowledgments: All funding sources (including grant identification) should be credited in the Acknowledgments section. Authors should also describe the role of the study sponsor(s), if any, in study design; in the collection, analysis, and interpretation of data; in the writing of the report; and in the decision to submit the paper for publication. If the funding source had no such involvement, the authors should so state.

In addition, people who contributed to the work but who do not meet the criteria for authors should be listed along with their contributions.

References: References should be numbered in the order in which they appear in the text. Citing of unpublished results, personal communications, conference abstracts, and theses in the reference list is not recommended but these sources may be mentioned in the text. In the reference list, cite the names of all authors when there are fifteen or fewer authors; if there are sixteen or more authors, list the first three followed by *et al*. Names of journals should be abbreviated in the style used in PubMed. Authors are responsible for the accuracy of the references. The EndNote Style of *BioScience Trends* could be downloaded at **EndNote** (*https://ircabssagroup.com/examples/ BioScience_Trends.ens*).

Examples are given below:

Example 1 (Sample journal reference):

Inagaki Y, Tang W, Zhang L, Du GH, Xu WF, Kokudo N. Novel aminopeptidase N (APN/CD13) inhibitor 24F can suppress invasion of hepatocellular carcinoma cells as well as angiogenesis. Biosci Trends. 2010; 4:56-60.

Example 2 (Sample journal reference with more than 15 authors):

Darby S, Hill D, Auvinen A, *et al*. Radon in homes and risk of lung cancer: Collaborative analysis of individual data from 13 European case-control studies. BMJ. 2005; 330:223.

Example 3 (Sample book reference):

Shalev AY. Post-traumatic stress disorder: Diagnosis, history and life course. In: Post-traumatic Stress Disorder, Diagnosis, Management and Treatment (Nutt DJ, Davidson JR, Zohar J, eds.). Martin Dunitz, London, UK, 2000; pp. 1-15.

Example 4 (Sample web page reference):

World Health Organization. The World Health Report 2008 – primary health care: Now more than ever. *http://www.who.int/whr/2008/whr08_ en.pdf* (accessed September 23, 2022).

Tables: All tables should be prepared in Microsoft Word or Excel and should be arranged at the end of the manuscript after the References section. Please note that tables should not in image format. All tables should have a concise title and should be numbered consecutively with Arabic numerals. If necessary, additional information should be given below the table.

Figure Legend: The figure legend should be typed on a separate page of the main manuscript and should include a short title and explanation. The legend should be concise but comprehensive and should be understood without referring to the text. Symbols used in figures must be explained. Any individually labeled figure parts or panels (A, B, *etc*.) should be specifically described by part name within the legend.

Figure Preparation: All figures should be clear and cited in numerical order in the text. Figures must fit a one- or two-column format on the journal page: 8.3 cm (3.3 in.) wide for a single column, 17.3 cm (6.8 in.) wide for a double column; maximum height: 24.0 cm (9.5 in.). Please make sure that the symbols and numbers appeared in the figures should be clear. Please make sure that artwork files are in an acceptable format (TIFF or JPEG) at minimum resolution (600 dpi for illustrations, graphs, and annotated artwork, and 300 dpi for micrographs and photographs). Please provide all figures as separate files. Please note that low-resolution images are one of the leading causes of article resubmission and schedule delays.

Units and Symbols: Units and symbols conforming to the International System of Units (SI) should be used for physicochemical quantities. Solidus notation (*e.g.* mg/kg, mg/mL, mol/mm^2/min) should be used. Please refer to the SI Guide *www.bipm.org/en/si/* for standard units.

Supplemental data: Supplemental data might be useful for supporting and enhancing your scientific research and *BioScience Trends* accepts the submission of these materials which will be only published online alongside the electronic version of your article. Supplemental files (figures, tables, and other text materials) should be prepared according to the above guidelines, numbered in Arabic numerals (*e.g.*, Figure S1, Figure S2, and Table S1, Table S2) and referred to in the text. All figures and tables should have titles and legends. All figure legends, tables and supplemental text materials should be placed at the end of the paper. Please note all of these supplemental data should be provided at the time of initial submission and note that the editors reserve the right to limit the size and length of Supplemental Data.

5. Submission Checklist

The Submission Checklist will be useful during the final checking of a manuscript prior to sending it to *BioScience Trends* for review. Please visit Download Centre and download the Submission Checklist file.

6. Online Submission

Manuscripts should be submitted to *BioScience Trends* online at *https://www.biosciencetrends.com/login*. Receipt of your manuscripts submitted online will be acknowledged by an e-mail from Editorial Office containing a reference number, which should be used in all future communications. If for any reason you are unable to submit a file online, please contact the Editorial Office by e-mail at *office@ biosciencetrends.com*

8. Accepted Manuscripts

Page Charge: Page charges will be levied on all manuscripts accepted for publication in *BioScience Trends* (Original Articles / Brief Reports / Reviews / Policy Forum / Communications: $140 per page for black white pages, $340 per page for color pages; News / Letters: a total cost of $600).

Misconduct: *BioScience Trends* takes seriously all allegations of potential misconduct and adhere to the ICMJE Guideline (*https://icmje.org/recommendations*) and COPE Guideline (*https://publicationethics.org/files/Code_of_conduct_for_journal_editors.pdf*). In cases of suspected research or publication misconduct, it may be necessary for the Editor or Publisher to contact and share submission details with third parties including authors' institutions and ethics committees. The corrections, retractions, or editorial expressions of concern will be performed in line with above guidelines.

(As of August 2026)

BioScience Trends
Editorial and Head Office
Pearl City Koishikawa 603,
2-4-5 Kasuga, Bunkyo-ku,
Tokyo 112-0003, Japan.
E-mail: office@biosciencetrends.com